

Landsat-based monitoring in the parks of the Northern and Southern Colorado Plateau Networks

Executive Summary

Authors

Robert E. Kennedy, Yang Zhiqiang, Department of Forest Ecosystems and Analysis, Oregon State University, Corvallis OR 97331

Warren B. Cohen, Pacific Northwest Research Station, USDA Forest Service, 3200 SW Jefferson Way, Corvallis OR 97331

Executive summary

The parks of the Northern and Southern Colorado Plateau Networks (N&SCPN) identified remote sensing as a potential tool to monitor changes in vegetation at a landscape scale. Through a partnership with researchers at Oregon State University (OSU), a number of target landscape changes were identified that may be observable using remotely sensed data (Table 1, Yang et al. 2005). There are many possible sources of remotely sensed data; however, imagery from the Landsat Thematic Mapper (TM) satellite was considered the best overall compromise for conducting long-term monitoring, with low cost, unparalleled consistency and historical depth, and prospects for future continuity. Over the course of several years, collaborators at OSU worked with staff from the N&SCPN on a multi-stage project to evaluate the potential utility of Landsat imagery for monitoring vegetation on the Colorado Plateau. The initial stage of the project focused on baseline and single-time-frame mapping. Because of the difficulties encountered at this stage, later work focused on detection and interpretation of change, using increasingly sophisticated methods.

Table 1. Remote sensing based framework of CP monitoring objectives

Change	Identified as	Examples of interpretation
Fire (prescribed fire and wildfire)	Type conversion Change in proportions Change in degree of membership	“Conifer → bare soil (severe burn)” “Conifer cover decreases 20% (partial burn)” “Becomes less like a conifer forest, more like a C4 grassland (burn with invasion)”
Mortality	Change in proportions Change in degree of membership	“Pinyon pine cover decreases 50%” “Becomes less like PJ forest, more like shrub or grass”
Encroachment	Change in proportions Change in degree of membership	“PJ cover increases by 40%” “Becomes less like native grassland, more like PJ”
Grazing effects	Change in proportions Change in degree of membership	“Decrease in total cover by 50%” “Becomes less like C3 grassland, more like sage or C4 grassland”
Structure of wooded systems	Changes in tree cover and height	Mid-seral ponderosa pine stand now mature
Invasives	Type conversion Change in proportions Change in degree of membership	“C3 → C4 (complete conversion)” “C4 cover increases 100%” “Becomes less like C3 and more like C4”
Build-up or development (urban, agricultural, some recreation)	Type conversion Change in proportions Change in degree of membership	“Shrub → urban (urban development)” “Urban increases 100%” “Becomes less like shrub, more like urban”

Baseline mapping

Identification of change requires both information about the starting condition and the creation of models to identify vegetation types from the Landsat imagery. Thus, substantial effort was initially aimed at baseline mapping. Baseline maps from the NPS Vegetation Mapping project are both extremely rich in information and generally high in spatial detail, but are limited to the parks proper and their immediate vicinity and to a single occasion. Expanding the temporal and spatial scope with Landsat imagery would provide context for monitoring within the parks. Work focused on Mesa Verde (MEVE) and Canyonlands (CANY), which had no NPS Vegetation

Mapping products at the time of the studies, and at Zion, which did have a completed NPSVM map.

Key conclusions from this stage of the project included

- As expected from the initial literature review, the soil signal dominates the spectral response in most of the areas of N&CPN, making vegetation discrimination difficult under any circumstance when Landsat data are used. This is a limitation inherent to the data, regardless of the spectral indices being used or the data analysis method employed.
- Mapping vegetation components with Landsat is done most robustly for forest and woodland vegetation cover. When thematic maps such as those from the NPSVM program are available, aggregation to simpler, spectrally-separable classes is feasible and relatively accurate.
- Available reference data are generally inadequate for the purposes of training and testing maps with Landsat data. New airphoto interpretation can fill some gaps, but is costly, and even airphoto interpretation lacks the separability needed to go beyond aggregated class labels with confidence.

Because of these challenges, the N&SCPN and OSU groups determined that the potential utility of Landsat data for baseline mapping alone was lower than that desired by the parks, but that some of the methods explored for baseline mapping may be relevant when used in the context of change detection.

Two-date change detection

Detection of landscape change was thus the next major focus. Change detection studies focused on MEVE, ZION, and Wupatki National Monument (WUPA). At the onset of the project, the N&SCPN were interested in the potential to apply the method known as “POM change detection” (for “probability of membership” change) that OSU had developed for the parks of the North Coast and Cascades Network (NCCN). However, unlike the situation in the NCCN, existing land cover maps were available, and thus new methods to aggregate and merge the existing landcover maps with the spectral strategies of the POM were developed. Also, because of the different ecosystem properties of the two networks and the expected difficulties of working in soil-dominated systems, OSU also examined other change detection approaches based on statistical models between the imagery and airphoto-interpreted estimates of component cover characteristics.

Key conclusions from this stage of the project included

- Reference data are an even greater bottleneck for many change-detection approaches than they are for single-date mapping, as reference data must be both appropriate for remotely-sensed models and consistent across time. Rarely are such data available. Validation of change results is thus particularly challenging.

- Detection of landscape change is possible using either continuous-variable maps or the POM (probability of membership) approach originally envisioned for these projects. The former approach is primarily limited to forest and woodland cover types. Landcover classes in the POM-change approach were limited to fairly broad labels that may not be useful for some the N&SCPN's goals.
- Any map of change using only two dates of imagery is suspect in these ecosystems because vegetation phenology and year-to-year variance in precipitation cause many potential false-positive spectral changes.

As was the case with baseline mapping, these results showed that the methods tested were appropriate for some uses, but the level of detail needed by the N&SCPN were greater than was generally feasible. Thus, on both of the primary efforts of the initial agreement between OSU and the parks, the potential utility of monitoring with Landsat imagery was inconclusive at best.

Many-date change detection

Hope for possible utility came from parallel work conducted by OSU for other parks and for other projects. Rather than map landscape change by comparison of two dates of imagery, OSU developed methods to detect trends across time-series of many years of imagery. A primary benefit of this approach is that year-to-year changes caused by phenology, sun angle, or ephemeral weather events can fade to noise around longer-term trends. Also, change is defined for each pixel relative to its own spectral trajectory, not relative to other pixels. In theory, the influence of cross-pixel variation in soil brightness would become less of an impediment than for more traditional methods. Additionally, the availability of stacks of imagery allows for more robust interpretation of the satellite imagery itself for validation using tools developed in-house at OSU (known as "TimeSync"). If these interpretation tools were applicable in the CP, many of the potential problems with reference data could potentially be avoided. Because of these potential advantages, a small pilot project was funded under a new agreement between OSU and the N&SCPN to investigate the potential utility of the new method (termed "LandTrendr") in the parks.

Key conclusions from this stage of the project included:

- LandTrendr segmentation captured many of the key disturbance processes of interest, including fire, insect mortality, and apparent drought disturbance, as well as growth/recovery processes
- Change mapping in herbaceous areas would likely require new rules to link spectral change to increase or decrease in cover, but these new rules would likely be generally applicable once found
- Linking POM labeling to LandTrendr was technically successful, resulting in yearly landcover maps with potentially large information content.
- However, POM labeling required aggregation of classes that altered the detailed class labels

- Additionally, the spectral conditions present directly after a change result in labels that often do make ecological sense; true labeling will require significant effort to develop post-disturbance spectral class labels that are different from those applicable to the rest of the landscape
- TimeSync interpretation was much more challenging in the non-forest and non-woodland areas of the CP than expected, suggesting that this validation approach is still not sufficient to replace inadequate reference data from existing sources.

At a teleconference in August 2009, OSU and the CP networks made progress toward evaluating which of the methods may be useful for actual implementation in the parks of the CP. The LandTrendr change maps appear to be the best balance of cost and utility, and the POM approaches (with two-date and LandTrendr + POM) are likely too costly to justify the further research needed to fully understand and implement them.

Report organization

There are three chapters and one large appendix in this document.

Chapter 1 summarizes research conducted under a multiyear agreement between Oregon State University (OSU) and the parks of the Northern and Southern Colorado Plateau Networks (N&SCPN) to investigate the potential of Landsat satellite imagery for mapping baseline conditions and for detection of landscape change. This chapter is a distilled version of a longer, more detailed report that was provided to the parks earlier. Appendix 1 is the original full report.

Chapter 2 reports on research carried out under a separate, shorter-term agreement between the same parties, with the goal of testing whether a newer approach to mapping change with many years of Landsat imagery may overcome challenges revealed in work conducted in the first project.

Chapter 3 looks ahead to suggest which components of Landsat-based monitoring may be feasible and useful for the parks of the N&SCPN.

Landsat-based monitoring in the parks of the Northern and Southern Colorado Plateau Networks

Chapter 1: Summary of report on initial pilot studies

DRAFT

Contents

	Page
1. Introduction	3
1.1 Characterizing NPS indicators using remote sensing	3
1.2 Dataset review, literature review, and study plan	5
2. Methods	7
2.1 Pilot study sites and data	7
2.2 Image preprocessing	7
2.3 Baseline mapping	7
2.3.1 Baseline mapping with continuous variables	7
2.3.2 Baseline mapping with thematic labels	7
2.4 Change detection methods	8
3. Results	10
3.1 Baseline mapping	10
3.1.1 Mesa Verde National Park	10
3.1.2 Canyonlands National Park	12
3.1.3 Zion National Park	14
3.1.2 Wupatki National Monument	17
3.2 Change detection	18
3.2.1 Mesa Verde National Park	18
3.2.2 Canyonlands National Park	19
3.2.3 Zion National Park	19
3.2.4 Wupatki National Monument	24
4. Summary and Conclusions	26
4.1 Key observations	26
4.1.1 Baseline mapping	26
4.1.2 Vegetation change	27

1. Introduction

National Park Service (NPS) units of the Northern and Southern Colorado Plateau Inventory and Monitoring Networks (NCPN and SCPN, respectively) have complex vegetation patterns that are shaped by natural processes and human management on lands both inside and outside parks. Understanding the combined effects of natural and anthropogenic processes across greater park ecosystems requires monitoring of vegetation and related variables and processes using consistent conceptual approaches across broad geographic areas. For this reason, the Colorado Plateau (CP) networks selected land use/land cover, landscape vegetation pattern or landscape structure, land or vegetation condition, and disturbance patterns as core vital signs to monitor.

Four landscape indicators associated with the vital signs were identified (Table 1). As monitoring these indicators requires consistent measurement across large areas over time, remote sensing was identified as a promising tool. CP network personnel collaborated with Oregon State University and the US Forest Service (collectively referred to here as OSU) to develop a project to study the potential role of remote sensing in monitoring, and to write protocols that incorporate the most successful approaches to remote-sensing based monitoring.

The project was initially divided into three subtasks: study plan development (which included dataset and literature reviews), pilot studies, and protocol development. The initial study plan was submitted and approved separately, and the initial pilot studies ensued. After completion of the initial pilot studies, which yielded less than satisfactory results, a new set of pilot studies was developed and executed that included testing of additional methods. The second set of pilot studies (referred to here as LandTrendr-POM) is reported in chapter 2, and the final protocols follow from those studies. In this report, we provide a summary of the initial pilot studies, including motivation for these and for the subsequent studies. For greater detail, see the full initial pilot studies report (Appendix 1).

1.1 Characterizing NPS indicators using remote sensing

Several indicators in Table 1 can not be directly mapped with remotely-sensed data, but are landscape indicators with levels of abstraction one or more steps removed from remote sensing data (Figure 1). Products from the bottom two layers of what we refer to as the “remote sensing layer cake” are not of direct interest to the parks, but are the foundations upon which the desired indicators must be based. These include the raw electromagnetic energy measured by a sensor and the clean imagery that has received a variety of pre-processing procedures.

Landsat-based monitoring in the parks of the Colorado Plateau

Table 1. Initial estimated desired resolutions for four landscape indicators and associated changes to be monitored with remotely sensed data in the NPS Northern and Southern Colorado Plateau Inventory and Monitoring Network parks.

Vital Sign	Landscape Indicator	Changes/ Features to Monitor	Thematic Resolution	Spatial Resolution	Temporal Resolution
Land use /Land cover (LULC)	Land use/Land cover (LULC)	Type conversions Boundary changes	Anderson Level II or equivalent	2-5m at small parks 30m at medium and large parks	every 5 years
Landscape vegetation pattern	Vegetation pattern	Type conversions Boundary changes	NVCS ¹ formation level or NatureServe ecosystem level	2-5 m at medium parks 30m at large parks	every 5 years
Vegetation or Land condition	Vegetation condition (ground cover and/or bare ground ² , and age class distribution ³)	Changes to ground cover; Changes in age class distributions for wooded systems	Continuous data set layer Continuous data set layer for wooded systems (detect changes at alliance level)	2-5m at small parks 30m at medium and large parks	every 5 years
Disturbance patterns	Disturbance patterns	Type, extent, and severity of major disturbances	Data set layer	30m for medium and large parks	Annual trends

¹ National Vegetation Classification System (Federal Geographic Data Committee, FGDC).

² Monitoring modifications to cover for selected ecosystems.

³ Example: where and how much of a park's forest is young, middle-aged, or old-growth? Monitoring this indicator may only be possible for selected ecosystems

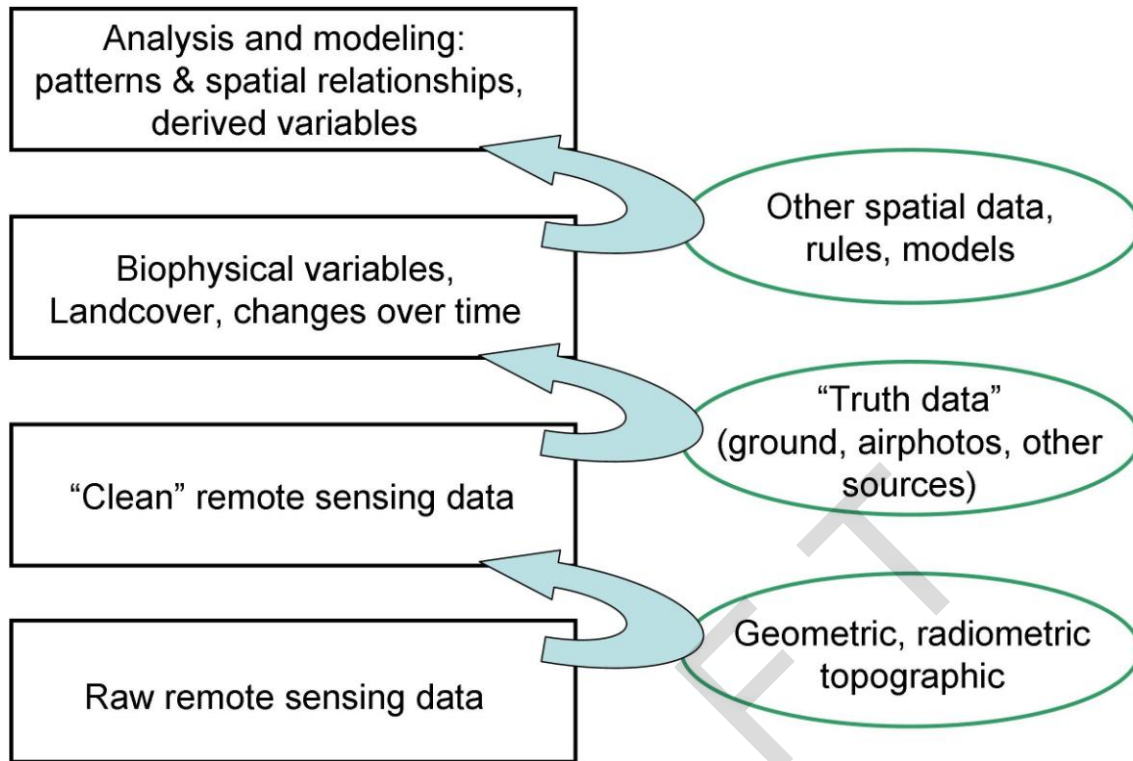


Figure 1. The "layer cake" of remote sensing. Although the information in the top two layers is ultimately of interest in ecological monitoring, its effective development depends on a good foundation in the lower two layers, which are the realm of remote sensing science and the focus of much of the work in the pilot studies.

Several of the indicators desired by the parks are found only in the top two layers of the layer-cake. Basic biophysical variables and related ecological and change data layers are transformed from the clean imagery, but rely on models and the availability of high quality ancillary data. This layer is still within the realm of remote sensing, but represents an end point for the remote sensing analysis. The top level is more in the realm of landscape ecology rather than remote sensing. Land-use labeling is an example of this level of analysis; in that cover types derived from the third layer are labeled according to spatial context and expert understanding of the system. An extensive area of the grass cover type, for example, might be labeled differently if its spatial context were a city rather than an agricultural valley. Similarly, an analysis of spatial patterns (e.g., patch analysis) might use land cover types as an input variable, and then apply various spatial distance rules to characterize patterns of cover types over a large area. Similarly, ascribing a disturbance agent might involve expert visual interpretation or assignment based on explicit rules that include consideration of the shape of the disturbance, the land cover type in which it occurred, and its position on the landscape. The top layer of the remote sensing layer cake was beyond the scope of work for these pilot studies.

1.2 Dataset review, literature review, and study plan

The dataset review revealed useful sources of data and other resources around which pilot studies were designed. To assess what reference data were available at the park and network levels, the OSU collaborators made direct visits to individual parks, data managers, GIS coordinators, and other interested or helpful contacts. Special efforts were made to locate and assess the quality and

Landsat-based monitoring in the parks of the Colorado Plateau

usefulness of historical field data and airphotos. The cost of acquiring supplemental data was also investigated. One of the most important existing reference datasets was the NPS Vegetation Mapping product (NPSVM). The detailed NPSVM maps have thematic resolution and precision greater than what may be accomplished through satellite-based remote sensing, and thus could not be used in their most detailed form. Because of their potential value, however, we spent significant effort developing methods to incorporate the field and airphoto data and the map products from the NPSVM into the pilot studies.

Given costs associated with acquisitions of satellite remotely sensed data, and the needs of large amounts of remote sensing data over time for monitoring across the CP parks, it was decided that Landsat and MODIS data were the most economical satellite remote sensing data for broad usage. MODIS data was the focus of other pilot studies; thus, the pilot studies outlined in our study plan focused on use of Landsat data for mapping and monitoring.

The literature review concentrated on uses of Landsat data for mapping in arid and semi-arid systems. An important highlight from the literature review was the fact that soil signatures dominate spectral response in arid and semi-arid systems. This is a problem that is pervasive in the literature and suggests that the capability for detailed vegetation mapping using satellite sensors in such systems is limited.

Another highlight from the literature was that there are two basic approaches for mapping vegetation: thematic and continuous-variable approaches. Thematic labeling results in a familiar vegetative type or land cover type map, with a handful of discrete land cover classes. The number of classes distinguishable with satellite remote sensing data is generally much smaller than the number that could be achieved with on-the-ground or even airphoto-based measurement, but can be done more consistently and quickly across large areas. Continuous-variable approaches attempt to describe the landscape in terms of proportional representation of different cover types within image pixels.

The appropriateness of reference data used to characterize the land surface was also highlighted as an important consideration when mapping with satellite data. Appropriateness is a function of both the type of measurements recorded on the ground and the spatial and temporal precision and representativeness of those data. All of these concepts apply equally to mapping of land cover at a single point in time and at multiple points in time. Detecting change over time adds constraints to the reference data, as the ideal reference must be representative and consistent for multiple measurement occasions over time.

The study plan set up specific pilot studies whose goals were to test the different means of preprocessing Landsat satellite imagery, linking with reference data, and analyzing relationships in support of the goals in Table 1. The focus was on the use of existing, reliable methods, applying or modifying them as necessary for the specific situation encountered in the CP ecosystems. These were developed and tested in park-based pilot studies involving four CP parks. A 2-tiered approach involving baseline mapping and change detection was used in conducting the pilot study. Initial efforts were focused on baseline mapping of Mesa Verde National Park (MEVE), CO and Canyonlands National Park (CANY), UT. Change detection was the focus for Wupatki National Monument (WUPA), AZ and Zion National Park (ZION), UT.

2. Methods

2.1 Pilot study sites and data

For MEVE and CANY, NPS vegetation maps (NPSVM) were not available for this study. For MEVE, 147 plots to be used in making the map were available and examined here. For CANY, 913 plots were available for analysis. The NPSVM for ZION and WUPA were available for use in this study. Additionally, at ZION there were 1:12,000 and 1:40,000 true color photos, and at WUPA there were 1:12000 1996 color-IR photos.

The dates of Landsat imagery used in this study were selected to match field plot data, map data, and/or airphoto data, as appropriate. The specific dates chosen were a balance between best match of dates and cost and availability. To the extent possible, for change detection the additional dates of imagery were chosen to match the initial dates.

2.2 Image preprocessing

All the images used were preprocessed according to current best practices in remote sensing. This included orthorectification, atmospheric correction, and radiometric normalization.

2.3 Baseline mapping

We investigated approaches to developing and/or geospatially extending baseline maps of land cover. There were two general approaches for creating baseline maps: continuous variable mapping and thematic mapping. Significant effort was initially placed on exploring both approaches to baseline mapping at MEVE and CANY, with a thorough investigation of the utility of using reference plot data from the NPSVM project. Initially, similar efforts were to be carried out at two additional parks (WUPA and ZION), but the NPSVM plot data proved to be less robust for our purposes than we had hoped. Plot data were used at CANY for both continuous and thematic mapping, but only for thematic mapping at MEVE. At MEVE, we undertook a small new study to understand whether newly interpreted airphoto data could be used in place of the NPSVM data for continuous-variable mapping. While we showed that such airphoto-based interpretation could be effectively used for mapping of some cover types, the time involved in airphoto interpretation prevented us from replicating that effort at other parks. For the WUPA and ZION studies, we focused all efforts on change detection approaches.

2.3.1 Baseline mapping with continuous variables

There are many approaches for continuous estimation of biophysical features. All methods attempt to derive a mathematical relationship between a variable of interest (e.g., percent vegetative cover) and spectral data from satellite imagery. Here, we sought methods that could be readily applied to different parks and to different date of images. This criterion places more weight on simple, robust methods than on nuanced, more complex methods that require significant site-specific tuning.

2.3.2 Baseline mapping with thematic labels

Where continuous-variable approaches essentially seek gradients in spectral space that correspond to gradients in features on the ground, thematic methods seek discrete regions in spectral space that correspond to discrete cover types on the ground. For thematic mapping, a reliable thematic system with the appropriate thematic resolution is needed for successful thematic mapping, using either supervised or unsupervised classification. For the parks involved in this pilot study, some have a complete vegetation map, while others only have field plot data.

Accordingly, different methods were applied to the different parks for evaluating effective methods for thematic mapping.

2.4 Change detection methods

As with baseline mapping, changes over time can be described using either continuous variables or categorical labels. In parks where continuous-variable modeling was conducted, change was inferred by subtracting the continuous-variable estimates at different times. In cases where there was a complete NPSVM, the vegetation map was used as the training data in a modified probability-of-membership (POM) change detection approach (Figure 2).

With traditional clustering, the tasseled cap spectral space of a selected Landsat image would be partitioned into spectrally separable clusters by unsupervised classification. Because of sparse vegetation cover in most of the CP parks, most variation in spectral space was associated with variation in soil brightness, which expresses as variation in a single index – tasseled-cap brightness. Because unsupervised classification methods partition spectral space according to minimization of variance within clusters, these methods tend to partition the spectral space along the brightness. Very little variation in vegetative cover is captured if traditional unsupervised classification of unaltered spectral space is attempted. Because many of the important monitoring goals of the CP parks involve vegetation, clustering should better capture the range of vegetative type and cover. Therefore, it is preferable to have spectral clusters occupy the full spectral space. This is the basis for POM, which is based on a combination of unsupervised and supervised classification, and designed to fully populate a selected spectral space (i.e. tasseled cap) with spectral classes.

A first step used in the application of POM was to standardize the tasseled cap spectral space. Standardization minimized the dominance of soil brightness, by normalizing the data such that all three tasseled cap spectral axes (brightness, greenness, and wetness) were given equal weight in the unsupervised classification. The standardization was performed on the selected base image, and then unsupervised classification (using a standard k-means algorithm) was used to partition the standardized spectral space of that base image into 50 spectral clusters.

Landsat-based monitoring in the parks of the Colorado Plateau

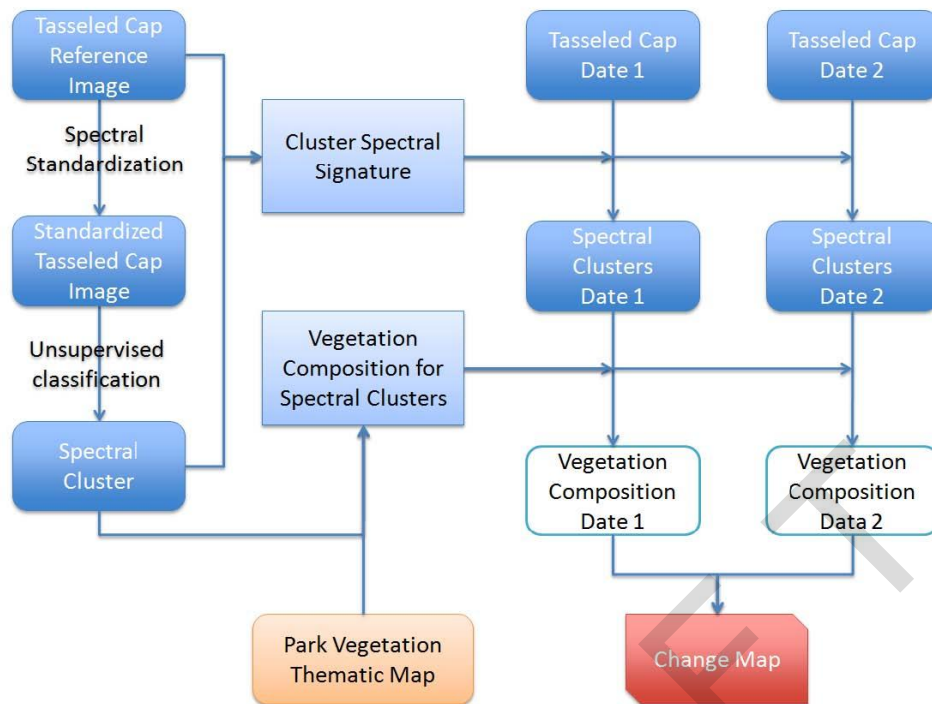


Figure 2. A diagram of POM thematic change detection approach. The spectral space of a reference image near in time to the date of the park vegetation thematic map is clustered using unsupervised methods (left-hand column). The spectral clusters (next column to the right) are described as proportions of park vegetation thematic categories, and also used to derive maps of spectral clusters from any date 1 and any date 2 of the tasseled-cap imagery (right-hand columns). The thematic descriptions of these clusters are then applied to the maps of spectral clusters to create maps of vegetation composition at both dates (lower right boxes), which are finally compared to create change maps.

The spectral clusters emerging from the unsupervised classification were used in two ways (Figure 2). First, the means and covariance matrices associated with the pixels in each cluster are used to define the shape of each cluster in spectral space. This is the typical approach for describing classes, and is equivalent to the approach used in maximum likelihood classification and the original POM approach developed for the NCCN protocols. These means and covariances can then be used in a supervised classification approach to create multi-layer probability of membership images that define for each pixel its probability of belonging to each of the 50 original unsupervised classes. At this point, the 50 classes have no meaning that can be attached to cover type on the ground. Thus, the second use of the clusters is to link them with the park vegetation thematic map. To characterize or assign meaningful labels to these spectral clusters, the existing vegetation map was used to characterize the vegetation composition of each of the spectral clusters derived from the baseline image, resulting in a matrix showing the vegetation composition (as defined by the park vegetation map) of each of the spectral clusters (derived for the 50 spectral clusters). The derived vegetation map (based on NPSVM) can be used further for change detection using either a direct map contrast method or a continuous-variable approach similar to that of the POM approach previously developed for NCCN.

3. Results

3.1 Baseline mapping

3.1.1 Mesa Verde National Park

For baseline mapping, the field data were problematic for several reasons. They were all smaller than a single Landsat pixel, which required extremely high GPS accuracy. Even with accurate GPS positioning, misregistration in the Landsat imagery resulted in the pixels being offset from their true locations on the ground. Because of high spatial frequency in local vegetation composition and density, the combined effect was to link spectral data to wrong mix of vegetation cover, weakening or invalidating statistical relationships required for mapping. In addition, other problems with the field data minimized their value for linkage with Landsat data. The spectral variability across the park was not adequately sampled, and thus full representation of the vegetation conditions was lacking. Some plots were in topographic shadows and were best excluded from statistical relationships.

Continuous modeling

For baseline mapping with continuous models, in addition to the problems described above, the field data were broadly categorical. This greatly limited their utility for deriving continuous estimates.

Given these problems with the NPVS field data for continuous cover modeling, we photo-interpreted 143 1-ha plots (Figure 3) almost exclusively within the park boundary using air photos from 2003 and 2004. Cover proportions of needleleaf, broadleaf, herbaceous, and open were interpreted following standard approaches for airphoto interpretation; no other detail could be reliably interpreted.

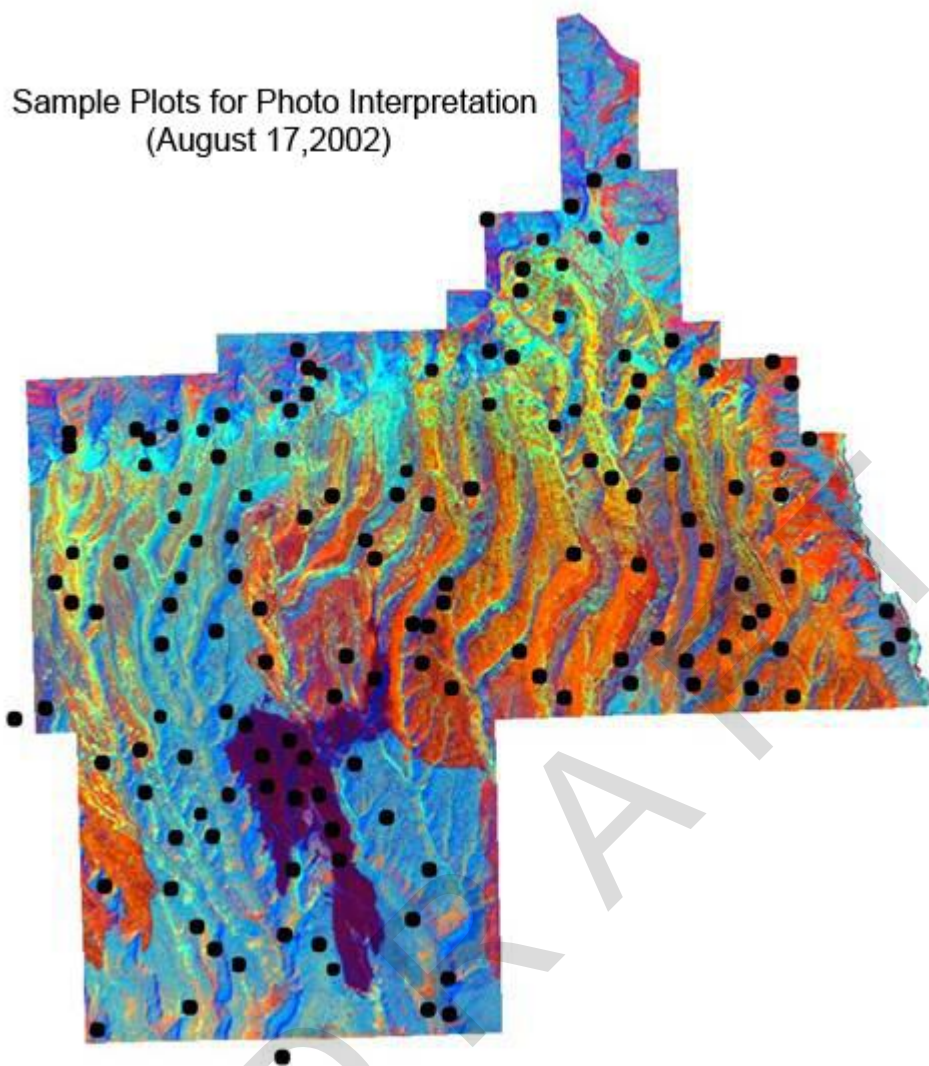


Figure 3. Sample plots for photo interpretation at MEVE, overlaid on a tasseled cap, false-color Landsat TM image.

Various mixtures of photo-interpreted vegetation components (needleleaf, broadleaf, herbaceous, open) were related to spectral data to determine which could be most accurately modeled: the individual vegetation components, woody vegetation (needleleaf + broadleaf), and all vegetation (woody + herbaceous). The spectral data considered were the Landsat bands and several spectral vegetation indices, including tasseled cap indices (brightness, greenness, and wetness), NDVI, SAVI, NDMI, and Angle (a new tasseled cap index).

Among the vegetation components examined, only woody vegetation cover exhibited a good relationship with spectral indices. The index having the lowest prediction error was Angle (Figure 4), followed by NDVI and wetness. The non-linear Angle model had an R-squared of 0.84 and the cross-validation RMSE was 11.4%.

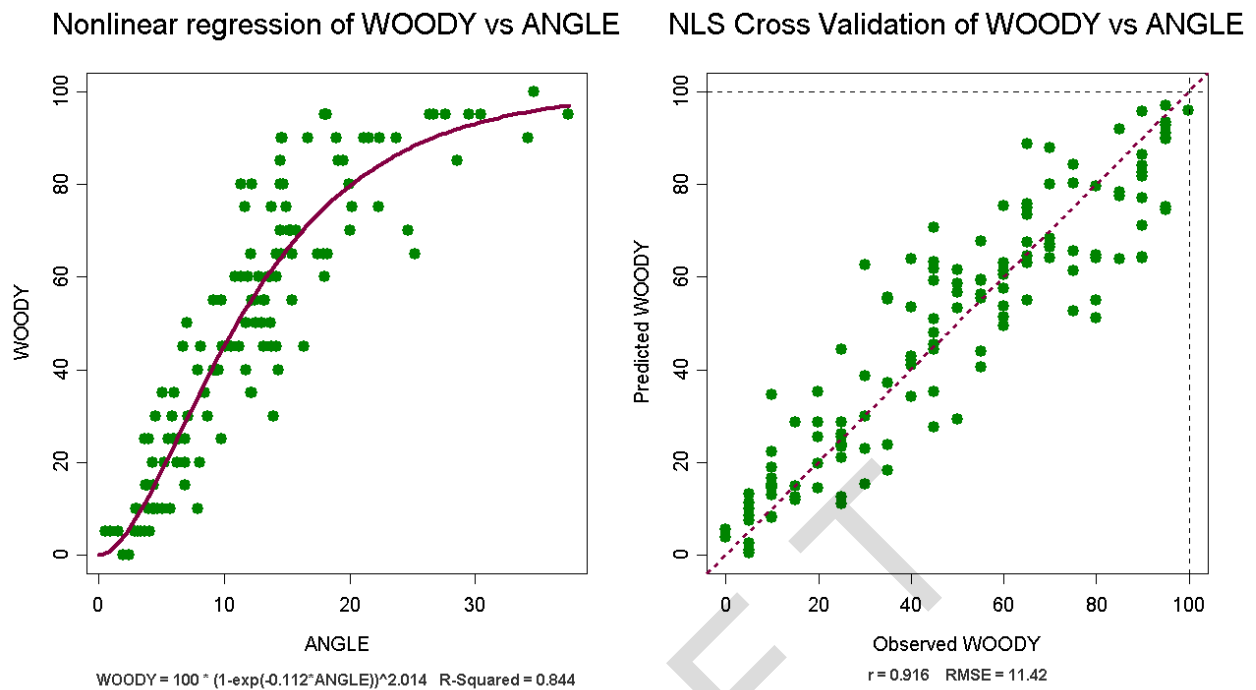


Figure 4. The model for woody cover based on Angle (left) and the cross-validation results (right).

Thematic classification

Without a vegetation map of the park, we had no choice but to use the NPSVM field data to derive thematic classifications at MEVE. There were too many basic classes for Landsat mapping; thus, we examined aggregated classes, including association name, physiognomy, and leaf phenology. To determine which level of aggregation could be mapped with any degree of accuracy we examined inter-class maximum likelihood spectral separability. One immediate problem for classification was the lack of sufficient plot data to represent each of the various classes in class schemes under consideration. For example, there were 29 association classes and only 102 usable NPSVM plots. Of the eight leaf-phenology classes, only two classes had more than 8 samples. For physiognomic class, less than half of the classes had enough plots to derive meaningful statistics. As a result, we could not sufficiently evaluate the degree to which standard thematic classification is a viable alternative for mapping vegetation cover at MEVE.

3.1.2 Canyonlands National Park

As no NPSVM map was available for the park, we focused on making use of the field plot data for baseline mapping. Many of the same challenges with field plots observed at MEVE existed at CANY. Shape and size of field plots varied (circular, rectangular, square), and all plots were less than one Landsat pixel in area. Similarly, we found that many plots were (1) not representative of local conditions or in mixed conditions (Figure 5, left); (2) in topographic shadow (Figure 5, right); or (3) geographically misregistered. To minimize these concerns, we visually screened all plots and retained only those that were square or circular and not in shadow. A total of 712 plots remained.

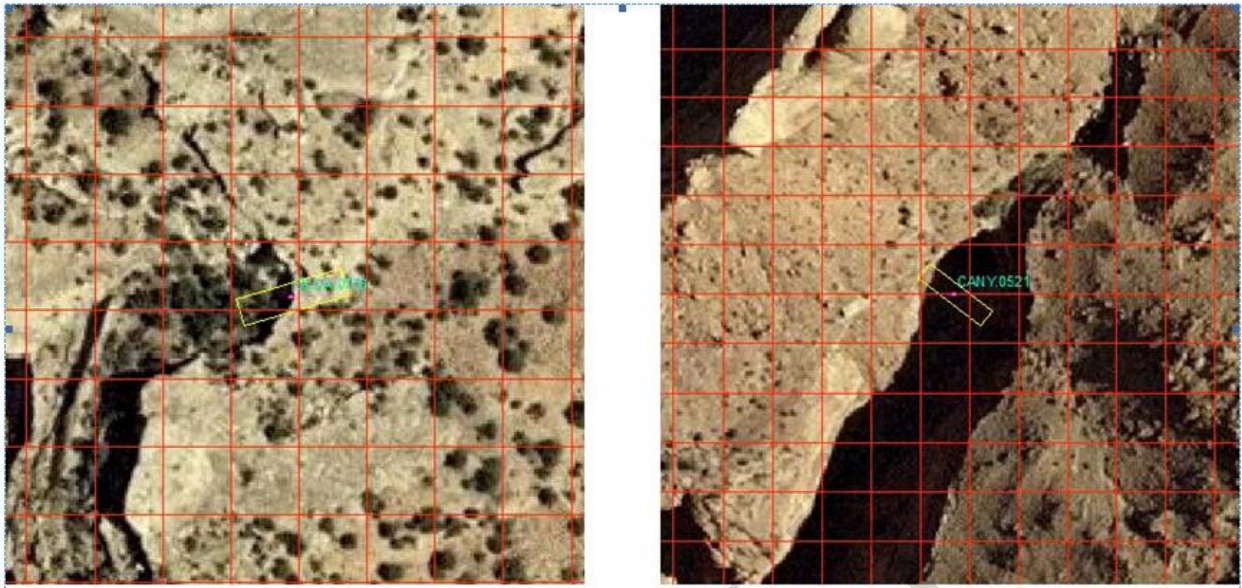


Figure 5. left: non-representative plot; right: shadow

Continuous modeling

Although CANY field survey data recorded cover information in categories, in contrast to MEVE, the resolution of these cover categories was sufficient for continuous modeling. Field plot records contained cover estimates for emergent tree, canopy, subcanopy, tall shrub, shrub, dwarf shrub, herb (graminoid, forb, fern, and seedling), nonvascular, vine, and epiphyte. Based on these data, five summary vegetation variables were created:

Tree = emergent + canopy + subcanopy
Shrub = tall shrub + shrub + dwarf shrub
Herb = graminoid + forb + fern
Woody = tree + shrub
AllVeg = tree + shrub + herb

Exploratory analysis between the five summary vegetation variables and the spectral indices was done using scatterplots. Similar to the MEVE results, woody cover was the only cover attribute with a reasonable relationship to spectral data, and thus was the only one examined further. Relationships of woody vegetation with NDVI, and the tasseled cap brightness, greenness, wetness and angle were evaluated.

All vegetation indices, and several when used in combination, yielded similar results. As shown in Figure 6, R-square values were low (~0.30). However, as with MEVE, RMSEs of predictions from cross-validation were around 10%. This indicates that prediction strengths for woody cover at each park were nearly equal, but because of the low range of cover percent at CANY, the cover model does not have much utility, as indicated by the low R-square.

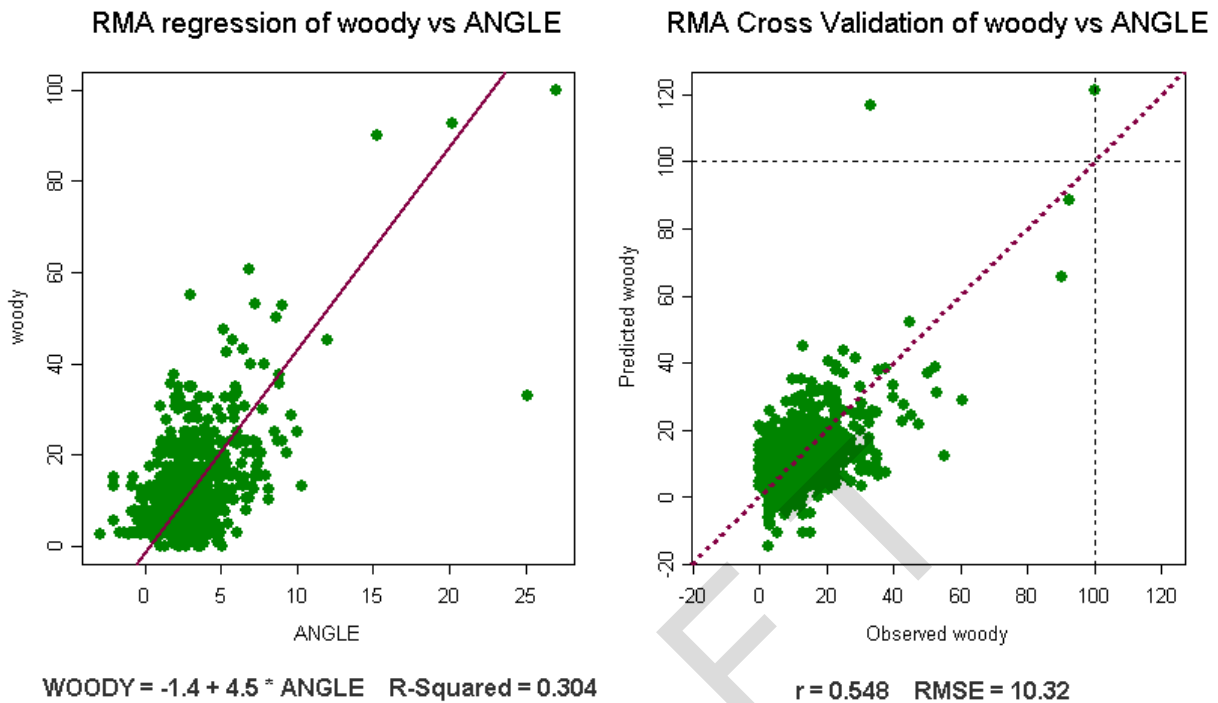


Figure 6. Woody cover model with angle index.

3.1.2.1 Thematic mapping

There were no promising results for thematic mapping from CANY.

3.1.3 Zion National Park

The ZION NPSVM project collected data from 346 field plots. These plots were a mixture of circular (11.3m radius), square (20m), and rectangular (40m x 10m or 40m x 20m) shapes, and all of the same problems/caveats associated with field plot data at MEVE and CANY existed here also. There was also an NPSVM available for use.

3.1.3.1 Continuous modeling

For continuous modeling, the field data had an additional problem not encountered at MEVE or CANY. Here, cover for vegetation strata was estimated in 10% intervals for each stratum, including Emergent, Canopy, Sub-canopy, Tall Shrub (>2m), Short Shrub (<2m), Dwarf-shrub (<0.5m), and Herbaceous. When added together, numerous plots had over 100% total cover, indicating an obvious overlap in cover among the various layers. We examined various relationships with spectral data for a number of combinations of the basic cover variables, as for MEVE and CANY, but no relationships were good enough to use in mapping.

3.1.3.2 Thematic mapping

At ZION there was a completed NPSVM available. The map was used to derive statistical relationships between classes of interest and spectral vegetation indices. We did this for the 76 classes in the basic map, and for aggregated classes, including vegetation association,

physiognomy, and ecological group. For each level of aggregation, we examined the spectral separability of Landsat data within the pixels associated with that group.

Among the 76 basic classes, only 19 were present across more than 1% of the map, the most abundant being *Pinus-Juniperus* Woodland Complex (22%), followed by Navajo Formation (10%), *Pinus ponderosa* / *Arctostaphylos patula* Woodland (8%), *Quercus gambelii* Shrubland Alliance (7%), *Pinus-Juniperus/Quercus gambelii* (6%), and *Pinus ponderosa/Quercus gambelii* Woodland (5%). For the 19 classes, a confusion matrix revealed an overall accuracy of 24%, with very high commission error and omission rates. Similarly, results for physiognomic classes the results were poor.

There was poor spectral separability among the full set of NPSVM association classes. However, via exploratory analysis, we determined that spectral separability was good for some aggregation of the association classes (Figure 7). Overall accuracy for this classification was above 80%, as were the accuracies of most of the individual classes.

DRAFT

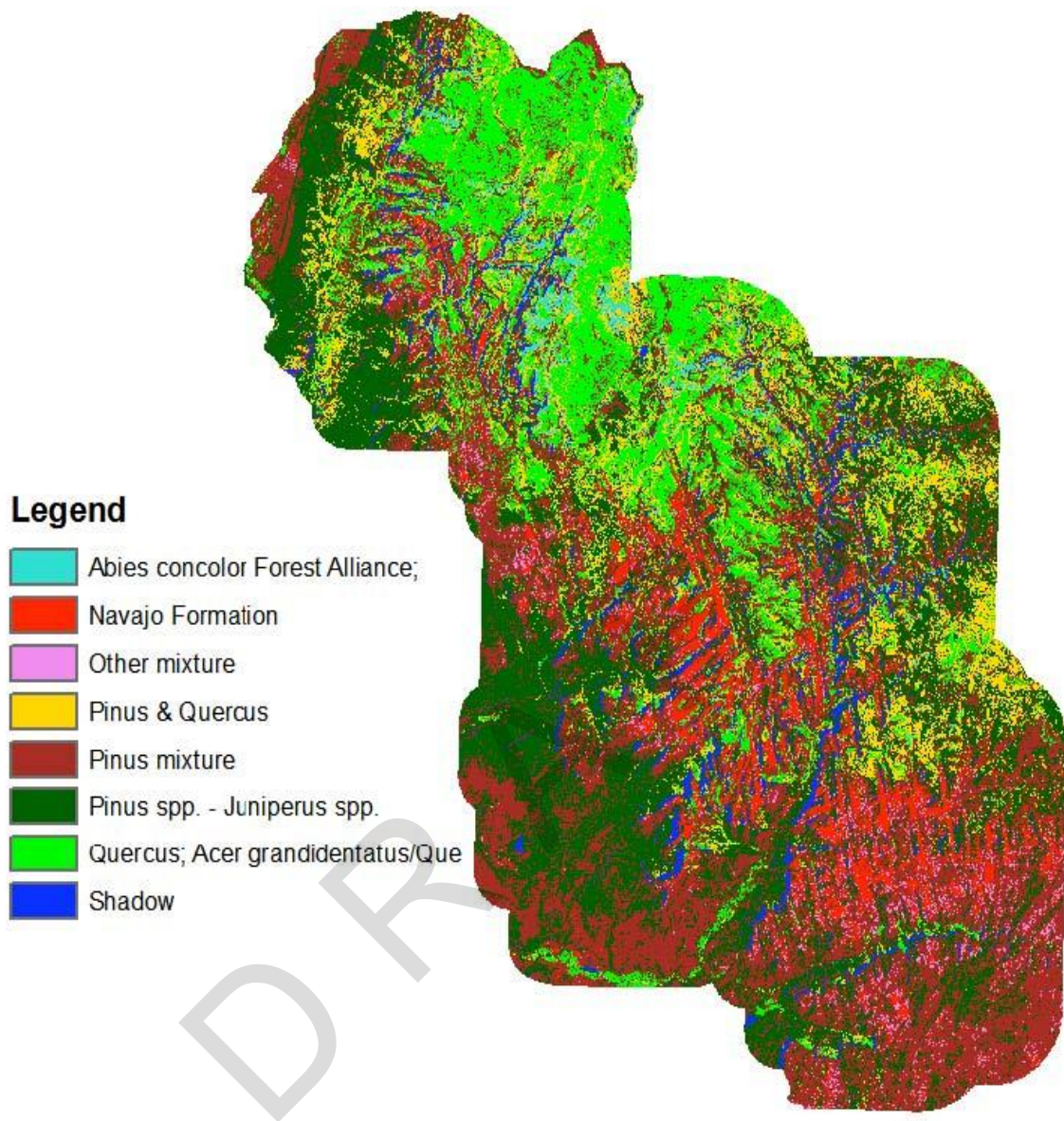


Figure 7. ZION vegetation classification based on aggregated NPSVM vegetation associations.

We also aggregated several of the NPSVM ecology classes into broader groups, after determining that the basic groups were not spectrally separable (Figure 8). For this aggregated set of classes, there was a 78% overall accuracy, with most classes having above 70% accuracy.

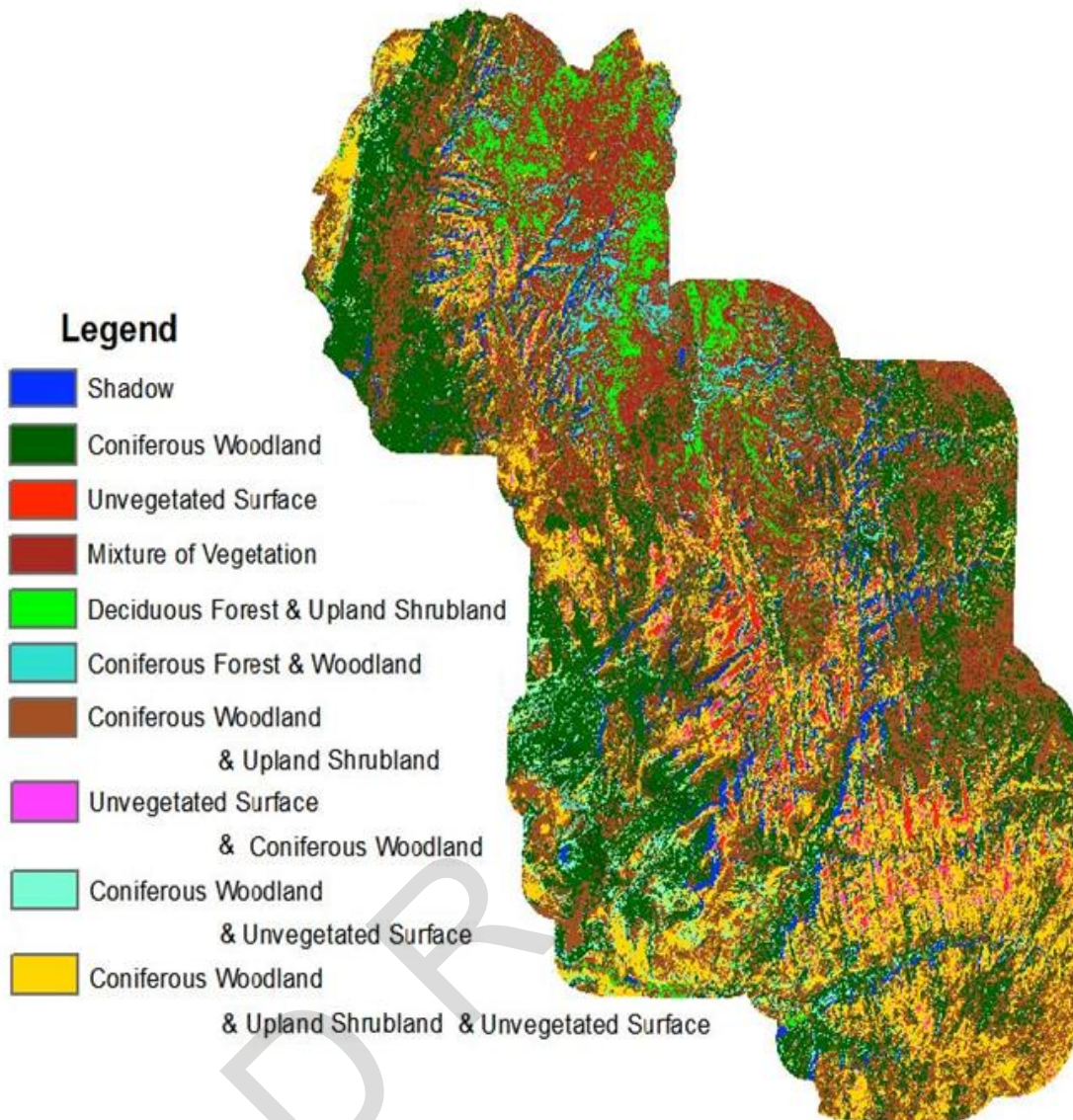


Figure 8. Map of ZION based on ecological groupings.

3.1.2 Wupatki National Monument

Minimum effort was devoted to baseline mapping for WUPA because the project's focus had shifted to change mapping.

3.2 Change detection

3.2.1 Mesa Verde National Park

The woody vegetation cover model using tasseled cap angle (described earlier) was applied to selected images from 1999 to 2002 (Figure 9). Using these results, changes in woody vegetation between selected dates was directly calculated by subtraction, with changes occurring across the full range from -100% to +100% vegetation change (Figure 10). This approach produces visually-realistic maps of change that are expressed in units that have meaning to the user on the ground, but caution should be used in interpreting these as no reference data were available to conduct an accuracy assessment.

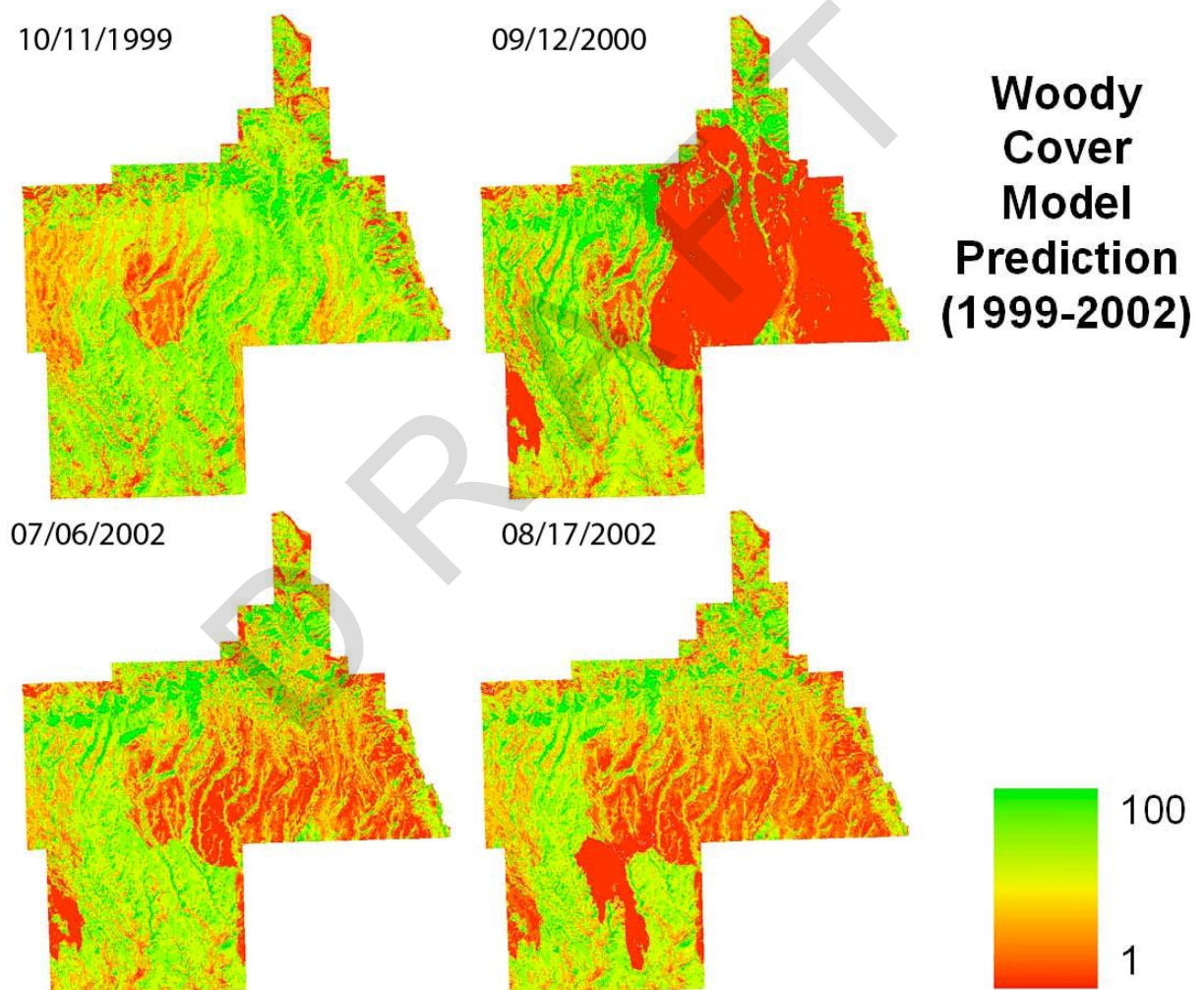


Figure 9. Woody vegetation cover modeled with angle at MEVE from 1999 to 2002.

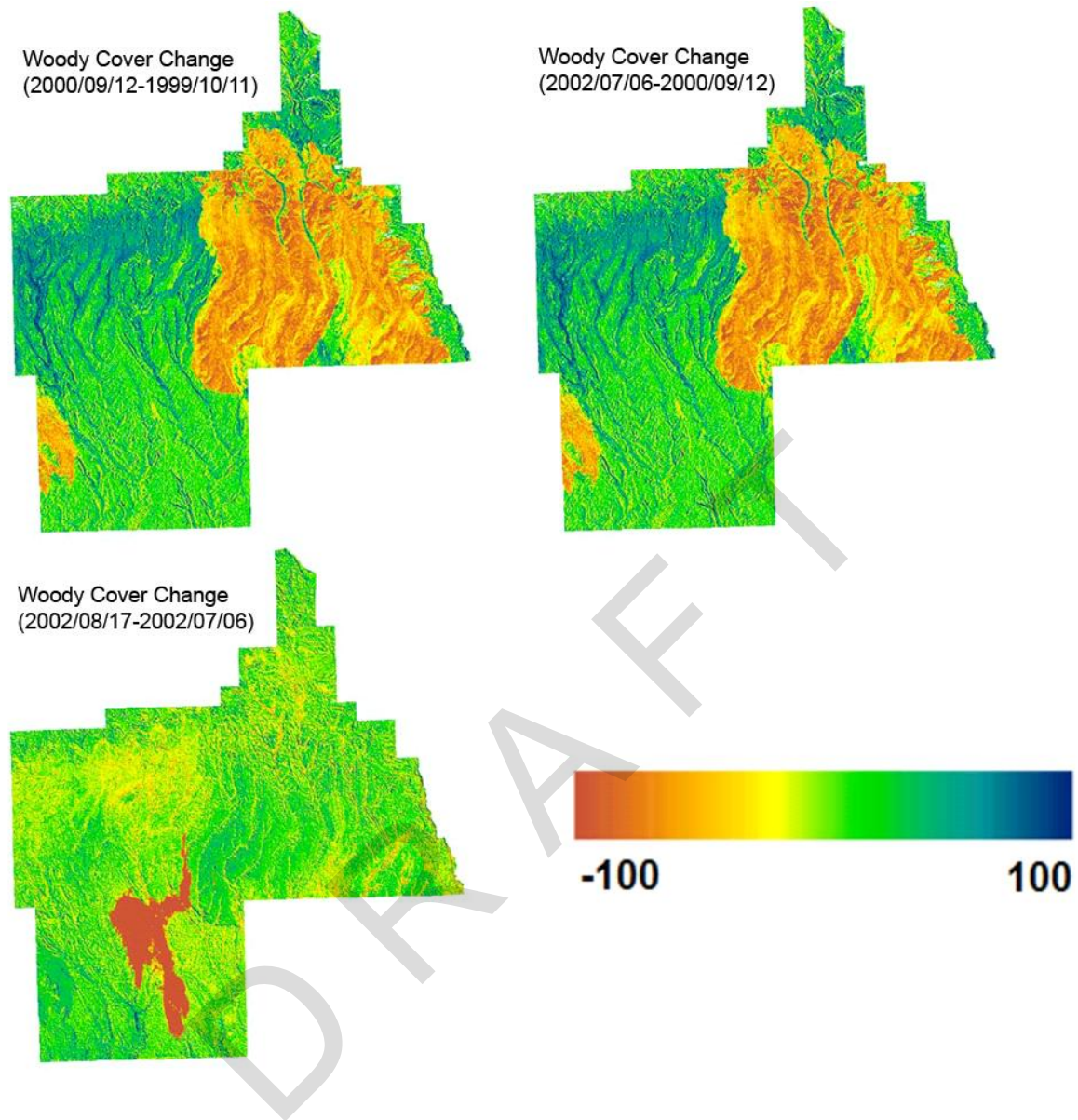


Figure 10. Woody cover change for MEVE

3.2.2 Canyonlands National Park

No change detection analyses were conducted for CANY.

3.2.3 Zion National Park

The modified NCCN POM method depicted in Figure 2 was applied to ZION. Because of high terrain variability, the park was divided into NW and SE facing slopes. Instead of taking the NPSVM vegetation classes directly from the vegetation map, we evaluated different aggregation methods. For each of the polygons defined in the vegetation map, we relabeled it as one of a new set of 19 POM vegetation classes (Table 2), which was based on physiognomic, ecology, and cover information for each polygon. The polygon map was then rasterized with a unique identifier assigned to each of these 19 POM groups. To match the resolution of Landsat image, the resolution of the rasterized image was set to 30m.

Landsat-based monitoring in the parks of the Colorado Plateau

Table 2. NPSVM aggregated POM vegetation classes used for change detection at ZION.

Class	Name
1	Barren
2	Deciduous Forest
3	Herbaceous Vegetation
4	Open Shrubland
5	Closed Gambel Oak
6	Semi-closed Gambel Oak
7	Other Shrubland
8	Open Coniferous Forest
9	Closed Coniferous Forest
10	Semi-open Coniferous Forest
11	Closed Coniferous Woodland
12	Coniferous Woodland Mixed Shrub
13	Gambel Oak mixed Coniferous Woodland
14	Open Coniferous Woodland
15	Water
16	Floodplain Woodland
17	Land Use
18	Streams
19	Agriculture

Separately, unsupervised k-means classification was used to partition the standardized tasseled cap space into 50 POM spectral clusters each for SW and NE aspects of ZION. Spectral signatures for the spectral clusters defined in standardized spectral space were derived and used for supervised classification for the other image dates (1999 and 2006 Landsat images). The relative likelihood of each POM vegetation class intersecting with each POM spectral class was calculated (Table 3).

Landsat-based monitoring in the parks of the Colorado Plateau

Table 3. Relative likelihood of each POM vegetation class being a member of each POM spectral class.

PHYS_CLASS_NAME	Barren	Herbaceous		Open Shrubland	Closed Gambel Oak	Semi-closed Gambel Oak	Other Shrubland	Open Coniferous	Closed Coniferous	Semi-open Coniferous	Closed Coniferous Woodland	Coniferous Woodland Mixed Shrub	Oak mixed Coniferous Woodland	Open Coniferous Woodland	Floodplain Woodland	Water	Land Use	Streams	Agriculture
		Deciduous Forest	Vegetation																
Phys_class_1	2383	9	18	643	3	8	371	1	0	2	17	262	40	713	0	2	21	21	129
Phys_class_2	2075	1	2	248	5	2	22	0	0	4	5	97	5	399	0	1	73	4	14
Phys_class_3	2096	13	73	754	10	19	925	0	1	7	41	673	86	1145	0	4	30	38	337
Phys_class_4	1739	5	28	192	0	3	168	0	0	4	5	62	18	211	0	6	10	11	189
Phys_class_5	1916	16	186	948	8	27	1150	3	1	13	44	1313	137	1383	0	6	40	41	576
Phys_class_6	775	91	88	372	41	90	849	7	5	18	95	780	254	1233	0	28	95	47	517
Phys_class_7	2599	3	103	514	8	4	382	3	0	8	26	182	20	781	0	3	169	12	204
Phys_class_8	1969	4	358	1132	12	7	1108	0	2	7	55	483	47	1562	2	20	201	49	888
Phys_class_9	2422	6	93	1010	25	7	2032	0	6	13	157	359	36	1067	3	17	316	62	331
Phys_class_10	1190	36	425	1011	31	54	1869	0	2	13	173	2522	435	1999	0	6	80	55	686
Phys_class_11	1710	3	1457	1951	7	20	2639	2	1	25	48	1589	86	2127	2	27	146	54	1603
Phys_class_12	1077	147	230	640	112	242	1874	7	15	51	449	2232	822	2630	2	74	140	105	658
Phys_class_13	1220	42	427	1274	54	91	2392	5	9	31	412	4145	618	3586	0	64	154	80	1178
Phys_class_14	3021	8	458	1676	17	14	2679	1	10	22	340	1512	42	3109	4	47	439	110	777
Phys_class_15	891	406	345	444	309	547	1949	20	44	75	621	1393	942	1574	5	214	258	171	628
Phys_class_16	1173	51	237	963	111	122	2238	10	11	36	1022	5185	874	3862	3	107	154	123	360
Phys_class_17	2773	15	229	1398	26	32	1960	5	15	34	1237	5260	146	4620	9	95	373	151	179
Phys_class_18	974	134	293	595	321	257	2337	8	51	106	1569	3398	1270	3191	4	239	162	188	155
Phys_class_19	1174	44	162	739	70	105	1761	2	21	43	2739	6965	513	3910	2	144	120	166	36
Phys_class_20	3179	9	75	1070	25	44	907	7	7	35	653	3268	82	2911	2	33	126	62	4
Phys_class_21	3687	16	21	883	37	94	561	7	15	92	1003	2283	117	2177	12	42	14	79	3
Phys_class_22	5179	19	21	690	78	82	708	24	31	167	556	797	244	1337	37	75	7	69	9
Phys_class_23	1419	33	60	790	88	102	1146	14	22	66	4308	7011	395	4266	3	113	69	168	9
Phys_class_24	758	189	307	375	404	387	2367	16	75	123	2588	3562	1139	2933	7	259	95	195	45
Phys_class_25	1114	32	43	471	154	134	964	12	36	86	6239	5159	729	2971	2	99	25	78	5
shadow	0	0	0	0	0	0	0	0	0	0	0	0	0	0	0	0	0	0	0
Phys_class_27	1704	32	19	473	108	114	768	15	39	107	4668	2760	658	2150	3	52	8	58	2
Phys_class_28	711	179	127	284	477	449	1896	22	118	163	3685	3706	1281	2468	5	276	55	161	24
Phys_class_29	719	101	46	189	514	295	1401	32	221	222	5150	3061	1497	1882	3	187	26	109	7
Phys_class_30	580	428	633	245	537	677	1946	28	69	110	784	1166	842	1160	11	268	173	122	171
Phys_class_31	351	818	674	148	551	605	1265	19	68	95	192	217	288	265	7	235	170	94	420
Phys_class_32	385	406	136	157	963	618	1610	24	166	218	3199	1779	1591	1386	3	275	67	114	7
Phys_class_33	410	847	647	764	1046	1076	2796	31	106	164	1476	1181	1117	1114	7	367	116	164	56

*Note: not all the spectral clusters are shown

This process created images of likelihood in terms of selected aggregated vegetation classes. For simplicity the most likely class map is shown in Figure 11. Changes were mapped by comparing the most likely class-images for the two dates (Figure 12). Note that there are situations where the most likely class could be very similar to the second likely class for a given pixel, and that for those situations, it might be useful to examine the second likely class also. As an alternative, a rule can also be defined to name those pixels as a mixture of the different composite classes. Our approach here, for Figure 12, was to apply an additional filter to minimize false change associated with classes that were not spectrally separable. The change map in Figure 12 describes change on the landscape using the spectral data, but transformed those data into land cover labels that have meaning to the park. This is the essence of POM change detection.

Landsat-based monitoring in the parks of the Colorado Plateau

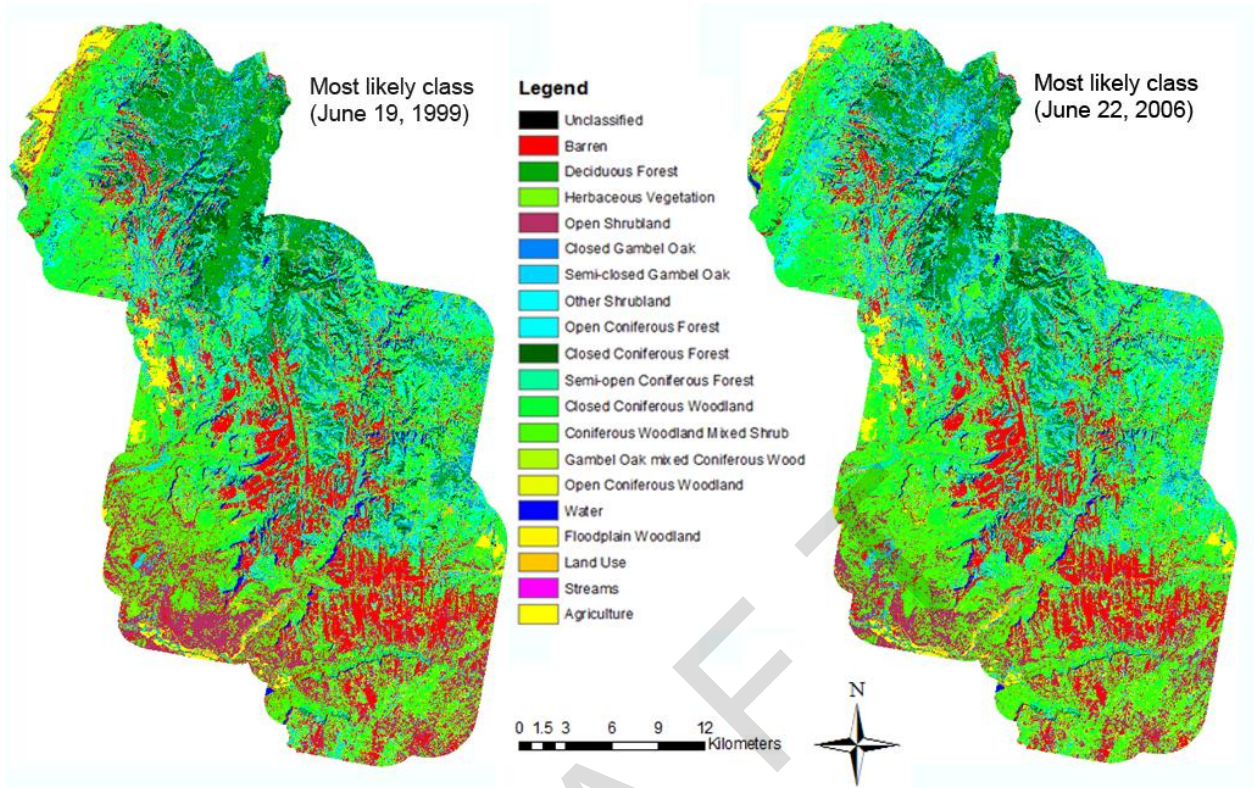


Figure 11. Most likely POM vegetation classes for ZION for 1999 and 2006.

Landsat-based monitoring in the parks of the Colorado Plateau

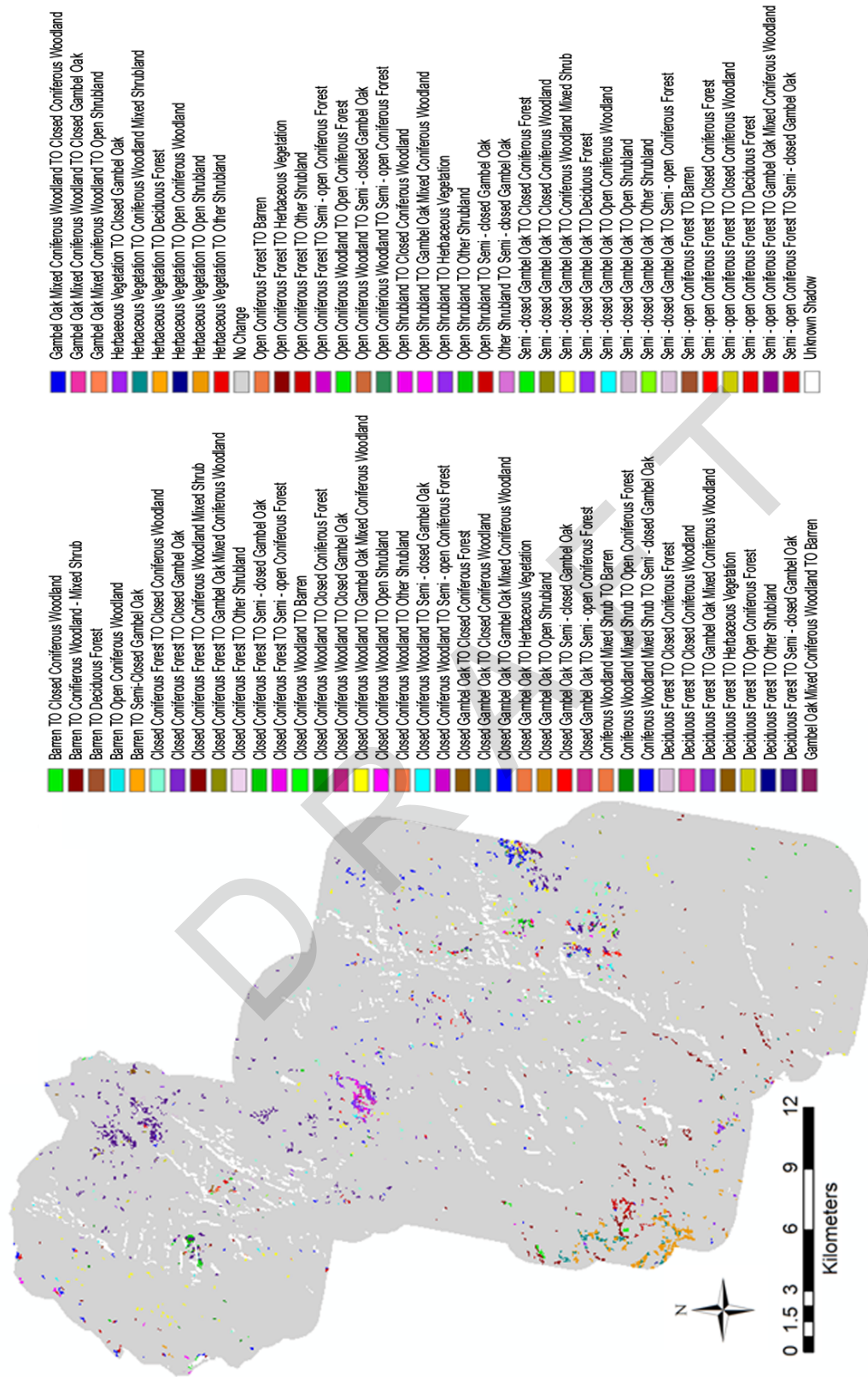


Figure 12. Most likely change between 1999 to 2006 at ZION from POM change detection.

Validation is an essential step to assess the quality of map. In the context of developing POM-based change detection map for ZION, there was a lack of multi-date reference data corresponding to the image dates analyzed. Available data sources for validation were TM images and sometimes two years of DOQs (digital orthoquads; both color and B/W). In the original NCCN protocols for change detection, we described an approach for direct interpretation of the Landsat imagery as a first phase in potential validation (the S2S validation strategy). Because such an approach is based on the same dataset from which the change maps are produced (the Landsat imagery), a complementary validation approach using DOQs is desirable. Here, we tested the feasibility of conducting a two-date DOQ validation strategy.

Results from DOQ-interpreted change with POM change from ZION must be interpreted with care (Table 4). More than two-thirds of the plots show no change or are in the agricultural land use. With so few actual change plots, a plot-by-plot error matrix is essentially meaningless statistically. Therefore, this table presents only the total count in each category (each row) derived from the DOQ interpretation and from the POM approach. As such, it indicates that the POM and the DOQ approaches agree well in overall landscape proportions of the different classes, but it should not be construed as a true error assessment of the POM method. To build a defensible error matrix, plot count would need to be increased by approximately an order of magnitude or more, which was impractical. Generally speaking, however, the DOQ interpretation approach appeared to be technically feasible, and the comparison with the POM results was straightforward.

Table 4. Validation interpretation for ZION and POM based changes.

Type	DOQ Interpretation	POM Most Likely
No change	63	67
Agriculture	11	0
Decrease Shrub	8	8
Increase Shrub	5	9
Decrease Tree	5	14
Increase Tree	3	2
No Image	4	0
Shadowed	1	0
Total	100	

3.2.4 Wupatki National Monument

The method used to derive change maps for ZION was repeated for WUPA. The most likely class for each pixel for two dates was derived (Figure 13).

Landsat-based monitoring in the parks of the Colorado Plateau

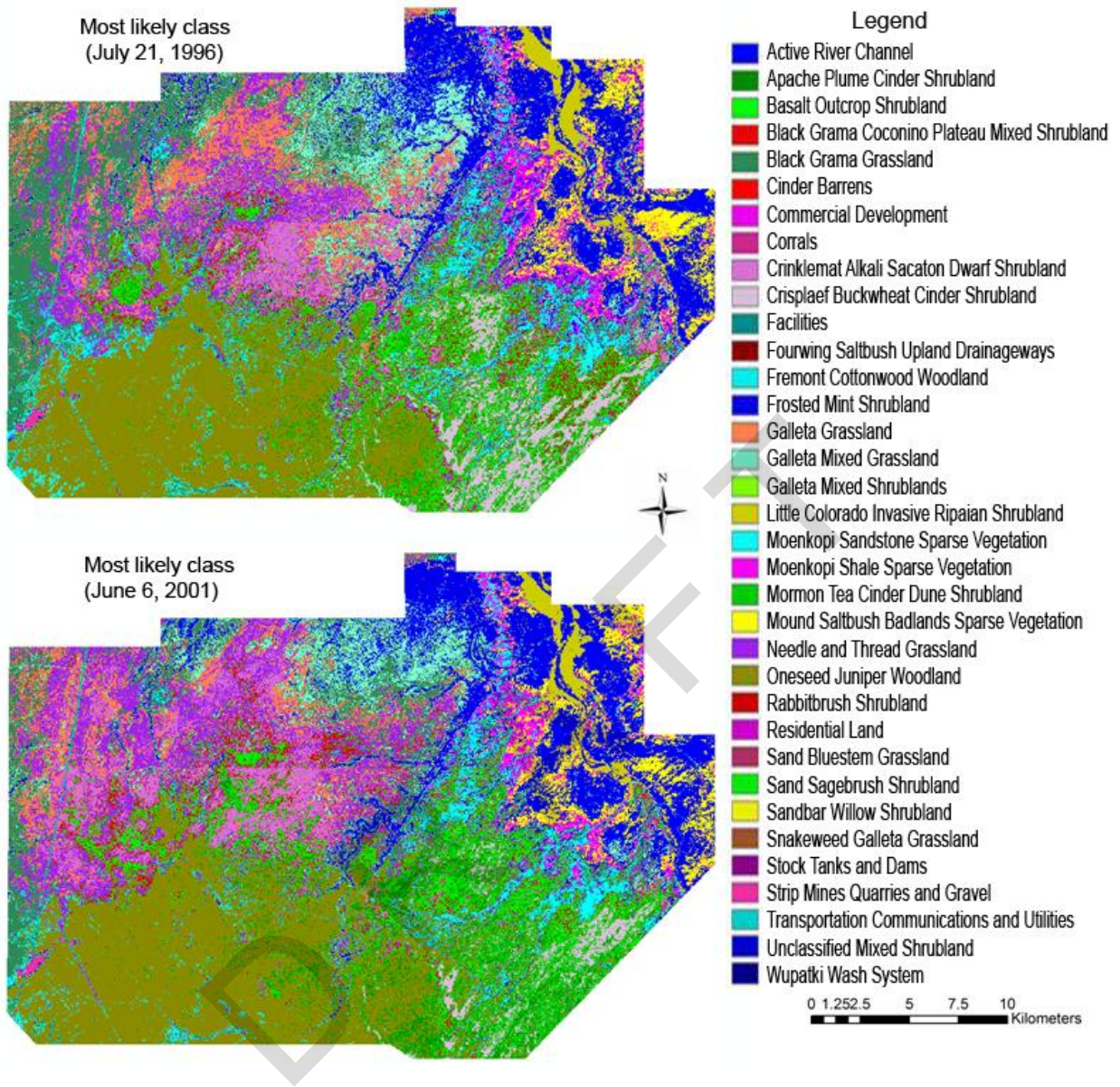


Figure 13. Most likely class in WUPA for 1996 and 2001.

A direct comparison of the two most likely classes was used to generate a change image (Figure 14). As for ZION, due to the similarities between NPS vegetation classes, and how most likely classes were labeled, when change detected by comparing the most likely classes and the pair of classes was not spectrally separable, then it was considered as no change. Without a reliable change data source for change that occurred, it is hard to validate the change detected between 1996 and 2001.

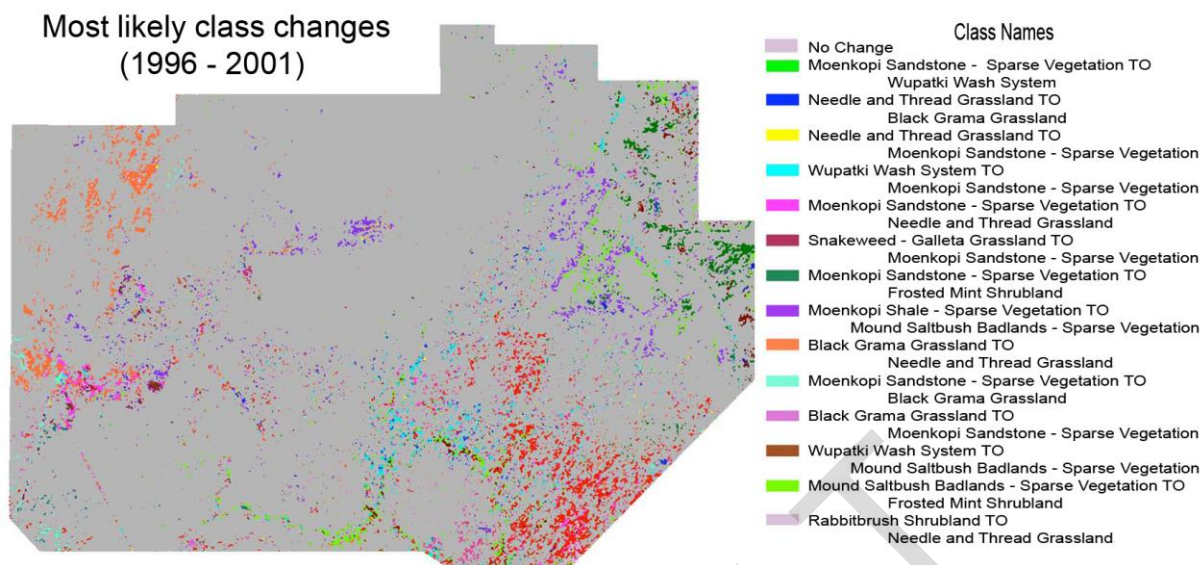


Figure 14. Most likely classes that have changed (using POM) from 1996 to 2001 at WUPA.

4. Summary and Conclusions

In general, these pilot studies showed that the use of Landsat imagery for baseline mapping and change detection within the parks of the CP requires great care. Results from MEVE and CANY suggest that continuous-variable modeling of woody cover is possible, particularly if more reference data are available. Results at CANY and ZION suggest that mapping based on the NPSVM maps is also possible, but that special aggregation of spectrally-similar vegetation classes must occur before mapping can be robust. Finally, the modified NCCN POM approach shows promise in capturing and labeling the changes that occur over time, but that spectral noise caused by variation in vegetation phenology and sun angle could lead to false positives or negatives, a problem common to all two-change detection approaches.

4.1 Key observations

4.1.1 Baseline mapping

Field plots collected in support of the NPSVM program were often not appropriate for our mapping purposes. Plots were often (1) not representative of local conditions; (2) in topographic shadow; and (3) misregistered geographically. Manual filtering of problematic plots can provide a reasonable set of potentially usable plots.

Woody vegetation was consistently the only vegetation variable that could reliably be modeled with continuous variables. Reference data for such model building must resolve cover into a sufficient number of categories for continuous variables. The derived tasseled cap angle consistently worked well for predicting cover. Predictions of woody cover within +/-10% absolute cover were possible at both MEVE and CANY. However, because woody cover at CANY tops out at 40%, this absolute error is proportionally large and perhaps larger than is tolerable for some applications. Additionally, the resources needed for photo-interpretation of woody cover in parks where field data are not well resolved may be unrealistic.

For baseline landcover mapping, the field plots did not sample all landcover classes equally. Combined with the general issues of field data, this meant that rules for classified map generation often did not allow for sufficient spectral separation between classes. Significantly more plots would be needed, at potentially great expense, to compensate for this effect. Therefore, we conclude that the NPSVM field plot data alone are not a pragmatic means of building Landsat-based landcover maps in these systems.

Landcover maps based on Landsat data are more appropriately constructed using existing NPSVM maps based on airphotos and field data. The NPSVM vegetation classification can be grouped according to vegetation name, ecological type, or physiognomic types. In all three cases, the original class labels contain too much spectral overlap among classes, in part because of the inherent spectral similarity of some classes and in part because some classes are so rare that statistical summaries are unreliable. For both vegetation name and ecological type groupings, thematic aggregation is needed to obtain sufficient spectral separability to produce reliable maps.

4.1.2 Vegetation change

Direct differencing of continuous-variable woody cover at two dates can provide maps of change in woody cover. However, two cautions are needed. First, direct differencing of maps derived from state-variable models compounds the error in both of the state maps. Second, that error is relatively high in systems with low absolute woody cover (such as within CANY).

The POM approach for change detection does appear to be feasible, and improvements to the method conducted in part for this project means that changes in land cover can be characterized in terms of the cover classes familiar to the parks.

Change maps can be validated with DOQ interpretation, but because change is relatively rare occurrence on the landscape, a random sample would require many hundreds of plots to produce error estimates statistically stable enough to fully characterize the error appropriately.

While two-date POM mapping appears to capture the spectral variation appropriately, the spectral variation itself may be caused solely by vegetation phenological change that cannot be separated from actual land cover change. This is essentially unavoidable when using only two dates of imagery, but we expect that a trajectory-based approach that incorporates many sequential years of imagery can significantly reduce this effect.

**Landsat-based monitoring in the parks of the
Northern and Southern Colorado Plateau Networks**

Chapter 2: LandTrendr for improved change detection

DRAFT

Contents

	Page
1. Introduction.....	3
2. Methods.....	4
2.1 Overview.....	4
2.2 LandTrendr	5
2.2.1 Preprocessing	6
2.2.2. Segmentation.....	9
2.2.3. Mapping	11
2.3. LandTrendr + POM	14
2.3.1. Temporal smoothing.....	15
2.3.2. POM development	15
2.4 Testing at Grand Canyon, Wupatki, and Zion	16
2.5 TimeSync	17
3. Results.....	20
3.1 Grand Canyon	20
3.1.1 LandTrendr	20
3.2 Zion.....	24
3.2.1 LandTrendr	24
3.2.2 LandTrendr + POM	32
3.3 WUPA.....	42
3.3.1 LandTrendr	42
3.3.2 LandTrendr + POM	53
3.4 TimeSync	55
4. Discussion.....	57
5. Summary.....	59
6. Literature Cited.....	60

1. Introduction

A primary goal of long-term monitoring is to gain an understanding how ecosystems function and respond to change through space and time. To understand how the ecosystems of the national parks of the Colorado Plateau are changing, the park monitoring networks of Southern Colorado Plateau (SCPN) and Northern Colorado Plateau (NCPN) have identified land use/land cover, landscape vegetation pattern or landscape structure, land or vegetation condition, and disturbance patterns as core vital signs to monitor. Because the areas to be monitored can be large, but the spatial detail required for management is typically fine-grained, we have been working with the N&SCPN to investigate the utility of moderate resolution (30m-250m grain size, Franklin et al. (2002)) satellite imagery to aid in characterizing land cover change over time.

Initial studies focused on two goals (Chapter 1 of this document). First, we examined the best approaches to map and validate static land cover using imagery from the Landsat Thematic Mapper (TM) sensors, using both field data and airphotos as training and testing datasets. Second, we examined whether a change detection approach (Probability of Membership, or POM, classification) developed for mesic parks of the North Coast and Cascades Network (NCCN) could be applied in the dry conditions of Colorado Plateau (CP) parks. After testing at a variety of parks in the CP, we arrived at three overarching conclusions. First, existing plot- and airphoto-based reference data was generally of poorer quality than ideally needed for satellite based mapping. Geolocation error, small grain size of field plots, and lack of consistently-measured variables were key obstacles. Second, static land cover mapping was most successful for variables related to woody cover. Herbaceous cover was extremely difficult to model from spectral data, in part due to inadequacy of reference data and in part to the extremely dominant soil background in most of the CP parks. Finally, change detection with the standard POM approach was hampered by the highly variable phenological condition of the parks. When any two dates of imagery were compared, year to year variations in condition or phenological state of the vegetation causes significant variations in the signal that confound efforts to identify a threshold separating change from no-change. A threshold value high enough to avoid all such noise will miss many real changes, and a threshold value low enough to capture change will include too many false positives to be useful. This obstacle would stand in the way of any traditional change detection approach that based change information on the differencing of two dates of imagery.

In this report, we summarize a pilot study to determine whether a new change detection approach we have developed may overcome some of these obstacles. The new approach, called LandTrendr (Landsat-based Detection of Trends in Disturbance and Recovery), uses trajectory-based approaches to extract coherent trends from a stack of more than two decades' worth of annual satellite imagery. By examining trends across many years of imagery, the signal-to-noise ratio is increased and the random effects of phenological variability are reduced in importance. However, the LandTrendr algorithms were initially developed for forested systems, which are generally more spectrally stable than are non-forested systems, and it was unclear to what extent they would be applicable in the CP parks. Therefore, the goal of this pilot study was to determine whether the LandTrendr approaches could be adapted for the CP, and whether they could be effectively merged with the static land cover POM mapping approach. As a secondary effort, we

also sought to evaluate whether an interpretation tool we have developed for validation of LandTrendr outputs in forested systems (TimeSync) would be applicable in the parks of the CP.

2. Methods

2.1 Overview

LandTrendr algorithms could augment landscape monitoring either alone or in combination with the POM change mapping strategies tested earlier for the CP (Figure 1). The core of the LandTrendr algorithms is a segmentation process that simplifies the temporal trajectories of pixels through a stack of Landsat Thematic Mapper imagery. In the standard incarnation of LandTrendr, the segments of the simplified time series are then labeled as disturbance or growth based solely on a single spectral index, and then filtered to eliminate changes in estimated percent cover that are below a user-specified threshold. Percent cover estimates are derived strictly from the relationship between the single spectral index and estimates of percent vegetative cover. In the LandTrendr + POM structure, the segmentation of the time series based on a single index is used to guide a process of temporal smoothing of other spectral indices. To the extent that the segmentation minimizes phenological and other noise, these temporally smoothed spectral indices are stable across years, essentially creating a consistent spectral space for every year in which imagery is available. This spectral space can then be used in a standard POM approach, where spectral space is converted to probability-of-membership space for all spectrally-separable classes in an externally-supplied land cover map. This allows creation of maps of land cover for every year where imagery is available. Both LandTrendr alone and LandTrendr + POM were tested for this pilot project.

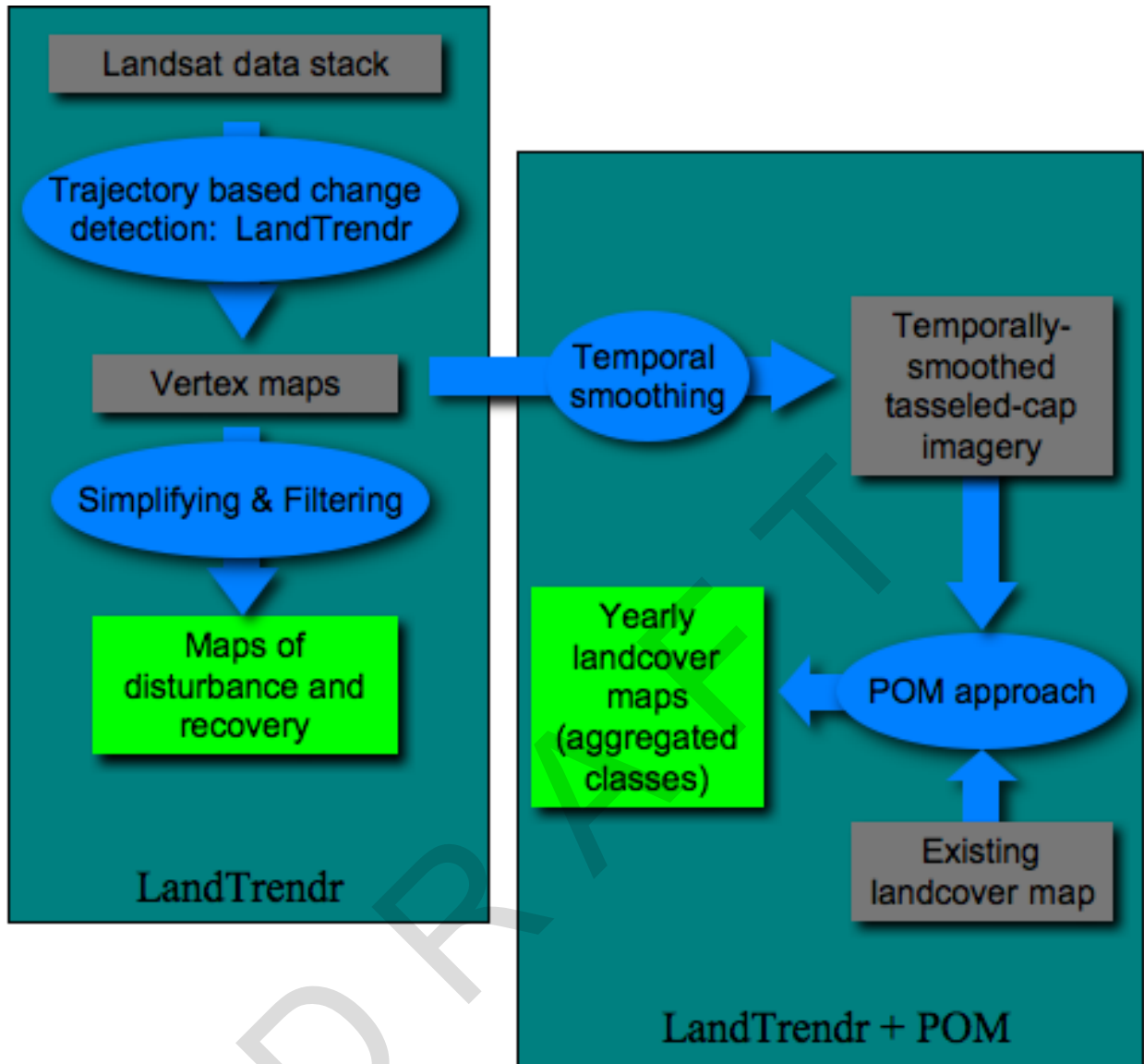


Figure 1. Schematic showing the relationship between LandTrendr processing alone and LandTrendr + POM processing.

2.2 LandTrendr

The LandTrendr algorithms involve a series of preprocessing, segmentation, and mapping steps, shown in Figure 2. Each step has a series of sub-steps described in detail below.

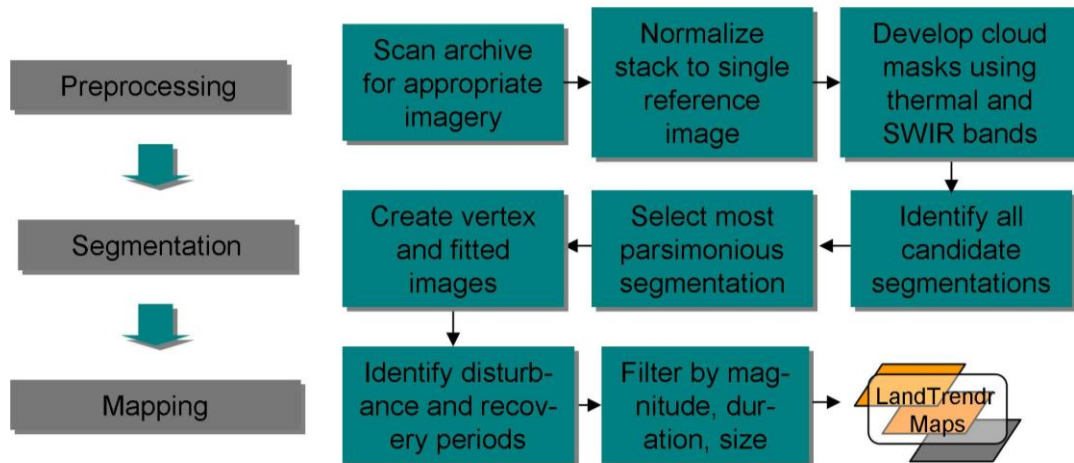


Figure 2. The overall workflow of LandTrendr

2.2.1 Preprocessing

Pre-processing is a key step in any remote sensing monitoring study (Kennedy et al. 2009). It describes a set of steps to convert essentially raw imagery into a form useful for analysis in monitor. In the case of LandTrendr, two components deserve special attention. First, because comparison will be done using all images in a stack simultaneously, consistency across images is paramount. Second, because large volumes of data are used, automation in data processing is critical to making the methods feasible. These considerations come into play at all stages in preprocessing: image acquisition, radiometric normalization, and cloud-screening.

2.2.1.1 Acquiring images

With the Landsat archive now open and cost-free, there is little penalty to acquiring as many images as needed for analysis. Rather than search for cloud-free images, we instead place highest weight on images that are consistent in terms of phenology and sun angle. The particular time of year chosen for image acquisition can vary depending on the study or the ecosystem of interest, but will be somewhat constrained by availability of images in the Landsat archive.

Reducing phenological variability in source imagery recognizes its potential confounding effect on year to year spectral signal. This is a consideration in two-date change detection, as well, but with only two dates of imagery, avoiding clouds is more important. In the case of dense temporal stacks of imagery, a masked cloud pixel in one image date is likely to be “bracketed” by non-clouded pixels in dates before and afterwards, making the penalty for clouds relatively low. Therefore, more prominence can be given to stabilizing the phenological signal, which would be much more difficult to compensate for or mask than the cloud signal. Appropriate images are selected and downloaded from the USGS’s GLOVIS website (<http://glovis.usgs.gov>, Figure 3).

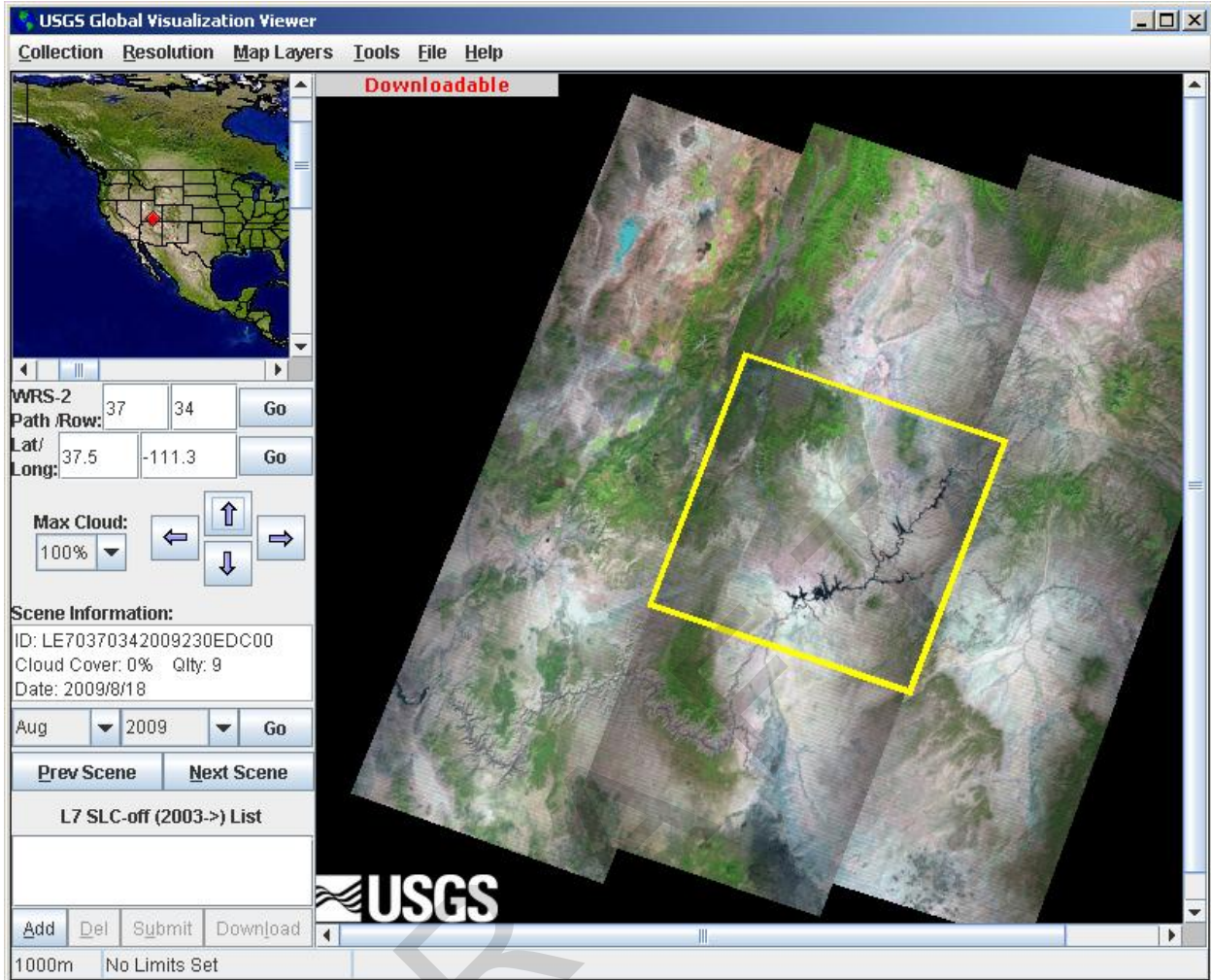


Figure 3. The USGS' Glovis site for identifying, ordering, and downloading free Landsat Thematic Mapper imagery.

2.2.1.2 Atmospheric correction and normalization

We used the same simple atmospheric correction approach described in our work previously (Kennedy et al. 2007). For a single reference year, we applied the COST correction to convert from Digital Counts to apparent surface reflectance. The COST correction includes a standard Dark Object Subtraction (DOS) correction to account for additive noise caused by aerosols, and then also includes a multiplicative correction using a first approximation of atmospheric transmission based on the cosine of the sun's zenith angle at the time of image acquisition.

The COST-corrected reference image was then used as the base for relative radiometric normalization of the remainder of the images in the stack. We used the MADCAL automated approach for detection of stable targets, as evaluated by Schroeder et al. (2006), but applied to the special case of normalizing many images in a stack. Whereas the standard MADCAL routines derive relationships between images using a single 1000 by 1000 pixel subset, we have modified this to allow any arbitrary number of subsets. Additionally, each subset is tested for robustness for each target image /reference image pair before its no-change pixels are considered

part of the larger population, thereby weeding out subsets that have clouds or other anomalies on any given target image. Therefore, a single set of potential subsets is identified for use on all images in the stack, without the need to hand-pick clear-image subsets for each image pair. The relative normalization process can therefore proceed relatively quickly without significant human intervention. Typical stable pixels within a scene range from dark, invariant shadows, to stable vegetation, to bright non-vegetated surfaces (rocks, sand, etc.). From these pixels a band-by-band linear regression determines the normalization coefficients to relate a given input image to the COST reference.

2.2.1.3. Cloudscreening

It is critical to remove both clouds and cloud shadows. Our approach was to compare each target image in a stack against a single cloud-free reference image chosen by the analyst. For each target image, an automated algorithm calculated two continuous-variable scores, one for clouds and one for cloud shadows (Figure 4a and 4b). These scores were derived from combinations of spectral bands and, when available, the thermal band. The analyst then manually viewed these cloud scores as grey-scale images, and determined an appropriate numerical threshold to separate cloud from non-cloud or cloud-shadow from non-cloud-shadow. These values were then used in an automated algorithm that develops binary masks for cloud and for cloud shadow, combines them, and then adds a buffer to allow for cloud-edge effects on neighboring pixels. This approach is fairly labor-intensive because each image's cloud and cloud-shadow images must be evaluated by an interpreter.

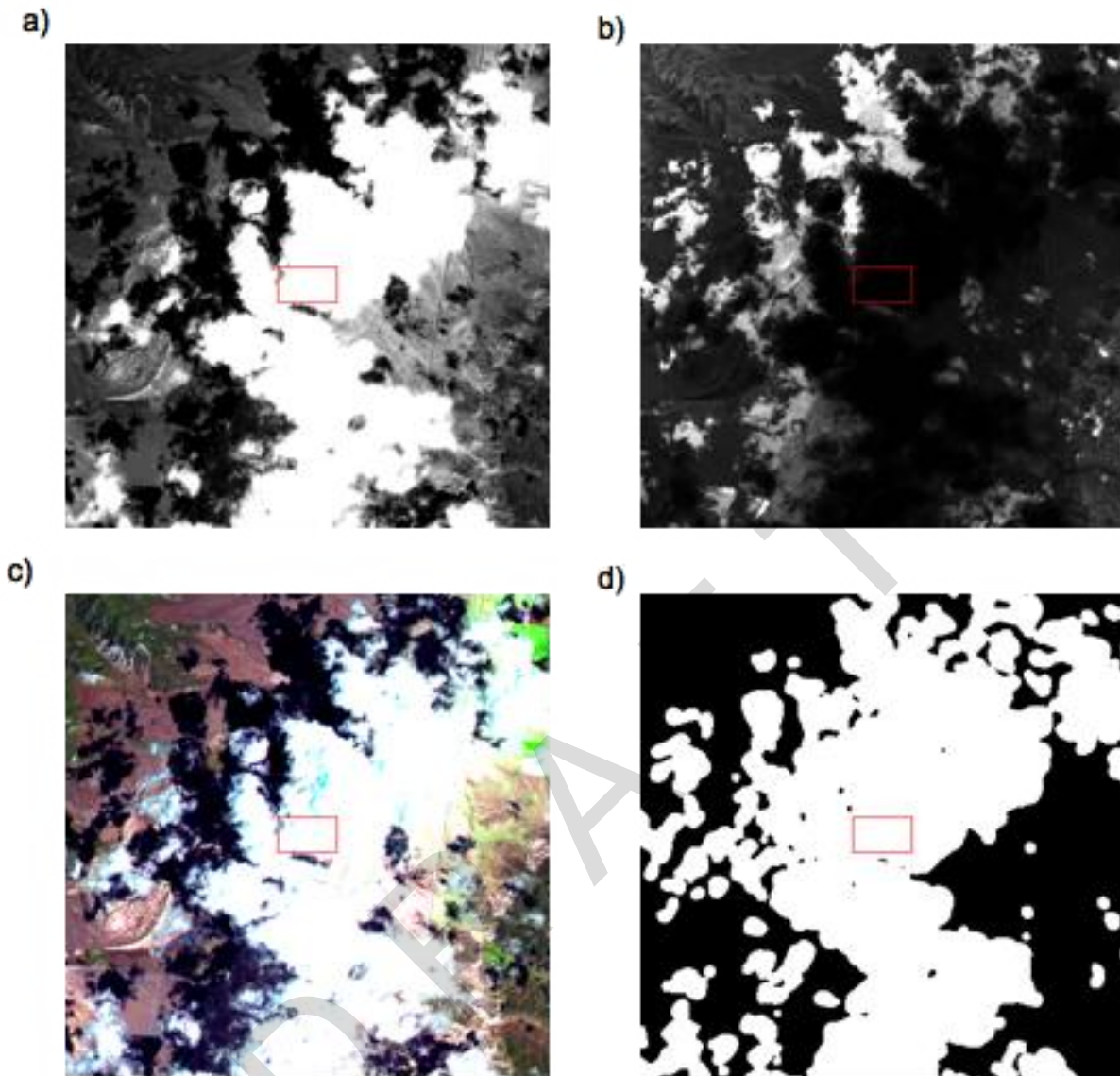


Figure 4. The cloud-masking process. For each image, a cloud score (a) and a cloud shadow score (b) image is produced. Part (c) shows the original image using a false-color 5,4,3 composite. For each image in (a) and (b), the analyst identifies a threshold below which cloud or cloud shadow is present, which is fed to a masking algorithm that combines the two into a mask (d).

2.2.2. Segmentation

The core of the LandTrendr process is temporal segmentation: the identification of periods within a time-series where a consistent process is occurring, either stability, increase, or decrease in a selected spectral index (Figure 5a). For example, a time-series running from 1985 to 2006 may be described as a single, stable segment with endpoints in 1985 and 2006, or by a single slowly increasing or decreasing trend with the same endpoints. Alternatively, a single abrupt disturbance in the year 1992 would result in a three-segment trajectory, with a stable initial period from 1985 to 1991, an abrupt change from 1991 to 1992, and a slow return from 1992 to 2006 (e.g. the green trace in Figure 5a).

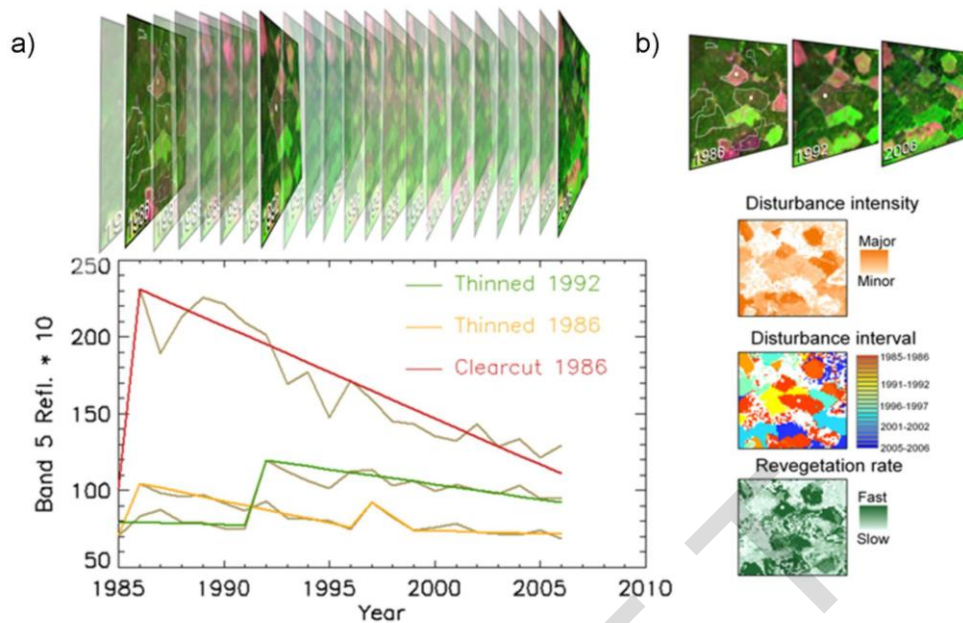


Figure 5. The segmentation and labeling phases of LandTrendr. a) Spectral values of a single index are extracted for a pixel in dense stack of images (grey traces). Signal extraction techniques are used to identify the years (x-axis) that form logical endpoints of segments describing consistent processes over time, and to find the vertex values (y-axis) for those years that minimize overall residual error in the fitted trends (colored traces). b) The endpoints, slope, magnitude, direction, and length of each segment can be described for each pixel in map form and used to infer the process occurring in a given time period.

Segmentation occurs at the pixel scale as follows. For each pixel, the spectral values of a single index are extracted for each year in the stack. Although any spectral index could be used, we focus on the tasseled-cap wetness index (Crist and Cicone 1984) and on the normalized burn ratio (NBR), which has been used in national parks as a means of observing fire severity (van Wagtenonk et al. 2004). Both indices include the short-wave infrared bands of Landsat, which are increasingly recognized as critical for detecting many types of change (Asner and Lobell 2000; Brown et al. 2000; Healey et al. 2006; Royle and Lathrop 2002; Skakun et al. 2003). If there are multiple images supplied for a given year in the stack, the algorithm chooses the best one based first on masking (clouded pixels are not chosen) and then date (pixels from the image closest to the median date for all images in the stack are preferred). If peak of growing season imagery is chosen, then this criterion will identify the pixels closest to that peak, unless they are cloudy, in which case images successively further from the peak will be chosen. The first segmentation algorithm then examines the time-series for all years that appear to represent turning points – either upward or downward – in the overall trajectory. These turning points are referred as vertex years in the trajectory, since they describe potential endpoints of segments. Selection of these candidate vertex years is a critical step that can be achieved with several different approaches, including evaluation of slope change with and without each vertex and deviation of the point from a longer-term straightline trend. Weight can also be given to years that precede or follow large disturbances, assuming that disturbance signals have a consistent directional character.

Once a target number of candidate vertex years are chosen, a second set of algorithms then identifies the most parsimonious path through the vertex years (the x-axis) to describe variation in the signal (y-axis). These fitting algorithms are used again later in the LandTrendr + POM process (see next section). A third algorithm then identifies and removes the vertex whose removal caused the least increase in residual variance, and then the second set of algorithms is reapplied to the smaller set of potential vertices. This vertex removal and trajectory recalculation is repeated until only one segment (with two endpoints) remains. Finally, another algorithm determines which number of segments represents the best overall description of the trajectory.

The vertex years and vertex values of this “best description” of the trajectory are the foundational pieces of information for all further mapping. The vertex years and the values of the spectral index at those vertex years are written to output files for later processing. In addition to the vertices at the endpoints of segments, the fitted values at each year along the segment are also written to a “fitted value” image that has as many layers as there are years in the input image data.

2.2.3. Mapping

This fitted image could itself be used to display spatial patterns in the trajectories of pixels across an image and compared visually with other datasets to understand if a particular known phenomenon is being captured by the segmentation process. However, the information is not summarized in a manner that can be interpreted quickly or quantitatively. Often, the richness of the information exceeds the needs of most users, and it also contains unwanted information. Therefore, to make use of the data, rule-based approaches must be applied to the vertex data to distill the information into simpler forms that can be mapped easily. In essence, we seek to extract from a given trajectory its most salient or distinctive features while ignoring its uninteresting features. This requires a sequence of processing steps.

2.2.3.1. Segment-merging

First, each segment is identified as a disturbance or recovery segment by virtue of its direction of change in the spectral index value. The rule linking direction of change to disturbance or recovery is based on knowledge of the index involved: for both wetness and NBR, increases in the index value (toward greater positive values) are generally associated with increases in vegetative cover, and decreases in index value with decreases in vegetative cover. Therefore, if a segment moves from a lower to a higher value in either index, it is labeled recovery, and if the segment moved from higher to lower value, it is labeled disturbance. This rule, while simple and generally applicable, does not hold under certain circumstances (discussed later).

In some cases, an observed trajectory will be best described by a sequence of segments that includes two or more successive segments of the same type (either disturbance or recovery) with slightly different slopes. This is particularly common in post-disturbance recovery dynamics, where an initially steep rate of recovery of vegetative cover gradually slows as time-since-disturbance increases (Figure 6a). Some disturbance types also occur over long periods, with segments of slower and faster disturbance rate. For many applications, the component segments are not as interesting as the overall start and end of the disturbance and recovery process, and the total change from start to finish. To report those data, adjacent segments need to be coalesced.

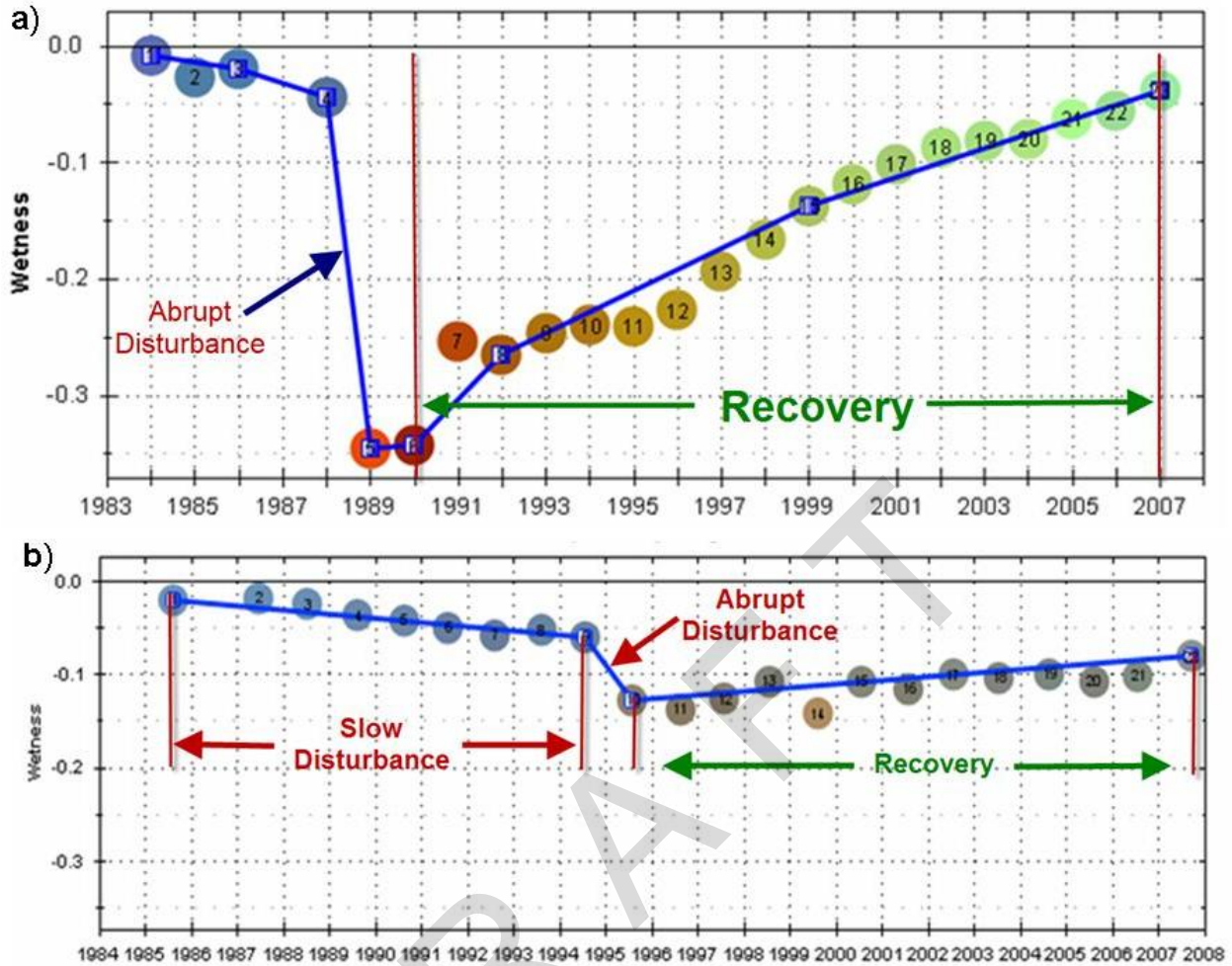


Figure 6. In many cases, the segmentation of a trajectory results in adjacent segments of the same type (disturbance or recovery) that differ only slightly in slope. a) In this example, the post-disturbance recovery period includes three straightline segments whose coalescing would simplify the information content greatly without sacrificing the key information about start, end, and overall magnitude of recovery. b) Although some adjacent segments of similar type can be coalesced, others contain useful and distinct information. Here, a slow disturbance is followed by an abrupt disturbance; coalescence in this case would remove useful information about two distinct processes.

However, we need to avoid coalescing potentially interesting and distinct processes. For example, an insect-related mortality event in forests may cause long, slow mortality with a gradually increasing disturbance signal (Figure 6b). If that is then followed by a fire with an abrupt, steep spike of disturbance, the two segments describe processes that are ecologically quite distinct and should be retained as separate pieces.

For LandTrendr processing in the CP, we used a simple threshold of angle-difference between segments to determine which adjacent segments of the same type are coalesced. Segments with similar angles in the spectral index/year space are coalesced, while those sharply different angles will be retained separately. The angle threshold for coalescence is parameter that can be altered as desired by an analyst.

2.2.3.2. Filtering by magnitude and duration

One drawback of the segmentation approach is its potential susceptibility to “overfitting,” whereby an undesirable small noise event is captured as a meaningful segment. Relative to a simple two-date change detection, these “false positive” signals are greatly reduced in frequency, but they still occur. Therefore, in the LandTrendr processing flow, a thresholding process was used to remove from maps segment information that was indistinguishable from noise.

In the forested systems where LandTrendr was developed, the thresholding process is based on an estimate of percent vegetative cover. Percent vegetative cover is estimated using statistical models linking photointerpreted percent vegetative cover with the spectral index used for LandTrendr change detection. For example, a random sample of pixels could be chosen from across a Landsat scene, and at each pixel an analyst would use airphoto interpretation to estimate percent vegetative cover. (This is done using the TimeSync utility described below). These photointerpreted estimates of cover could then be linked to the pixel values of the NBR index, and a simple regression approach used to estimate the relationship between NBR and percent cover. Once determined, this percent cover model would be applied to the fitted vertex values in a trajectory segmentation, and any segments whose starting and ending vertices were closer in percent cover to each other than a given percent cover threshold would be considered “no-change.”

This process was not directly applicable in the CP. As noted in chapter 1, percent cover models are too noisy for many of the systems in the non-forested parks of the CP. However, to test the general approach, we developed a simple alternative to the detailed estimate of percent cover: for the index being used (either wetness or NBR), we noted index values associated with areas on the landscape that were visibly non-vegetated or visibly vegetated, and used a simple interpolation between these high and low values to estimate percent cover. This highly simplified approach would need substantial tuning for each park, and – given the known difficulties estimating percent cover in these systems (as noted in the introduction) – may be a critical step for methodological improvement if LandTrendr were to be implemented in the arid systems of the CP. *Alternatively, if change need not be measured in units of percent cover, spectral index thresholds (i.e. in the units of the original spectral index) can also be employed, and could be tailored for each park/ecosystem.* This would require substantially less effort.

Once percent cover estimates were related to either the NBR or the wetness index used for segmentation, filtering was applied differentially to disturbance and recovery processes. For segments associated with a disturbance event, the pre-disturbance cover and the relative magnitude of disturbance were considered in the filtering process. Disturbance segments that began in conditions having too little vegetation were considered noise, as were disturbance segments whose magnitude of cover change was too small. The change-magnitude criterion was adjusted relative to the duration of the disturbance process: short-duration disturbance segments are more likely to be identified through overfitting, and therefore require a greater magnitude of change to be considered meaningful than are segments that persist across many years of data. As an important detail, this threshold could be calculated either directly or relative to the starting cover estimate; for all disturbance filtering tested here, we used the relative cover change. For segments associated with recovery events, a single magnitude of cover change was used for filtering.

At the end of this process, the remaining segments associated with each pixel’s temporal trajectory could be mapped in one of several ways. First, disturbance or recovery segments were generally mapped separately. Within either type, maps of start year, duration, or magnitude of change could be mapped.

2.2.3.2. Filtering by patch size

Depending on the desired map outcomes, it was also possible to filter mapped changes (either disturbance or recovery) to a minimum patch size. Patches were defined as groups of adjacent pixels (using 8-neighbor rule) whose start-year of disturbance or recovery was similar. For this pilot project, we filtered disturbance polygons to an 11-pixel (approximately 1 ha) size, meaning that groups of disturbance pixels had to include at least 11 adjacent pixels to be mapped.

2.3. LandTrendr + POM

Although the LandTrendr algorithms are useful for producing labeled maps of disturbance and recovery, they only capture and label such change in one spectral dimension at a time. A single spectral index does not carry the full range of information contained in the larger spectral space, which limits the degree to which conditions and changes can be labeled. Therefore, a key component of our work has been to build links between LandTrendr and the probability-of-membership (POM) approach that we tested in the two-date mode for the CP. The goal was to minimize the problematic phenological noise in two-date change detection and rely on LandTrendr to pick up the changes and then label them with POM.

The overall process of integration involves three broad steps (Figure 7). First, LandTrendr algorithms are used to create temporally-smoothed images that remove any non-informative year-to-year variation from the images. Then the single date of imagery closest to the park-specific cover map is used in the standard POM process to develop probability-of-membership lookup-tables that link the fitted spectral space to the park-specific cover map. Finally, those rules are applied to the spectral values of all fitted images to produce labeled maps based on the NPS map labels.

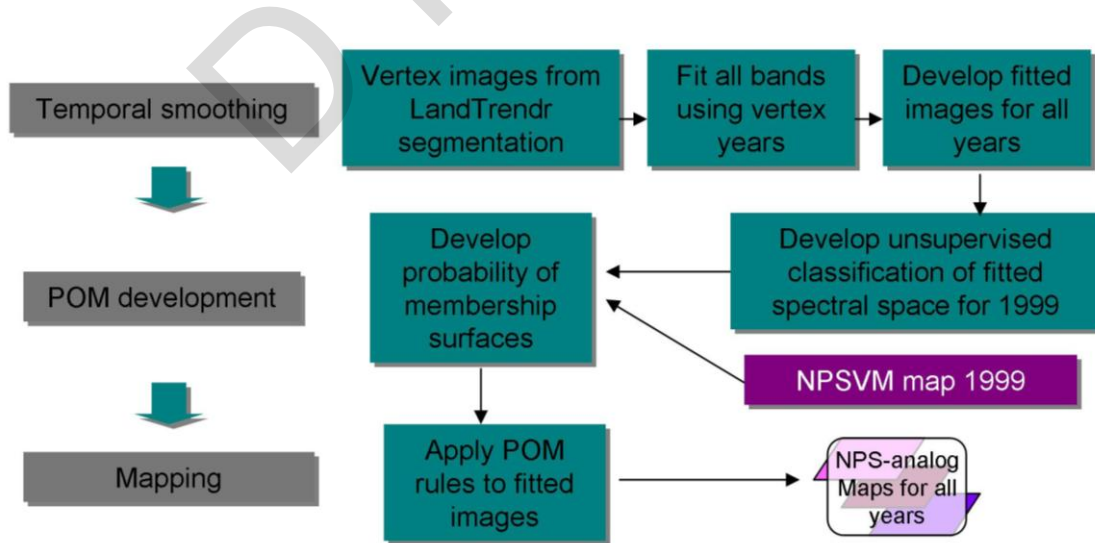


Figure 7. Overall workflow of LandTrendr + POM for a park with a 1999 landcover map from the NPS Vegetation Mapping (NPSVM) mapping program.

2.3.1. Temporal smoothing

The link between LandTrendr and the POM approach is temporal smoothing of the raw spectral data. LandTrendr segmentation is applied as described in the prior section on a single spectral index or band, but rather than derive maps from the summary characteristics of the segments, we force other spectral bands to conform to the temporal segmentation of the single index (Figure 8). Vertex years from the NBR fitting are fed to the LandTrendr fitting algorithms (described in the segmentation section above) to determine the most parsimonious path through the observed values in another spectral band, given fixed vertex years. Fitted values for each year for each band are recombined by year to create fitted “pseudo-images” that are temporally-smoothed representations of the original data. Although the vertex years are defined by the single index used in the original segmentation, the pattern of increasing and decreasing value of the segments between vertices varies by index. This allows capture of greater spectral dimensionality than from the single index alone.

2.3.2. POM development

The POM approach was designed as an attempt to merge the mapping perspectives of remote sensing scientists and ecologists. Remote sensing scientists approach mapping from the perspective of signal content within the spectral space defined by a satellite sensor, aggregating and separating land cover classes according to their distinctiveness in spectral space. Ecologists approach mapping from the perspective of ecologically-meaningful distinctions in vegetation and abiotic types, aggregating and separating land cover classes according to the functional processes or the species of interest. These two worldviews often do not produce maps with the same labels, so an approach is needed to build a compromise map that captures the essential elements of both views.

The POM approach begins with the premise that a single-date, airphoto- and/or field-based map exists and is meaningful to park specialists. This was true at Zion National Park and Wupatki National Monument, where the NPSVM map was developed from airphoto data and subsequent field training and validation. As we showed in our prior project with the CP, this map contained far more detail in terms of land cover class than could be

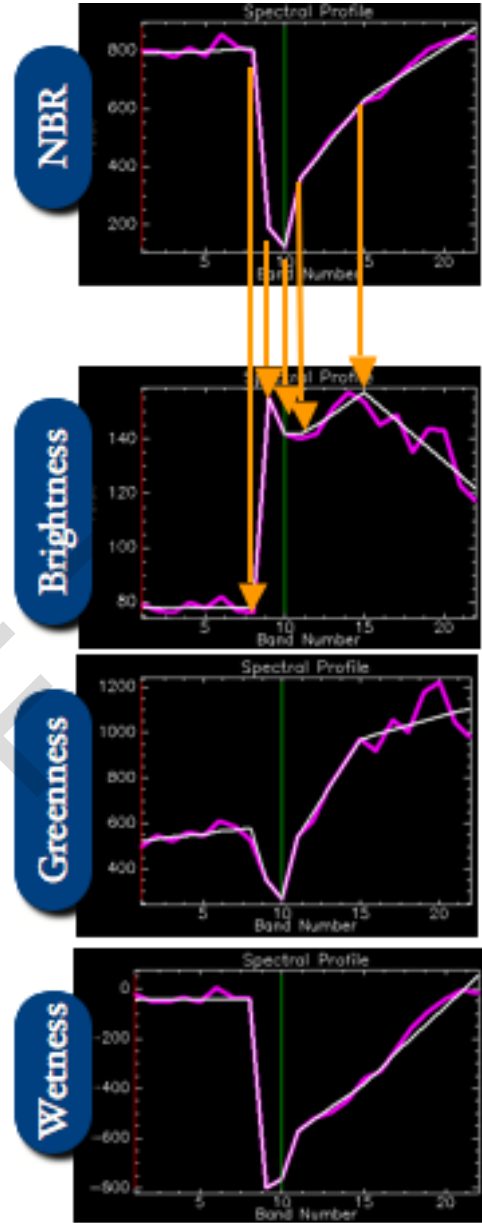


Figure 8. Once LandTrendr algorithms have been applied to a core index (here, the NBR, at top) other spectral indices (here, the tasseled-cap indices) can be smoothed using a constrained segmentation driven by the vertex years of the original segmentation

captured from spectral distinctions alone. When classes were aggregated into simpler definitions, the satellite data could create reasonable maps.

Separately, the spectral space of the pseudoimage closest in date to the year of the NPSVM map was partitioned. A standard k -means non-parametric partitioning algorithm was used to create a set of image “spectral classes” that optimally divide the spectral space. We used 50 classes for all investigations in this report. The classes have no inherent meaning in terms of land cover, but capture the distinctions in spectral space on the landscape. Thus, the unsupervised classification results can be considered one optimal approach to characterizing the variability in condition on a landscape, as reflected in the spectral variability. For each unsupervised class, we calculated Gaussian likelihood surfaces that represented the probability of membership (POM) in each class for all parts of the spectral space.

Integration of the NPSVM and unsupervised classes is central to the POM approach. Each Gaussian probability surface was overlaid on a similar Gaussian probability surface for the NPSVM classes to result in an amalgam probability surface for each NPSVM class. The mathematical integration ensured that all areas of spectral space were covered, and also that all NPSVM classes had the potential to be mapped. However, this process also penalized NPSVM classes that were spectrally ambiguous – NPSVM classes with broad distributions in spectral space dilute their probability surface over a larger area, reducing the probability of being selected as the label for any particular portion of the space. NPSVM classes that were spectrally distinct, on the other hand, were more likely to be chosen as labels for some portion of the spectral space. Thus the POM mapping process is an unbiased approach to creating maps where the ecological distinctions have manifestations in spectral space. The final product of this process is a POM lookup table that links the spectral values in the pseudoimages to the probability of membership in the aggregated NPSVM landcover classes. By applying these lookup table rules to any of the yearly pseudo-images created using methods described in section 2.3.1, a new landcover map was created for the year of that pseudo-image. In this manner, a stack of landcover maps was created for the park in question for every year.

2.4 Testing at Grand Canyon, Wupatki, and Zion

We applied the LandTrendr approaches at several parks in the CP networks. At GRCA, we only tested the LandTrendr. Without a recent landcover map from GRCA, we did not attempt LandTrendr + POM. At both WUPA and ZION, we conducted a LandTrendr run, with the simple percent cover estimation, and the LandTrendr + POM mapping. WUPA and ZION were chosen in part because of availability of source maps obtained during our prior work at these parks, and in part to represent a wide range of vegetative cover conditions. ZION includes more forest cover similar to that in which LandTrendr was developed, while WUPA is dominated by non-forest cover that was expected to test the limits of the LandTrendr approaches.

For each park where LandTrendr was run, stacks of Landsat imagery were acquired and processed as described in the above sections. Table 1 provides an example of the density of Landsat imagery used, in this case for Zion NP. Shown are the year and Julian Day (1-365) for each image. Nearly every year is represented.

Table 1. List of images for Zion

Platform	Image Date
TM	1984-161
	1986-166
	1987-185
	1988-188
	1989-174
	1990-177
	1991-164
	1992-167
	1993-185
	1994-188
	1996-162
	1998-183
	1999-170
	2001-167
	2002-178
	2003-181
	2004-184
	2005-186
2006-173	
2007-176	

LandTrendr was run on the NBR index for Grand Canyon and Zion, and on the tasseled-cap wetness index for WUPA. Table 2 describes the parameters used at all parks. At most six segments were allowed in the segmentation phase. Setting disturbance weight to zero removes any preference in the segmentation algorithm for vertices adjacent to apparent disturbance events; experience gained in these parks showed that disturbance events do not always manifest typical disturbance signals with single spectral bands in non-woody, open systems like those in the CP. Turning off the disturbance weight threshold therefore gave equal weight to all changes.

Table 2 Parameters used in Landtrendr (1984-2007)

Parameter	Parameter values	Comments
Number of segments	6	At most 6 segments
Disturbance weight factor	0	
Segment merging	15 degree angle for disturbance and recovery	
Abrupt disturbance vegetation loss threshold	10	
Slow disturbance vegetation loss threshold (20 years duration)	5	
Disturbance size	11 pixels	

2.5 TimeSync

Recognizing the expanded need for reference data necessitated by the LandTrendr yearly outputs, the only possible reference dataset that has both the spatial and temporal scope of our maps is the imagery itself. Building on the strategies for satellite-to-satellite image interpretation laid out in the original protocols we developed for POM mapping (Kennedy et al. 2007), we have developed a new software tool to aid in interpretation: TimeSync. TimeSync is a platform that allows a trained interpreter to quickly label trends and events in a time series of imagery. Our

goal here was to determine whether TimeSync could be useful for interpretation in the ecosystems of the CP parks.

Figure 9 shows TimeSync windows for a plot chosen for examination in Zion NP. In each figure, a block of small image chip windows is shown on the top portion of the figure. Each image chip is extracted from a single date of imagery, and shown in the false-color tasseled-cap rendition. The target plot is always in the center of each image chip. Below each block of image chips is a spectral trajectory graph for the plot of interest. The y-axis in these plots can be any spectral index. The interpreter identifies segments of consistency, much as the LandTrendr segmentation algorithms do. In this case, however, the interpreter uses all possible tools to make the interpretation of the processes occurring for the plot, including spatial and spectral clues, as well as high-resolution DOQs as available. For many areas, we use GoogleEarth to provide the single-date, high spatial resolution imagery sometimes needed to resolve ambiguity in the Landsat imagery.

DRAFT

Landsat-based monitoring in the parks of CP

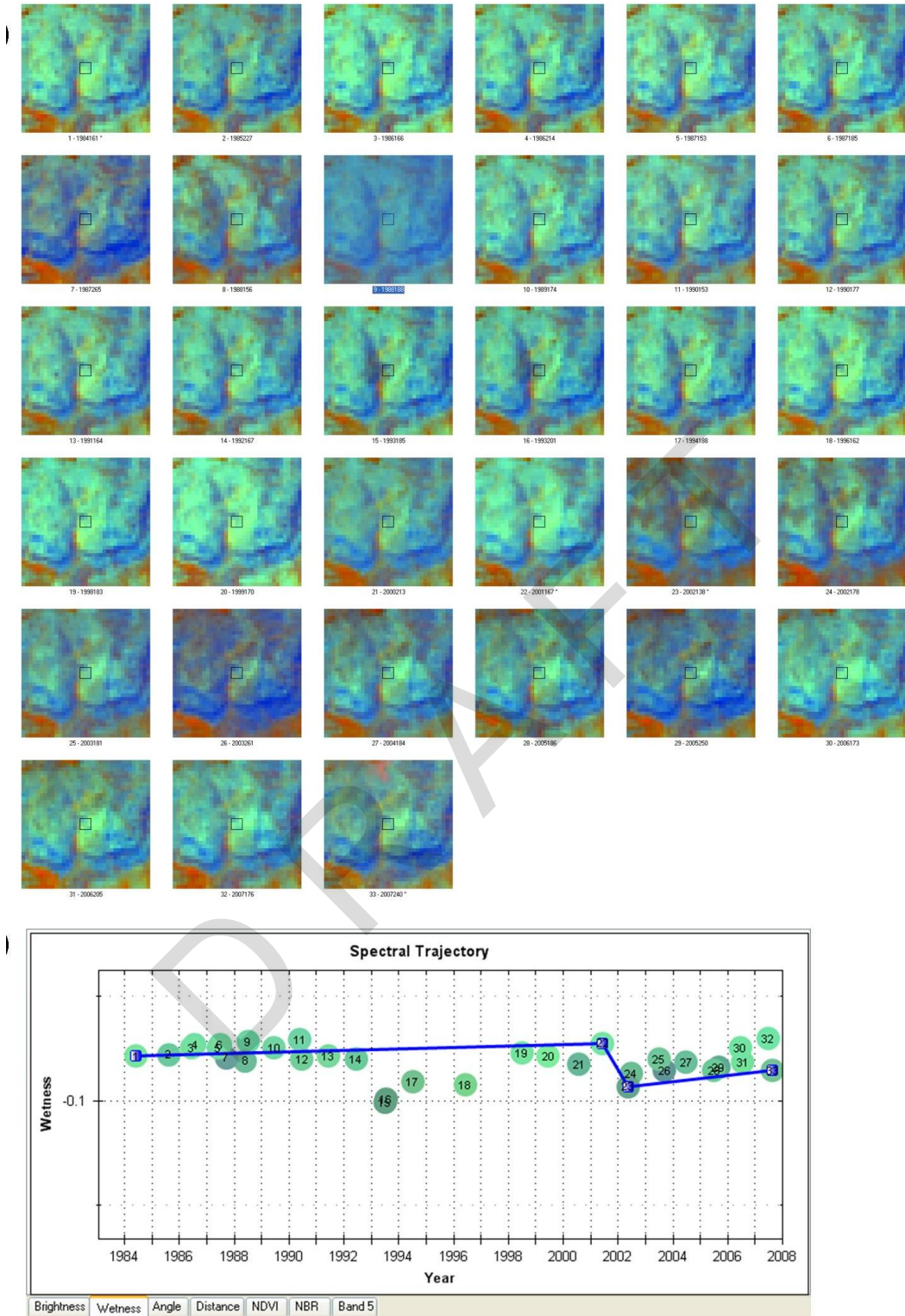


Figure 9. The interpretation windows of TimeSync, the software tool developed to quickly view, interpret, and label time-series Landsat data. a) Image chips centered on the target plot, showing false-color tasseled-cap imagery for every year (and in some cases, multiple images per year). b) The spectral trajectory of the target plot on the tasseled-cap wetness scale. This plot was interpreted to be disturbance that occurred between the 2001 and 2002 images.

As the interpreter segments the time series, he or she populates a database that is wrapped into the TimeSync tool. A variety of attributes are ascribed to each segment in the trajectory, including a label for the event or process, a likely cause, and an indication of the confidence the interpreter has in making those calls. These data can then be used in conjunction with the segment data itself (start and end year) to assess how well the automated algorithms capture the essential processes of a given plot. Note that the TimeSync tool is a manual interpretation conducted on single points on the landscape; LandTrendr is a set of algorithms that are applied automatically across the landscape to create maps.

The TimeSync tool is envisioned as both a standalone assessment as well as a unifying foundation for other independent reference data. As a standalone tool, the TimeSync interpretations are not a true validation, since they are based on the same imagery as the algorithms used to make the maps being assessed. However, we have been struck by how much more information is brought to bear on interpretation when the entire time series of data is available. For many ecosystems, the calls made in TimeSync are likely to be quite good. As a unifying foundation for other reference data, TimeSync can be applied anywhere on the landscape to overlap opportunistically with any other dataset or with local knowledge of disturbance processes. For example, a given reference source may be field plot data collected in a single year. The point locations can be fed to TimeSync, interpretations of dynamics conducted for the plots, and then compared with the field data to examine how well the TimeSync data capture whatever information content is in the point data. Similarly, opportunistic use of two dates of airphotos, or separate geospatial mapping efforts, can be undertaken through sample-based LandTrendr interpretation and comparison for the overlap period.

For this pilot study, we used the TimeSync approach to examine a handful of randomly-placed plots in both Zion and Wupatki to determine whether the visual interpretation of the imagery is possible in these arid systems. This effort was not the focus of the pilot project, and thus was intended simply as a subjective and initial assessment.

3. Results

3.1 Grand Canyon

3.1.1 *LandTrendr*

LandTrendr at GRCA was run using the NBR index on an image stack running from 1984 to 2008. At the most basic level, the LandTrendr segmentation algorithms produce output images of the desired index (here, NBR) with each year of input data mirrored with a year of fitted output data, resulting in this case in a 25-layer output image. This output image stack contains essentially the entire information content of the fitting process, and can be viewed year by year. For quick assessment of the information content of the segmentation, three layers at a time can be viewed as RGB composites, with areas that are stable taking on tones of black to white, and areas that have changed appearing in different colors. Figure 10 shows one such view for the North Rim of the Grand Canyon, where conifer forests dominate and a variety of disturbance and growth processes have been occurring since 1985. When the information is displayed in this manner, it provides clues about what is happening on the ground that can be investigated at specific points with profile tools in an image processing package that allow examination of the source spectral data and the fitted spectral data (Figure 11). In this case, many of the pixels on

the North Rim show evidence of prolonged loss of vigor or mortality, indicated by long slow declines in the NBR index. In some cases, these long, slow declines are followed by fire events that are also captured in the pixel-level segmentations.

To examine potential causes of the decline, other data can be brought into an analysis. In Figure 12, we add polygon data from the Forest Health Protection program of the USDA Forest Service, acquired in this case from Jeff Hicke (University of Idaho, personal communication). FHP polygons are hand-drawn by expert observers flying in fixed-wing aircraft across forests of much of the western U.S. Although rich in thematic detail, the spatial properties of these data make them difficult to bring into analytical frameworks, as the entire polygon is assigned a single damage class and the polygons themselves can sometimes be of questionable spatial precision. When used in concert with LandTrendr data that are highly spatially specific and accurate, however, a richer picture of pest-related forest mortality may be achievable.

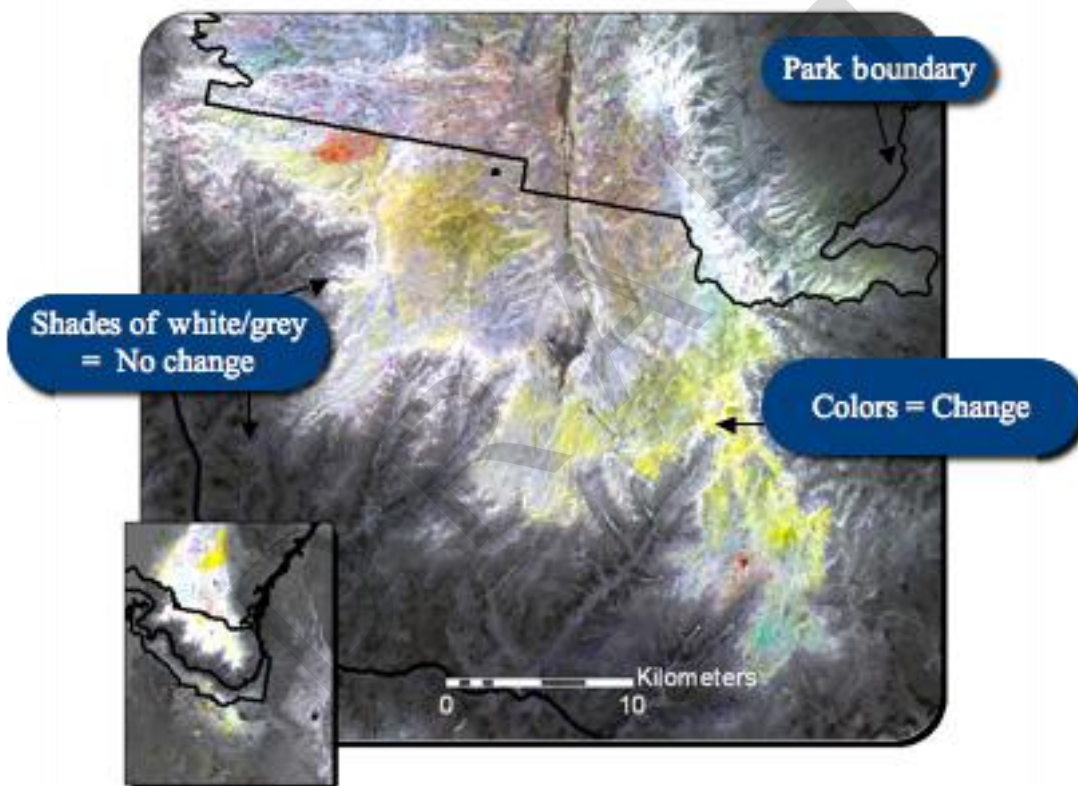


Figure 10. Initial segmentation outputs for the north rim of the Grand Canyon. This image shows three years from a stack of fitted NBR imagery, with 1985, 1994, and 2007 in the red, green, and blue tones, respectively. Shades of black, grey, and white indicate areas where spectral values have not changed over time, whereas the colored tones indicate areas where spectral values were higher or lower in one or more of the displayed years. Reds and yellows correspond to areas that experienced loss of vegetation from the first or second period to the last period whereas blue and cyan tones correspond to areas that saw increased vegetative cover.

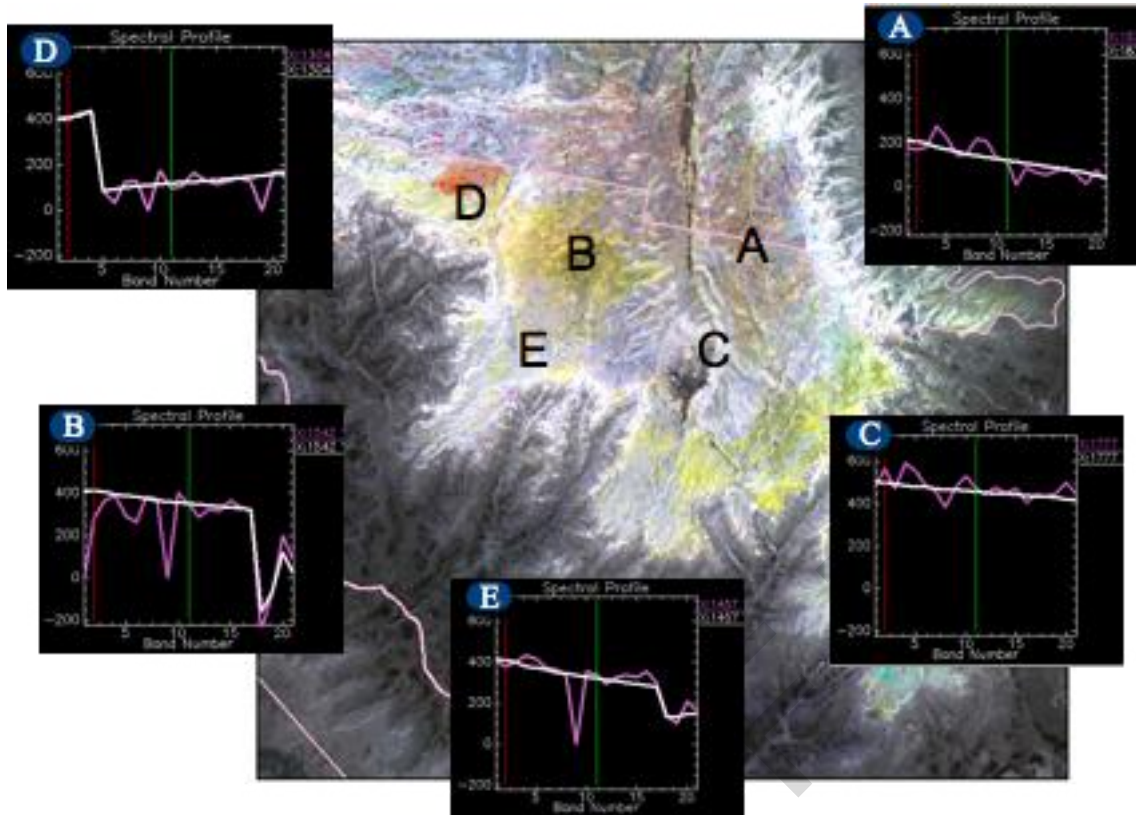


Figure 11. Source (purple) and fitted (white) trajectories for the NBR index at selected points on the North Rim, Grand Canyon. For the NBR index, decreases in value over time are associated with loss of vegetation. Trajectories A and C show prolonged decrease in the vigor of the forests through the entire period. Trajectories B and E show similar loss of vigor followed by abrupt fire events. Trajectory D shows an abrupt fire event early in the period, followed by slow increase of vegetation corresponding to post-fire regrowth.

Using the simple approach described in section 2.2.3.2 to develop a percent vegetative cover estimate from NBR data, we then filtered the disturbance information from these segmentation runs of LandTrendr by percent cover (at the pixel scale), aggregated all remaining pixels into patches based on year of onset, and converted all patches to ArcGIS shapefile format for viewing (Figure 13). Each polygon retains information on the magnitude of disturbance (as a mean value for all pixels in the patch), the duration of disturbance, and the estimate of pre-disturbance vegetative cover. In this example, year of disturbance onset is shown. Recall that filtering was applied to *relative cover change*, meaning that the same absolute change in cover would appear higher in areas with low initial vegetative cover (for example, many of the areas on the upper right of figure 13). Disturbances that last over the entire time period are those with long-duration segments of decline, such as points A and C in Figure 11. In this figure, only one disturbance is shown, but map of all potential disturbance events (multiple events per pixel) are possible.

Landsat-based monitoring in the parks of CP

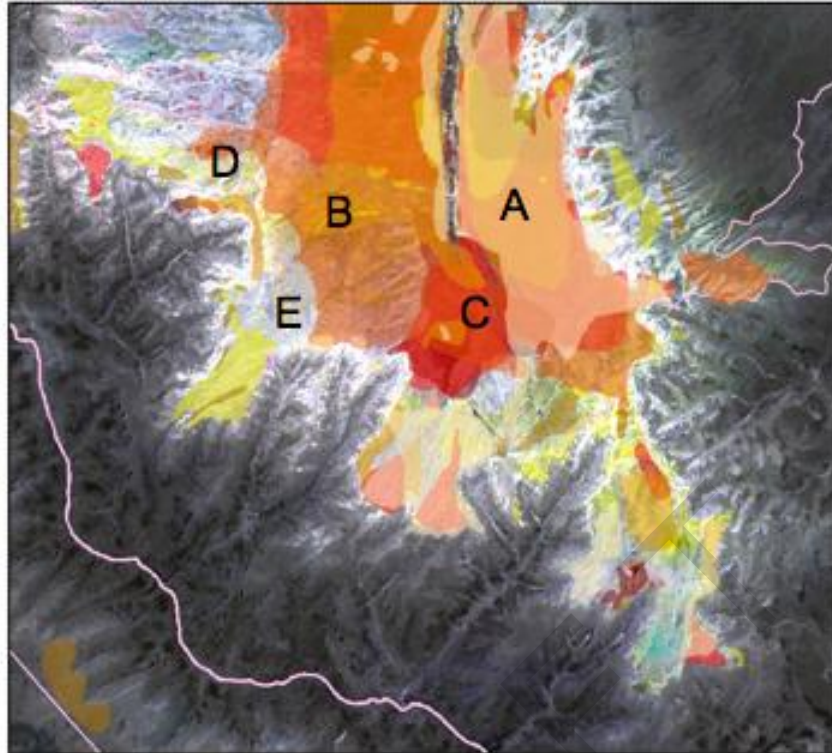


Figure 12. Forest Health Protection polygon data (red and yellow polygons) associated with insect activity overlaid on the fitted images of Figures 10 and 11. Polygon colors are associated with the different years of observation for the period 1997 to 2005.

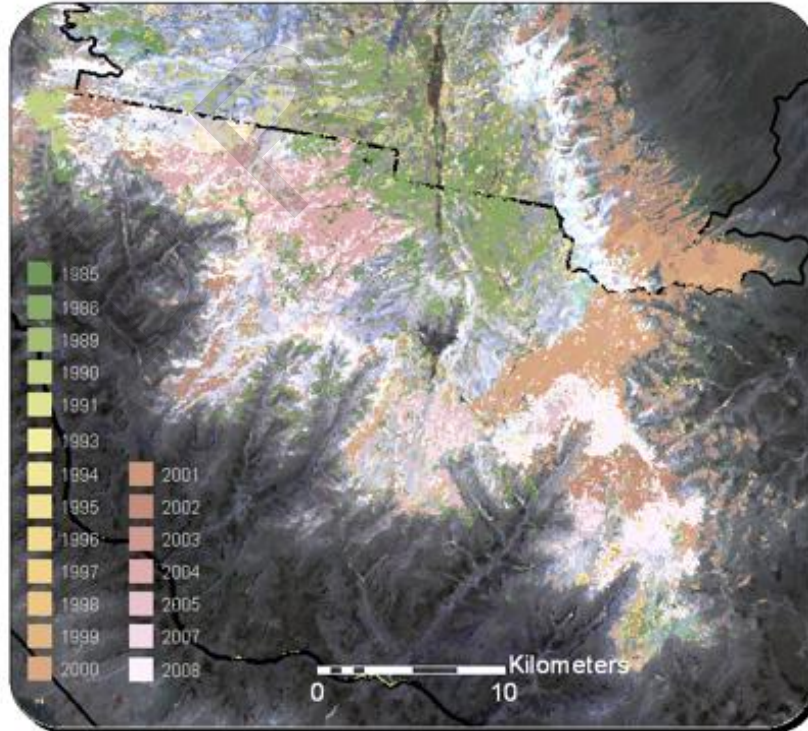


Figure 13. LandTrendr disturbance outputs for the same area shown in Figures 10-12, filtered by percent cover and patch size. Year of disturbance onset is shown; for disturbances that occur over the entire period, year of onset is the beginning of record (e.g. 1985).

3.2 Zion

3.2.1 LandTrendr

We applied LandTrendr segmentation and filtering algorithms to Zion NP using NBR as the index on which segmentation was based. Figure 14 places Zion NP in its elevation and Landsat spectral context

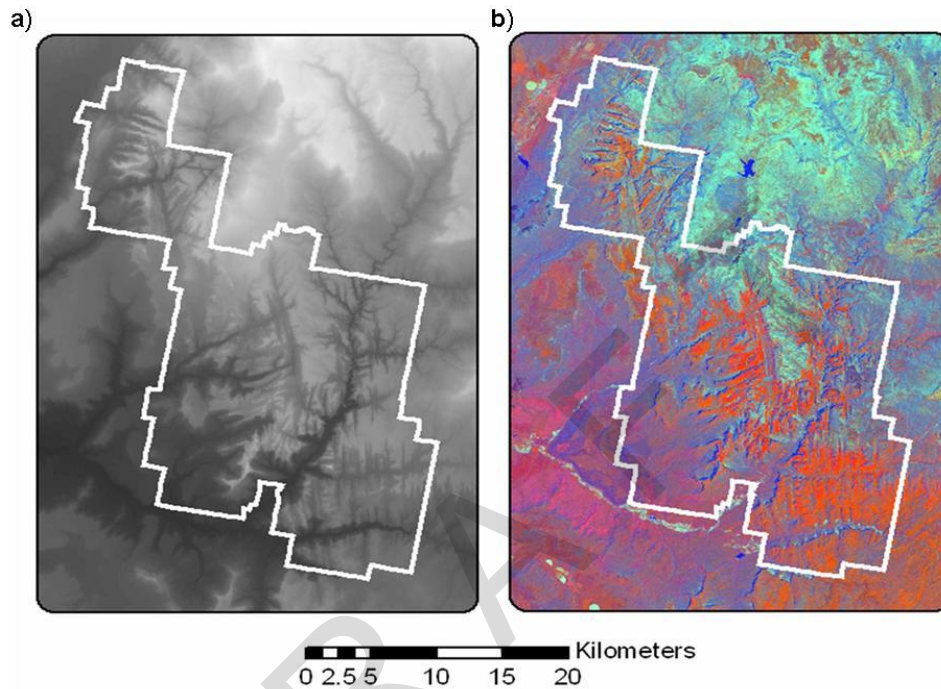


Figure 14. Zion National Park and environs. Park boundary overlaid on a) a digital elevation model and b) a false-color tasseled-cap image from 2006. Tasseled-cap imagery is displayed with brightness in red, greenness in green, and wetness in blue colors. Bare areas appear in red tones, forested areas in cyan and blue tones. Sparse shrub varies depending on the degree of canopy shadowing of background, and ranges from orange to magenta to deep blue.

As observed at GRCA, the LandTrendr algorithms appear to capture well the events and processes in areas of Zion NP with woody cover. Figure 15 shows the filtered output map for severity of disturbance for the park. Fire polygons obtained from the park are overlaid, showing good correspondence with the LandTrendr disturbance estimates. Note that the LandTrendr outputs offer pixel-level estimates of vegetation loss from the fire event, as shown in Figure 16 for the 2001 Langston fire. Also note that areas of the park show apparent disturbance not associated with fire. Figure 17 shows a close-up of one such area that experienced long-duration disturbance with temporal characteristics similar to those observed on the North Rim Grand Canyon. Other disturbed areas not associated with fire may be related to the 2002 drought event. Figure 18 shows a close-up of one such area which appeared to suffer significant loss of vegetation in 2002 that had not recovered after the drought had passed. From the simple “disturbance/recovery” binary labeling scheme afforded by LandTrendr alone, it is impossible to determine whether this was associated with mortality of one component of these systems, or due to loss of vigor or leaf area without actual mortality of the vegetation.

The limitation of a single-index label is also illustrated by the absence of a 2006 fire from the disturbance map shown in Figure 15. Upon further investigation (Figure 19), it was apparent that this fire was indeed detected during the segmentation phase, but was dropped in the filtering process because the pre-disturbance percent cover estimates suggested it had not been vegetated. Clearly, the rules for filtering disturbance data would need to be tuned to the conditions of the park before reliable filtered maps could be produced. However, the raw information from the segmentation is always retained, and various approaches for post-processing and mapping from this raw information could be employed or developed as the specialized knowledge of the parks increases. As this knowledge base increases, the types of change detectable and mappable with the LandTrendr outputs should increase.

Finally, processes of increased growth (encroachment, regrowth, succession) can be captured (Figure 20), although again the specific process occurring cannot be labeled beyond the general observation of increased vegetative cover.

DRAFT

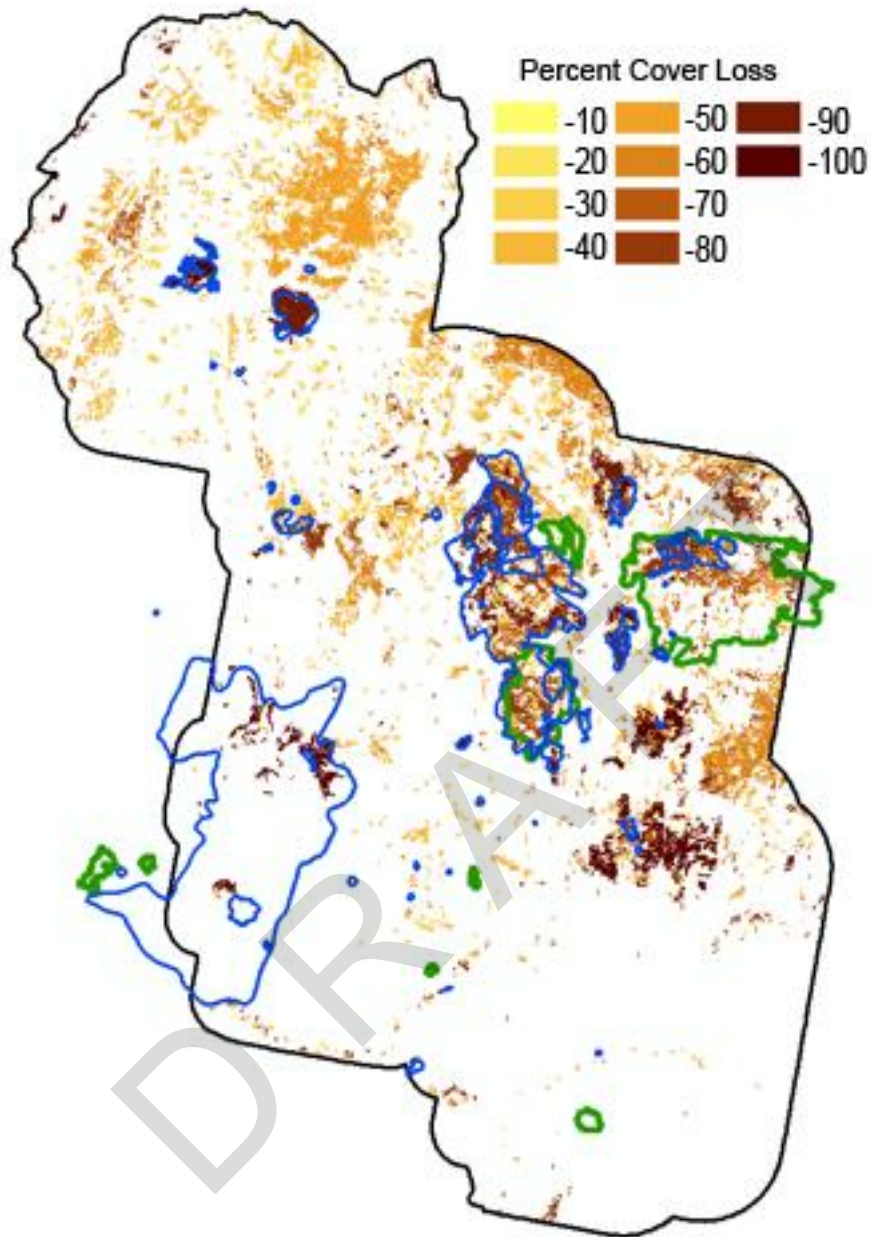


Figure 15. Filtered LandTrendr disturbance severity map for Zion NP, with known fire polygons overlaid. Green polygons are fires that occurred before the period of Landsat record and are for reference only. Blue polygons are those to which LandTrendr should be responsive. Note extensive areas of apparent loss of cover not associated with fire, as well as a fire event in the southwest portion of the park that was not labeled in this disturbance map. Both are addressed in the subsequent figures.

Landsat-based monitoring in the parks of CP

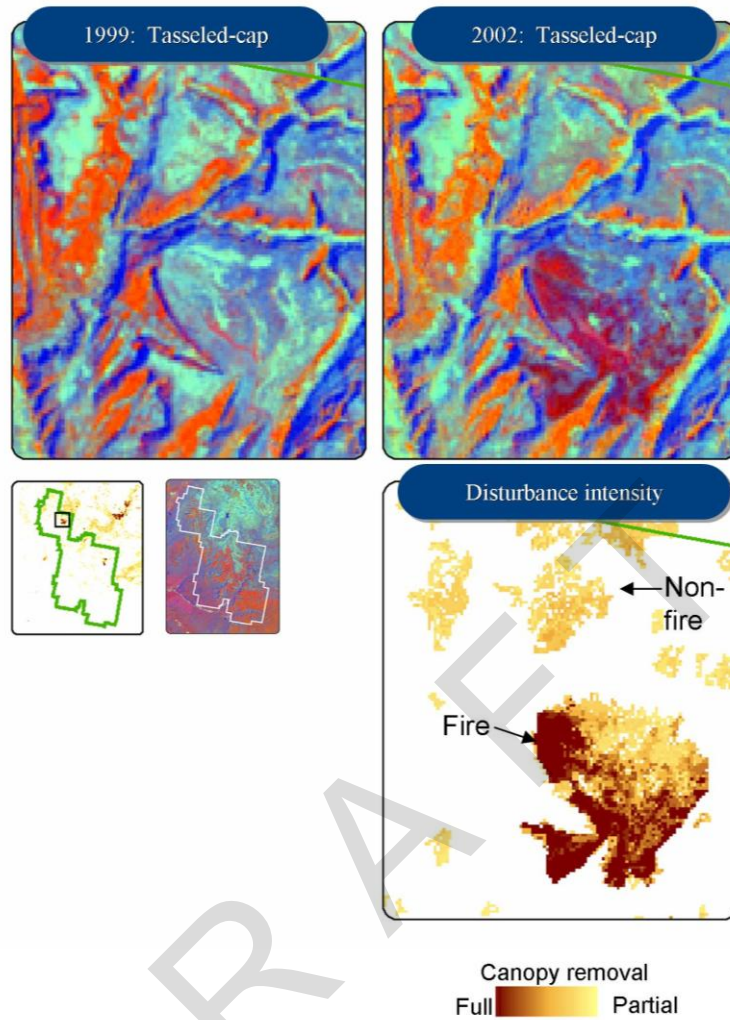


Figure 16. Detail of LandTrendr disturbance mapping for the 2001 Langston Fire. The fire itself shows a range of canopy removal intensities. Note the significant areas of partial canopy removal not associated with the fire.

Landsat-based monitoring in the parks of CP

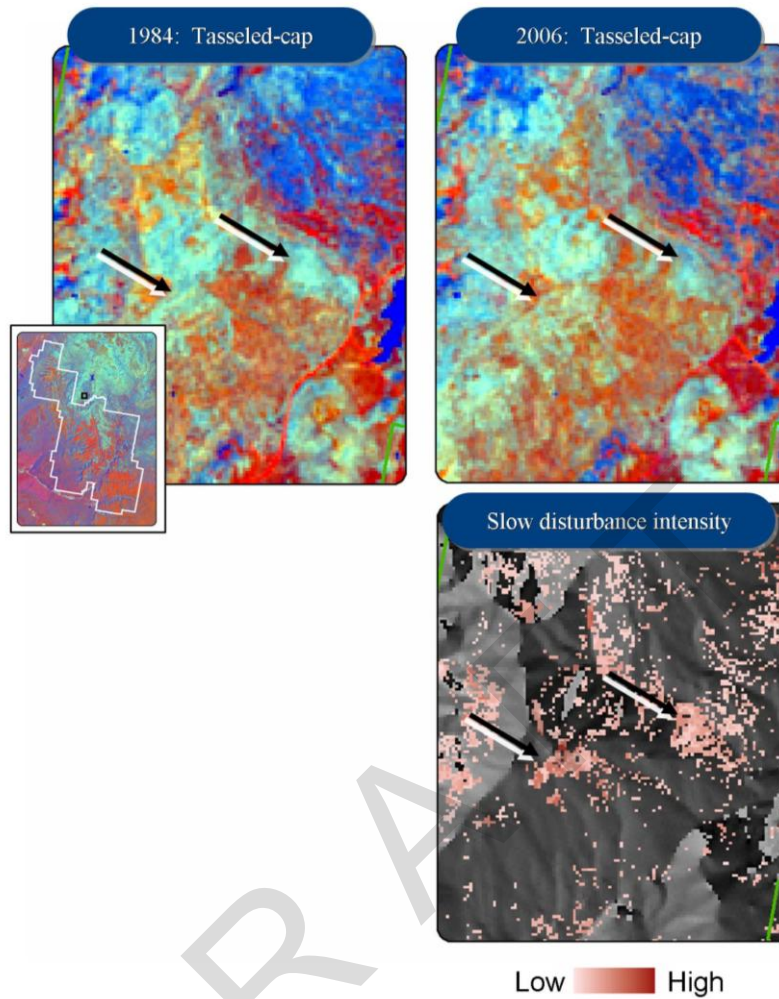


Figure 17. LandTrendr maps of slow disturbance in forested systems just outside the park. Arrows help identify which areas are affected in the two image dates. In both cases, the decreases in cover are subtle but real, suggestive of either insect mortality or delayed effects of forest management.

Landsat-based monitoring in the parks of CP

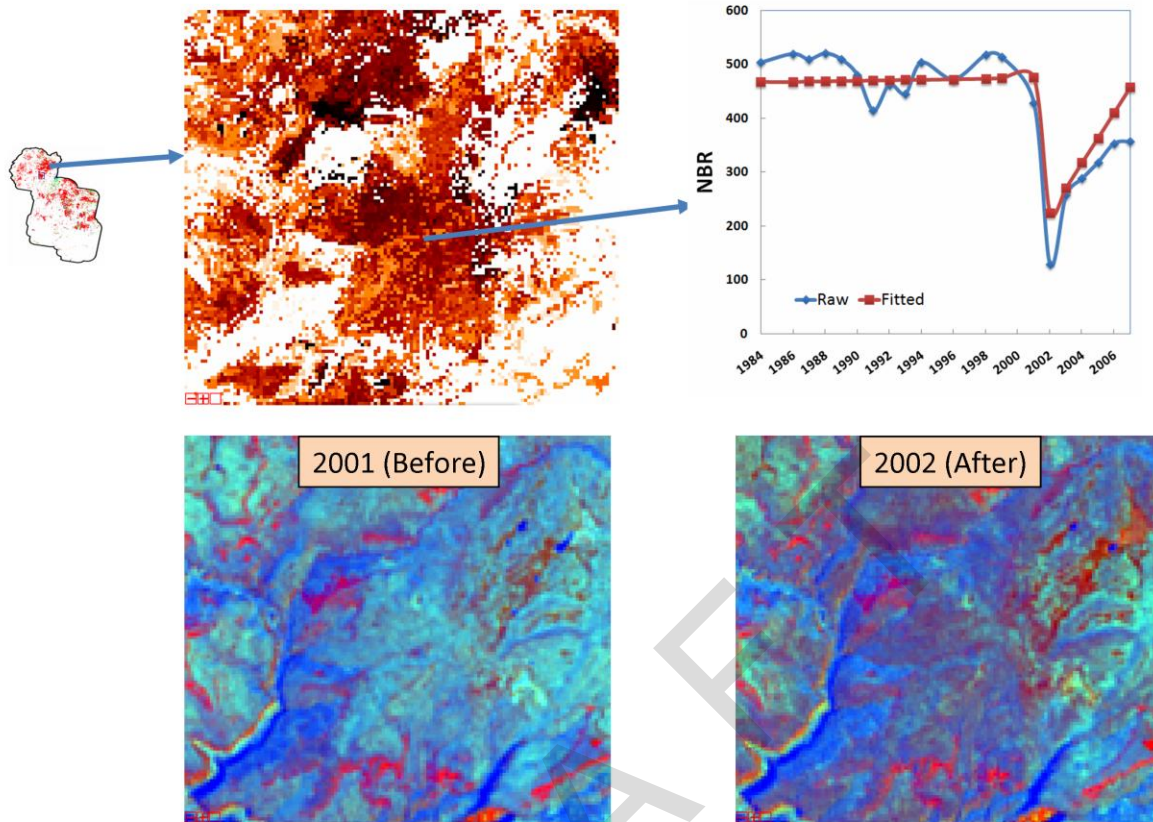


Figure 18. LandTrendr disturbances noted for the northern portion of Zion NP in the year 2002 that was not associated with a fire polygon. This disturbance event had persistence beyond just the year 2002 (see trajectory), suggesting that although it may have been triggered by the 2002 drought event, it caused longer-term impacts on the vegetation.

Landsat-based monitoring in the parks of CP

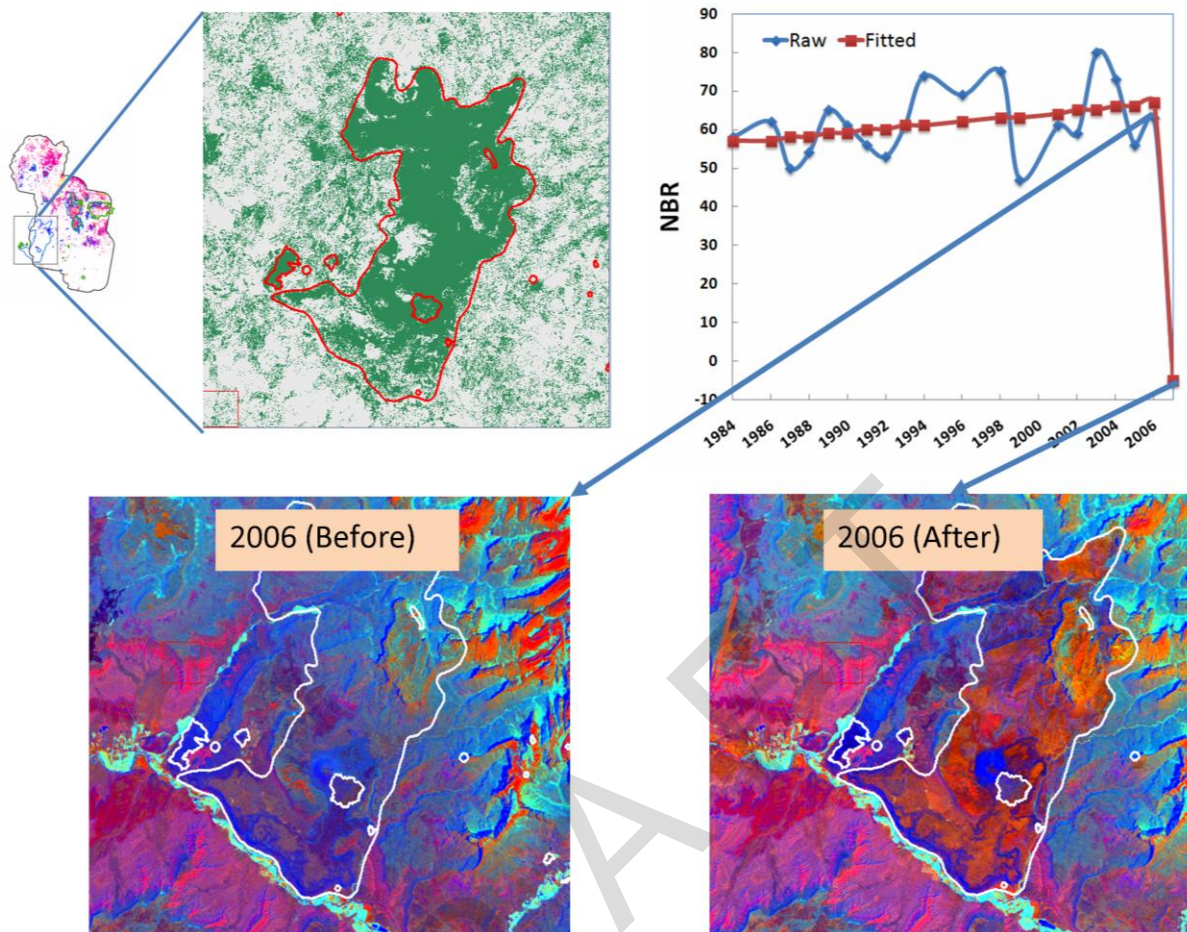


Figure 19. Closer examination of the 2006 fire at Zion that was eliminated in the disturbance filtering process. a) A close-up of the LandTrendr segmentation vertex image, showing that the impact of the fire was indeed captured by LandTrendr, a fact corroborated by the trajectories of individual pixels in the fire (b). However, the starting NBR value before the fire (between 50 and 70) was so low that the starting cover estimates fell below our standard pre-disturbance threshold for detection, resulting in the pixels associated with the fire being masked. For reference, we also show false-color tasseled-cap images before (c) and after (d) the fire.

Landsat-based monitoring in the parks of CP

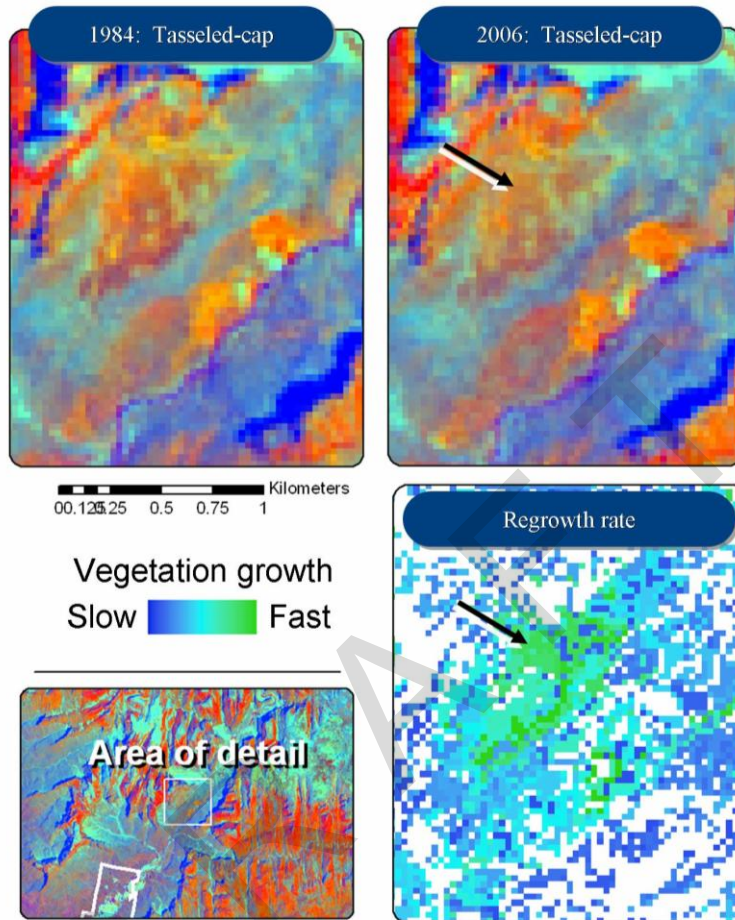


Figure 20. LandTrendr map of vegetative growth for a portion of Zion NP. In the patch noted by the arrow, tasseled-cap values progress slowly from dark reds to increasingly yellow as greenness increases.

3.2.2 LandTrendr + POM

The core of the LandTrendr + POM approach is the creation of temporally smoothed spectral data spaces on which a standard POM methodology can be applied. Development of procedures and code to create these temporally smoothed images was a major focus of our work in this project.

A visual example of the result of the fitting process at Zion NP is shown in Figure 21. At the scale of the whole landscape, the fitted and original tasseled-cap images appear very similar. Close examination, however, shows that the original 2002 image had large areas with apparently lower vegetation cover, as indicated by darker red tones in the vegetated northeastern third of the image in Figure 21. The fitted tasseled-cap image removes much of this effect, indicating that the LandTrendr algorithms determined that much of the 2002 vegetation change was ephemeral, caused either by different phenological status at the time of image acquisition or by a single-year change in vegetation vigor, such as that caused by the drought event in 2002. Importantly, however, the areas of the landscape where the 2002 event was *not* ephemeral – i.e. that experienced sustained effects – manifest that effect in the 2002 fitted image.

The distinction between the original and fitted 2002 images is even more apparent in the two-date image differencing shown in Figure 22. The original imagery found large swaths of the area north and east of the park to be brighter and less vegetated (as indicated by red tones in the difference image) in 2002 versus 1999. In the difference of the fitted image, however, only areas where the change persisted are captured as change. From the perspective of long-term landscape dynamics, the persistent change is likely to be more relevant than the ephemeral change.

The results in Figures 21 and 22 suggest that the fitting process has significantly reduced the year-to-year variation in spectral signal, as we had hoped. Such variability was determined in the pilot project to be a primary obstacle to interpretation of two-change detection maps in the CP parks. Although imagery alone cannot verify whether the remaining changes in Figure 22 are real, the likelihood of them being false change is significantly reduced. Nevertheless, direct visits in the field would be needed to corroborate or deny the observations.

Landsat-based monitoring in the parks of CP

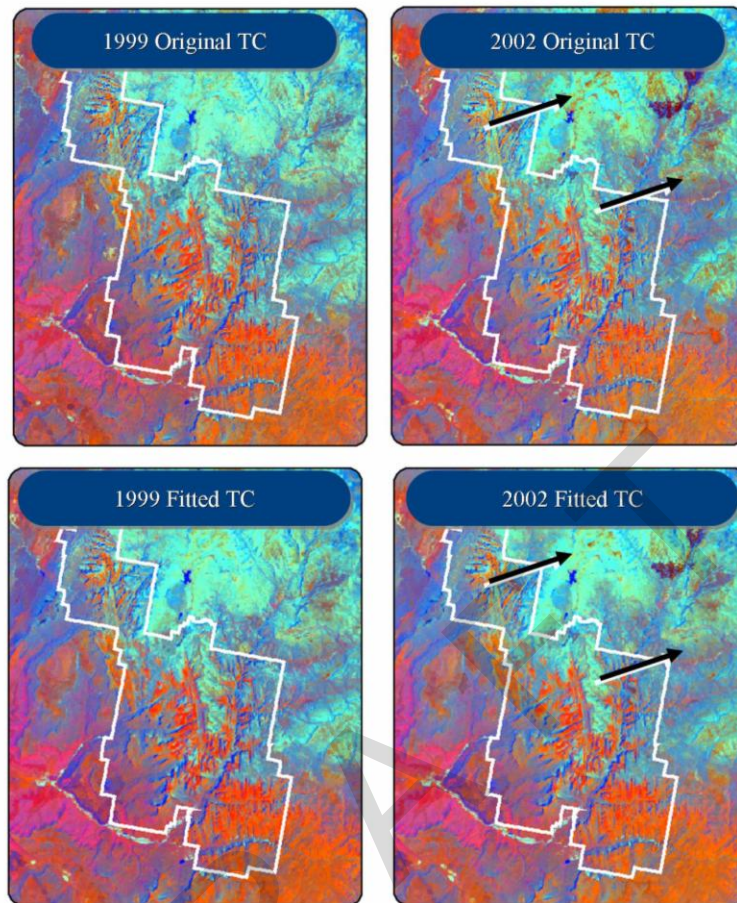


Figure 21. Comparing original tasseled-cap imagery with that derived from the fitting process of LandTrendr. Note that much of the northeastern quadrant of the image shows less vegetation (more dark red tones in a matrix of cyan and blue tones) in the 2002 original image, but that these ephemeral effects disappear in the fitted image.

Landsat-based monitoring in the parks of CP

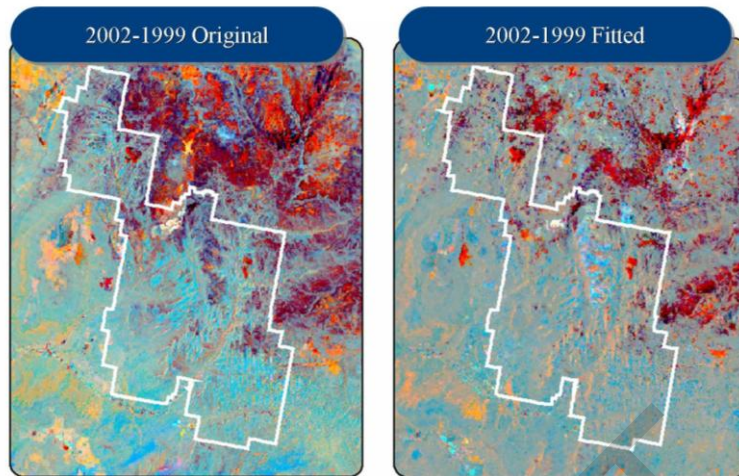


Figure 22. Examining the effect of fitting on two-date differencing of tasseled-cap imagery. Greyish tones are areas with relatively little spectral change, while colors denote change, with reds indicating less vegetative cover. Note that the unfitted imagery shows broad patterns of apparent spectral change, but that the fitted imagery only shows a subset of those changes whose spectral signal persists, indicating higher likelihood of actual change.

After fitted tasseled-cap images were produced, the POM process was applied. We developed a simplified set of class labels based on the original NPSVM labels for Zion NP, augmented with our experience from the prior project to guide aggregation rules. Table 3 shows the class labels used for mapping at Zion NP.

Table 3. Rules used to aggregate NPSVM map labels at Zion NP.

New class name	Source classes and rules
Barren	Physiognomic class: Barren
Deciduous forest	Ecological group: Deciduous forest
Herbaceous	Physiognomic class: Herbaceous
Open shrubland	Physiognomic class: Closed canopy shrub; <25% cover
Closed Gambel oak	Physiognomic class: Shrubland; Vegetation name: Gambel oak; 75-100% cover
Semi-closed Gambel oak	Physiognomic class: Shrubland; Vegetation name: Gambel oak; 25-75% cover
Other shrubland	Physiognomic class: Shrubland not belonging to prior categories
Open coniferous forest	Ecological group: Coniferous forest; 5%-25% cover; Shrub; 0-25% cover
Closed coniferous forest	Ecological group: Coniferous forest; 75%+ cover
Semi-open coniferous forest	Ecological group: All remaining coniferous forest
Close coniferous woodland	Ecological group: Coniferous woodland; 75%+ cover
Coniferous woodland mixed shrub	Ecological group: Coniferous forest; 25 % cover; Shrub 50-75% cover; Not Gambel oak
Gambel oak mixed coniferous woodland	Ecological group: Coniferous forest; 25 % cover; Shrub 50-75% cover; Gambel oak
Open coniferous woodland	Ecological group: All remaining coniferous woodland

These groupings are one slice through the labeling space of the original map. We applied the standard POM process to the NPSVM park map using these grouping and applied them to the fitted 1999 tasseled-cap image for Zion, resulting in the fitted POM map shown in Figure 23. We note both broad agreements in spatial pattern, but also significant loss of detail in class names. The loss of specific classes from the NPSVM map indicates that they were spectrally ambiguous relative to some other similar class. For example, the “closed Gambel oak class” in the aggregated NPSVM map appears to have spectral characteristics that span other classes, notably the “deciduous forest” class. Similarly, the “open coniferous woodland” class appears to be spectrally ingested into both the “barren” and the “coniferous woodland mixed shrub” classes. In practice, most of the POM-derived map is composed of these classes: “deciduous forest,” “coniferous woodland mixed shrub,” “closed coniferous woodland,” “other shrubland,” and “barren.” Note that the “land use” and “agriculture” classes are *land use* labels, not land cover, and thus were not included in the training set for POM. Therefore, pixels falling in these classes are labeled by POM according to the spectral properties of the landcover class to which there are most similar spectrally.

The loss of information caused by ambiguity in class labels is offset by the utility of creating land cover maps for every year in the record. Figure 24 shows a subset of the yearly land cover maps for the area including Zion NP. Notable in the yearly cover maps is the consistency of the spatial patterns over time. Where land cover changes occur in these maps, they are likely associated with real change.

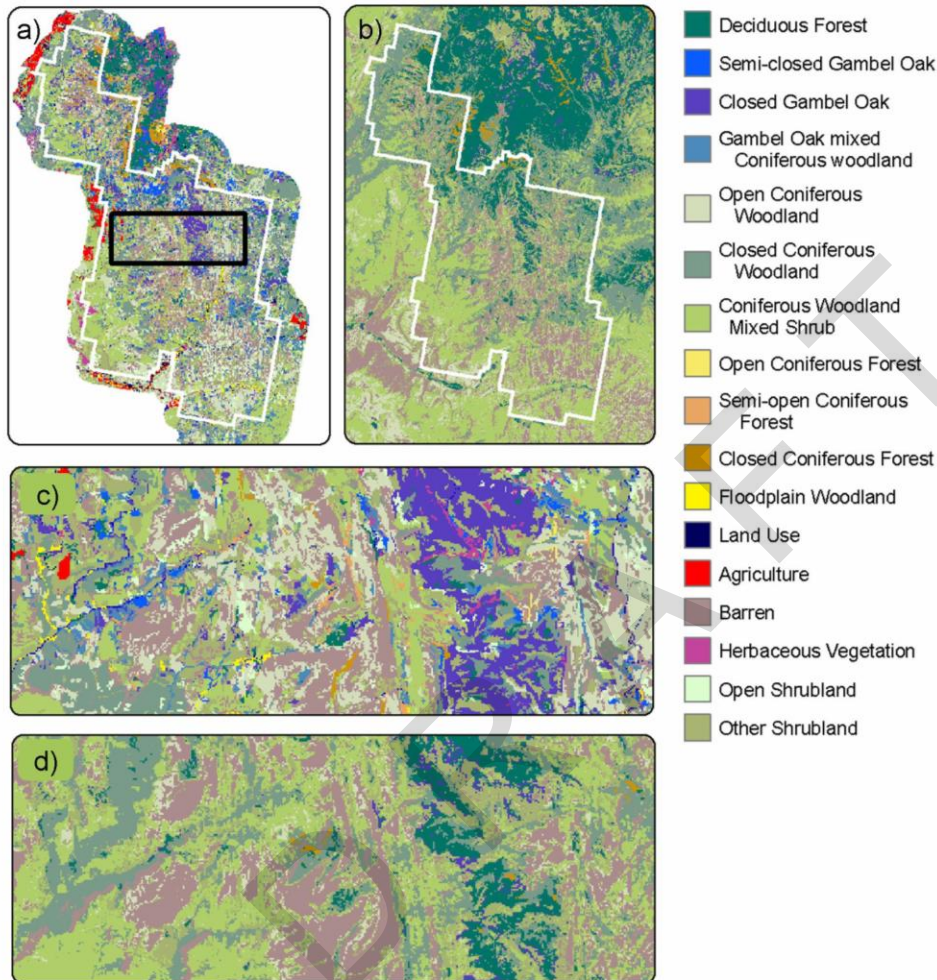


Figure 23. Comparing spatial patterns of cover class labels from the NPSVM map and the Landsat-derived POM map for 1999. a) NPSVM classes have been aggregated according to the rules described in Table 1 of the text. b) Because many of the classes in the NPSVM are not spectrally separable, the POM mapping process places pixels from the spectrally indistinguishable classes into those classes which are closest to them in multivariate space. c) and d) Close-up views of the area shown in the black rectangle in a).

Two detailed examples provide illustration for the type of information content contained in these maps. Figure 25 shows how the Langston Fire (originally shown in Figure 16 above) affected landcover. Before the fire, the area that would eventually burn was a mixture of closed coniferous woodland, closed coniferous forest, and deciduous forest according to the aggregated class map. In the first growing season after the fire, much of the land cover reflected loss of vegetation, as classes transitioned to less-vegetated conditions. By 2006, however, some of the

original spatial patterns of land cover had returned to the portions of the fire that did not burn as intensively, though some other areas saw persistent change in cover. In addition to noting these patterns, it is also instructive to note the consistency of land cover class labels for areas just outside of the burn area, indicating that much of the non-informative spectral change has indeed been removed from mapping.

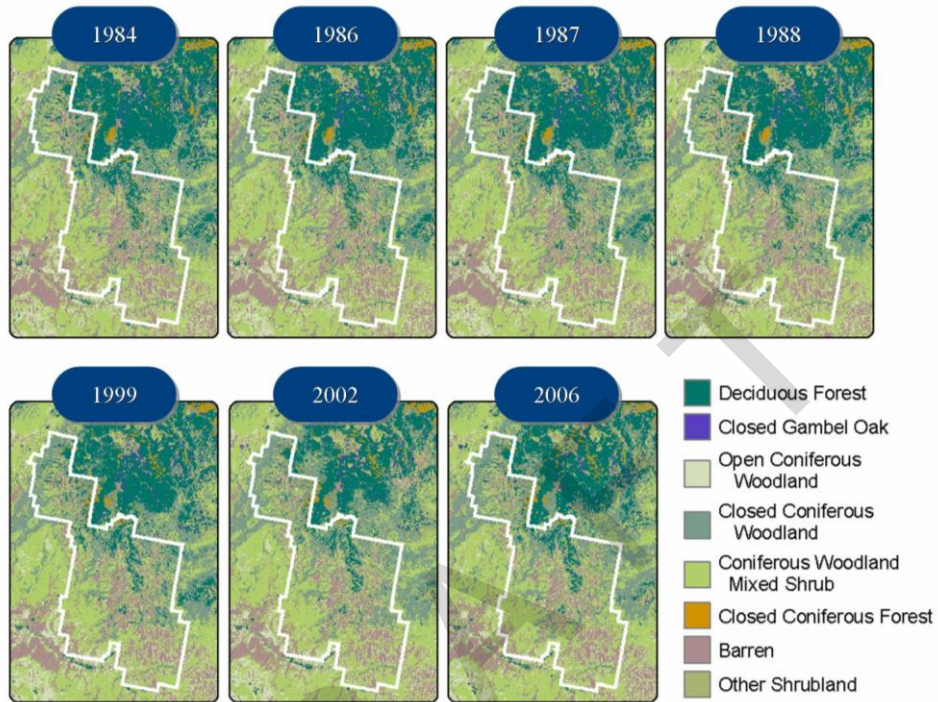


Figure 24. POM-based landcover maps for a selection of years in the stack. Each year's map is based on POM rules developed using temporally-smoothed tasseled-cap data, resulting land cover maps that change little from year to year, except in places where actual change has occurred (see Figure 10). Note: Only the dominant land cover classes are shown in the legend, although in theory the entire set of classes listed in Figure 8 applies.

Landsat-based monitoring in the parks of CP

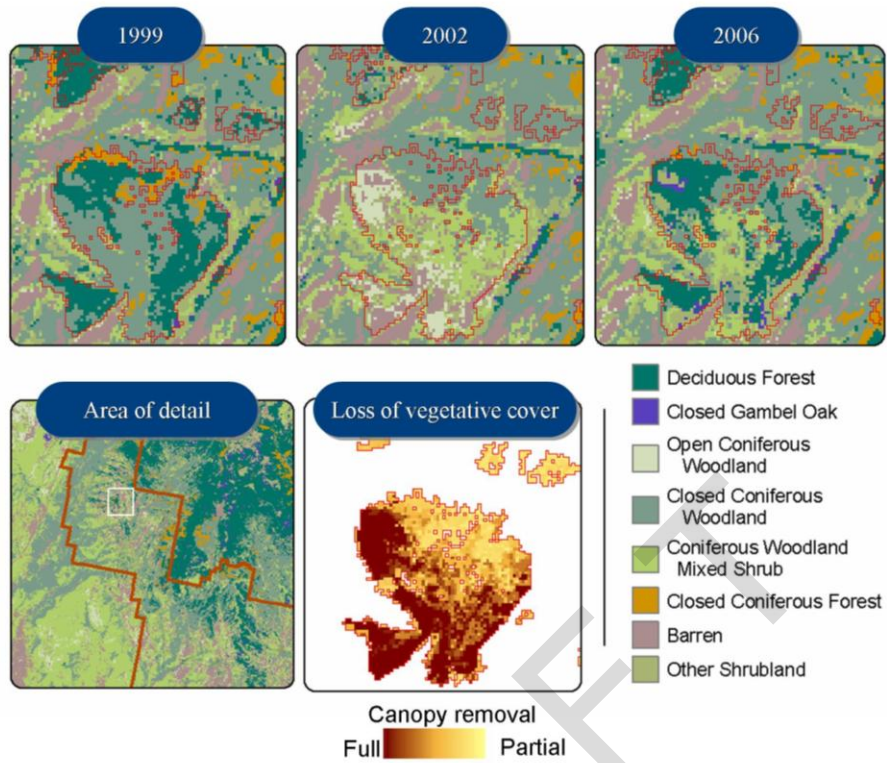


Figure 25. Effect of fire on POM-based landcover maps. The October 2001 Langston Fire changed the mapped cover type from deciduous forest, closed coniferous woodland, and closed coniferous forest in 1999 toward less-vegetated classes in 2002, such as coniferous woodland / mixed shrub, open coniferous woodland, and barren. By 2006, however, some portions of the fire had returned to the cover type preceding the fire and some remained in less-vegetated classes.

Landsat-based monitoring in the parks of CP

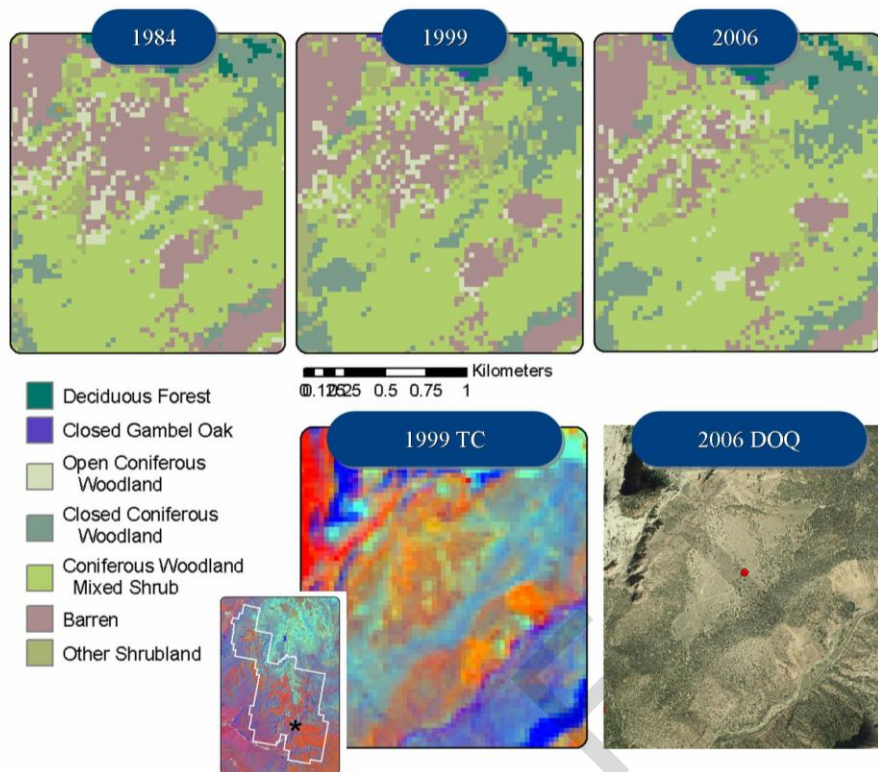


Figure 26. Apparent increase in vegetative cover over a 20+ year period, as captured by POM maps derived from LandTrendr-temporally-fitted imagery. Cover classes progress from generally barren to increasingly vegetated over the time period, suggesting a slow infilling of shrub vegetation.

Because one of the strengths of the LandTrendr approach is detection of long, subtle trends, slow increase in apparent vegetation cover can also be captured in the derived cover maps. Figure 26 shows how the vegetation increase originally shown in Figure 20 manifests itself in the land cover maps. This figure is striking in illustrating how a subtle effect that could not be resolved with simple two-date change detection can be more confidently mapped using information from the entire temporal trajectory.

The POM approach also reveals weaknesses in the assumptions that underlie most satellite-based land cover maps. Figure 27 shows the progression of POM land cover classes associated with the areas first shown in Figure 18, presumably associated with the drought event of 2002. As expected, the spectral changes caused by the fire result in changes in the POM labels from 2001 to 2002, and these persist through 2007 for several areas. However, the actual labels for those post-disturbance classes do not appear to be ecologically possible: deciduous forest in 2001 converts immediately to Open Coniferous Forest and Closed Coniferous Woodland in 2002. Based on these class calls alone, one would be challenged to infer that this is indeed a disturbance-mediated transition. From a strictly spectral perspective, however, these labels are consistent with what is seen in the tasseled-cap images associated with these changes. In 2002, there is indeed loss of greenness (indicative of loss of deciduous forest leaf area), but there is also a decrease in overall brightness of the area, perhaps caused by increased shadowing from remaining woody vegetation or by dark burn scars.. This darkening and increased shadow is

similar spectrally to the natural spectral condition of intact conifer canopies and conifer woodlands, even though the canopies in this area may or may not include actual conifer species.

These observations suggest that the cover labels associated with particular regions of spectral space may need to be altered for immediately-post-disturbance conditions. Most maps based on satellite spectral data can only capture conditions at a single date, and such post-disturbance conditions rarely can be adequately separated in this static mapping mode. Because the POM approach is based on a static map, and because the yearly POM maps are simple applications of the static mapping rules, our POM maps also suffer from this ambiguity. While no straightforward recourse is available to solve this problem given the data at hand, it points to a potential need for change in land cover mapping philosophy. For the purposes of interpreting some types of land cover change from the POM maps, it represents an important caution on how users interpret the changing POM classes over time. It should be noted, however, that this effect is likely only relevant for disturbances that remove only a portion of the vegetative canopy, because these cause novel combinations of partial shadow and vegetative cover. Full removal of the canopy removes the shadowing effect.

DRAFT

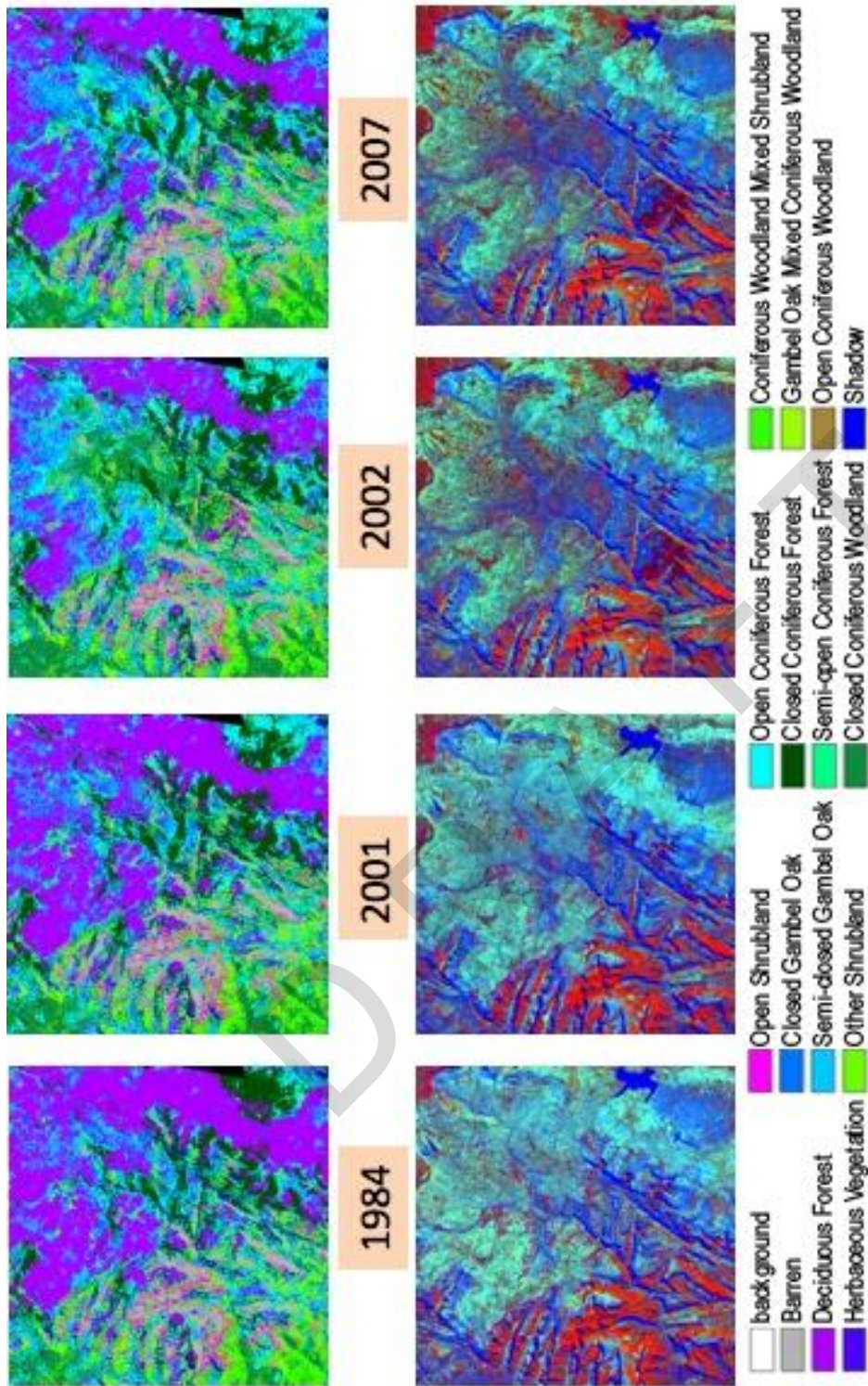


Figure 27. An example of LandTrendr + POM capturing land cover changes apparently associated with the 2002 drought for the area shown originally in Figure 18. Areas largely classified as deciduous forest moved abruptly in 2002 to spectral conditions more similar to conifer forests. While some areas had returned to pre-2002 labels by 2007, much of these remained in an altered cover class condition. Possible reasons for the conifer-class labels are discussed in the text.

3.3 WUPA

3.3.1 *LandTrendr*

Application of LandTrendr to Wupatki National Monument was expected to test the bounds of the method. LandTrendr algorithms were developed for woody systems quite different from the arid non-woody systems that dominate at WUPA. After experimenting with both NBR and tasseled cap wetness indices, we determined that wetness was a more robust means of capturing processes at WUPA than NBR. All subsequent results are thus based on wetness. Because of the limited scope of this pilot project, we did not explore a full suite of spectral indices.

Fitted outputs show that LandTrendr at WUPA detected a variety of events or processes with spatially coherent patterns (Figure 28). As with Figures 10-12 at GRCA, these images are color composite of three layers of fitted output data, with grey-scale tones indicating no detectable change and colors corresponding to some type of change. Much of the area in the northern half of the monument appears to have undergone change, as indicated by the magenta tones, and some smaller patches of change are evident throughout. Because the wide range of wetness values compresses the color stretch, visualization of this fitted image at the scale of the park is difficult. By focusing on just a smaller part of the monument with known fires (Figure 29), the narrower color stretch allows richer interpretation of fitted data information content. Based on these data, it appears that the LandTrendr segmentation captures the fire events.

The same cannot be said for juniper mortality. Comparing the LandTrendr fitted outputs to a polygon provided by the NPS outlining an area of juniper mortality suggests that the segmentation is not capturing any coherent signal in the area (Figure 30). Closer examination shows that there may be some promise in detecting change in this area, but that at best the effect is very subtle in the spectral signal, and that much of the area shows no noticeable change (Figure 31). It is unclear whether the lack of spectral change is because the change in vegetative condition is too subtle, or because the change in condition of the target vegetation is compensated by other change in non-target vegetation (herbaceous understory or shrubs, for example). Direct observation in the field would be necessary to determine whether this is in fact a true “false negative.”

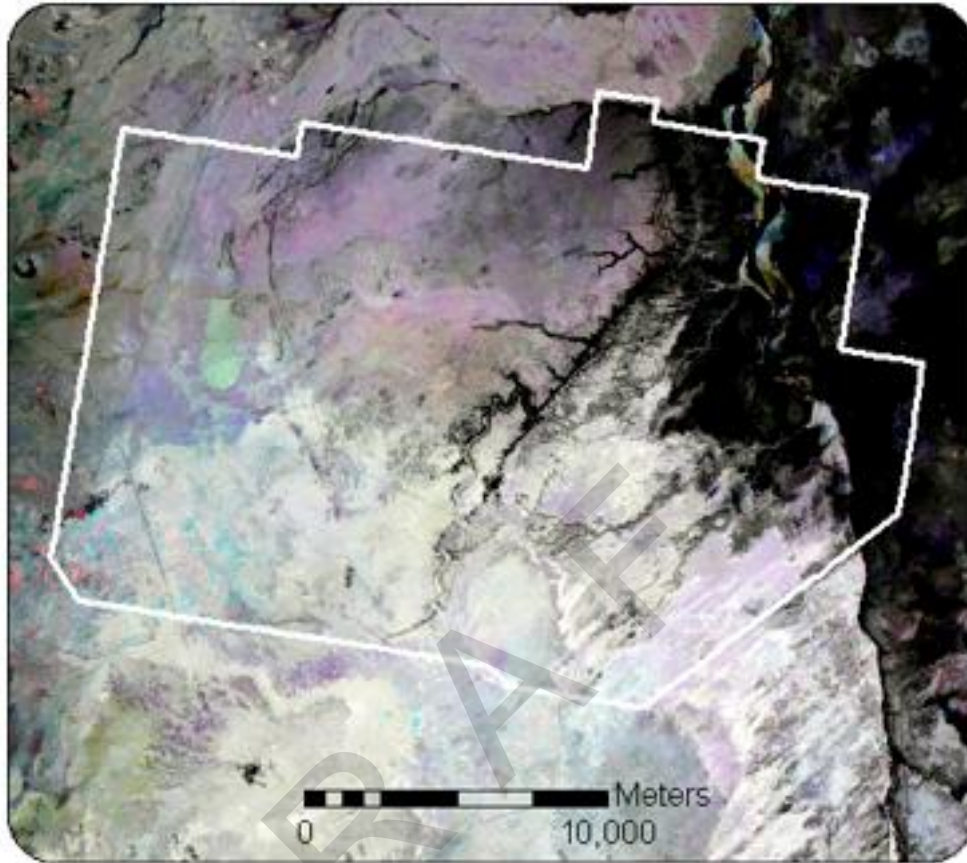


Figure 28. LandTrendr fitted outputs for Wupatki National Monument (WUPA). Shown are years 1984, 1996, and 2008 from fitted wetness outputs. As in Figures 10-12 for Grand Canyon, black to white tones indicate no-change, while colors suggest change has occurred.

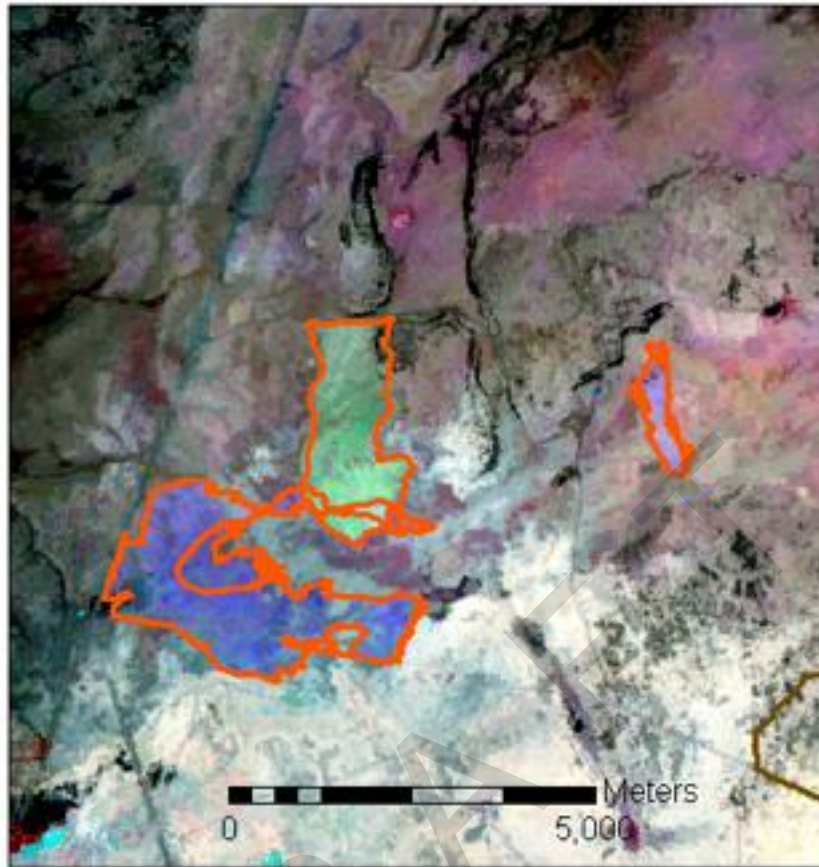


Figure 29. A closer examination of fitted outputs and fire events at WUPA. Fire polygons are shown in orange. LandTrendr segmentation appears to capture these fire events, as well as other dynamics on the landscape.

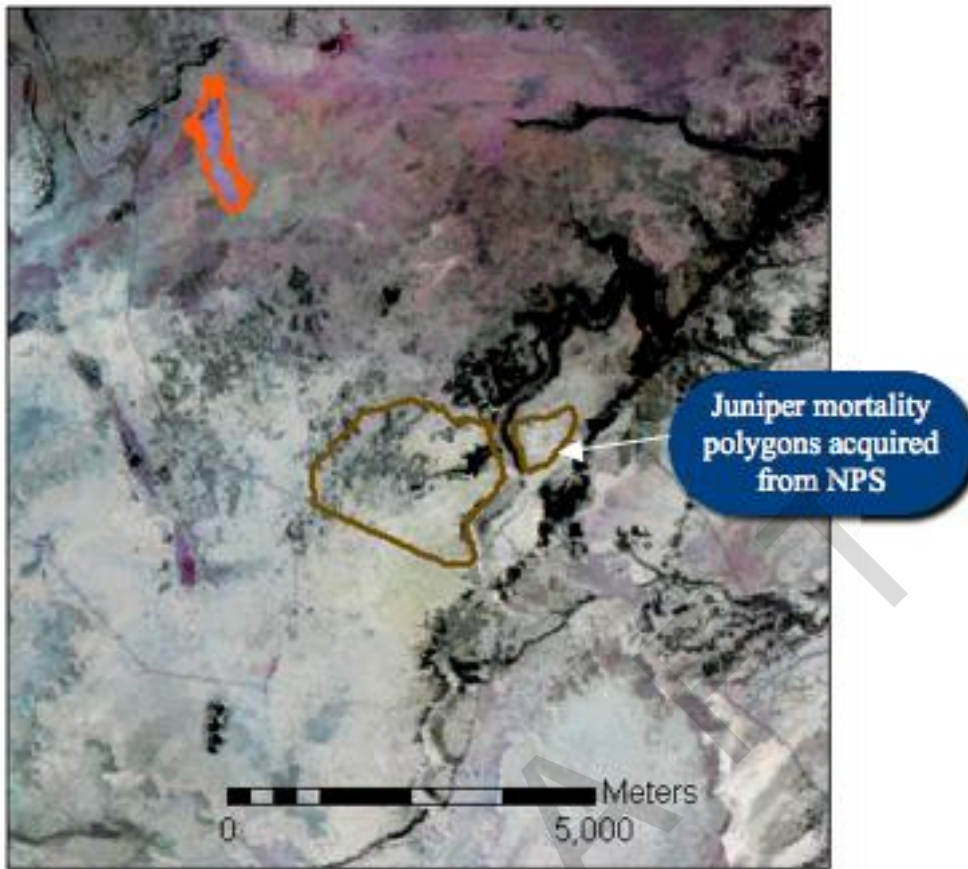


Figure 30. LandTrendr fitted data with an overlay of polygon data from the NPS indicating an area of juniper mortality (brown outline). LandTrendr does not appear to capture any of this mortality event (as indicated by absence of color in this fitted output image).

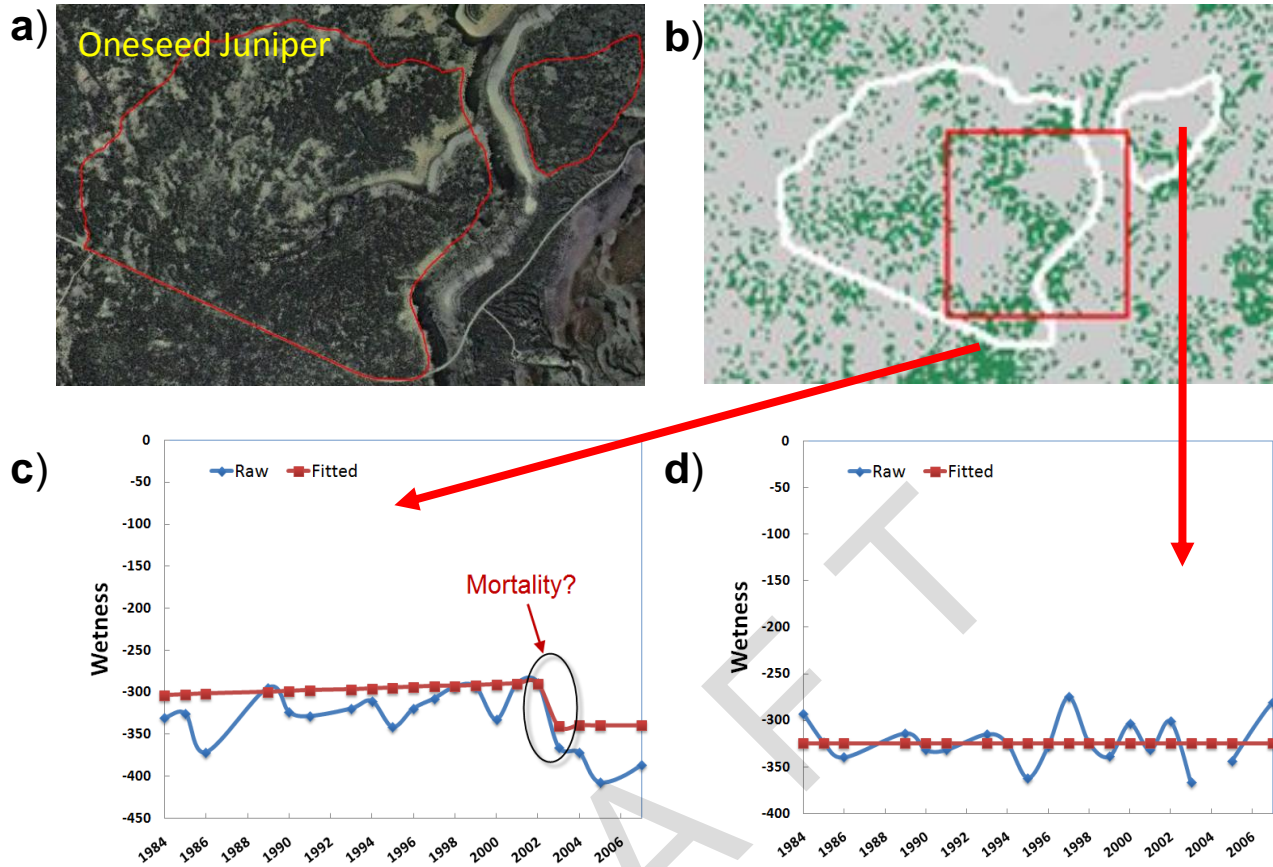


Figure 31. Closer examination of the juniper mortality area indicated in Figure 30. a) A digital orthoquad image of the area. b) A map of pixels showing a segmentation vertex in the year 2003 (in green), indicating that parts of this polygon appeared to see some evidence of change. c) An example of a “green” pixel from part b. The signal is very slight, although may be sufficient to be captured. d) Much of the area shows no sign of coherent spectral change over time.

Spatial patterns also emerged when the LandTrendr fitted outputs were filtered using vegetative cover and patch size thresholds. Figures 32 and 33 show filtered outputs for segments of decreasing and increasing wetness, respectively. In woody systems, decreasing wetness is typically associated with loss of vegetative cover and disturbance, while increase in wetness is associated with increasing cover and regrowth. [Note that the use of the term “wetness” for this spectral index is by historical convention only; actual water or wetness is likely not the driver of this index in these systems.] Close examination of Figures 32 and 33 shows that this is not necessarily the case for the grassland systems of WUPA. The fire events originally shown in Figure 29 are visible, for example, in the western half of the monument, but the direction of change is opposed to what would be expected in a woody system. Figure 34 illustrates this in detail for the 1995 West fire. When the fire burned in 1995, wetness actually increased markedly, and only began to decrease again after the fire. Thus, the initial fire event was captured for the correct year in the filtered image for increasing wetness (Figure 33), a result contrary to that expected from woody systems. This behavior was not an anomaly: The same behavior was found in the 2002 Antelope fire, suggesting that the signal of fire in these grassland systems is consistent, albeit opposed in sign to that expected in woody systems. Based on the dark

appearance of the post-fire images, wetness appears to be responding to the charred soil caused by the fire rather than to rapid regrowth of herbaceous vegetation (which would be bright). Date ranges for these images are constrained to similar periods within the growing season, and the consistency of this effect in two image stacks (both for Zion and WUPA) further corroborates the generality of this phenomenon. Collectively, these examples illustrate that it is not feasible to simply label trajectories as “disturbed” or “recovering” from the perspective of a single index in these arid grasslands, and that filtered mapping in WUPA (and likely in other similar parks of the CP) will require more investigation before disturbance and growth labels can be robustly applied. But the generality of this particular effect suggests that new approaches would have more than esoteric utility. In all cases, we expect indices anchored in the short-wave infrared (such as the NBR and wetness) to be more stable from year to year than those based on the near-infrared and visible (such as NDVI), likely making them more useful for capturing subtle change.

Despite the ambiguity of labeling, the filtered data corroborate an interesting pattern first observed in the original segmentation outputs shown in Figure 28. The northern portion of the monument and the areas outside the monument appear to be experiencing changes with coherent spatial patterns. Figure 36 shows that these patterns have coherent temporal characteristics as well: wetness decreased from the beginning of observation until the mid-1990s, whereupon it shifted abruptly in sign toward increasing wetness. The effect appears to span the ownership boundary, suggesting it is not a simple function of management, but the cause of this phenomenon is not clear from the spectral data alone. Nevertheless, this example shows the potential utility of the trajectory approach in flagging apparently coherent patterns, allowing direct investigation on the ground to understand what may be occurring.

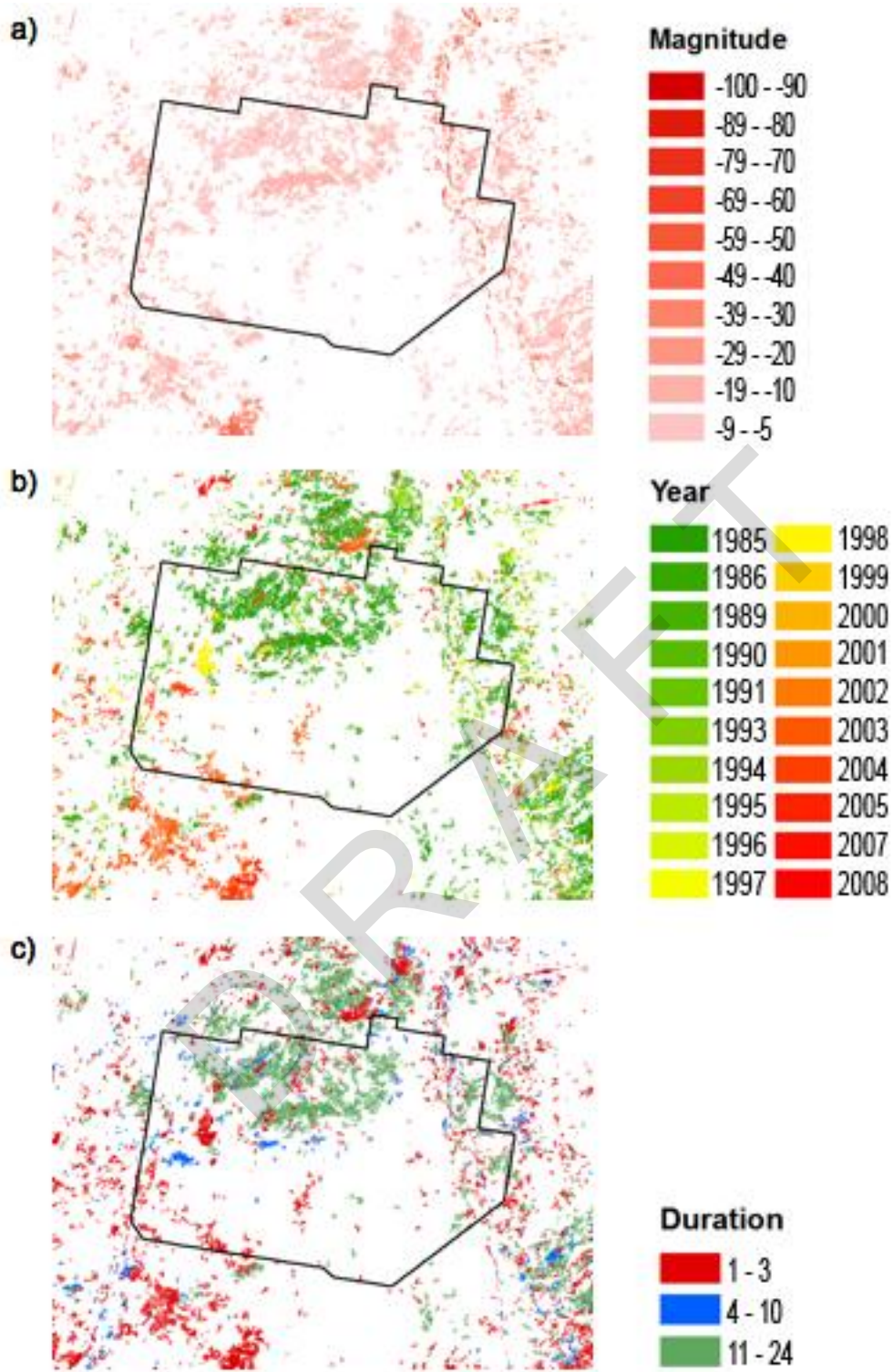


Figure 32. Filtered LandTrendr outputs for events related to declining wetness, typically associated with loss of vegetation in woody systems. a) Relative vegetation loss b) Year of onset c) Duration (in years).

Landsat-based monitoring in the parks of CP

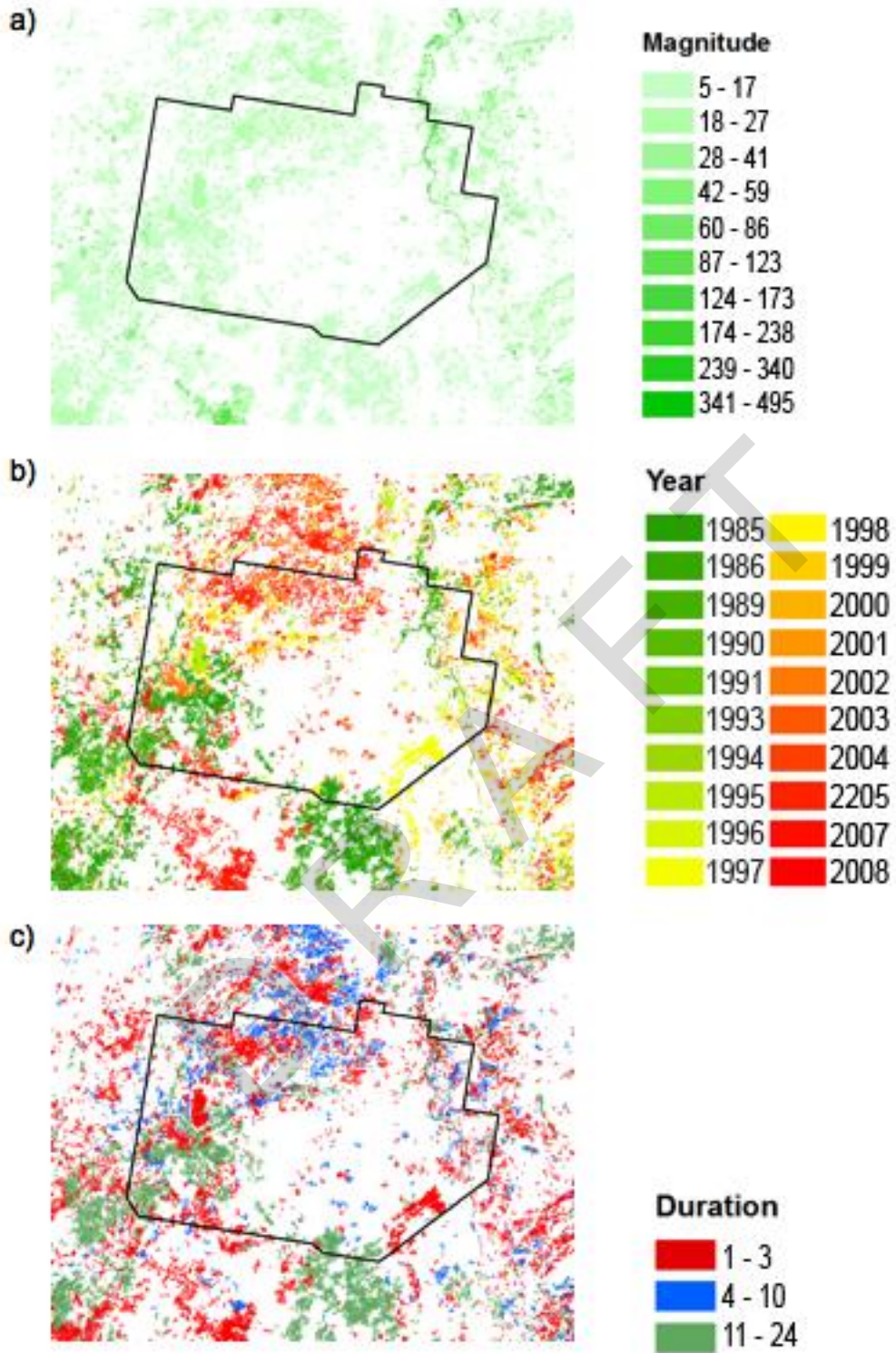


Figure 33. Filtered LandTrendr outputs for events related to increasing wetness, typically associated with increase of vegetation in woody systems. a) Relative vegetation gain b) Year of onset c) Duration (in years).

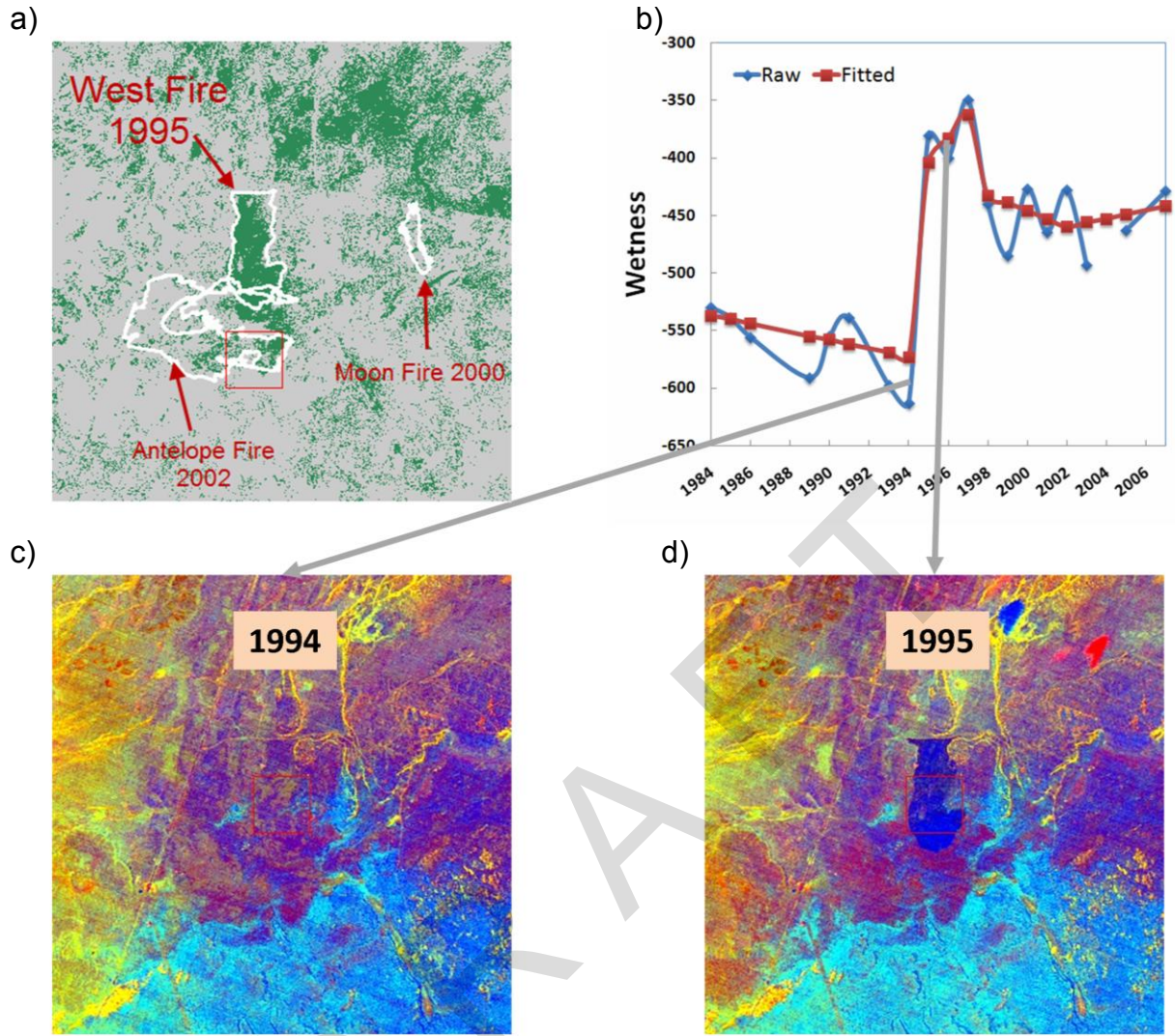
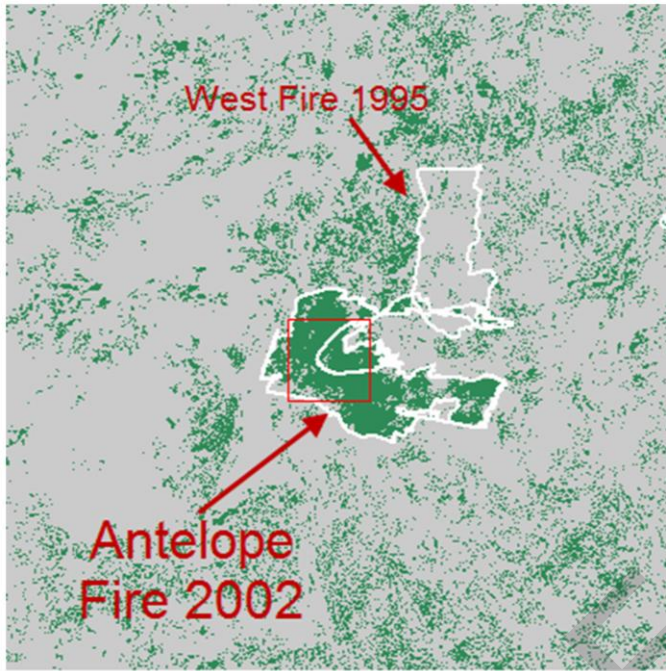


Figure 34. Closer examination of the 1995 West Fire. a) An image showing pixels in green whose segmented trajectory showed a vertex in 1995. The West fire outline is clearly visible. b) The wetness trajectory for a single pixel in the West fire. Unlike the case for woody systems, wetness increased markedly when the fire passed through. c) Tasseled-cap brightness, greenness and wetness in the Red, Green, and Blue bands, respectively for 1994 c) and 1995 (d).

a)



b)

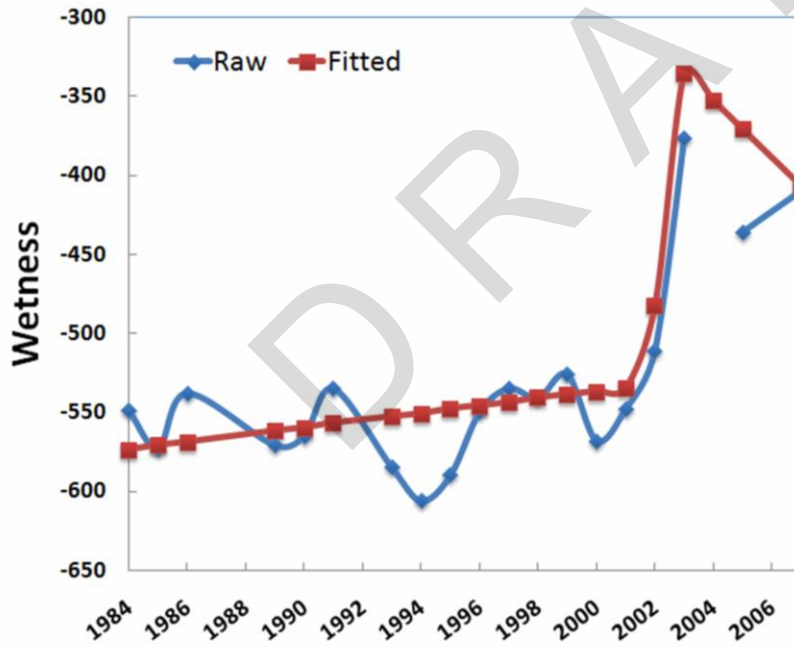
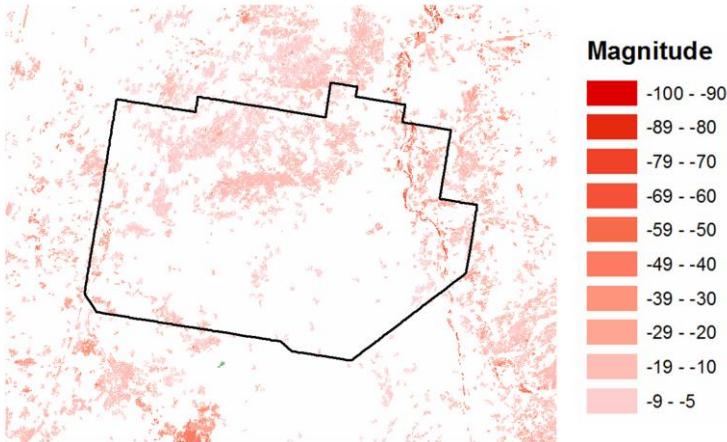
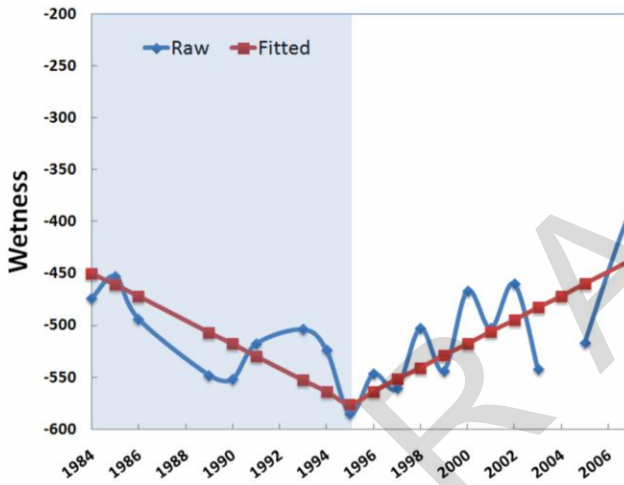


Figure 35. Details of the 2002 Antelope fire, showing a similar increase in wetness after the fire. a) The vertex image for 2002. b) The wetness trajectory of a typical pixel from the fire.

a)



b)



c)

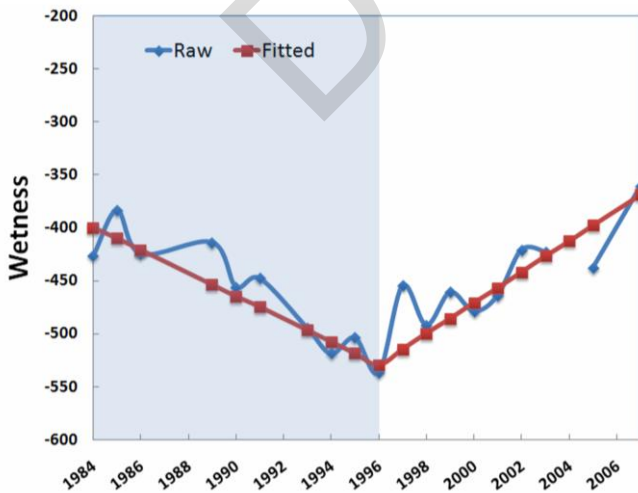


Figure 36. Much of the northern half of WUPA appears to have undergone coherent change in wetness that changed sign in 1996. Both pixels shown here are in areas classified as “Galleta Mixed Grasslands”. The phenomenon appears to be occurring both inside and outside of the monument.

3.3.2 LandTrendr + POM

As was the case at ZION, the transition at WUPA from the NPSVM classification to the POM class map resulted in an overall agreement in broad spatial patterns but a rearrangement of class dominance and, to some degree, landscape position (Figure 37). Application of the POM across years at the monument shows similar stability in class label seen at ZION (Figure 38), which is a promising result given that variability in the spectral signal at WUPA was a significant impediment to change mapping in the two-date case tested under our prior project.

An important question is whether the POM approach can resolve the ambiguity in the labels observed with the single-index LandTrendr runs described in section 3.3.1. Focusing on just the fire events, we see that the POM class labels do indeed change when the fires occur, but that the class labels are again not intuitive indicators of fire (Figure 39). For example, the 1995 West fire converted an area dominated by “Galleta Grassland” to one dominated by “Fourwing Saltbrush Upland Drainages.” Similarly, the 2002 Antelope fire involved substantial conversion to the “Active River Channel” class, which is clearly not an appropriate label for this part of the landscape.

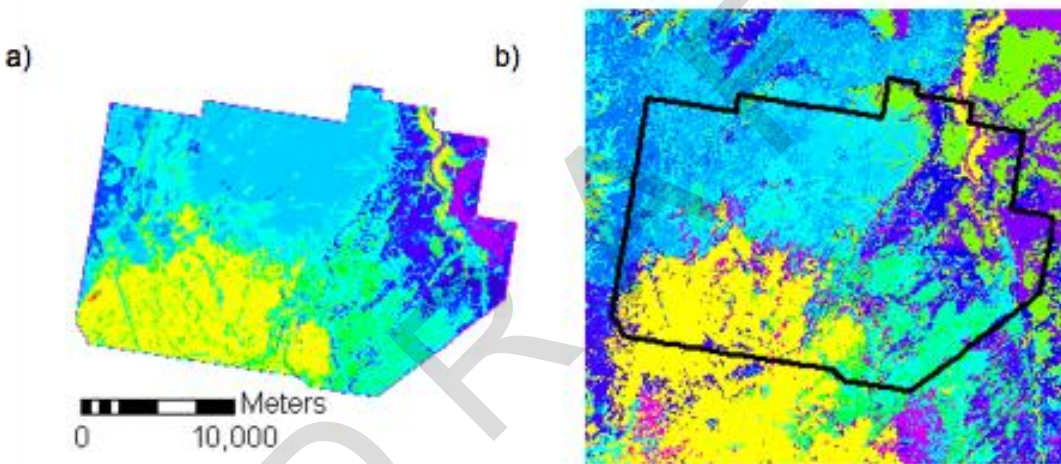


Figure 37. The POM approach applied to WUPA, a) Landcover for the monument based on 1996 airphotos (legend shown on Figure 38). b) POM landcover for 1995. While general patterns are similar, details diverge. In particular, the magenta tones in the POM map correspond to the “active river channel” class in the original map, suggesting that the land-use designation of the original class should be better defined in terms of vegetation components.

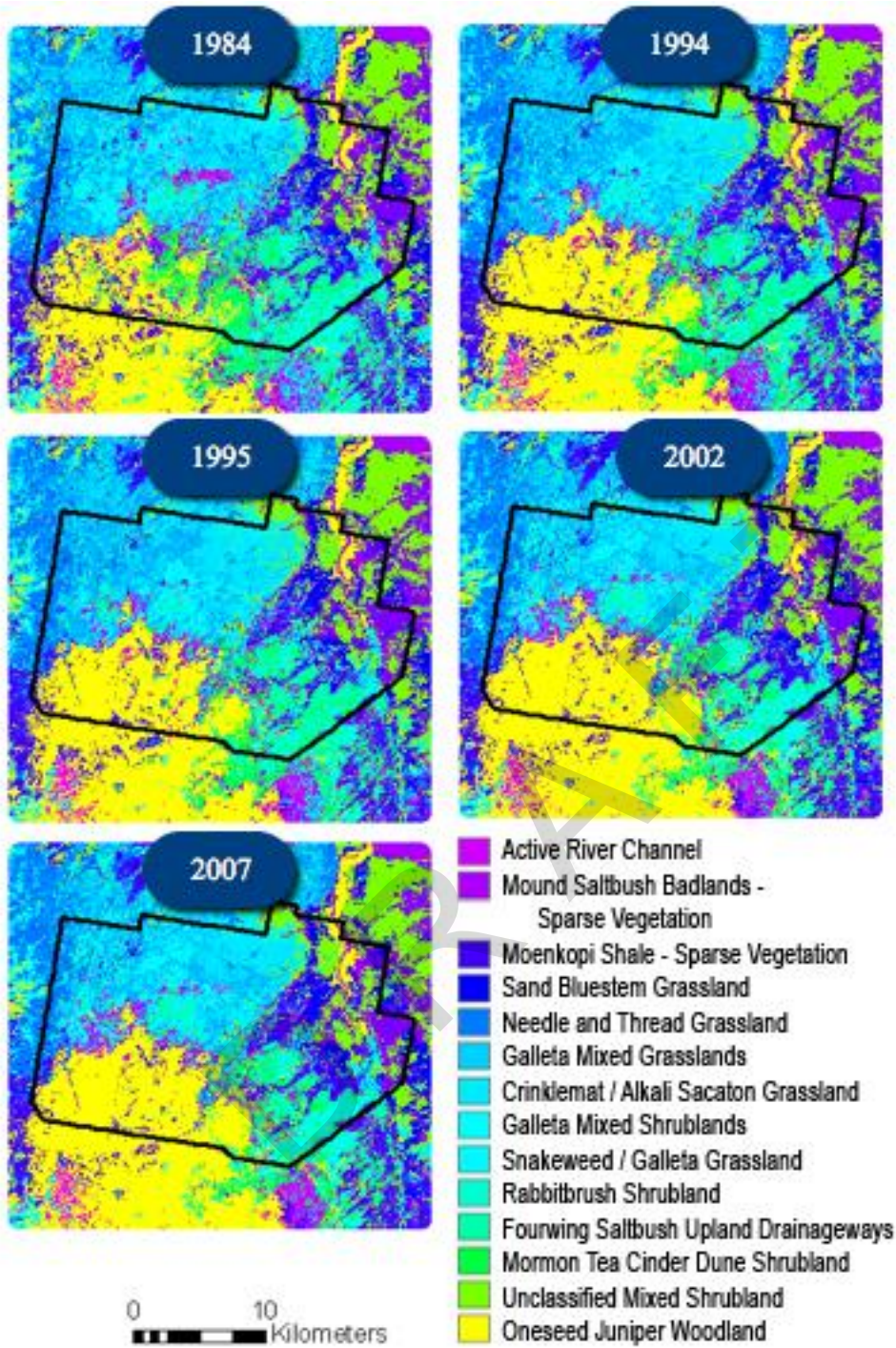


Figure 38. Application of the POM to multiple years at WUPA.

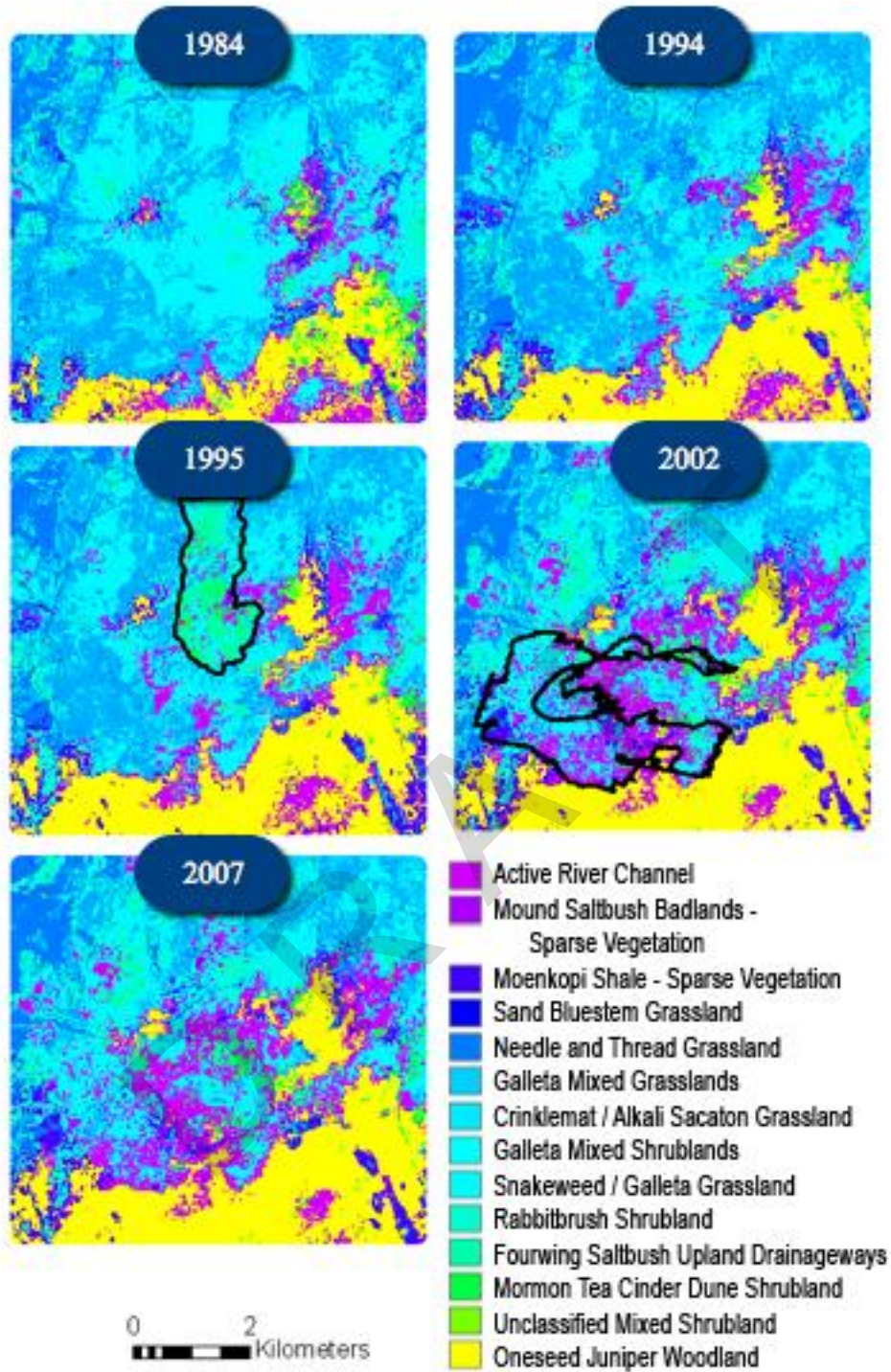


Figure 39. Multiple years of POM classification for fire events at WUPA. The 1995 West and 2002 Antelope fires are captured as changes in land cover type, but the utility of the class labels for inferring the actual change that has occurred is unclear.

3.4 TimeSync

TimeSync was developed as a means of interpreting trajectories in forested systems. We did not know whether it would be applicable in the sparsely- to non-vegetated systems of parks in the

CP. We first examined a set of random points in and around Zion NP, but found most of them to be stable (no-change). We then chose a set of points based on areas that LandTrendr identified as having changed, so we could understand what LandTrendr was labeling change. Two of the examples are shown in Figure 9 above and Figure 40 here.

Our overall assessment of TimeSync in Zion is as follows:

- We are able to see and confidently label some change in brighter areas of the landscape, as well as stability in those areas. We are also able to see change in darker targets, but our confidence is lower in some of these change calls than we would like.
- Phenological variability makes interpretation difficult in these systems, even with the full complement of yearly images. In many cases, phenological noise has a coherent spatial and temporal pattern that rivals actual change. The example in Figure 40 shows how even a fairly obvious change has a magnitude of spectral change not unlike the variability in the supposedly stable signal that preceded the disturbance.
- In open systems, disturbances such as low-intensity fire may cause short-lived spectral change that has a temporal signature not unlike phenological noise, exacerbating the difficulty in separating this noise from real signal.

The bottom line is that image-based interpretation is difficult to do. We will have moderate success, but it is likely that more specific work would be needed to develop better interpretation rules. More importantly, ancillary datasets for validation that complement the TimeSync interpretations are likely to be more critical here than in more vegetated ecosystems.

Landsat-based monitoring in the parks of CP

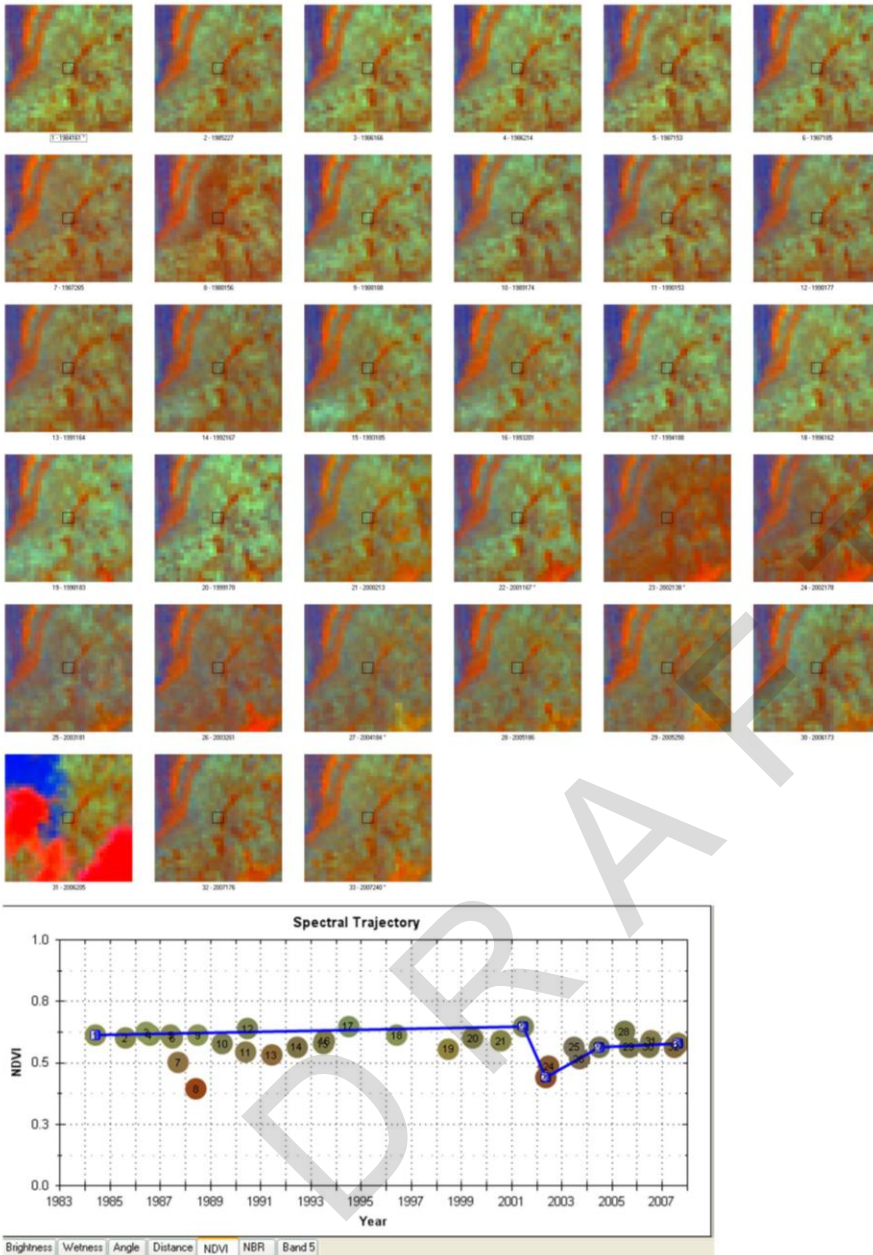


Figure 40. Apparent change in cover as interpreted using TimeSync. Note the significant variability in spectral signal before and after the event identified as meaningful (2001 to 2002).

4. Discussion

This project was envisioned as a test of the potential effectiveness of bringing LandTrendr into the landscape dynamics strategy for the parks of the CP. Because of funding constraints, the test was limited to answering whether the existing LandTrendr algorithms, joined with new fitting algorithms to the POM approach, could be applied directly to the ecosystems of the CP. In large part, the need for this test was driven by the general lack of positive results when applying simple two-date change detection approaches at the parks of the CP. Based on the results shown

in this document, it appears that the trajectory-based segmentation captures many important phenomena occurring in the parks, but that the filtering and labeling phases would require more tuning to be applicable to these arid systems.

LandTrendr segmentation performed better than we expected across the three tested parks. Knowing that the segmentation should perform reasonably in the more heavily wooded sections of the parks, the central question was at what lower bound of woody cover the algorithms would fail. The results at WUPA suggest that the segmentation itself may be applicable even in the grassland systems of the parks, in addition to the woodland and forested upslope areas. Fires in these systems were largely captured (Figures 34, 35, & 39), and a coherent downward and upward trend in wetness in grassland-dominated areas was detected (Figure 36). Additionally, capture of slow increase in cover at ZION, presumably due to regrowth or ingrowth of sparse vegetation, was also a notable positive element (Figure 26), as was the capture of slow loss of cover or increase in mortality in the forests of the north rim of the Grand Canyon (Figures 11 & 12). Thus, we are encouraged that the information content of the image stacks and that the core LandTrendr algorithms used to extract change are both robust.

The challenge in application of LandTrendr in the CP occurs when moving from the segmentation phase to the filtering and labeling phase, particularly in the non-woody systems. First, the direction of spectral signal change for disturbance and growth can be confounded. Fires in Wuptaki grasslands caused spectral changes that were the reverse of what we typically label disturbance in more densely vegetated systems (Figures 34 and 35). Our current approach to distinguishing between disturbance and growth processes requires that disturbance have a consistent spectral sign. A second important challenge comes from the percent cover model estimation needed for filtering. As noted in our prior work for the CP, it is very difficult to develop continuous-variable vegetation cover models from spectral data in the CP. When some cover model is needed for filtering, the uncertainties associated with the model manifest in either the filtering of real change, or conversely the non-filtering of noise. This effect will be most problematic for areas that have low vegetation cover (e.g. the fire in Zion, Figure 19), which includes large areas of most of the CP parks. Addressing this issue would require either further improvement of the cover models, alteration of the thresholds at which change is allowed, or development of novel approaches to filter noise, perhaps using spatial information as well as spectral information.

The second important methodology examined for this report was bringing the trajectory-approach into the POM mapping realm. The critical connection between the two strategies for which methods were developed creation of fitted tasseled-cap image spaces (Figure 1). Again, based on the results presented in this report, this step was successful. The fitted imagery for Zion NP illustrated both the congruence of the fitted and original images for places that are unchanged, as well as the power of the fitted image in separating ephemeral from sustained change (Figure 22). It is important to note that any changes not captured in the segmentation process will not be reflected in the fitted spectral space, and that any false changes captured by LandTrendr will introduce noise in the fitted maps. Phenology and bright soil backgrounds will likely still be significant challenges in the CP parks, even though their impact should be greatly diminished.

The conversion of fitted spectral space to class labels using the POM approach offers a similar mix of caution and optimism. It is clear that labels defined from existing NPSVM maps do not translate smoothly into the spectral space needed for the POM approach (Figures 23 and 37). This is likely due to a mix of two factors: the spectral ambiguity of the NPSVM class labels and the forcing of class labels into Gaussian probability-envelopes. We can envision several methodological changes to this process that may improve the spatial congruence of the source and POM maps, including an iterative labeling, comparison, and adjusting process. As the methodology currently stands, some users in the parks will find the aggregated class labels insufficient at first blush. Despite this shortcoming, we believe that the change information captured in the LandTrendr + POM approach is promising. In several examples, the use of labels before and after disturbance events illuminates the effects of both slow and fast processes (Figures 25 and 26). We are also encouraged by the consistency of the LandTrendr+POM class labels for areas that have apparently not changed.

The use of the LandTrendr + POM labels also illuminates a challenge in landcover mapping when a method allows capture of subtle disturbance events. Class labels based on spectral space alone may differ for roughly static portions of the landscape and those portions that have experienced disturbances, particularly when that disturbance subtly alters but does not remove the vegetation canopy (Figure 27).

When considering the utility of these different approaches, the NPS must also consider means of evaluating outputs. As we noted in our prior work with the CP, it is difficult to find historical or current reference data on which remote sensing analysis can be built. This problem is amplified with yearly stacks of data. Thus, we spent a small effort testing whether the rules we use for TimeSync interpretation can be applied in the CP. The conclusion is similar to that of LandTrendr filter and labeling: for the more woody areas, TimeSync interpretation is likely to be useful, but for the less-vegetated portions of the park, considerable ecosystem-specific training or rule development would be needed to make TimeSync a reliable partner in the process.

5. Summary

We developed and tested new tools to integrate LandTrendr and POM for Zion National Park. LandTrendr disturbance and recovery maps appeared to be plausible, especially in areas of the system with more vegetative cover. Our new code to develop fitted images functions well and also appears to produce reasonable image outputs. When combined with the NPSVM map, we produced yearly vegetation maps with greatly-simplified landcover labels. Changes in those labels over time appeared to be congruent with spectral properties in the imagery, but otherwise are difficult to validate. TimeSync validation appears to have moderate promise for these ecosystem types, but will likely be unable to resolve a fairly high portion of possible subtle change processes or events.

6. Literature Cited

- Asner, G.P., & Lobell, D.B. (2000). A biophysical approach for automated SWIR unmixing of soils and vegetation. *Remote Sensing of Environment*, 74, 99-112
- Brown, L., Chen, J.M., Leblanc, S.G., & Cihlar, J. (2000). A shortwave infrared modification to the simple ratio for LAI retrieval in boreal forests: An image and model analysis. *Remote Sensing of Environment*, 71, 16-25
- Crist, E.P., & Cicone, R.C. (1984). A physically-based transformation of thematic mapper data-- The TM tasseled cap. *IEEE Transactions on Geoscience and Remote Sensing*, GE 22, 256-263
- Franklin, S.E., Lavigne, M.B., Wulder, M.A., & Stenhouse, G.B. (2002). Change detection and landscape structure mapping using remote sensing. *Forestry Chronicle*, 78, 618-625
- Healey, S.P., Yang, Z., Cohen, W.B., & Pierce, D.J. (2006). Application of two regression-based methods to estimate the effects of partial harvest on forest structure using Landsat data. *Remote Sensing of Environment*, 101, 115-126
- Kennedy, R.E., Cohen, W.B., Kirschbaum, A.A., & Haunreiter, E. (2007). Protocol for Landsat-based Monitoring of Landscape Dynamics at North Coast and Cascades Network Parks. In, *U.S. Geological Survey Techniques and Methods: USGS Biological Resources Division*
- Kennedy, R.E., Townsend, P.A., Gross, J.E., Cohen, W.B., Bolstad, P., Wang, Y.Q., & Adams, P.A. (2009). Remote sensing change detection tools for natural resource managers: Understanding concepts and tradeoffs in the design of landscape monitoring projects. *Remote Sensing of Environment*, 113, 1382-1396
- Royle, D.D., & Lathrop, R.G. (2002). Discriminating *Tsuga canadensis* hemlock forest defoliation using remotely sensed change detection. *Journal of Nematology*, 34, 213-221
- Schroeder, T.A., Cohen, W.B., Song, C., Canty, M.J., & Yang, Z. (2006). Radiometric Calibration of Landsat Data For Characterization of Early Successional Forest Patterns in Western Oregon. *Remote Sensing of Environment*, 103, 16-26
- Skakun, R.S., Wulder, M.A., & Franklin, S.E. (2003). Sensitivity of the thematic mapper enhanced wetness difference index to detect mountain pine beetle red-attack damage. *Remote Sensing of Environment*, 86, 433-443
- van Wagtenonk, J.W., Root, R.R., & Key, C.H. (2004). Comparison of AVIRIS and Landsat ETM+ detection capabilities for burn severity. *Remote Sensing of Environment*, 92, 397-408

**Landsat-based monitoring in the parks of the
Northern and Southern Colorado Plateau Networks**

Chapter 3: Looking forward

DRAFT

Contents

	Page
1. Introduction.....	3
2. Clarifying uncertainties.....	4
2.1 Spectral indices	4
2.2 Dates of image acquisition.....	5
2.3 Linkage with MODIS-based products.	5
2.4 Attribution of change	5
2.5 Applicability in different ecosystem types.	10
3. Approaches to implement change mapping in the CP	12
4. Literature Cited	16

DRAFT

1. Introduction

In the studies summarized in Chapters 1 and 2, OSU developed and tested a range of approaches for utilizing Landsat imagery in support of monitoring in the parks of the N&SCP. Each study was framed primarily as a pilot, with the goal of understanding feasibility and providing sideboards on utility for the parks. With these studies complete, the N&SCP must now determine if any of the approaches described in those chapters may fit into the actual monitoring plans for the two networks.

Significant progress toward this goal was made during a teleconference between OSU and representatives of the N&SCP in August 2009. That teleconference focused on evaluating the findings from the pilot study summarized in Chapter 2, but because the work with LandTrendr was motivated by inadequacies in the two-date change methods described in Chapter 1, the discussion moved to broader topics of feasibility of any of the methods described in both chapters. From the written comments on OSU's prior version of Chapter 2, and from the discussion in August teleconference, it became clear that the N&SCP require more specific information on several issues to make informed decisions about how to proceed.

- How can implementation of the LandTrendr approach actually be achieved? Are there logical separations of effort between a remote-sensing type contractor and the staff in the parks?
- How much would those approaches cost?
- Given the challenges working with imagery in areas dominated by bright soil backgrounds, how applicable are these methods for the open systems of the parks? Are other spectral indices or methods more applicable? Would different dates of image acquisition improve results?
- How much of this work may be captured in the MODIS-based approaches being developed separately?

Even with those uncertainties, two areas of agreement arose:

- The use of trajectory information for maps of change (LandTrendr) appears to be the method with most hope of utility in the parks
- The uncertainties in labeling classes using any approach (Chapter 1), including using the LandTrendr + POM approach (Chapter 2), make their use less desirable from the strict perspective of cost and uncertain benefit.

This chapter is designed to address the issues described above.

2. Clarifying uncertainties

2.1 Spectral indices

Issue: Would use of different spectral indices improve results or be more appropriate for the non-woody systems of the CP?

The use of novel spectral indices (Huete 1988) and spectral unmixing (Elmore et al. 2000; Roberts et al. 1993; Smith et al. 1990) is common in remote sensing studies in arid and semi-arid systems, but largely absent from our reports. Rather, our research has tended to focus on either the development of study-specific linear combinations of the spectral bands (as in woody vegetation modeling in MEVE, Chapter 1), or on existing spectral indices that take into account the Shortwave Infrared (SWIR) regions, such as the tasseled-cap (Crist and Cicone 1984) or the normalized burn ratio (van Wagtenonk et al. 2004). Our approach is based on three factors.

First, spectral unmixing is largely untenable because the spectral space of the parks of the CP is dominated by the soil brightness variation. In practice, the spectral unmixing largely reduces to a one-dimensional axis of soil brightness, with the vegetation signal occupying a small orthogonal axis of variation. Spectral unmixing is mathematically more stable when the components occupy a more balanced distribution of spectral space. We initially explore the potential to derive models of percent cover from the spectral unmixing space, but recognized that this approach is mathematically equivalent to direct modeling of percent cover from the spectral data without transformation through endmembers. Thus, the spectral unmixing approach had no clear conceptual or practical benefit relative to other approaches to tap the spectral space.

Second, the use of the SWIR bands has been shown repeatedly to improve interpretation of spectral data in both arid and non-arid systems (Asner and Lobell 2000; Brown et al. 2000). Because the tasseled-cap transformations incorporate components of the shortwave bands in all three primary spectral indices (brightness, greenness, and wetness), we have found this transformation to be generically interpretable across most ecosystems. The NBR focuses on the contrast between the near infrared and the SWIR bands, and it too is used frequently in dry (although not necessarily arid) systems.

Third, the development of novel spectral bands in dry systems requires good reference data to build site-specific relationships (Cingolani et al. 2004; Rogan et al. 2002). As we have shown repeatedly, the reference data already in hand for the CP parks is largely not appropriate for building these relationships because the data were not collected with remote sensing models in mind. Indeed, several of our efforts described in Chapter 1 were efforts to tailor site-specific information and models from available reference data, and these were not feasible because of the reference data.

Because of these constraints, we have proposed working with known spectral indices for LandTrendr change detection, but any novel spectral indices can be used in the LandTrendr paradigm if desired. In our LandTrendr work with the Sierra Nevada Network (SIEN), we recently found that the use of the tasseled-cap Brightness index, which is essentially a measure of overall albedo, appeared to be more effective at capturing the potential encroachment and densification of woody vegetation at treeline than did the SWIR-based NBR index. Because the cost of running LandTrendr on different spectral indices is minimal compared to the costs of

preprocessing image stacks and conducting field work, we advocate experimentation and diversification as knowledge of local conditions and patterns increase over time. It is likely that other spectral indices may eventually emerge as useful indicators of particular types of change. Initially, however, the use of simple indices represents the best compromise of cost and potential utility.

2.2 Dates of image acquisition

Issue: Why were the dates of imagery used in the LandTrendr chapter chosen? Would different periods of the growing season be more appropriate?

For the LandTrendr project, we used imagery that we already had ordered and processed for Chapter 1 pilot studies to do our evaluations. The reference image for those stacks was based on dates of airphotos, because the original intent of those images in the work done for the Chapter 1 studies was to link the imagery to those airphotos. The small scope of the LandTrendr add-on project precluded expansion or experimentation with other dates of imagery.

However, given that the imagery has become freely available, and that images are available for the CP parks across the season for many years, it is possible to envision a wide range of actual image stack choices. There is no particular need to be limited to the stacks used in the Chapter 2 work, and we agree that the use of a different date range, or perhaps of two separate stacks at two strategic points in the growing season, may improve results. Conducting this work, however, would require more effort in both pre-processing and interpretation.

2.3 Linkage with MODIS-based products.

Issue: How much of the utility of the products in Chapter 2 could be captured with the MODIS products being conducted under a separate project for the CP?

We are not aware of the details of the MODIS projects being developed for the CP, but are aware of other MODIS-based efforts to map change at broad scales.

MODIS grain size is an order of magnitude larger than Landsat grain, which may be an issue for many of the landcover transitions of interest to the parks. For broad, landscape-wide patterns, the MODIS data are likely useful. Our sense from interactions with the CP is that even Landsat pixels are perceived as too large, which suggests that the MODIS information would fill a different need than that met by the Landsat data. They are certainly complementary.

MODIS data are also of relatively short duration for detecting long-term trends. Many examples of long-term change in vegetation require the long-duration record of the Landsat archive to distinguish from background noise.

2.4 Attribution of change

Issue: How would the CP ascribe change agents for the spectral change information captured by LandTrendr?

Attribution of change agent is higher in the “remote sensing layer cake” described in Chapter 1 than is detection and labeling of change itself. As described in Chapter 1, moving from maps of change to models of how the change occurred requires that analysts bring new, external information (either data, models, or conceptual understanding) to bear on foundational change

maps. Shape, landscape position, and character of spectral change all contribute to the ability to ascribe an agent to a particular change event.

Ultimately, attribution of change is a process that is best conducted by experts in the ecosystems of interest – i.e. the parks themselves. However, we continue to update and improve our mapping products, and since the conclusion of Chapter 2's original work have expanded the suite of change products available from which attribution can be made. Recognizing the difficulty of utilizing fitted imagery (such as that shown in Chapter 2's Figure 10 and 11) for direct interpretation or quantification, we have developed a tool to quickly label pixels according to user-defined rules for segment type, duration, and sequence (Figure 1). For example, pixels exhibiting spectral patterns indicative of chronic loss of vegetation vigor can be captured as a cohesive change-label group and visited in the field to understand the process occurring in that class (Figure 2).

DRAFT

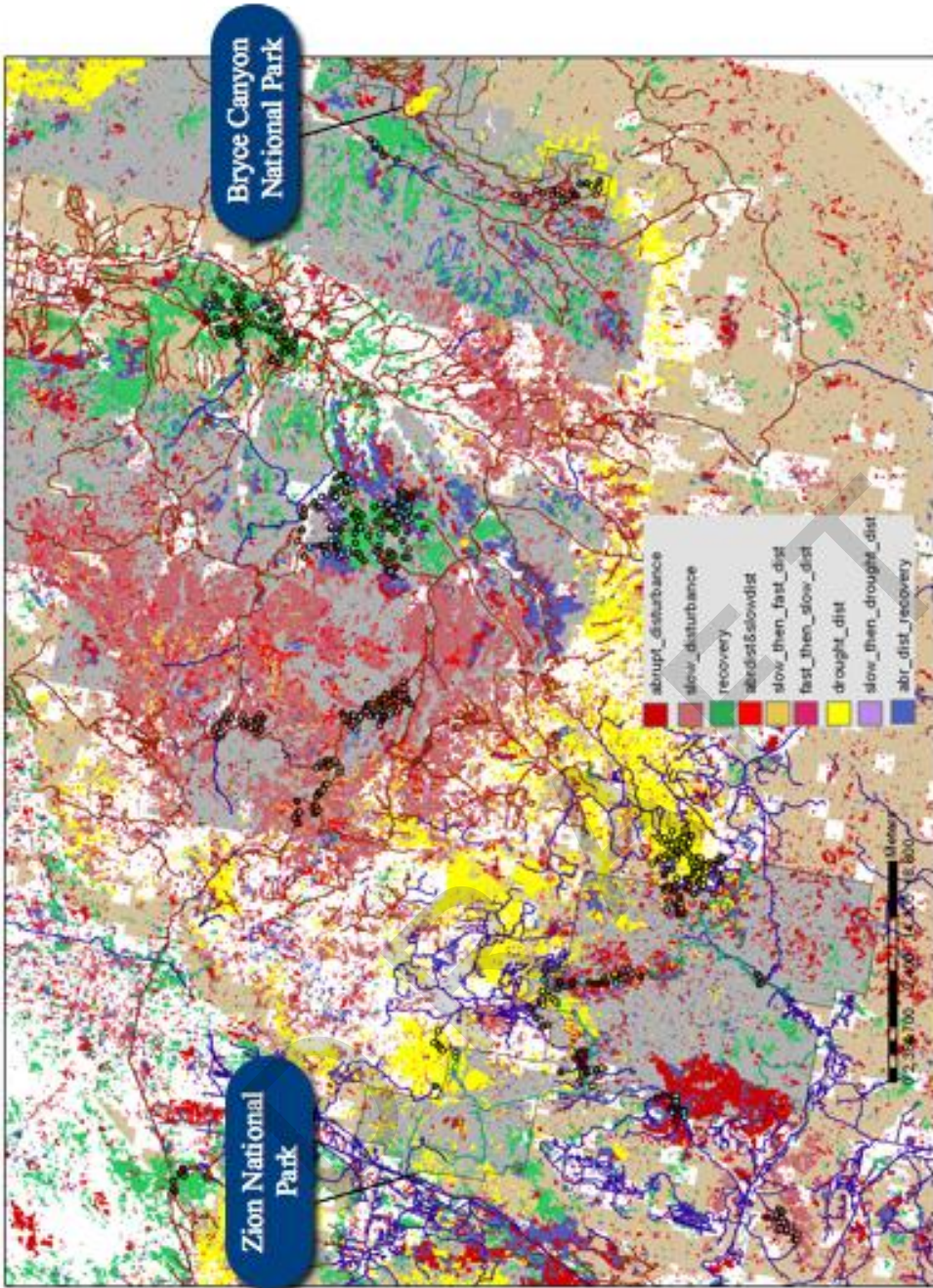


Figure 1. New approaches for labeling change from LandTrendr outputs. Classes of change are defined by the user to capture particular types, durations, or sequences of spectral trends and events. These labels are based entirely on the change of information, and could be linked with other geospatial data to improve labeling of change agent.

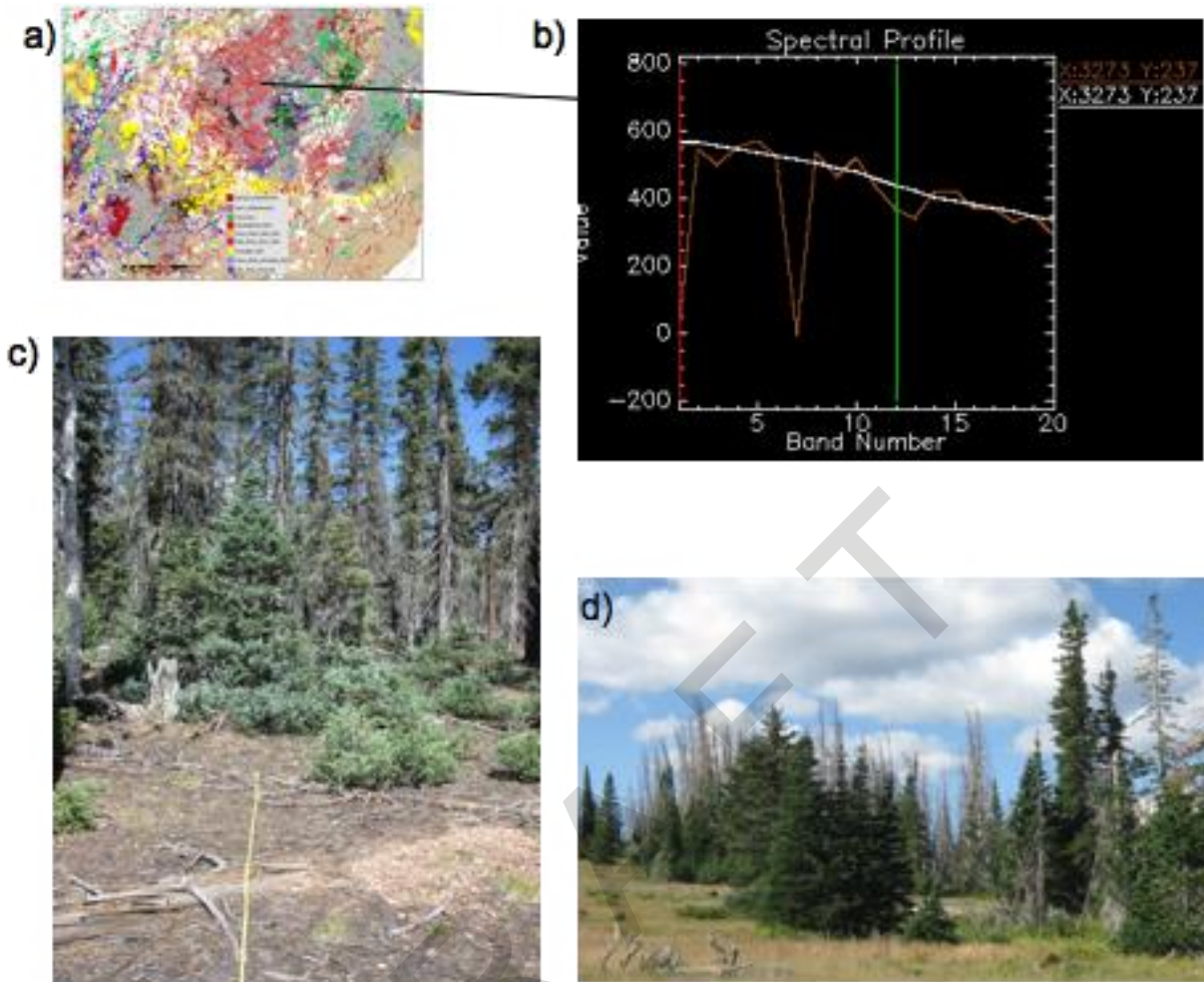


Figure 2. From the change-labeled map in Figure 1, reproduced here in a), the chronic loss of vigor in spectral space (b) captured in the “slow disturbance” category can be visited in the field (c) and (d) to link with insect-related mortality in the forests on the plateaus.

Based on our own field work in both the CP and the SIEN parks in 2009, we expect that the change label approach may be a valuable addition to the process of ascribing change. We identified a class of change consistent with growth or encroachment (Figure 3) in healthy pinyon pine woodlands. The positioning of this class on the landscape in contrast to other areas where pinyon pine mortality occurred during the recent drought may provide insight into the mechanisms of that mortality. Because the change classes provide coherent spatial groupings that can be placed on the landscape, other insights may arise. For example, we isolated all areas that showed disturbance in the peak of the drought (2002), and draped those changes along with other change classes on the digital elevation model of the plateau connecting Zion and Bryce parks. The disturbances occurring in 2002 were low-intensity and grouped along the upper facet of the slopes of the plateaus, suggesting an ecological community or hydrological similarity in the impact of the 2002 drought.

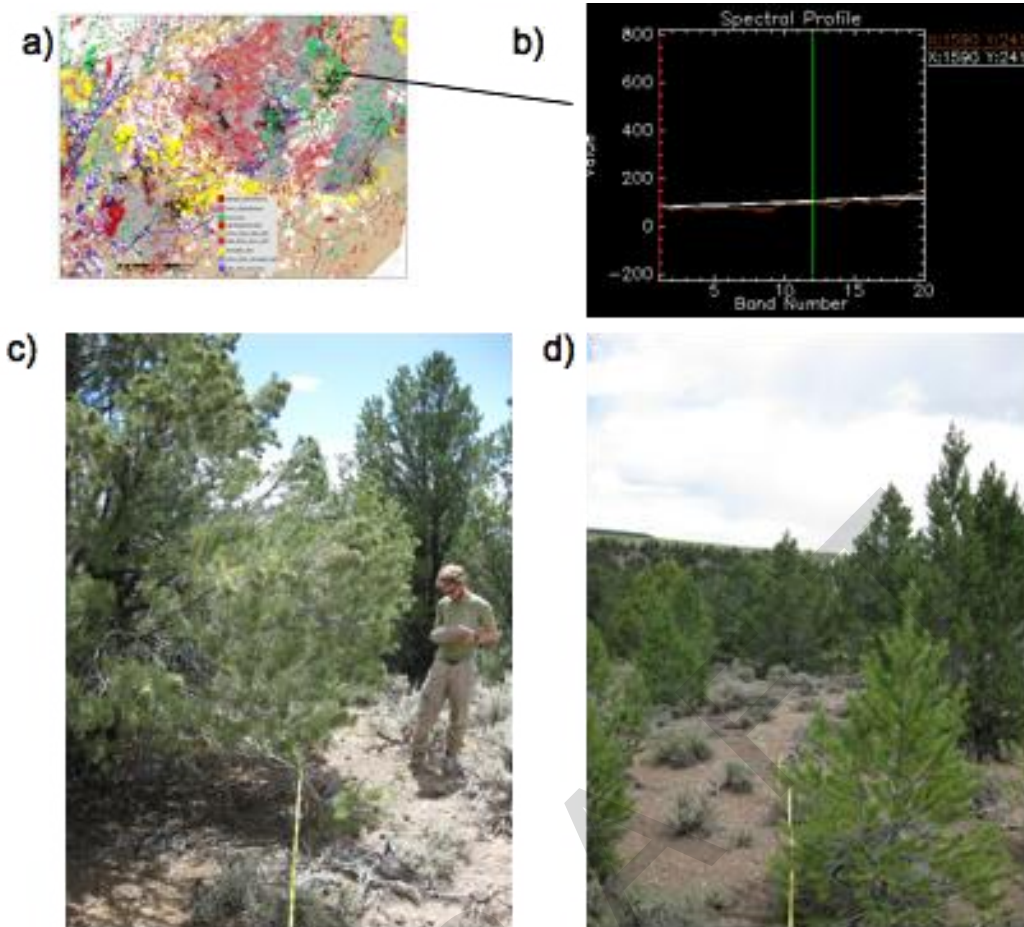


Figure 3. As in Figure 2, but for long-duration, subtle increase in apparent vegetative component (b). Field visits show that this spectral signal occurs in healthy pinyon woodlands with no evidence of well-documented pinyon mortality experienced elsewhere (c) and (d).

Although attribution of change must ultimately bring in other rules or understanding (beyond the change labels themselves), we expect that the change information captured in the change labels maps may make that process and rule-making more feasible and robust.

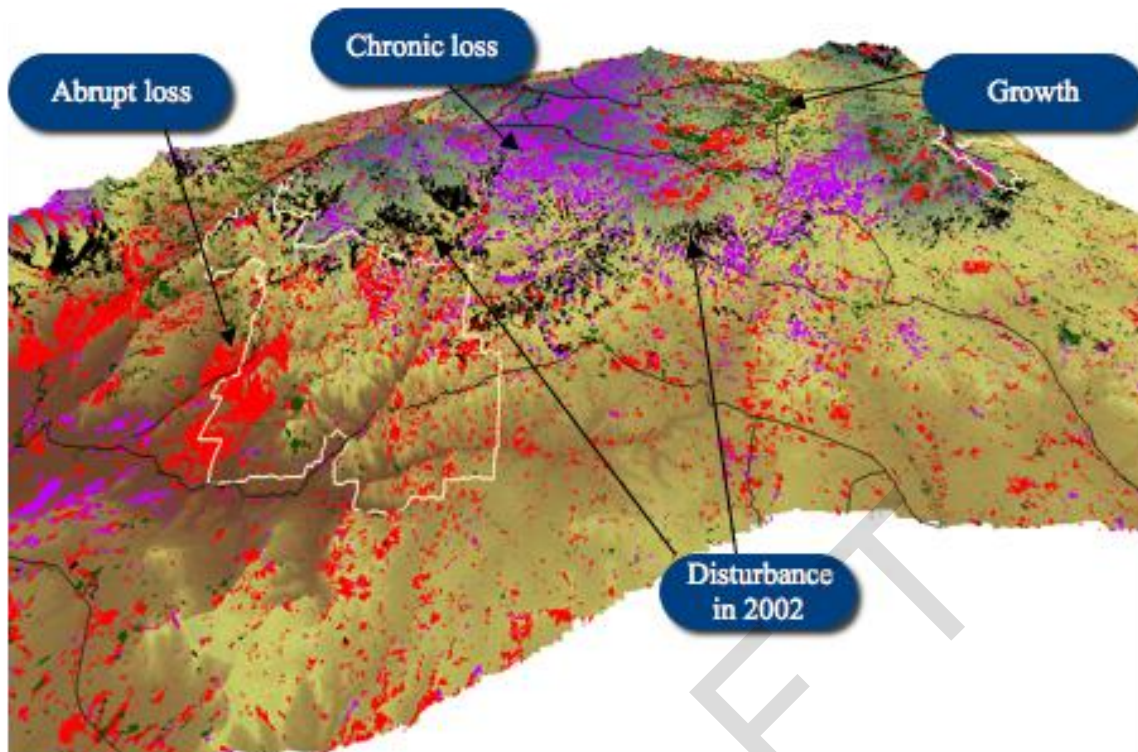


Figure 4. When draped over the virtual landscape, the change labels (here shown in different colors to contrast with underlying topographic model) can further point to interesting patterns. Here, disturbances occurring in the peak drought year of 2002 are shown to occur along the same topographic facet of the plateau, suggesting similarity in either hydrologic or ecological community impact of the drought.

2.5 Applicability in different ecosystem types.

Issue: Given that much of the CP park systems are non-woody, how well will these methods work? Where are these methods likely to be most effective?

The dominance of soil spectral properties in herbaceous and sparse arid systems is of particular concern for any remote-sensing project conducted in the CP. For this reason, when conducting the work for Chapter 2, WUPA was considered representative of the herbaceous and more arid conditions that will be encountered in the CP parks. Our results in WUPA show that even the herbaceous-dominated areas of the monument exhibited cohesive temporal trends (such as those shown in Figure 36 of Chapter 2), but that these trends are difficult to interpret using knowledge of spectral change in woody systems. In woody systems and woodlands, the change labels appear to be largely consistent with the patterns expected. While the limited scope of our pilot study prevents us from conducting new analysis of the accuracy of the LandTrendr change maps in different ecosystem types, our experiences running the LandTrendr algorithms in WUPA, Zion, Bryce, and GRCA provides us with a general sense of their applicability in different ecosystems. These are summarized in Table 1.

Landsat-based monitoring in the parks of CP

Table 1. Applicability of the LandTrendr-based approaches for different ecosystem types of the CP.

Ecosystem type	Robustness of change information	Interpretability of change information	Comments
Mixed conifer forests	High	High	Analogous to types where LandTrendr was developed.
Deciduous/evergreen broadleaf	Moderate	Moderate to high	Deciduous systems are more variable from year to year, but changes in spectral direction are consistent with those in mixed conifer
Woodland	Moderate	Moderate to high	Primary uncertainty is whether background vegetation compensates for change in woody component; otherwise, spectral signal is likely to be largely interpretable.
Shrubland	Low to moderate	Moderate	Shrublands are likely to show even greater variability in spectral response than woodlands, but interpretation should be similar.
Grassland	Low to moderate	Low	Grasslands may have coherent signals, as shown in WUPA, but interpretation of the change over many years has not yet been done and is thus uncertain.
Rock/bare ground	Low	Low	LandTrendr is likely not appropriate for these systems.

For conifer-dominated forests at higher elevation, LandTrendr change information will be reliable and readily interpreted. For open woodland types (such as juniper and pinyon types), we also expect that mortality (both from abrupt disturbances and slower, spreading processes caused by insects or drought) will be largely achievable, although the apparent juniper mortality in SE WUPA raises some uncertainty as to the degree to which such mortality will be captured. Unpublished work by a student in the OSU lab has shown that the spectral signal of pinyon decay in the areas south of the Grand Canyon is both detectable and mappable. For open woodland types, it also appears that densification or encroachment is likely feasible. Shrubland types are likely variable, but patterns of spectral change (if detectable) are expected to be either interpretable or consistent once new patterns emerge. Grasslands are clearly the most uncertain types for mapping, but our experience in WUPA suggests that even these systems may show consistent trends in spectral signal over time. However, these systems are known to be highly

noisy in terms spectral response, and the patterns of spectral evolution over 20 years are largely unexplored and untested.

3. Approaches to implement change mapping in the CP

Of the methods for change detection explored in Chapters 1 and 2, we expect that the use of LandTrendr change maps will likely represent the best balance of cost and likely utility (Table 2). The assessments captured in Table 2 are based on the expert judgment of the OSU collaborators, and are first-approximations meant to capture the relative costs of the different approaches. Actual implementation costs and utility are unknown until implemented.

Table 2. LandTrendr-based change detection and attribution options for the N&CPN

Change detection	Attribution	Effort/cost	Likely utility
POM change with two-date change	From class labels	Setup: Moderate; Ongoing: Moderate	Low
	From change labels alone	Setup: low to moderate; Ongoing: low	Moderate
LandTrendr based on single-season stacks, with change labeling from trajectories alone	As prior, but with rule-based approaches to attribute change based on landscape position, type, etc.	Setup: Development of rules may be high; Ongoing: low to moderate	Moderate-to-High
	As prior, but with field validation of change areas	As prior, but ongoing costs moderate to high	High
LandTrendr based on two-season stacks, with development of new approaches for labeling and attribution	From changes in spectral space alone	Setup: moderate to high; Ongoing: low	Moderate-to-High
LandTrendr with single-season stacks, plus POM mapping	From POM change labels	Setup: Low (for parks already studies) or Moderate (for new parks); Ongoing: Moderate	Moderate
	As prior, but with additional rule-based approaches	Setup: High; Ongoing: Moderate	Moderate

If the LandTrendr route were chosen, Table 3 provides a sketch of the relative costs of different flavors of both change detection and validation. Of particular note is the distinction between setup costs (which are relatively high for the image processing side of the work) and ongoing costs (which are relatively low for image processing). In all cases, better validation is a primary determinant of overall cost.

Landsat-based monitoring in the parks of CP

Table 3. Options for LandTrendr-based monitoring in the N&CPN

<i>Mapping method</i>		<i>Validation</i>	
		<i>Setup costs</i>	<i>Ongoing costs</i>
LandTrendr (LT) with existing single-season image stacks	TimeSync		
LandTrendr (LT) with existing single-season image stacks	Airphoto interpretation	Low	Low
	Field-validation	Low	Moderate
LandTrendr (LT) with existing two-season image stacks	TimeSync	Low to moderate	High
LandTrendr (LT) with existing two-season image stacks	Airphoto interpretation	Moderate to high	Moderate
	Field-validation	Moderate to high	High

The relative costs shown in Tables 1-3 do not provide actual estimates of the human capital needed to achieve any particular combination of options. Given our understanding of the goals and cost constraints of the CP parks, we provide in Table 4 a first approximation of the actual person-week costs of carrying out different steps in the processing and analysis of LandTrendr change maps for three contiguous Landsat scenes, including all parks and non-park areas within each scene. We chose a count of three scenes for this example because single-scene processing often splits larger parks, and because processing of all possible scenes in the CP (approximately 17 scenes, see Figure 5) is likely beyond the scope of funding within the parks.

Actual costs of each person-week depend on both the entity conducting the work and on the funding instrument used. These estimates of person-weeks assume the work is being conducted by staff trained in the aspect of each task well enough that little startup training is required.

Landsat-based monitoring in the parks of CP

Table 4. Expected costs for change mapping in parks in three adjacent Landsat scenes.

Item	Person-weeks	Performed by	Comments
Setup			
Pre-processing single-season (two-season) stacks	12 (24)	Remote sensing lab	Image identification, downloading, importing, radiometric processing, normalization, cloud-screening
LandTrendr segmentation and change labeling using standard approaches for single (two) seasons	8 (12)	Remote sensing lab	With two to three indices (NBR, NDVI, Brightness), using standard change labels and minimum map-unit filtering, quality control
Yearly updates			
Addition and pre-processing of new images, re-running LandTrendr for single season (two season)	6 (9)	Remote sensing lab	Entire stack re-run once new images added.
Validation / corroboration			
Validation with TimeSync of change and no-change areas	6 to 12	Park staff and either remote sensing lab or network staff	Highly variable and dependent on plot count, availability of high-resolution photos, and on interactions with park staff to aid in interpretation
Validation with airphotos	8 to 12	Park staff and either remote sensing lab or network staff	Assumes two dates of reliable airphotos
Validation in the field	2 to 12	Park staff and either remote sensing lab or network staff	Depends entirely on field sampling methods and goals
Setup / updates			
Interpretation of patterns, attribution of change	4 to many	Park staff and either remote sensing lab or network staff	Depends on the degree to which novel rules are developed and on the number of agents desired

Given the specialized nature of the processing and analysis, particularly the image processing steps, it is assumed that most parks and park networks will not have staff on hand to immediately conduct this work. Startup training is highly variable, but would enjoy highest likelihood of success if the responsible individuals were already adept in geospatial data analysis, had academic exposure to image processing and remote sensing concepts, and were familiar with the ecological and monitoring goals of the networks. Other resources needed include secure storage of approximately 150 gigabytes of data per scene initially, a robust multi-CPU workstation to process imagery, and software licenses for ENVI/IDL (approximately \$2000) and ArcGIS (which is typically already on-hand). Statistical analysis packages are also required, but also are typically available.

Based on conversations with both the CP network and with other national park networks, it appears that one model for implementation of the LandTrendr change mapping approach would be for OSU to oversee a transition period of change mapping to several park networks. Setup costs associated with processing image stacks, which requires significant image processing

Landsat-based monitoring in the parks of CP

expertise, would be handled by the OSU collaborators, with fixed costs (computing, software, office space) prorated across networks and effort expended on each network proportional to the contribution by each network. A dedicated position at OSU would process imagery for all park networks in a similar manner, allowing for economies of scale in startup and training, and would provide a single contact point for technology transfer to the parks. Tech transfer would focus on updating stacks each year, and on development of capacity within the parks for handling change

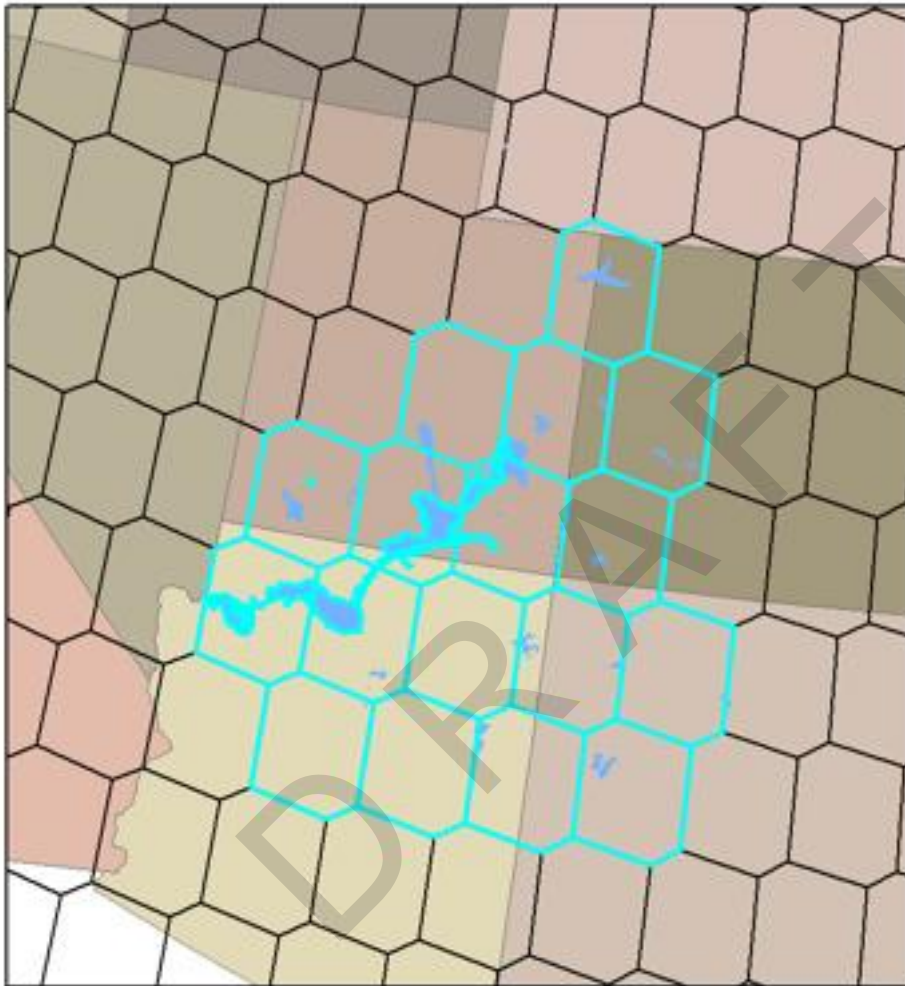


Figure 5. In the Colorado Plateau, approximately 17 Landsat scenes (shown as turquoise polygons) cover nearly all parks.

maps and attributing agents of change. As a first approximation, tech transfer duties could be expected to add approximately 20% time to the OSU position's person-weeks listed in Table 4. The period of transition should be two to three years, to 1) provide enough support to attract a quality candidate to OSU to fulfill the role and 2) to provide time for tech transfer to occur after the initial period of actual mapping and validation. At present, the SWAN, NCCN, and SIEN park networks have also expressed interest in this model, but no firm commitments have been solicited at this point.

4. Literature Cited

- Asner, G.P., & Lobell, D.B. (2000). A biophysical approach for automated SWIR unmixing of soils and vegetation. *Remote Sensing of Environment*, 74, 99-112
- Brown, L., Chen, J.M., Leblanc, S.G., & Cihlar, J. (2000). A shortwave infrared modification to the simple ratio for LAI retrieval in boreal forests: An image and model analysis. *Remote Sensing of Environment*, 71, 16-25
- Cingolani, A.M., Renison, D., Zak, M.R., & Cabido, M.R. (2004). Mapping vegetation in a heterogeneous mountain rangeland using Landsat data: an alternative method to define and classify land-cover units. *Remote Sensing of Environment*, 92, 84-97
- Crist, E.P., & Cicone, R.C. (1984). A physically-based transformation of thematic mapper data-- The TM tasseled cap. *IEEE Transactions on Geoscience and Remote Sensing*, GE 22, 256-263
- Elmore, A.J., Mustard, J.F., Manning, S.J., & Lobell, D.B. (2000). Quantifying Vegetation Change in Semiarid Environments: Precision and Accuracy of Spectral Mixture Analysis and the Normalized Difference Vegetation Index. *Remote Sensing of Environment*, 73, 87-102
- Huete, A.R. (1988). A soil-adjusted vegetation index (SAVI). *Remote Sensing of Environment*, 25, 295-309
- Roberts, D.A., Smith, M.O., & Adams, J.B. (1993). Green vegetation, nonphotosynthetic vegetations, and soils in AVIRIS data. *Remote Sensing of Environment*, 44, 255-269
- Rogan, J., Franklin, J., & Roberts, D. (2002). A comparison of methods for monitoring multitemporal vegetation change using Thematic Mapper imagery. *Remote Sensing of Environment*, 80, 143-156
- Smith, M.O., Ustin, S.L., Adams, J.B., & Gillespie, A.R. (1990). Vegetation in deserts: I. A regional measure of abundance from multispectral images. *Remote Sensing of Environment*, 31, 1-26
- van Wagendonk, J.W., Root, R.R., & Key, C.H. (2004). Comparison of AVIRIS and Landsat ETM+ detection capabilities for burn severity. *Remote Sensing of Environment*, 92, 397-408

Appendix 1

The use of Landsat imagery in baseline mapping and change detection in National Park Service units of the Northern and Southern Colorado Plateau Networks:

Report on Pilot Study

Zhiqiang Yang¹, Robert Kennedy¹, Warren Cohen²

¹Department of Forest Ecosystems and Society, Oregon State University

²Pacific Northwest Research Station, USDA Forest Service

August 22, 2008 (Revised November 10, 2009)

1. Introduction

National Park Service (NPS) units of the Northern and Southern Colorado Plateau Inventory and Monitoring Networks (NCPN and SCPN, respectively) have identified a need for long-term monitoring of landscape patterns and land use change. Monitoring land use, land cover, vegetation pattern, and vegetation condition within and surrounding NPS units is critical to understanding present and future ecosystem states and dynamics, biodiversity patterns, available habitats, movements of organisms, and flow rates of energy and materials. The studies reported in this document examined the potential utility of remote sensing technology to aid such monitoring.

1.1 Motivation

The natural systems of all Colorado Plateau (CP) parks are affected by past and current human management on lands both inside and outside parks. The legacies of livestock grazing and altered fire regimes influence the types and densities of vegetation, which in turn influence abiotic processes such as fire, nutrient cycling, and water flow. Outside the parks, increased development and intensification of land use practices (e.g., grazing, logging, recreation) on bordering lands have several ecological consequences, including sharper contrasts (edge increases) in vegetation structure and function along park boundaries, change in the effective size of the parks' natural ecosystems, changes in ecological flows into and out of the park, loss of adjacent habitat, and increased exposure to human activity along park boundaries (Hansen and Jones 2004). The need to understand the combined effects of past management within parks and ongoing management outside parks impels monitoring of vegetation and land cover using consistent measurement tools across broad geographic areas.

These anthropogenic effects are overlaid on natural disturbance and successional processes that operate at the landscape scale. Disturbance to vegetation caused by fire, insects, and extreme climatic events (e.g., droughts, floods) affect the ability of the natural systems in the park to sustain the natural characteristics that the park managers are mandated to preserve, and must be observed and understood for managers to make informed decisions about response. Similarly, managers must have information on the spatial and temporal patterns of natural vegetative processes of establishment, succession, and vegetative community change as these, too, affect the character and resources of the park. These natural processes interact with past and current management strategies to give rise to new effects. For example, the combined effect of recent climate change (drought) and past fire suppression have created conditions that generally favor more frequent and intense fires, and have also produced stands with a tendency for elevated response to insect outbreaks (i.e., increases in extent and severity). These have collectively led to increased disturbance rates in semiarid and montane ecosystems across the Colorado Plateau.

For these reasons, the Colorado Plateau networks have selected land use/land cover, landscape vegetation pattern or landscape structure, land or vegetation condition, and disturbance patterns as core vital signs to monitor. Four landscape indicators associated with these vital signs have been identified (Table 1). For the most part, monitoring these indicators requires consistent measurement across large areas over time, making remote sensing technology a promising tool to aid in such monitoring. Therefore, the CP networks have been working with the OSU collaborators to develop a project to study the potential role of remote sensing in monitoring, and to write protocols that incorporate the most successful approaches to remote-sensing based

monitoring. The project was divided into three subtasks: development of study plan; pilot studies; and protocol development. This report covers only the pilot studies.

Table 1. Initial estimated desired resolutions for four landscape indicators and associated changes to be monitored with remotely sensed data in the NPS Northern and Southern Colorado Plateau Inventory and Monitoring Network parks.

Vital Sign	Landscape Indicator	Changes/Features to Monitor	Thematic Resolution	Spatial Resolution	Temporal Resolution
Land use/Land cover (LULC)	Land use/Land cover (LULC)	Type conversions Boundary changes	Anderson Level II or equivalent	2-5m at small parks 30m at medium and large parks	every 5 years
Landscape vegetation pattern	Vegetation pattern	Type conversions Boundary changes	NVCS1 formation level or NatureServe ecosystem level	2-5 m at medium parks 30m at large parks	every 5 years
Vegetation or Land condition	Vegetation condition (ground cover and/or bare ground ² , and age class distribution ³)	Changes to ground cover Changes in age class distributions for wooded systems	Continuous data set layer Continuous data set layer for wooded systems (detect changes at alliance level)	2-5m at small parks 30m at medium and large parks	every 5 years
Disturbance patterns	Disturbance patterns	Type, extent, and severity of major disturbances	Data set layer	30m for medium and large parks	Annual tree

¹ National Vegetation Classification System (Federal Geographic Data Committee, FGDC).

² Monitoring modifications to cover for selected ecosystems.

³ Example: where and how much of a park's forest is young, middle-aged, or old-growth? Monitoring this indicator may only be possible for selected ecosystems

1.2 Characterizing NPS indicators using Remote Sensing

Although necessary as a structure for conceptualizing monitoring in and around the parks of the CP, several indicators in Table 1 do not represent attributes that can be directly mapped with remotely-sensed data. Rather, the landscape indicators represent levels of abstraction one or more steps removed from remote sensing data. Figure 1 presents a useful heuristic (the “layer cake”) that illustrates the linkage between raw remote sensing data and the derived variables that may ultimately be of use to the parks. Clarifying this linkage is important in describing the overall scope of the work that is necessary for this project.

Although products from the bottom two layers of the progression in Figure 1 are not of direct interest to the parks, they are the foundation upon which the desired indicators must be based. At

the base layer are raw data measured by a sensor on a satellite or aircraft platform. These are simply spatial representations of electromagnetic energy received at the sensor. Proceeding from raw imagery to clean imagery requires “pre-processing” of the imagery, and results in maps of electromagnetic reflectance on the surface of the landscape. Our experience with remote sensing-based ecological monitoring at the North Coast and Cascades Network (NCCN) has emphasized that this step is critical for successful monitoring many of the properties of interest to the parks. Monitoring any of the indicators in Table 1 necessarily requires investigation of imagery over time, and thus normalization across image dates rises to critical importance in this stage. Therefore, one of the key themes of the work done for this project will be ensuring that preprocessing methods are thoroughly evaluated for the conditions found in the ecosystems of the CP Network of parks.

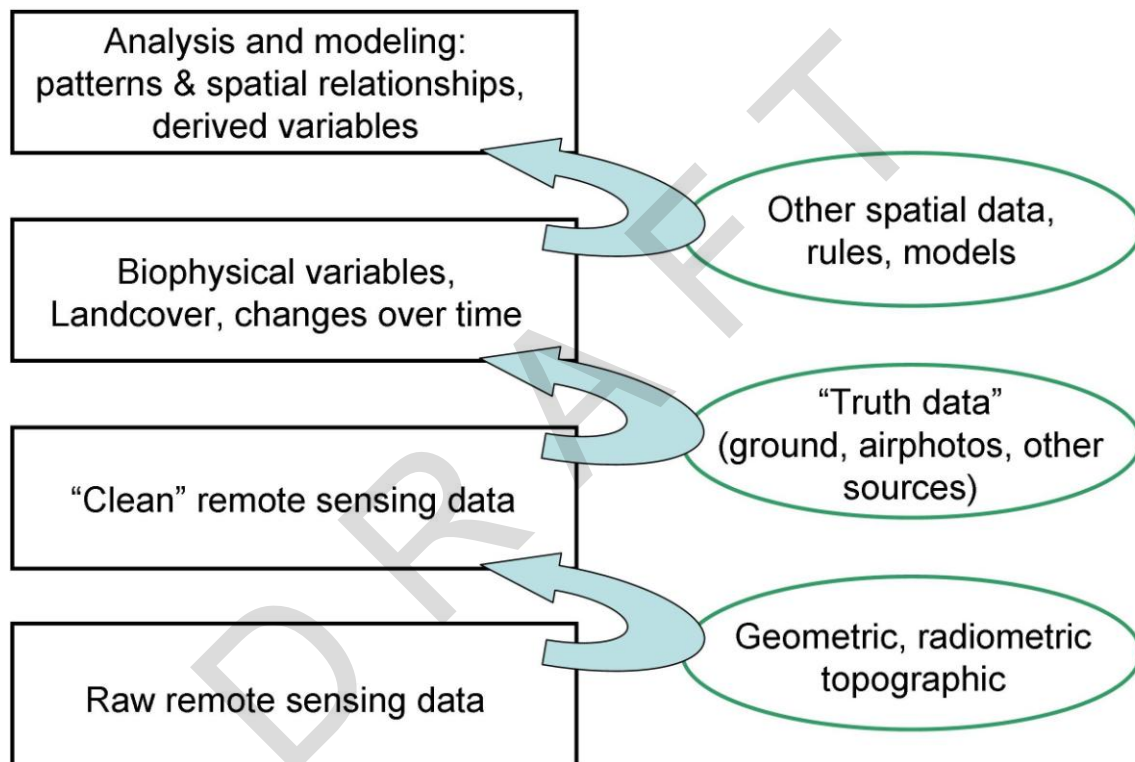


Figure 1. The “layer cake” of remote sensing. Although the information in the top two layers is ultimately of interest in ecological monitoring, its effective development depends on a good foundation in the lower two layers, which are the realm of remote sensing science and the focus of much of the work in the pilot studies.

Derived products at the third level of the “layer cake” in Figure 1 are those that begin to have relevance to the parks. These map products are built by linking cleaned maps of electromagnetic reflectance to ancillary data, such as field plots of percent vegetation cover or photo-interpreted plots of cover type. The linkage between a sample of ancillary data and remotely-sensed data is typically through a multivariate statistical model, where variation in attributes measured by ancillary methods is expressed as a function of variation in remotely-sensed reflectance. These relationships are then applied to remotely sensed data at locations where the ancillary data were not collected, resulting in a wall-to-wall map of estimates. The attributes being mapped can be either continuous or discrete variables.

At this third level, land cover types on the surface can only be distinguished according to their contrasting properties of electromagnetic reflectance (their “spectral reflectance”) as measured by a particular sensor. Integration of temporal variation in spectral reflectance can also be included at this level, taking advantage of seasonal changes in electromagnetic reflectance to further discriminate among types. The more similar the spectral reflectance properties of two cover types, the less likely those two cover types can be separately mapped. This has direct relevance for the properties in Table 1. Some of the distinctions in cover type may be quite separable, while others might be quite challenging. General predictions about cover type separability are possible from the literature and from our current experience with the spectral properties of common cover types, but direct testing is necessary to quantify the degree of separability of categorical variables, or the strength of a predictive equation for continuous variables, for the ecological systems of the CP. This also applies to monitoring changes in these attributes over time. Thus, a central goal of pilot studies has been assessing the degree to which affordable remote sensing technologies can separate indicators of interest to the parks, either at a single date or over time.

Assessing the appropriateness of a given remote sensing methodology necessarily requires that error properties of that method be quantified. Error properties can only be assessed by validation of derived maps or of the models used to build them. Therefore validation methods are integral to the testing and overall methodological development. For any methods that require analysis of change over time, evaluation of methodologies requires that retrospective validation be included as part of a pilot study design. The availability of historical truth data for validation is a strong constraint on testing of different methods and approaches for remote sensing based validation. Therefore, assessing the utility for remote sensing of reference data collected for other projects is an important component of several of the pilot studies reported here.

Several of the indicators desired by the parks are found only in the top layer of the layer cake. Progression to the final level requires that the remote sensing-based derived variables be integrated with other models or data. Land-use labeling is appropriate at this level: cover types at the derived-variable layer are labeled according to spatial context and expert understanding of the system. An extensive area of the grass cover type, for example, might be labeled differently if its spatial context were a city rather than an agricultural valley. Similarly, an analysis of spatial patterns (patch analysis, etc.) might use land cover types as an input variable, and then apply various spatial distance rules to characterize patterns of cover types over a large area. Finally, ascribing a disturbance agent might involve expert visual interpretation or assignment based on explicit rules that include consideration of the shape of the disturbance, the land cover type in which it occurred, and its position on the landscape. This final step is generally beyond the scope of the work conducted for these pilot studies, but the products of the pilot studies and of the protocols developed from them feed directly into the analytical structures needed to conduct this final step, and therefore, it is important to consider this step when carrying out the other steps.

1.3 Literature review, dataset review, and study plan

Before beginning pilot studies, the OSU collaborators and the CP developed a study plan to better articulate goals and to narrow questions into manageable study units. The study plan was built on findings of a literature review conducted by the OSU collaborators to establish a common framework for discussion.

The literature review identified existing, reliable methods that could be used to meet the monitoring objectives. It focused on three main topics: preprocessing of Landsat imagery; how to develop baseline maps; and how to do change detection. Subsequent data analysis was based on the findings from literature review and when necessary, modification to the methods from literature were applied to address questions for CP monitoring need.

The dataset review revealed useful sources of data and other resources around which pilot studies were designed. To assess what data may already be available at the park and network levels, the OSU collaborators made direct visits to individual parks, data managers, GIS coordinators, and other interested or helpful contacts. Special efforts were made to locate and assess the quality and usefulness of historical airphotos, and digital imagery, specifically Landsat, Aster, IKONOS, and Lidar, and other geospatial datasets. The cost of acquiring supplemental data was also investigated.

One of the most important existing datasets is the NPS Vegetation Mapping products (NPSVM). NPSVM is a NPS-wide vegetation mapping program, which uses airphoto interpretation and field measurements to develop a polygon-based vegetation map. The detailed NPSVM maps have thematic resolution and precision greater than what may be accomplished through satellite-based remote sensing, and thus could not be used in their most detailed form. Because of their potential value, we spent significant effort developing methods to incorporate the field and airphoto data and the map products from the NPSVM into the pilot studies. Details are provided in the methods section.

There were several key topics in the literature review that shaped the study plan. First, the low vegetative cover of many of the ecosystems in the CP was expected to make soil background reflectance an important player in all spectrally-based measurements. This is a well-known challenge of using optical data in dry ecosystems. Second, characterization of vegetative cover with remote sensing data can be accomplished using either thematic or continuous-variable approaches. Thematic labeling results in a familiar vegetative type or land cover type map, with a handful of discrete land cover classes. The number of classes distinguishable with satellite remote sensing data is generally much smaller than the number that could be achieved with on-the-ground or even airphoto-based measurement, but can be done more consistently and quickly across large areas. Continuous-variable approaches attempt to describe the landscape in terms of proportional representation of different cover types within image pixels. Two limitations affect both approaches: richness of the spectral data and appropriateness of the reference data used to characterize the spectral data. Spectral data richness is largely defined by the sensor being used, which for this study was determined to be the Landsat Thematic Mapper family of sensors. The appropriateness of reference data used to characterize the surface is a function of both the type of measurements recorded on the ground and the spatial and temporal precision and representativeness of those data. All of these concepts apply equally to mapping of land cover at a single point in time and at multiple points in time. Detecting change over time adds constraints to the reference data, as the ideal reference must be representative and consistent for multiple measurement occasions over time.

The study plan set up specific pilot studies whose goals were to test the different means of preprocessing satellite imagery, linking with reference data, and analyzing relationships in

support of the goals in Table 1. The focus was on the use of existing, reliable methods, applying or modifying them as necessary for the specific situation encountered in the CP ecosystems. These were developed and tested in park-based pilot studies involving four Colorado Plateau parks.

A 2-tiered approach involving baseline mapping and change detection was used in conducting the pilot study. Initial efforts were focused on baseline mapping of Mesa Verde National Park, CO and Canyonlands National Park, UT. Change detection was the focus for Wupatki National Monument, AZ and Zion National Park, UT.

2. Pilot study sites

2.1. Mesa Verde National Park (MEVE)

The NPS vegetation map (NPSVM) for MEVE was not available at the time of analysis, nor at the time of writing this report. However, the field plot data used in making the map were available, with a total of 147 field plots surveyed in 2003 and 2004. The plots were either 15x15m or 20x20m in size (Figure 2). A reference image from the year 2002 was acquired from the LEDAPS project (Masek et al. 2008). and used as a geometric reference.

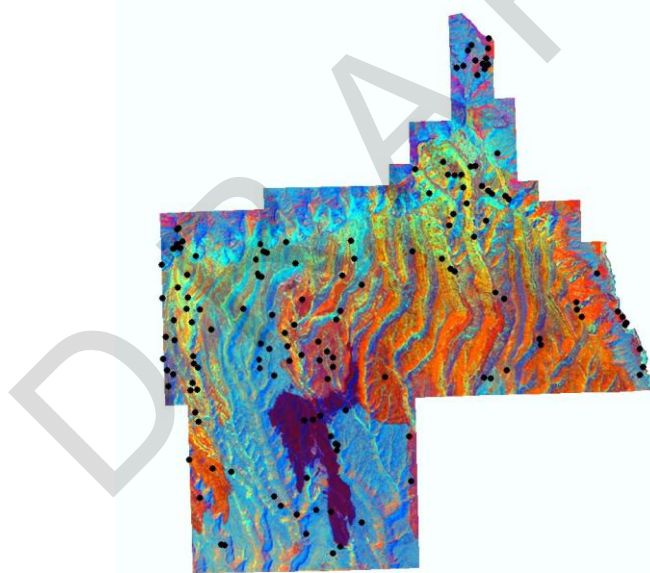


Figure 2. A false-color [tasseled-cap image] of MEVE from the year 2002, with locations of NPSVM field plots overlaid. Red tones correspond with sparse or non-vegetated soil and rock, dark blue tones with conifer cover, and cyan tones with mixed conifer and broadleaf or with broadleaf only.

2.2. Canyonlands National Park (CANY)

As with MEVE, there was no NPS vegetation map product available at the time of data analysis. Similarly, as of June 2008, the NPS vegetation mapping project is still in progress and no data are available. Again, however, NPS vegetation mapping field plots for CANY were available for use. There were 913 field plots available for analysis (Figure 3). As with the MEVE study area, a LEDAPS image was used for reference, this time from the year 2000. For baseline mapping, an image from 2004 was then geometrically referenced to that baseline 2000 image.

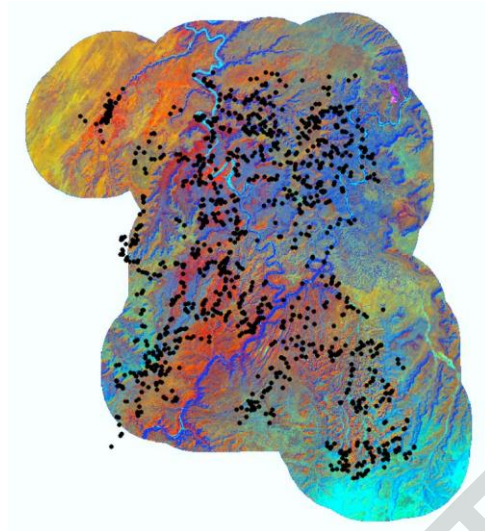


Figure 3. A false-color, tasseled cap 2004 image of CANY with 10 km buffer, with locations of NPSVM field plots overlaid.

2.3. Zion National Park (ZION)

At the time of this project, ZION had a complete vegetation map based on 1:12,000 and 1:40,000 true color photos from June 22 and 23, 1999 acquired by Horizons, Inc. Images from the Landsat Thematic Mapper (TM) are arranged in an address system of paths and rows, with path 38 row 34 covering all of ZION NP park. We chose a reference image from those produced by the LEDAPS project from July 18, 2001. Although orthorectified Landsat TM imagery is rapidly becoming available for no cost at the time of writing, this dataset was the only free source of such imagery at the time of processing. This image served as the foundational geometric and radiometric reference to which all other images were normalized. Because this image did not match to the date of the NPSVM map, however, we chose a second Landsat image from June 19, 1999 as the “baseline” image for mapping (Figure 4). For change detection, a later image from June 22, 2006 was selected and normalized to the 1999 image (Figure 4). All images were clipped to the park boundary, with a 1km buffer.

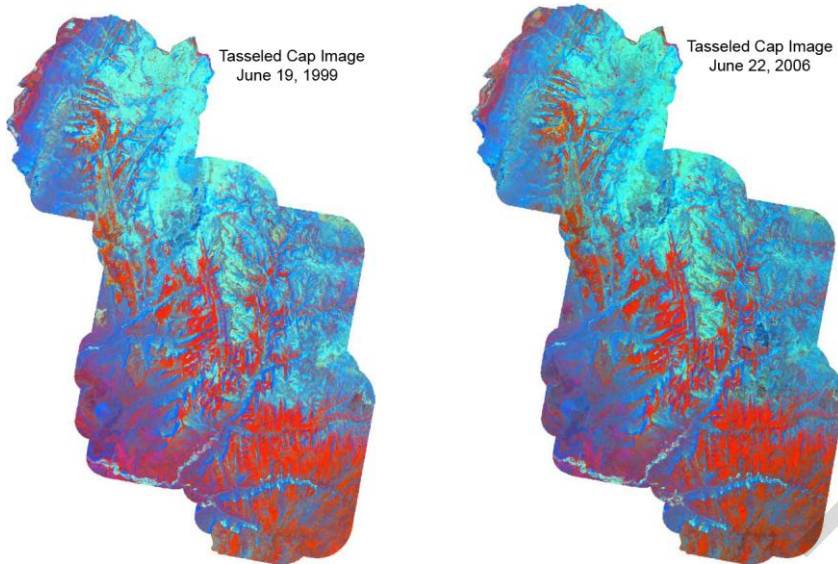


Figure 4. False-color, tasseled cap images of Zion National Park (with a 10 km buffer) from 1996 (left) and 2006 (right). Red tones correspond with sparse or non-vegetated soil and rock, dark blue tones with conifer cover, and cyan tones with mixed conifer and broadleaf or with broadleaf only.

2.4. Wupatki National Monument (WUPA)

WUPA also had a completed vegetation map from NPS vegetation mapping project at the time of this project. The map is based on 1996 Color IR photos acquired at 1:12000. As with the prior parks, the reference image for path 37 row 35 on June 6, 2001 was acquired from the LEDAPS project. For change detection, a second image from July 21, 1996 was acquired (Figure 5). A second image from May 30, 2006 was acquired, orthorectified, and used as the radiometric reference for the other images. All images were subset to the park boundary for further analysis.

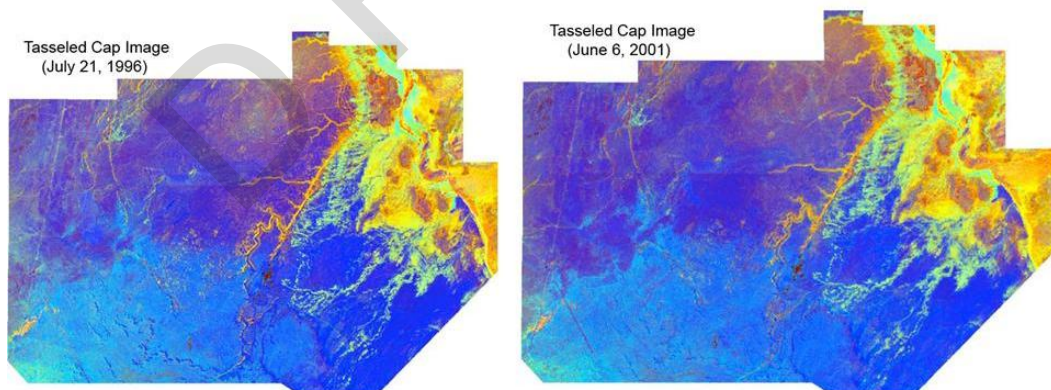


Figure 5. Tasseled cap image for WUPA (no buffer) from 1996 (left) and 2001 (right).

3. Methods

3.1. Image preprocessing

All the images used are subject to the preprocessing steps. In the subsequent section, image refers to images that have been preprocessed.

In all cases, the reference image referred to in section 4 was used at the geometric basis for any other image. Tie points were located using automated software (Kennedy and Cohen 2003) and orthorectification conducted in the ERDAS Imagine software package, with a 30-m digital elevation model used for vertical reference. All images were resampled to 25m resolution using cubic convolution resampling and were reprojected to UTM projection zone 12 and WGS84 datum.

Where appropriate, a single radiometric reference image was acquired for each park. First-order atmospheric correction using the COST method (Chavez 1996) was applied to the reference image, using methods described in the NCCN Landsat protocol (see SOP #2 in the online document: <http://pubs.usgs.gov/tm/2007/tm2g1/>). For change detection, all other images were normalized to the radiometric reference image using the MADCAL algorithms (Canty et al. 2004), which are also described in the NCCN protocol.

3.2. Baseline mapping methods

One of the overall project objectives was to investigate approaches to developing and/or geospatially extending baseline maps of land cover. There were two general approaches for creating baseline maps: continuous variable mapping (e.g., a percent tree cover map) and thematic mapping (e.g., extending the NPS vegetation map beyond its boundaries to the greater park ecosystem or GPE). Significant effort was initially placed on exploring both approaches to baseline mapping at MEVE and CANY, with a thorough investigation of the utility of using reference plot data from the NPSVM project. Initially, similar efforts were to be carried out at two additional parks (WUPA and ZION), but the NPSVM plot data proved to be less robust for our purposes than we had hoped (see below). Plot data were used at CANY for both continuous and thematic mapping, but only for thematic mapping at MEVE. At MEVE, we undertook a small new study to understand whether newly-interpreted airphoto data could be used in place of the NPSVM data for continuous-variable mapping. While we showed that such airphoto-based interpretation could be effectively used for mapping of some cover types, the time involved in airphoto interpretation prevented us from replicating that effort at other parks. Therefore, for the WUPA and ZION studies, we focused all efforts on change detection approaches.

3.2.1. Baseline mapping with continuous variables

There exist many approaches for continuous estimation of biophysical features: regression, mixture modeling, neural network modeling, etc. All methods attempt to derive a mathematical relationship between a variable of interest (for example, percent vegetative cover) and spectral data from satellite imagery. In the case of the CP parks, we sought methods that could be readily applied to different parks and to different date of images. This criterion places more weight on simple, robust methods than on nuanced, more complex methods that require significant site-specific tuning.

3.2.2. Baseline mapping with thematic labels

Where continuous-variable approaches essentially seek gradients in spectral space that correspond to gradients in features on the ground, thematic methods seek discrete regions in spectral space that correspond to discrete cover types on the ground. For thematic mapping, a reliable thematic system with the appropriate thematic resolution is needed for successful thematic mapping, using either supervised or unsupervised classification. For the parks involved in this pilot study, some have a complete vegetation map, while others only have field plot data.

Accordingly, different methods were applied to the different parks for evaluating effective methods for thematic mapping.

3.3. Change detection methods

As with the baseline mapping case, changes over time can be described using either continuous variables or categorical labels. In parks where continuous-variable modeling is conducted, change can be inferred simply by subtracting the continuous-variable estimates at different times. For example, in MEVE, woody vegetation can be estimated by relating photo interpreted vegetation cover with spectral data, and then applied to images from different dates. Estimation of change in woody vegetation cover would then be achieved by subtracting the modeled vegetation cover at the two different dates.

In cases where there is a complete NPS vegetation map, the vegetation map was used as the training data in a modified NCCN probability-of-membership (POM) change detection approach (Figure 6). The approach is based on a combination of unsupervised and supervised classification. A Landsat image near in time to the year and season of the NPSVM map was identified to represent the spectral space of the vegetation captured in the existing NPSVM map. Selection preference is given to images in the summer season, when phenological contrasts among vegetation types are most diagnostic.

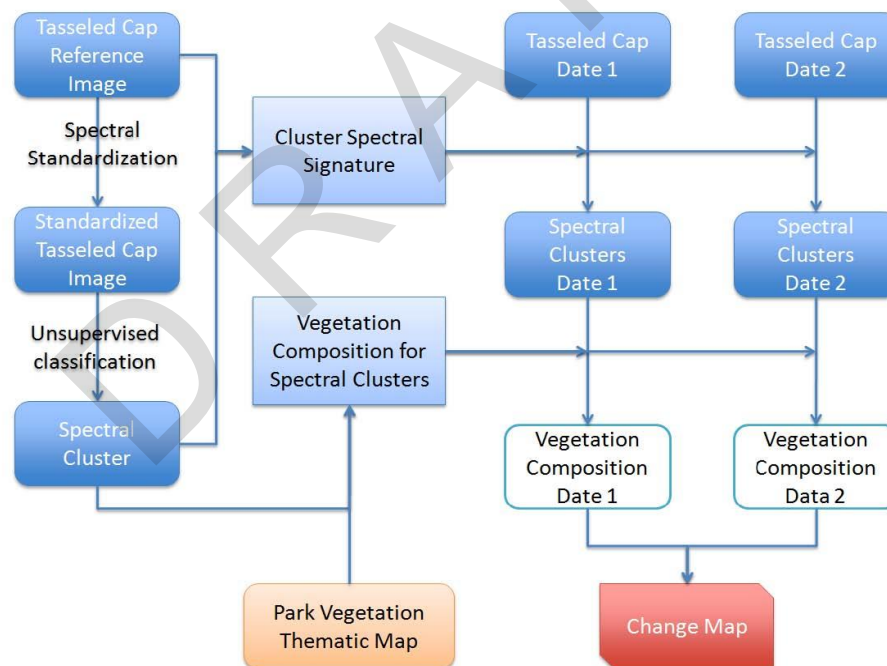


Figure 6. A diagram of the new POM thematic change detection approach. The spectral space of a reference image near in time to the date of the park vegetation thematic map is clustered using unsupervised methods (left-hand column). The spectral clusters (next column to the right) are described as proportions of park vegetation thematic categories, and also used to derive maps of spectral clusters from any date 1 and any date 2 of the tasseled-cap imagery (right-hand columns). The thematic descriptions of these clusters are then applied to the maps of spectral clusters to create maps of vegetation composition at both dates (lower right boxes), which are finally compared to create change maps.

The tasseled cap spectral space of the selected Landsat image was partitioned into spectrally separable clusters by unsupervised classification. However, because of sparse vegetation cover in most of the CP parks, most variation in spectral space was associated with variation in soil brightness, which expresses as variation in a single index – tasseled-cap brightness. Because unsupervised classification methods partition spectral space according to minimization of variance within clusters, these methods tend to partition the spectral space along the brightness. Very little variation in vegetative cover is captured if traditional unsupervised classification of unaltered spectral space is attempted. Because many of the important monitoring goals of the CP parks involve vegetation, clustering should better capture the range of vegetative type and cover. Therefore, it is preferable to have spectral clusters occupy the full spectral space.

We evaluated many approaches to fully populate the spectral space with equal-or close-to-equal-size spectral clusters. Among all the approaches examined, spectral space standardization is the most efficient, and thus was the approach we selected for all the data processing presented in change detection results presented in this document. Spectral space standardization is achieved using the following equation:

$$D_{i,j}=(D_{i,j}-D_i)/\text{std}(D_i),$$

where, $D_{i,j}$ is the spectral value for band i pixel j ; D_i is the mean value for band i ; and $\text{std}(D_i)$ is the standard deviation of all pixels in band i . This standardization step converts the original tasseled-cap space, where variation in one of the three tasseled-cap bands may dominate the signal, into a mathematical space that gives equal weight to brightness, greenness, and wetness. The standardization was performed on the selected base image, and then unsupervised classification (using a standard k-means algorithm) used to partition the standardized spectral space of that base image into 50 spectral clusters.

The spectral clusters emerging from the unsupervised classification were used in two ways (Figure 6). First, the means and covariance matrices associated with the pixels in each cluster are used to define the shape of each cluster in spectral space. This is the typical approach for describing classes, and is equivalent to the approach used in maximum likelihood classification and the original POM approach developed for the NCCN protocols. These means and covariances can then be used in a supervised classification approach to create multi-layer probability of membership images that define for each pixel its probability of belonging to each of the 50 original unsupervised classes. At this point, the 50 classes have no meaning that can be attached to cover type on the ground. Thus, the second use of the clusters is to link them with the park vegetation thematic map. To characterize or assign meaningful labels to these spectral clusters, the existing vegetation map was used to characterize the vegetation composition of each of the spectral clusters derived from the baseline image, resulting in a matrix M showing the vegetation composition (as defined by the park vegetation map) of each of the spectral clusters (derived for the 50 spectral clusters). Combining this matrix and the multi-layer likelihood image using the weighted sum, $L_v = \sum H_s * C_{s,v}$, where L_v is likelihood of class v in the NPS vegetation map, H_s is the likelihood for spectral class s from supervised classification; and $C_{s,v}$ is the composition of vegetation class v in spectral class s from the matrix. This derived vegetation map (based on the NPS vegetation map) can be used further for change detection using either a direct map contrast method or a continuous-variable approach similar to that of the POM approach previously developed for NCCN.

4. Results

4.1 Baseline mapping

4.1.1 Mesa Verde National Park

The original plan for baseline mapping was to build on relationships between spectral data and the field plot data acquired in the NPSVM project. We spent considerable effort attempting to make those field plot data usable for mapping. The field plot data from MEVE were all smaller than a single Landsat pixel, which would require high accuracy in field georeferencing (GPS positioning) to use the data for continuous modeling. However, even with accurate field positioning, misregistration in the Landsat imagery could result in the pixels being offset from their true locations on the ground. For model-building, this would result in linking inappropriate spectral data to the vegetation cover information measured in the field, which would weaken or invalidate the continuous models being built. In addition, there are other issues associated with some field plot data: the plot is not representative of the local condition; the plot is in topographic shadow; and (most importantly) the cover estimation in the field survey is categorical (Table 2).

Table 2. Cover classes used for MEVE NPSVM field plots.

Cover Class	CoverClassPercent
0	0%
1	1-5%
2	5-10%
2.5	10-25%
3	25-50%
4	50-75%
+	Trace
5	>75%
R	<1%

To make use of the field plot data to the maximum extent possible, all the MEVE field plots were manually examined with air photos for the issues mentioned above, except for plot size and cover estimation. After filtering out plots that were either obviously misregistered, falling in shadow, or non representative of local conditions, 102 out of the 147 plots remained. However, examination of remaining field plots with Landsat imagery indicated that the plots were not representative of all the park vegetation conditions – i.e. the conditions sampled by the plots were only a subset of all of the park conditions. Due to the aforementioned issues with the field plot, the continuous model derived from field plot data was judged to be inadequate.

Therefore, we opted for a different strategy. To build a continuous cover model, we photo-interpreted 143 1-ha plots (Figure 7) within the park boundary using air photos from 2003 and 2004. Cover proportions of needle-leaf, broadleaf, herbaceous, and open were interpreted following standard approaches for airphoto interpretation. Photo interpretation was done only within the park for two reasons: (1) we were relying only on the airphotos provided by the park; (2) for continuous modeling, the new photo interpreted plots within the park appeared to be representative of the cover proportion mixtures and ranges of the components that are photo interpretable across the GPE.

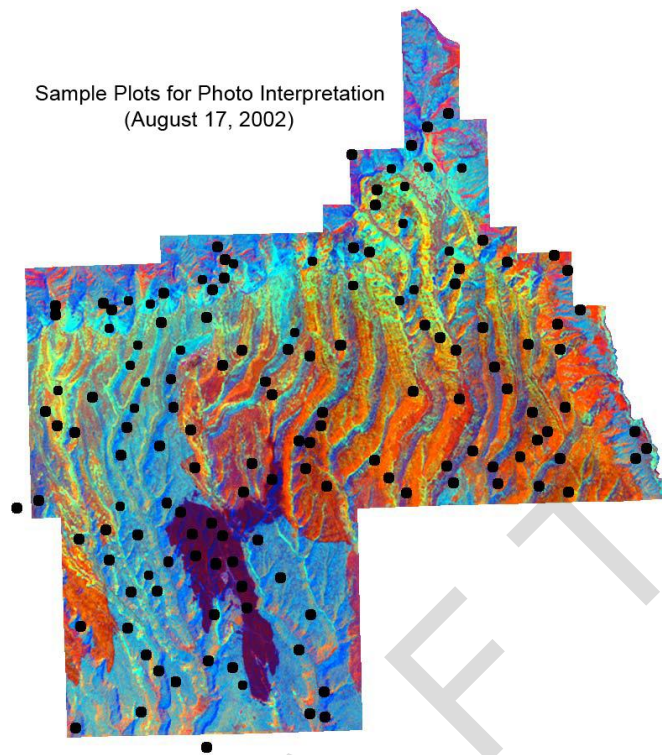


Figure 7. Sample plots for photo interpretation at MEVE, overlaid on a tasseled cap, false-color Landsat TM image.

The vegetation components available for continuous modeling are those vegetation proportions (needle-leaf, broadleaf, herbaceous, open) we obtained from photo interpretation. In addition to the individual vegetation component, woody vegetation (needle-leaf + broadleaf) and all vegetation (woody + herbaceous) were also evaluated as response variables. The spectral data considered were spectral raw bands from Landsat and related spectral transformations including tasseled cap indices, NDVI (Normalized Difference Vegetation Index), SAVI (Soil-adjusted Vegetation Index), NDMI (Normalized Difference Moisture Index), and a transformed tasseled cap index.

The Landsat image date is Aug. 17, 2002, which differs from the photo dates used in photo interpretation (2003 and 2004). This mismatch may generate potential errors for continuous modeling, especially those plots in recently-burned areas visible as dark magenta in Fig. 7. The burned area shows a dramatically different spectral signal from the unburned area. Therefore, those plots within the recent burned area were not used in the continuous modeling analysis.

We visually explored relationships between the vegetation components and all the possible spectral indices with scatter plots. Among the vegetation components examined, woody vegetation cover (needle-leaf plus broadleaf cover) showed a stronger relationship with spectral indices than the individual components did. Therefore, only woody vegetation and the spectral indices with stronger relationships (NDVI, tasseled cap transformation, and transformed tasseled cap space) are presented. All statistical analyses were conducted using R software.

4.1.1.1 Continuous Model

(1) NDVI

NDVI is a commonly used vegetation index in sparse vegetation systems, as it responds quickly to changes in vegetative cover as long as vegetative cover is less than approximately 100%. Based on our investigations, NDVI at MEVE shows a nonlinear relationship with woody vegetation cover. A nonlinear model in the form of $woody = 100 \times (1 - e^{k \times NDVI})^b$ was used. The scatter plot of NDVI with woody vegetation cover and the nonlinear model are shown in Figure 8 (left). The NDVI nonlinear model explains 80% of the variation in the woody vegetation cover. A leave-one-out cross validation for the woody cover and NDVI model shows an RMSE of about 13 percent (Figure 8, right).

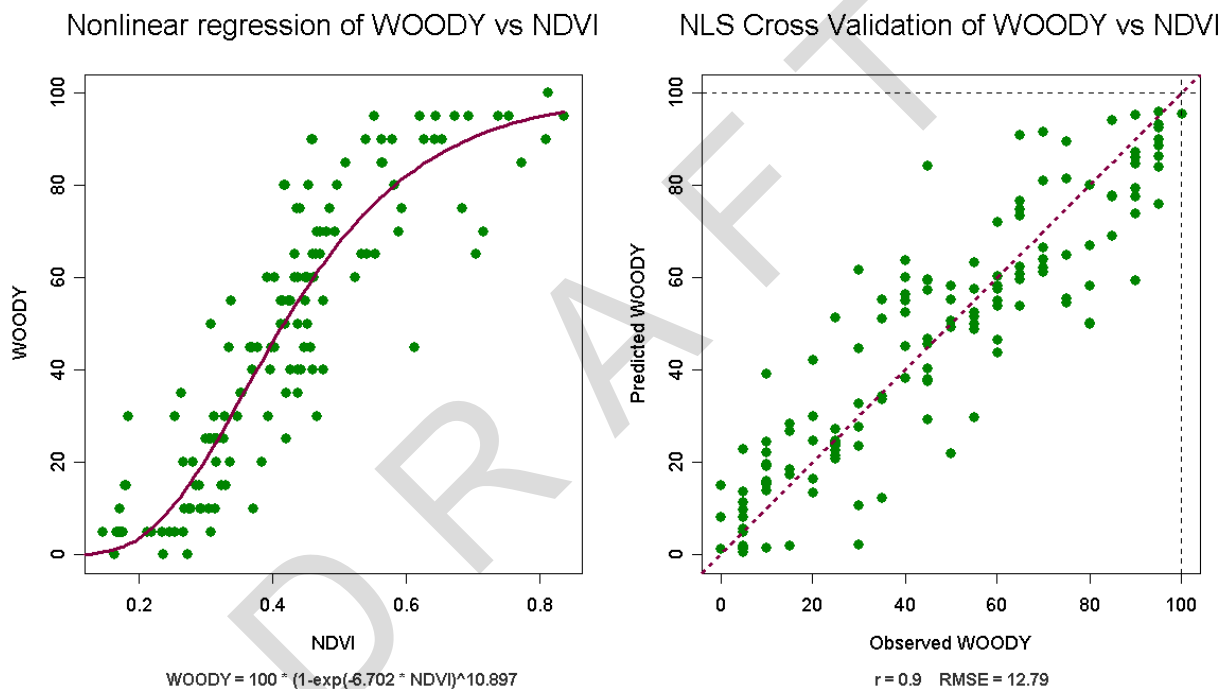


Figure 8. Photointerpreted woody vegetation cover at MEVE is well-predicted with NDVI. a) Woody cover vs. NDVI. b) Leave-one-out cross-validation comparisons of observed vs. predicted woody cover based on the NDVI model in part a).

(2) Wetness

Among the indices brightness (B), greenness (G), and wetness (W), wetness shows the strongest relationship with woody cover. Wetness and woody cover also show a nonlinear relationship (Figure 9), for which we used $woody = 100 \times (1 - e^{k \times wetness})^b$. The final model indicates that about 74% of the variation in woody cover can be explained by wetness alone. Leave-one-out cross validation showed an RMSE of 15%. The cross validation results also indicate that wetness has a potential tendency of saturation around 80% woody cover.

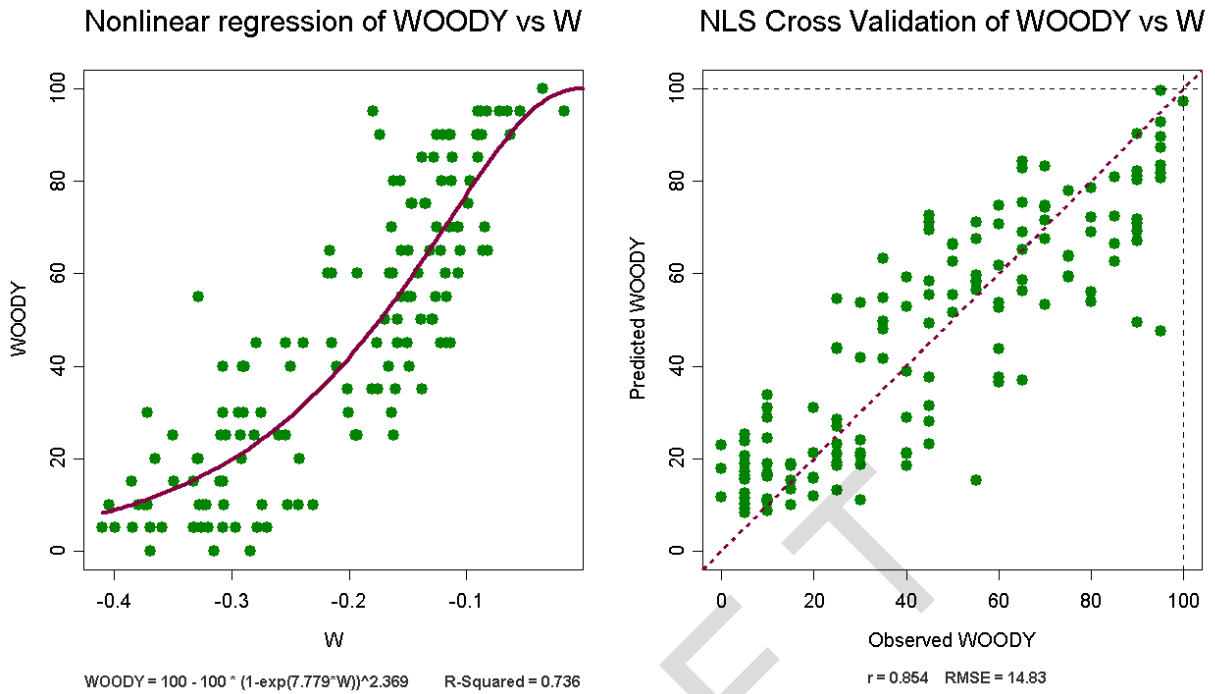


Figure 9. As in figure 8, but for tasseled cap wetness vs. woody cover.

(3) Transformation of Tasseled Cap

We developed a new data structure based on the properties of vegetation within the tasseled cap spectral space. Two new indices were derived from the tasseled cap spectral space: spectral angle (ANGLE) and distance to origin (DISTANCE) in brightness (B) and greenness (G) plane, where

$$\tan(\text{ANGLE}) = B/G$$

and

$$\text{DISTANCE} = \sqrt{B^2 + G^2}$$

ANGLE is directly related to vegetation cover, which is used to model woody cover in this study. A scatter plot of ANGLE (degrees) and woody cover is shown in the following graph (Figure 10, left). A nonlinear model was used to model woody cover: $woody = 100 \times (1 - e^{k \times ANGLE})^b$. Cross validation shows an RMSE of 11% (Figure 10, right).

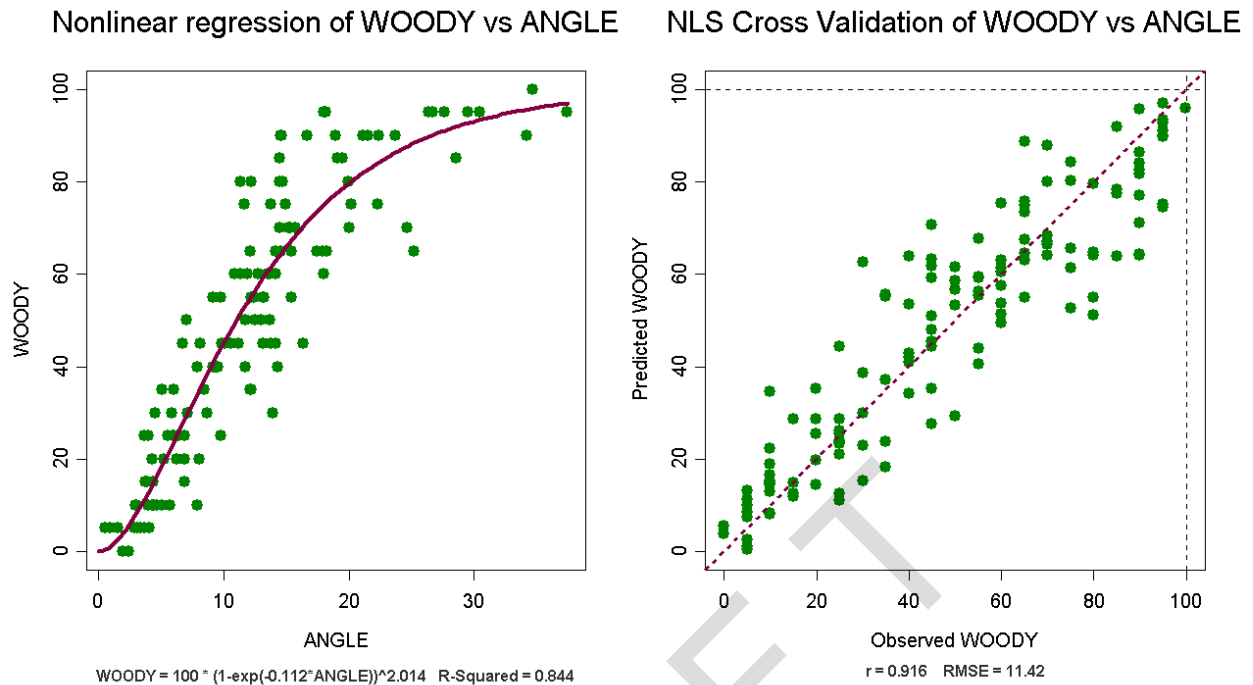


Figure 10. As in figure 8, but for the index “ANGLE” (derived from brightness and greenness) vs. woody cover.

4.1.1.2 Thematic Mapping at MEVE

Without a full coverage vegetation map of the park, we relied on the field plot data from the NPSVM project to evaluate to what level the NPSVM map classes can be mapped using Landsat data. Even though the field plot data did not seem to represent the GPE, this was the best data source available at the time of this study. There were different classifications used in the NPSVM. After examining these classification structures, we decided to evaluate three levels of aggregation of the NPSVM plot data labels: Association name, Physiognomy, and Leaf Phenology. Our objective was to determine which level of aggregation could be used for spectral classification. The metric we used was spectral separability, which is a measure of the distinctiveness in spectral space of the class labels in the aggregated classification. Spectral separability was based on the maximum likelihood classification approach, where distances in spectral space are a function of both position and spread of each class in spectral space.

(1) Association Name

According to the MEVE NPSVM vegetation classification system, there were 29 vegetation types (Table 3) used at the aggregation level of “association.” This is based on the file MEVE Classification FINAL.xls and on the field plot database obtained from NPS.

However, for the purposes of this study, there were only 102 usable field plots, and those are distributed unevenly among the classes. As a result, the full set of 29 vegetation types could not be evaluated for spectral separability using these field plots. To evaluate spectral separability, we would have needed to combine plots into more generic, aggregated classes. For example, the several *Pinus edulis* classes could have been lumped into a single *Pinus edulis* class. However, such aggregation was deemed to be redundant with the other aggregations already contained in

the classification system, and thus we did not pursue measures of spectral separability at the association level at MEVE. In the future, if more plots are obtained for each class, a spectral separability test could be conducted.

Table 3. NPSVM vegetation associations defined in MEVE field plots.

ID	Association Name
0	None
1	Pseudotsuga menziesii / Quercus gambelii Forest
2	Agropyron trachycaulum Semi-natural Herbaceous Vegetation
3	Amelanchier utahensis -Cercocarpus montanus Shrubland
4	Amelanchier utahensis Shrubland
5	Artemisia nova -Chrysothamnus nauseosus -Artemisia ludoviciana Shrubland
6	Artemisia tridentata / Chrysothamnus nauseosus Shrubland
7	Bromus inermis Semi-natural Herbaceous Vegetation
8	Bromus tectorum Semi-natural Herbaceous Vegetation
9	Cercocarpus montanus -Fendlera rupicola Shrubland
10	Comandra umbellata Herbaceous Vegetation
11	Juncus balticus Herbaceous Vegetation
12	Leymus cinereus Herbaceous Vegetation
13	Pinus edulis -(Juniperus osteosperma) – Amelanchier utahensis Woodland
14	Pinus edulis -(Juniperus osteosperma) -Peraphyllum ramosissimum -Eriogonum corymbosum Woodland
15	Pinus edulis -Juniperus osteosperma / Artemisia tridentata Woodland
16	Pinus edulis -Juniperus spp. / Cercocarpus montanus Woodland
17	Pinus edulis -Juniperus spp. / Quercus gambelii Woodland
18	Pinus edulis -(Juniperus osteosperma) / Stanlyea pinnata Woodland
19	Pinus edulis / Purshia tridentata / Poa fendleriana Woodland
20	Populus angustifolia / Populus fremontii -Bromus inermis Woodland
21	Post-Fire Mixed Herbaceous Vegetation
22	Prunus virginiana Shrubland
23	Purshia tridentata / Achnatherum hymenoides Shrubland
24	Quercus gambelii / Amelanchier utahensis Shrubland
25	Quercus gambelii / Symphoricarpos oreophilus Shrubland
26	Quercus gambelii Shrubland
27	Salix exigua / Mesic Forb Shrubland
28	Sandstone Pinus edulis -Juniperus osteosperma Barrens
29	Sarcobatus vermiculatus -Artemisia tridentata Shrubland

(2) Leaf phenology

There are eight leaf phenology types listed for the field plots (Table 4). The number of plots for each leaf phenology type varies greatly, and even at this level of aggregation there are few plots in most classes. With only three plots between them, the two types of Mixed evergreen were merged into one “Mixed evergreen” type. Spectral signatures for each leaf phenology type were extracted from the Landsat image for the field plots. The mean and two-standard deviation plots of classes in spectral space is shown in Figure 11.

Table 4. Leaf phenology and number of plots from NPSVM MEVE field plots.

Leaf Phenology		
PhenCode	Phenology	Number of Plots
1	Annual herbaceous	8
2	Cold-deciduous*	60
3	Drought-deciduous	0
4	Evergreen	25
5	Evergreen woody	0
6	Mixed evergreen/cold-deciduous	2
7	Mixed evergreen/drought-deciduous	1
8	Perennial herbaceous	4

Note: * The meaning of cold-deciduous is unclear. Among those plots labeled as cold-deciduous, some are dominated by herbaceous vegetation, and some are dominated by shrub vegetation.

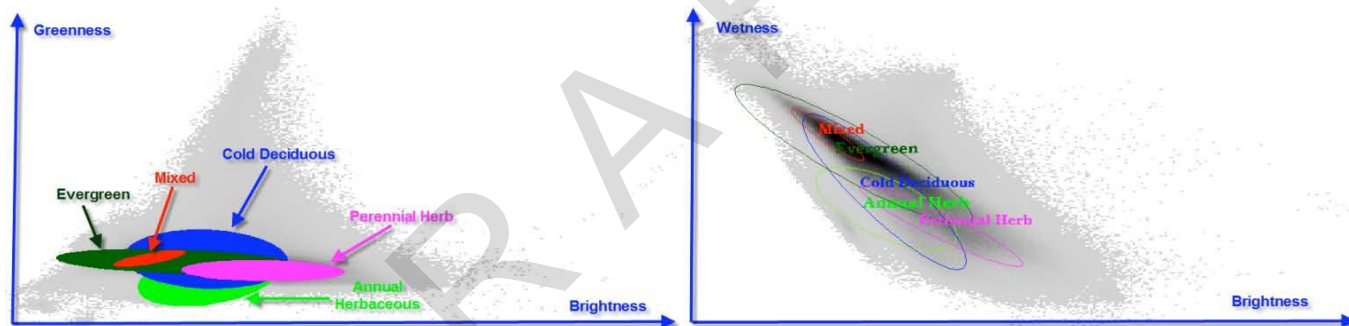


Figure 11. Spectral properties of pixels associated with leaf phenology labels at MEVE NPSVM field plots. (Left) Greenness vs. brightness, with greyed background area indicating the range of greenness and brightness values for the greater park ecosystem of MEVE, and colored class ellipsoids representing the mean + 2 standard deviations of leaf phenology classes. (Right) Similar graph for wetness vs. brightness.

With the extracted spectral signatures, a maximum-likelihood supervised classification was applied to the Landsat image data from Aug. 17, 2002. A comparison of classification results with the plot data was summarized in a confusion matrix or contingency table (Table 5).

Table 5. Contingency table for supervised classification of MEVE leaf phenology, with cell values indicating the plot count for each combination of observed and predicted class labels.

		Observed					
		Annual Herb	Cold-deciduous	Evergreen	Mixed	Perennial Herb	
Predicted	Annual Herb	5	11	1	0	0	17
	Cold-deciduous	0	29	2	0	0	31
	Evergreen	1	14	21	3	0	39
	Mixed	0	0	0	0	0	0
	Perennial	2	6	1	0	4	13
		8	60	25	3	4	100

In spite of the large overlap in the spectral space (Figure 11), the confusion matrix based on maximum likelihood classification (Table 5) shows some promise for spectral separation for leaf phenology classes with significant numbers of plots for training (e.g., Cold-deciduous and Evergreen show relatively high accuracy in the confusion matrix). All other types are so poorly represented in the plot data that their accuracies can be interpreted only in the broadest sense. The relative success with the two well-represented classes suggests that greater numbers of plots in other classes may allow reasonable classification. Note, however, that these comparisons are developed using the same set of data for training and testing (because of the extremely small sample sizes in most classes), and that therefore the error may be underestimated.

(3) *Physiognomic Class*

An alternative labeling scheme at MEVE is the “physiognomic class,” of which 10 are noted (Table 6). There are no field plots belonging to Dwarf Shrubland, Nonvascular, and Steppe classes. For the remaining seven physiognomic classes, we extracted spectral signatures from the pixels associated with the field plot data; developed maximum likelihood class plots, and applied the classification back to the images to produce error assessments. Figure 12 shows the plot means and two-standard deviation ellipsoids; Table 7 shows the contingency matrix for the classification.

Table 6. Physiognomic classes and number of plots from NPSVM MEVE field plots.

Physiognomic Class		
PhysCode	Physiognomic	Number of Plots
1	Dwarf Shrubland	0
2	Forest	10
3	Herbaceous	20
4	Nonvascular	0
5	Petran Chaparral	32
6	Shrub Herbaceous	10
7	Shrubland	9
8	Sparsely Vegetated	3
9	Steppe	0
10	Woodland	16

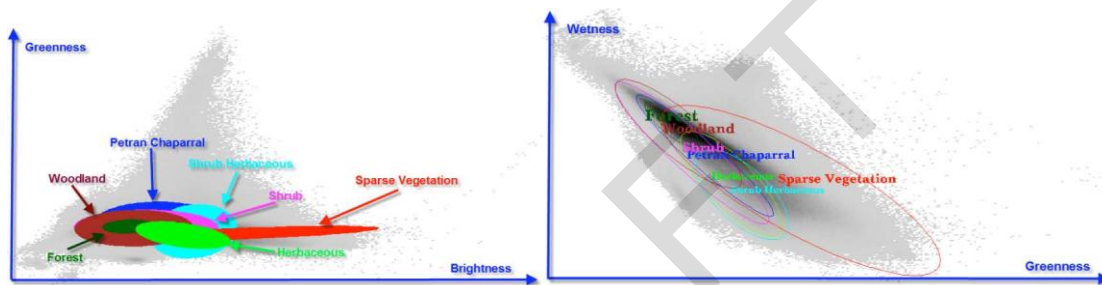


Figure 12. Physiognomic classes in tasseled cap spectral space.

Table 7. Contingency classes in tasseled cap spectral space.

		Observed							
		Forest	Herbaceous	Chaparral	Shrub Herb	Shrub	Sparse Veg	Woodland	
Predicted	Forest	8	1	7	0	2	0	8	26
	Herbaceous	0	14	6	4	1	2	0	27
	Petran Chaparral	0	1	11	1	1	0	1	15
	Shrub Herbaceous	0	2	5	4	1	1	1	14
	Shrubland	1	0	1	1	2	0	1	6
	Sparsely Vegetated	0	0	0	0	0	0	0	0
	Woodland	1	0	2	0	2	0	5	10
		10	18	32	10	9	3	16	98

4.1.1.3. MEVE baseline mapping summary

Without a complete vegetation map, and with only a small number of field plots from NPSVM, thematic mapping does not seem to be a productive approach at MEVE. Field plots have several issues that make thematic mapping difficult. First, the sample design is non-ideal for Landsat data classification in terms of plot size and distribution across the landscape. Second, there are too few plots relative to class label descriptors to fully evaluate the separability of field-defined classes in spectral space. Finally, even the best classification approaches appear to result in inadequate separability of classes, likely due to the broad range of vegetation and soil conditions in each class. With more plots, it may be possible to improve or resolve some of these issues, but the process is expected to remain challenging.

Continuous modeling based on photo-interpreted cover data shows promise for modeling woody tree cover. Among the various models examined, only NDVI, Wetness, and ANGLE were presented here. These three show a stronger relationship with woody cover than other spectral indices. The transformation of tasseled cap space to ANGLE is a novel way of interpreting the tasseled cap space that has a distinct advantage over NDVI by its use of spectral information from all the Landsat bands. Cross validation of the different models examined shows that the model using ANGLE had the smallest RMSE. Despite these positive findings, good results were only found with woody vegetation, and not for the other vegetation components. Moreover, the airphoto interpretation can only extract fairly broad descriptions of vegetation, and thus limits the richness of prediction that is possible. Therefore, the applicability of this approach is highly dependent on how the maps will be used.

Mixture modeling was also evaluated for MEVE, but was not successful. Mixture modeling is an approach to interpret the spectral space by defining areas of spectral space as mixtures of spectral “endmembers.” In this study, these endmembers were assumed to be pure representations of open, green vegetation, and shadow components. Although mixture modeling seemed to capture spectral variations visually, the interpretation of the mixture results would require many more reference plots or a separate classified map, neither of which was sufficient to apply it successfully here.

4.1.2 Canyonlands National Park

Work at CANY was similar to that conducted at MEVE. No NPSVM classified map was available for the park, and much effort focused on making use of field plots for baseline mapping.

Many of the same challenges with field plots observed in MEVE existed at CANY. Shape and size of field plots varied (circular, rectangular, square), and all plots were less than one Landsat pixel in area. Similarly, we found that many plots were often (1) not representative of local conditions (Figure 13, left); (2) in topographic shadow (Figure 13, right); and (3) misregistered geographically. The small plot size contributes to misregistration problems. To minimize these issues, we visually screened all plots and retained only those that were square or circular and that were not in shadow. This screening process yielded a total of 712 plots.

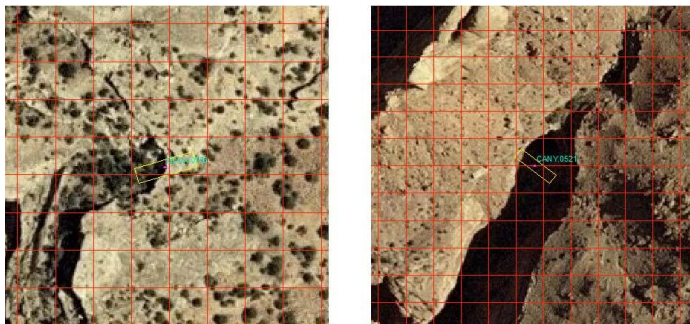


Figure 13. left: non-representative plot; right: shadow

Choosing imagery for modeling purposes was based on an investigation of phenological cycles recorded with MODIS sensors, which provide near-daily temporal resolution at a coarse spatial grain. Using MODIS NDVI, it was determined that full greenup at CANY does not reliably occur

in early spring; therefore, a late summer image (September 6, 2004) was selected. Using LEDAPS 2000 Landsat TM image as a geographic reference, the 2004 TM image was geometrically and terrain corrected using UTM12 GRS80 with 25m pixel size. The COST correction (Chavez 1996) was applied to the image to remove atmospheric effects and convert to apparent surface reflectance. Surface reflectance was then converted to tasseled cap indices and other vegetation indices including NDVI, NDMI, etc.

4.1.2.1 Continuous modeling

CANY field survey data recorded cover information in categories shown in Table 8. In contrast with the cover information recorded at MEVE, the resolution of these cover categories was sufficient for continuous modeling. Therefore, we did not do additional photo interpretation in CANY. The mid value of the cover category was used as the continuous estimation of cover for each field plot. Field plot records contained cover estimates for emergent tree, canopy, subcanopy, tall shrub, shrub, dwarf shrub, herb (graminoid, forb, fern, and seedling), nonvascular, vine, and epiphyte. Based on these data, five summary vegetation variables were created:

Tree = emergent + canopy + subcanopy
 Shrub = tall shrub + shrub + dwarf shrub
 Herb = graminoid + forb + fern
 Woody = tree + shrub
 AllVeg = tree + shrub + herb

Table 8. CANY cover classes and corresponding mid-point values (VALUE).

Cover Estimation			
CoverClass	Low	high	VALUE
(t)	0	0	0.1
0	0	0	0
01	5	15	10
01-a	5	10	7.5
01-b	10	15	12.5
02	15	25	20
03	25	35	30
04	35	45	40
05-a	45	50	47.5
05-b	50	55	52.5
06	55	65	60
07	65	75	70
08	75	85	80
09	85	95	90
10	95	100	97.5
P	1	5	2.5
T	0	1	0.5

Exploratory analysis between the five summary vegetation variables and the spectral indices was done using scatterplots. Similar to the MEVE results, woody cover was the only cover attribute

with a reasonable relationship to spectral data, and thus was the only one examined further. Relationships of woody vegetation with NDVI, tasseled cap transformation, and tasseled cap ANGLE are presented here.

(1) *NDVI*

The scatter plot of NDVI with woody vegetation cover and the regression equation are shown in Figure 14 (left). The NDVI model only explains about 34% of the variation in the woody vegetation cover. A leave-one-out cross validation for the woody cover and NDVI model shows an RMSE about 10 percent (Figure 14, right), similar to MEVE. However, because the overall range in woody cover is relatively small (most observations between 0 and 40% cover), this level of RMSE is more deleterious at CANY than at MEVE.

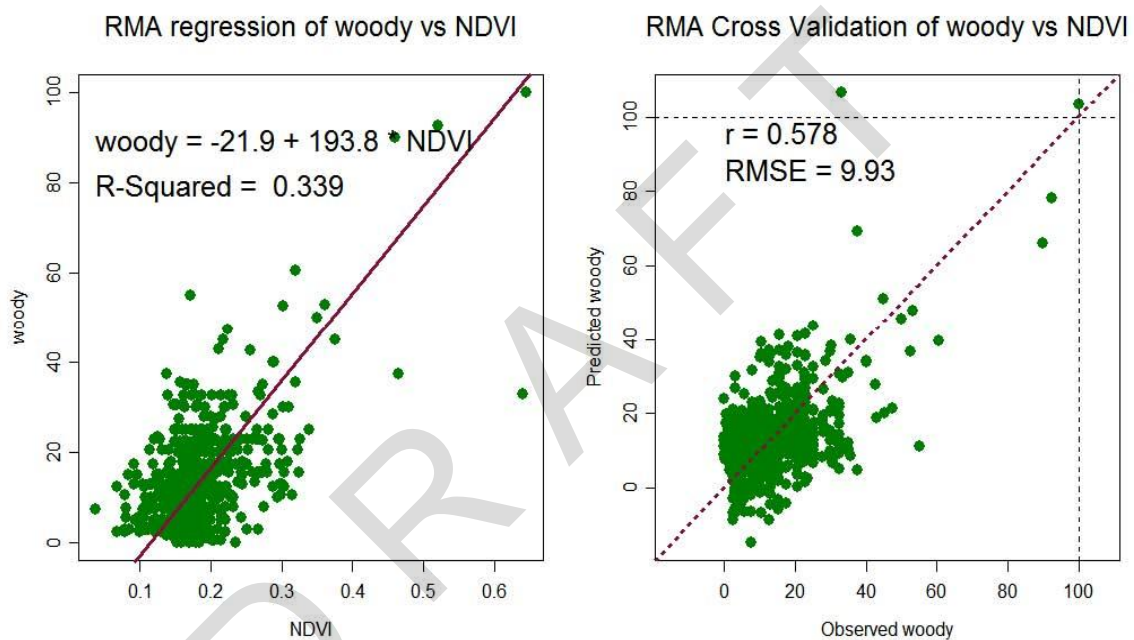


Figure 14. Scatterplot and regression of NDVI vs. woody cover at CANY (left). (Right) Leave-one-out cross-validation comparisons of observed vs. predicted woody cover based on the NDVI model.

(2) *Tasseled Cap*

Brightness, greenness, and wetness were all included in a stepwise regression model of woody cover. Since brightness and wetness were highly correlated with each other at CANY ($r = -0.88$), only brightness and greenness were used in the model (this combination gives a slightly better model in terms of r -squared than the greenness and wetness combination). The final model indicates that about 23% of the variation in woody cover can be explained. Leave-one-out cross validation shows an RMSE of 10% (Figure 15).

Multiple Regression Cross Validation of woody vs B + G

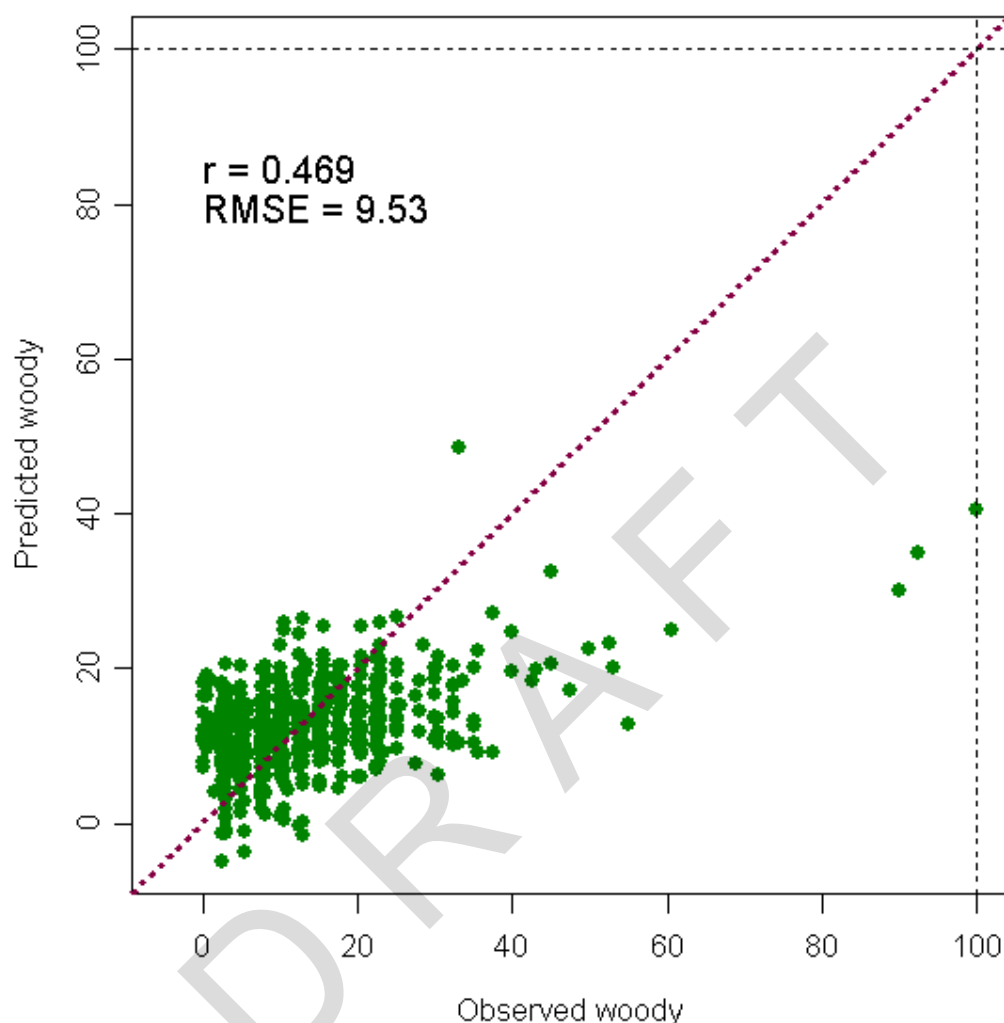


Figure 15. Woody cover model with tasseled cap brightness (B) and greenness (G).

(3) Angle and distance

The tasseled cap ANGLE index was compared to woody vegetation cover using reduced major axis regression, which balances errors in X and Y variables (as opposed to Y-variable only in standard linear regression). Using this model, for the TC ANGLE index explained approximately 30% of the variation in woody cover and cross validation showed an RMSE of 10% in terms of

woody cover (Figure 16).

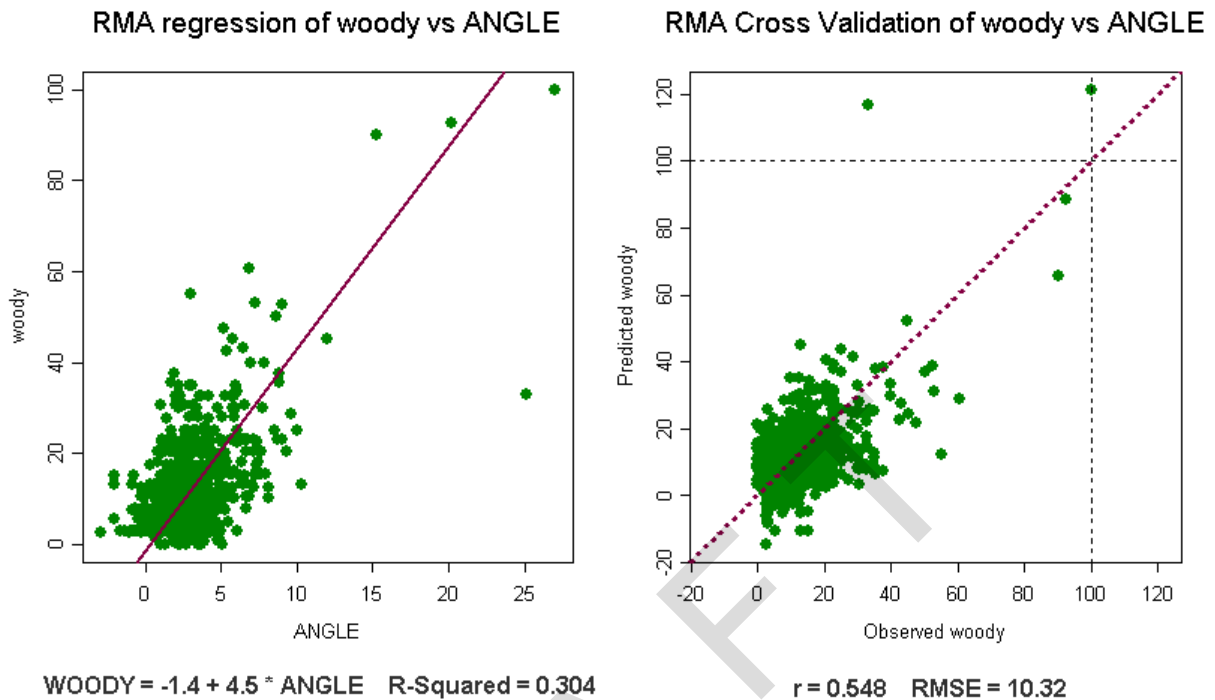


Figure 16. Woody cover model with ANGLE index.

4.1.2.2 Summary of CANY baseline mapping

As was the case with MEVE, the limitations of the reference data constrained the robustness of the mapping approaches possible at CANY. Because plot reference data for the NPSVM were not well-suited for Landsat data analysis, significant noise remained in all explored relationships. Although woody cover was again the most promising variable predicted by continuous models, it was only weakly predicted with spectral data. The low vegetation cover at CANY makes vegetation mapping particularly challenging in the absence of a robust, satellite-centric reference data set.

4.1.3 Zion National Park

Our work at Zion National Park was significantly different from that at MEVE and CANY because a completed NPSVM classified map was available for testing. We thus first focused on thematic mapping using that map as a base, examining three different levels of classification: vegetation class, physiognomy, and ecological group. For each level of aggregation, we examined the spectral separability of Landsat data within the pixels associated with that group.

4.1.3.1. Thematic mapping at Zion

(1) Vegetation Class

The ZION mapping project resulted in a total of 76 map classes at the level of vegetation class. The area covered by the classes is quite variable from class to class (Figure 17).

ZION Veg Name Distribution by Area

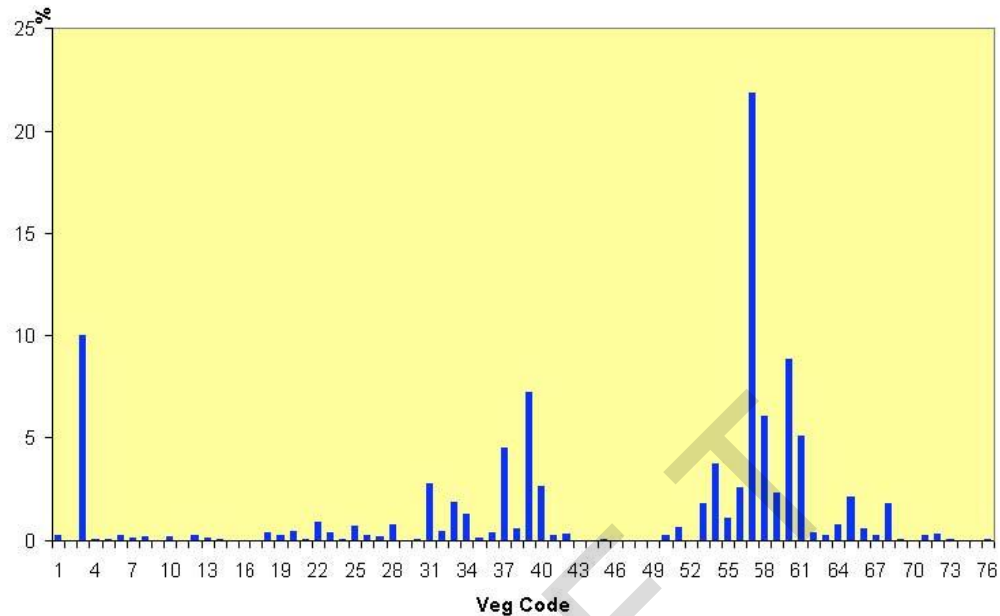


Figure 17. ZION NPSVM vegetation class by area mapped (percent of total).

Among the 76 vegetation classes, most of the classes inhabit less than 1% of the mapped area (Figure 17). The most abundant class is *Pinus-Juniperus* Woodland Complex (22%), followed by Navajo Formation (10%), *Pinus ponderosa* / *Arctostaphylos patula* Woodland (8%), *Quercus gambelli* Shrubland Alliance (7%), *Pinus-Juniperus/Quercus gambelli* (6%), and *Pinus ponderosa . Quercus gambelii* Woodland (5%). All the rest of the vegetation name classes cover less than 5% each.

Given the number and the distribution of the classes, it was unlikely that many classes would be separable with Landsat data. To evaluate the separability, only those classes covering more than 1% of the study area were used (Table 9).

Table 9. ZION vegetation class used in evaluation of spectral separability.

1	22	Dry Meadow Mixed Herbaceous Vegetation Mosaic
2	55	Populus tremuloides Forest Complex
3	34	Quercus turbinella - (Amelanchier utahensis) Colluvial Shrubland
4	68	Croplands and Pastures
5	53	Quercus gambelii Woodland
6	33	Cercocarpus intricatus Slickrock Sparse Vegetation
7	65	Abies concolor Forest Alliance
8	59	Pinus ponderosa Slickrock Sparse Vegetation
9	56	Juniperus spp. / Artemisia tridentata Woodland Complex
10	40	Mixed Mountain Shrubland Complex
11	31	Artemisia tridentata Shrubland Complex
12	54	Acer grandidentatum / Quercus gambelii Forest
13	37	Arctostaphylos patula Shrubland Complex
14	61	Pinus ponderosa / Quercus gambelii Woodland Complex
15	58	Pinus spp. - Juniperus spp. / Quercus gambelii Woodland Complex
16	39	Quercus gambelii Shrubland Alliance
17	60	Pinus ponderosa / Arctostaphylos patula Woodland
18	3	Navajo Formation (Sandstone)
19	57	Pinus spp. - Juniperus spp. Woodland Complex

We used the ZION vegetation classes (Table 9) and their corresponding field plot locations to acquire training data for a supervised classification of a July 18, 2001 image (see Section 4.3 above). Thus, this represents a possible best case for classification, assuming an accurate vegetation map. A confusion matrix for the supervised classification is shown in Table 10. The overall accuracy is 24%., and both commission error and omission error are very high.

Table 10. Confusion matrix of supervised classification of selected vegetation classes.

		ZION VEG CODE																			
		1	2	3	4	5	6	7	8	9	10	11	12	13	14	15	16	17	18	19	
SUPERVISED	1	3314	1110	745	337	2645	291	658	440	308	2677	2433	3296	1861	3692	3998	8787	4682	1937	4489	6.9
	2	1358	7996	152	101	6630	75	5258	158	50	3016	470	17578	1227	8416	7313	18637	1861	965	1741	9.6
	3	56	7	728	104	204	689	396	1016	334	900	296	90	1614	1707	357	1002	3842	5075	5865	3.0
	4	76	27	659	1804	567	659	307	1101	305	1239	578	316	2465	1462	385	1446	4270	5783	4280	6.4
	5	79	28	294	425	329	59	161	87	12	594	175	173	358	642	202	993	787	554	368	5.2
	6	37	2	650	3700	252	6791	129	6988	1275	219	1880	28	5258	1264	715	700	8765	24915	4728	9.9
	7	351	1018	674	90	1172	227	12206	527	64	4487	209	1523	3364	15199	7372	7304	6471	2589	7506	16.7
	8	14	0	309	663	77	732	56	1263	367	199	240	16	1684	416	340	283	3060	4134	2834	7.7
	9	743	42	2620	7022	443	5306	171	5710	19504	1093	10686	47	8147	1641	3784	1439	13529	17036	75789	11.2
	10	121	49	404	452	400	100	426	198	85	1735	214	434	1549	1031	1149	1527	1813	1247	2603	11.2
	11	752	58	1012	4372	1112	2796	194	3077	4175	1043	11901	76	6757	2753	4233	2512	13612	8218	16656	14.0
	12	2209	2674	324	211	3907	83	2029	151	28	4558	487	20525	1464	5147	5207	22522	1514	1070	1341	27.2
	13	0	0	7	5	4	8	2	5	0	5	6	1	12	20	2	10	28	95	11	5.4
	14	0	3	17	0	11	23	74	57	0	41	0	3	21	204	26	47	142	208	31	22.5
	15	931	267	2053	190	2739	387	2003	784	551	3928	1421	453	5377	8913	18425	10691	11986	2725	24761	18.7
	16	167	67	202	478	489	32	265	81	8	1041	126	646	464	989	591	2479	613	529	492	25.4
	17	8	2	91	28	53	95	39	153	49	76	51	2	282	326	124	269	783	612	657	21.2
	18	60	19	838	867	266	2893	499	3318	690	774	598	87	2762	1674	1138	1269	5576	35657	4516	56.2
	19	886	63	3747	769	1047	1751	825	3370	3165	4705	1924	197	10382	6229	16325	5509	24021	8478	1E+05	56.3
		29.7	59.5	4.7	8.3	1.5	29.5	47.1	4.5	63.0	5.3	35.3	45.1	0.0	0.3	25.0	2.8	0.7	29.3	43.2	24.4

It might be possible to merge ZION map classes into a set that is spectrally separable. For example, *Juniperus spp. / Artemisia tridentata* Woodland Complex could potentially be combined with *Pinus spp. -Juniperus spp.* Woodland Complex. By examining the dominant physiographic types in each of the 50 unsupervised spectral clusters, we determined that with the 2001-07-18 image, the potentially separable physiographic groups are Shadow; *Quercus/Acer* alliances; *Pinus/Juniperus* woodland alliances; *Pinus* mixture; *Pinus/Quercus*; Other mixtures; Navajo sandstone; and *Abies concolor* forest alliance (Figure 18). All the classes are mixtures of different associations.

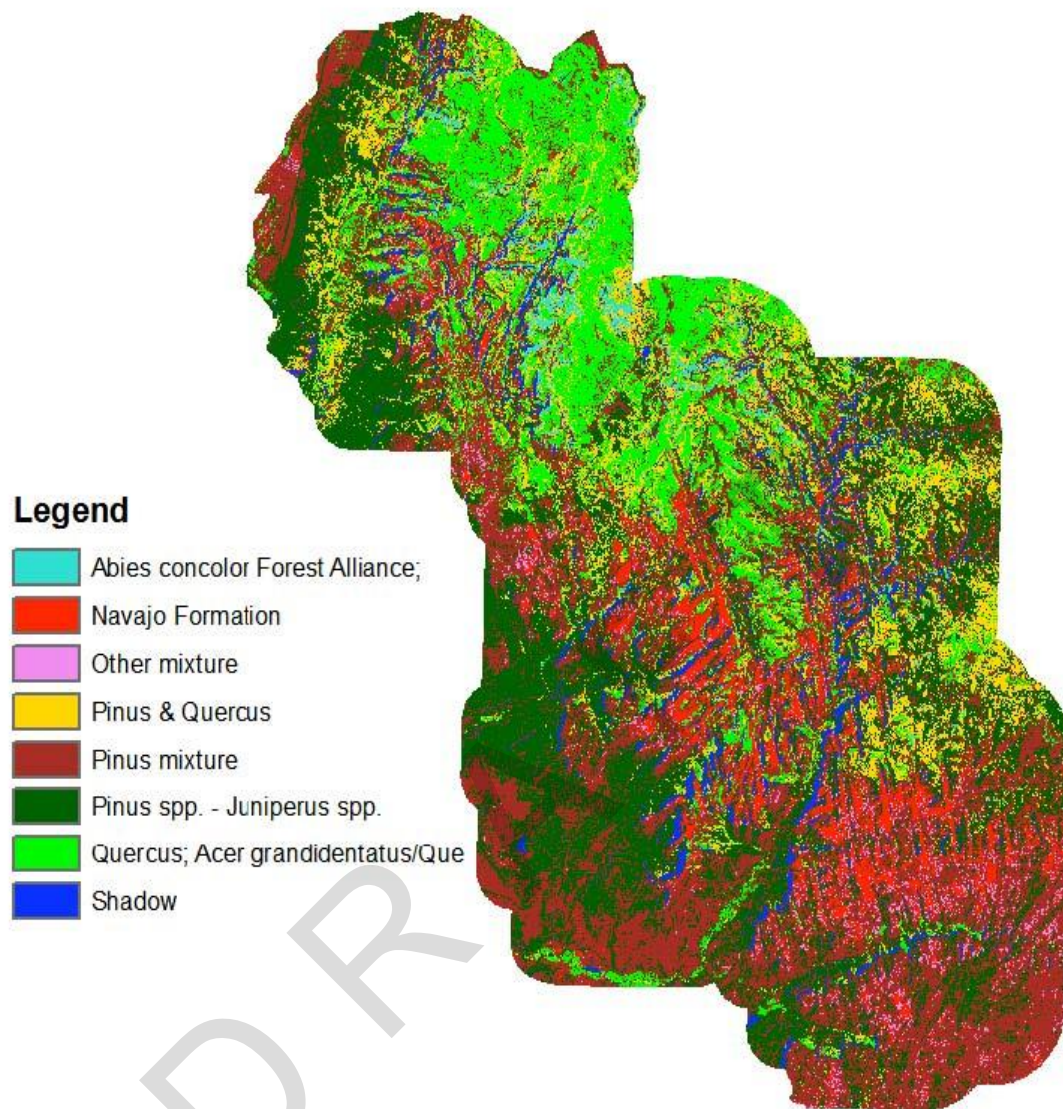


Figure 18. ZION vegetation classification based on NPSVM vegetation associations.

The tasseled cap spectral space was partitioned by the vegetation associations shown in Figure 18. Each ellipse in Figure 19 represents one standard deviation of the spectral signature around the mean and generally good separability among classes. In addition, transformed divergence values were calculated to quantify the separability of the classes (Table 11). In general, if the transformed divergence value is greater than 1900, then the classes can be separated; between 1700 and 1900, the separation is fairly good, and below 1700, the separation is poor. As expected, the separation of these aggregated classes was much better than for all vegetation classes shown in Table 10, and the overall accuracy improved to 80.5% (Table 12).

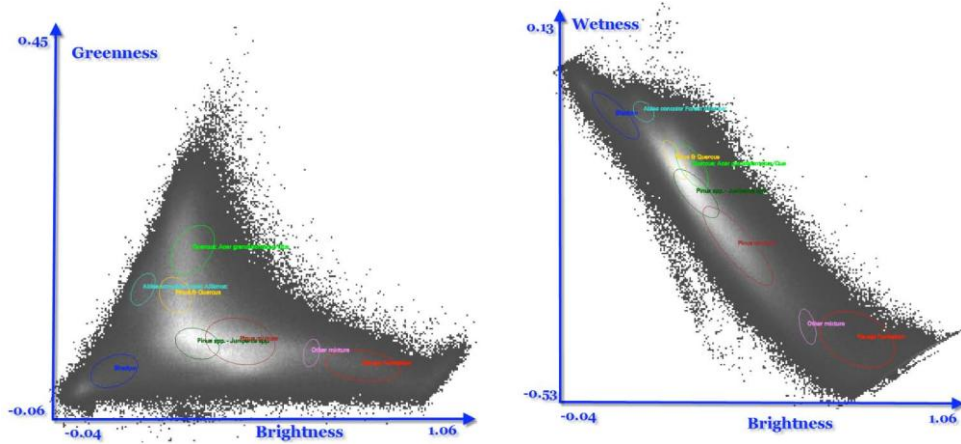


Figure 19. Partition of tasseled cap feature space by association classes.

Table 11. Transformed Divergence for association-based classes.

	1	2	3	4	5	6	7	8
1	0							
2	1923	0						
3	2000	2000	0					
4	1837	2000	1995	0				
5	1997	1950	2000	1931	0			
6	1994	1837	2000	1462	1308	0		
7	1937	2000	1768	892	1829	1925	0	
8	2000	2000	1984	2000	2000	2000	1998	0

1. Shadow
2. Abies concolor Forest Alliance;
3. Navajo Formation
4. Pinus spp. - Juniperus spp.
5. Quercus; Acer grandidentatus/Que
6. Pinus & Quercus
7. Pinus mixture
8. Other mixture

Table 12. Contingency matrix of supervised classification of vegetation associations.

	1	2	3	4	5	6	7	8	
1	40549	82	0	7849	0	0	8753	0	70.8
2	228	22524	0	0	0	2394	6032	0	72.2
3	0	0	62304	5	0	0	7103	7662	80.8
4	7	0	0	217594	0	7639	15607	0	90.3
5	0	9	0	178	164096	18831	3700	0	87.8
6	0	251	0	4734	9929	109466	197	0	87.9
7	76	129	429	125440	4401	6131	358792	1224	72.2
8	0	0	162	0	0	0	636	17061	95.5
	99.2	98.0	99.1	61.2	92.0	75.8	89.5	65.8	80.5

1. Shadow
2. *Abies concolor* Forest Alliance;
3. Navajo Formation
4. *Pinus* spp. - *Juniperus* spp.
5. *Quercus*; *Acer grandidentatus*/*Que*
6. *Pinus* & *Quercus*
7. *Pinus* mixture
8. Other mixture

(2) *Ecological group*

The Zion vegetation map also defined an ecological group (vegetation types sharing ecological processes) for each mapped polygon (Table 13). The area covered by each ecological group was quite variable among groups (Figure 20). A similar approach used for evaluating map class spectral separability was used to evaluate the spectral separability of ecological types. For this analysis, a supervised classification based on only the ecological group was performed. The overall accuracy for ecological group was 34% (Table 14).

Table 13. Vegetation ecology classes at ZION (according to NPSVM).

Ecology ID	ECOLOGY
	Coniferous Forest
	Coniferous Woodland
	Deciduous Forest
	Floodplain Woodland
	Land-Use
	Mesic Grassland
	Riparian Shrubland
	Unvegetated Surface
	Upland Grassland
	Upland Shrubland
	Wetland Herbaceous Vegetation
	Xeric Shrubland

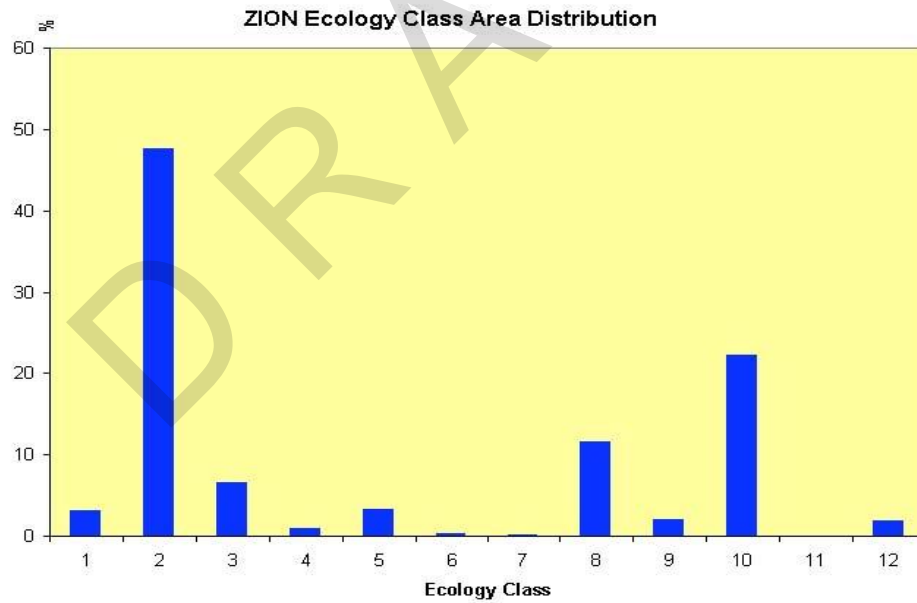


Figure 20. Area distribution by ecological class (see Table 13 for class name).

Table 14. Confusion matrix from supervised classification of the ecological types.

ZION ECOLOGY

		1	2	3	4	5	6	7	8	9	10	11	12	
SUPERVISED	1	15792	43435	3952	873	692	76	33	3642	564	20286	26	31	17.7
	2	4109	3E+05	3425	2472	5302	136	333	19561	2806	58826	32	764	72.9
	3	8476	40354	44140	1928	1677	1012	91	2968	3273	50084	85	19	28.6
	4	700	4449	822	653	802	60	86	1244	229	5229	22	23	4.6
	5	1205	23935	904	564	4247	28	78	11554	605	16610	14	202	7.1
	6	2942	16787	23486	1347	1998	2557	168	2353	6387	34680	239	50	2.7
	7	634	12937	590	1378	2734	22	478	3336	420	6421	23	289	1.6
	8	2310	36897	566	372	3382	14	56	59238	324	21389	15	1032	47.2
	9	948	43884	1803	879	3488	185	87	4971	2321	22920	11	391	2.8
	10	216	1570	187	86	179	12	8	629	54	1312	0	9	30.8
	11	372	795	900	743	2167	211	93	527	246	1983	131	24	1.6
	12	492	97671	495	917	14699	12	242	31695	8024	33333	16	20842	10.0
		41.3	44.9	54.3	5.3	10.3	59.1	27.3	41.8	1.3	0.5	21.3	88.0	33.8

Among the 12 ecological groups defined in the NPS vegetation map, only five of them (Coniferous Forest, Coniferous Woodland, Deciduous Forest, Unvegetated Surface, and Upland Shrubland) had real proportions large enough to be useful (i.e., greater than approximately 5%). The rest of the ecological groups only comprise a small portion of the landscape. Therefore, a new set of classes were defined based on these five groups. First, the spectral data were partitioned using a standard unsupervised classification algorithm, and compared with the distribution of the five dominant ecological groups. Based on this evaluation, 10 spectral groups were tentatively defined (Table 15).

Table 15. Spectral groups based on ecological groups.

ID	Vegetation Class Composition
1	Shadow
2	Coniferous Woodland
3	Coniferous Forest + Coniferous Woodland
4	Coniferous Woodland + Unvegetated Surface
5	Coniferous Woodland + Upland Shrubland
6	Mixture of vegetation with small proportion of unvegetated surface.
7	Deciduous Forest + Upland Shrubland
8	Coniferous Woodland + Upland Shrubland + Unveg surf.
9	Unvegetated surface + Coniferous Woodland/Upland Shrubland
10	Unvegetated Surface

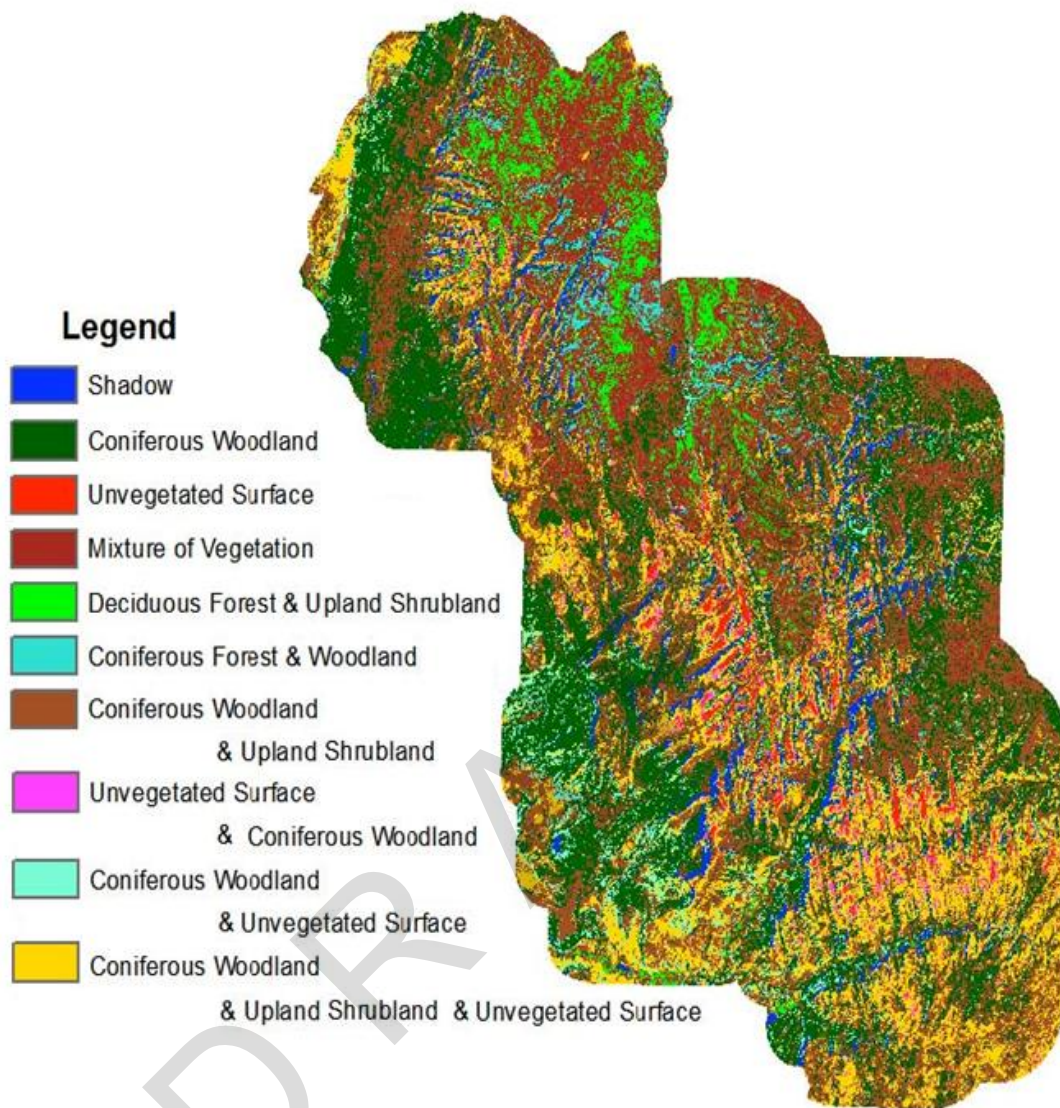


Figure 21. Map of ZION based on ecological groupings.

These spectral classes are mostly mixtures of the basic ecological groups defined in the NPS vegetation map (Figure 21). Both the spectral space (Figure 22) and transformed divergence metrics (Table 16) indicated that while the spectral separability of the ecological group-based classes are good, there still exists a large amount of confusion among some of the classes. For example, Coniferous Woodland is not very separable from mixture of Coniferous Woodland and Unvegetated Surface and mixture of Coniferous Woodland and Upland Shrubland. Evaluation of the contingency matrix indicates an overall accuracy of 78% (Table 17).

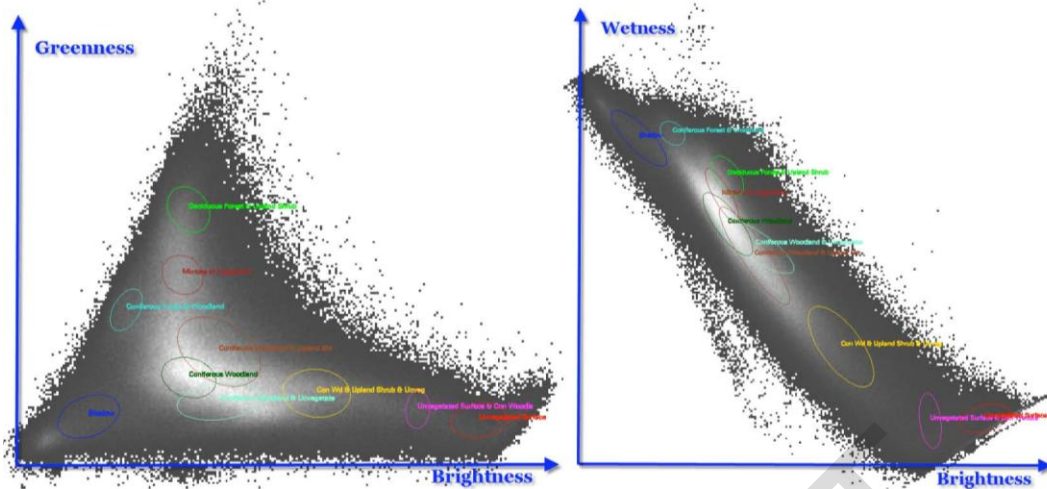


Figure 22. Partition of tasseled cap feature space by ecological group-based classes.

Table 16. Transformed divergence values for ecological group-based classes.

	1	2	3	4	5	6	7	8	9	10
1	0									
2	1817	0								
3	1923	1998	0							
4	1807	864	2000	0						
5	1941	877	2000	1482	0					
6	2000	1923	1935	1997	1452	0				
7	2000	1999	1955	2000	1959	1438	0			
8	1999	1839	2000	1611	1490	1998	2000	0		
9	2000	2000	2000	2000	2000	2000	2000	1993	0	
10	2000	2000	2000	2000	2000	2000	2000	2000	1857	0

1. Shadow
2. Coniferous Woodland
3. Coniferous Forest & Woodland
4. Coniferous Woodland & Unvegetated
5. Coniferous Woodland & Upland Shrubland
6. Mixture of Vegetation
7. Deciduous Forest & Upland Shrub
8. Con Wd & Upland Shrub & Unvegetated
9. Unvegetated Surface & Con Woodland
10. Unvegetated Surface

Table 17. Contingency table for ecological group-based classification.

	1	2	3	4	5	6	7	8	9	10	
1	39587	8957	80	0	0	0	0	0	0	0	81.4
2	13	178398	64	3088	11513	0	0	0	0	0	92.4
3	232	4791	22514	0	657	2293	0	0	0	0	73.8
4	991	66643	0	45196	6998	0	0	7544	2	0	35.5
5	11	76435	246	2679	326066	23101	296	3293	0	0	75.5
6	0	0	63	0	4034	97496	116	0	0	0	95.9
7	0	0	0	0	3072	10122	48802	4	0	0	78.7
8	26	719	28	966	25510	23	1	171646	51	2	86.3
9	0	0	0	0	0	0	0	3735	16297	577	79.1
10	0	0	0	0	0	0	0	1	284	16941	98.3
	96.9	53.1	97.9	87.0	86.3	73.3	99.2	92.2	98.0	96.7	78.1

(3) *PHYSIO* Classes

Each ZION vegetation polygon in the NPSVM maps was also assigned a *PHYSIO* type (Table 18). A supervised classification was applied to the Landsat image using the ZION vegetation map *PHYSIO* classes as training data. The contingency matrix (Table 19) indicates that the groups defined in the vegetation physiognomy map are not spectrally separable. The overall accuracy is 38% with accuracy varying among classes significantly (Table 19).

Table 18. ZION Vegetation map *PHYSIO* name.

PHYSIO ID	PHYSIO
1	Agricultural
2	Barren
3	Forest
4	Herbaceous Vegetation
5	Impoundments
6	Land-Use
7	Shrubland
8	Streams
9	Woodland

Table 19. Confusion matrix for ZION PHYSIO supervised classification.

		ZION PHYSIO Classes									
		1	2	3	4	5	6	7	8	9	
S U P E R V I S E D	1	10118	26527	2119	4090	37	1450	43334	1278	71731	6.3
	2	2268	45955	1299	603	16	978	18614	373	25232	46.2
	3	1387	6002	72394	8108	199	1892	81419	912	85291	28.1
	4	2741	6671	9093	9534	102	1164	45139	881	59408	7.1
	5	216	18920	2365	213	491	232	9510	284	22915	0.9
	6	2595	10811	743	1558	33	2506	14763	752	23991	4.3
	7	0	26	29	1	0	0	41	1	61	25.8
	8	295	1697	793	287	17	235	4346	343	7647	2.2
	9	2671	25109	8284	5798	73	2587	81336	2240	324280	71.7
		45.4	32.4	74.5	31.6	50.7	22.7	0.0	4.9	52.3	37.9

Because the physiognomic classes are already highly aggregated, we spent minimum effort testing different aggregations of the PHYSIO classes, and do not report any investigations here.

4.1.3.2. Continuous modeling

The ZION vegetation mapping project had 346 field plots. Most of the plots were either circular (11.3m radius) or square (20m), with just a few rectangular plots (40x10m or 40x20m). Cover for vegetation strata was estimated in 10% intervals for Emergent, Canopy, Sub-canopy, Tall Shrub (>2m), Short Shrub (<2m), Dwarf-shrub (<0.5m), Herbaceous, Non-vascular, Vine, Epiphyte. There is no non-vascular, vine, and epiphyte cover for all the plots surveyed, and they were excluded from further analysis. The remaining field cover data were grouped into tree (Emergent + Canopy + Sub-canopy), Shrub (Tall Shrub + Short Shrub + Dwarf-Shrub), Woody (tree + shrub) groupings. However, these cover data were not collected for analysis of Landsat imagery. An overlap existed between the different layers of vegetation, resulting in over 100% vegetation cover by simple addition of different layer's cover (e.g., plot ZION.200 = 130% shrub, 40% tree, and plot ZION.208 = shrub 60%, 90% tree). As a result, the aggregated cover estimation did not match the spectral data properly.

Spectral data evaluated for modeling vegetation cover were Landsat raw band reflectance, NDVI, the tasseled cap transformations (brightness, greenness, and wetness), and the tasseled cap ANGLE and DISTANCE metrics.

Given the small field plot size (less than 1 Landsat pixel), we extracted spectral data from a single pixel located at the plot center point. Unlike the situation at MEVE and CANY, no plot by plot screening was done before they were subjected to analysis.

Scatter plots were first used to evaluate the relationship between vegetation cover and spectral data. As an example, the scatter plot of tree cover is shown in Figure 23. The correlations among vegetation variables and spectral variables are shown in Table 20.

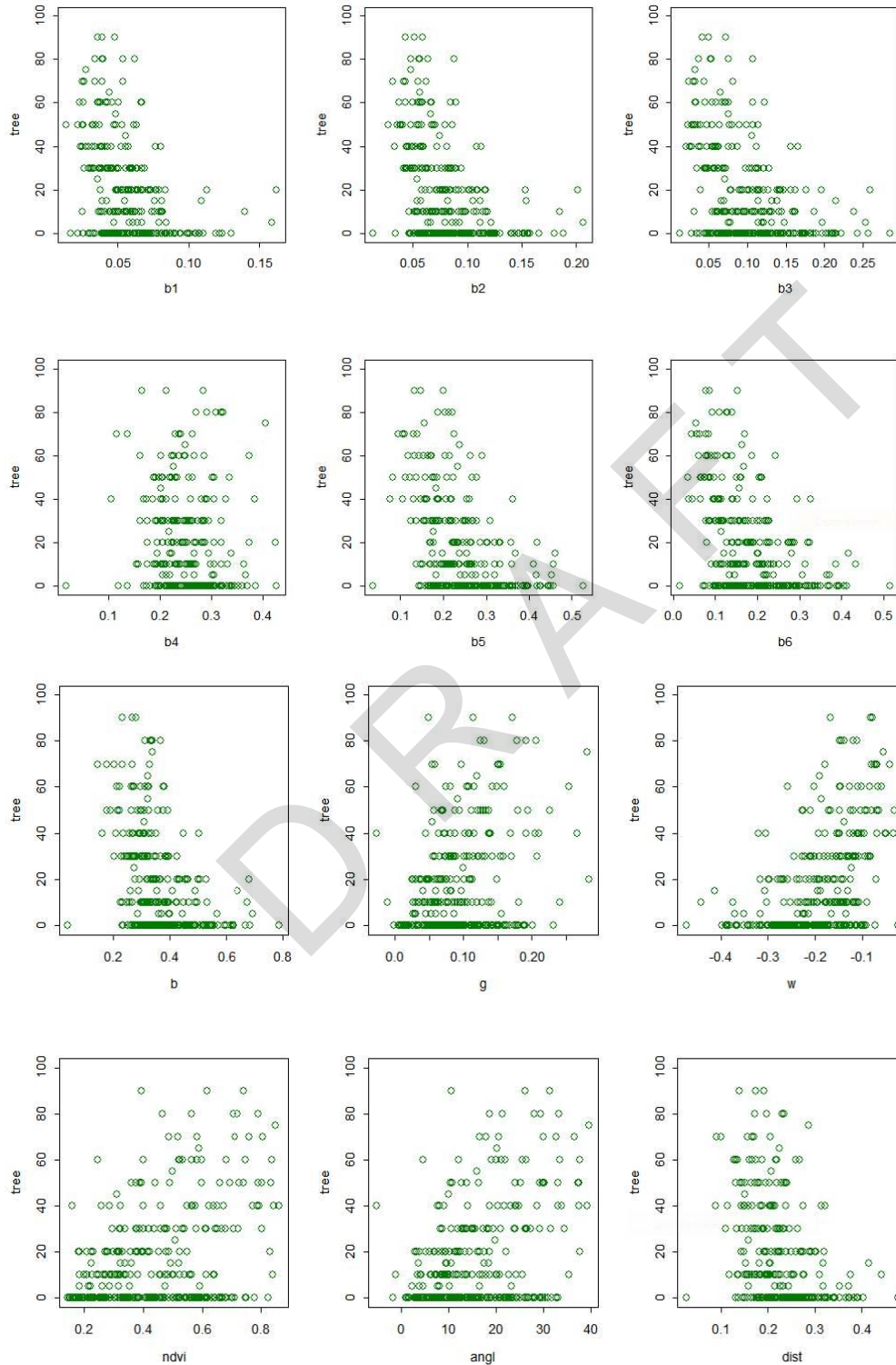


Figure 23. Scatterplots of tree cover vs. several spectral variables.

Table 20. Correlations among vegetation cover and spectral variables.

	b1	b2	b3	b4	b5	b7	b	g	w	ndvi	angl	dist	tree	shrub	herb	woody	tree2	woody2
b1	1.00												-0.36	-0.16	-0.22	-0.39	-0.35	-0.37
b2	0.97	1.00											-0.37	-0.15	-0.21	-0.39	-0.36	-0.37
b3	0.94	0.97	1.00										-0.40	-0.17	-0.22	-0.43	-0.39	-0.40
b4	0.28	0.40	0.32	1.00									-0.09	0.07	0.05	-0.01	-0.07	0.02
b5	0.85	0.88	0.90	0.46	1.00								-0.45	-0.08	-0.11	-0.39	-0.43	-0.35
b7	0.86	0.89	0.93	0.28	0.96	1.00							-0.44	-0.12	-0.17	-0.41	-0.42	-0.37
b	0.88	0.94	0.93	0.62	0.96	0.91	1.00						-0.39	-0.09	-0.14	-0.36	-0.37	-0.32
g	-0.64	-0.57	-0.65	0.50	-0.48	-0.64	-0.36	1.00					0.30	0.20	0.23	0.38	0.30	0.37
w	-0.81	-0.83	-0.87	-0.28	-0.97	-0.99	-0.89	0.60	1.00				0.45	0.09	0.13	0.40	0.44	0.36
ndvi	-0.81	-0.77	-0.85	0.19	-0.69	-0.81	-0.63	0.92	0.76	1.00			0.41	0.20	0.23	0.46	0.40	0.43
angl	-0.78	-0.73	-0.80	0.24	-0.69	-0.81	-0.59	0.94	0.78	0.99	1.00		0.42	0.19	0.20	0.46	0.41	0.43
dist	0.66	0.72	0.72	0.61	0.92	0.86	0.88	-0.21	-0.89	-0.44	-0.44	1.00	-0.34	-0.02	-0.03	-0.26	-0.32	-0.22

tree = Emergent + Canopy + Sub-canopy
shrub = Tall shrub + Short Shrub + Dwarf Shrub
woody = tree + shrub
tree2 = Emergent + Canopy
woody2 = tree2 + shrub

The weak correlations among vegetation cover and spectral indices could be attributed to a few factors:

- Small plot size increases the error associated with misregistration of plot locations.
- Small plot size increases the effects of local vegetation variation.
- Vegetation cover is estimated by vegetation strata. In reality, there exists overlap among vegetation strata, resulting in cover estimation error.

Given the weak relationship for the vegetation continuous model, these were not applied for baseline mapping and change detection. However, if photo interpretation were performed on new sample plots designed for Landsat-based mapping (to correct the factors mentioned above), there should be a strong relationship between vegetation components and spectral indices.

4.1.3.3. ZION Summary

Based on the ZION vegetation map, we explored the spectral separability of several different levels of classification defined in the ZION vegetation map, including association, physiognomy, and ecological group. Results indicated that some of these classifications, as defined in the ZION vegetation mapping project, were useful for Landsat analyses (up to 80% overall accuracy), but only when highly aggregated. Continuous modeling did not yield satisfactory results.

4.1.4. Wupaki National Monument

Minimum effort was devoted to baseline mapping for WUPA because the project's focus had shifted to change mapping. As noted in Figure 6, however, the intermediate products from change detection are maps that could be used as baseline mapping analogues (see sections 4.2.3 and 4.2.4 for more details).

4.2 Change detection

4.2.1 Mesa Verde National Park

The woody vegetation cover model using tasseled cap ANGLE (described earlier) was applied to selected images from 1999 to 2002 (Figure 24). Using these results, changes in woody vegetation between selected dates can be directly calculated by subtraction, with changes occurring across the full range from -100% to +100% vegetation change (Figure 25). This approach produces visually-realistic maps of change that are expressed in units that have meaning to the user on the ground, but caution should be used in interpreting such difference maps. Comparing two maps that have each been constructed with a linear model that has its own error can result in compounding error of prediction in the difference image.

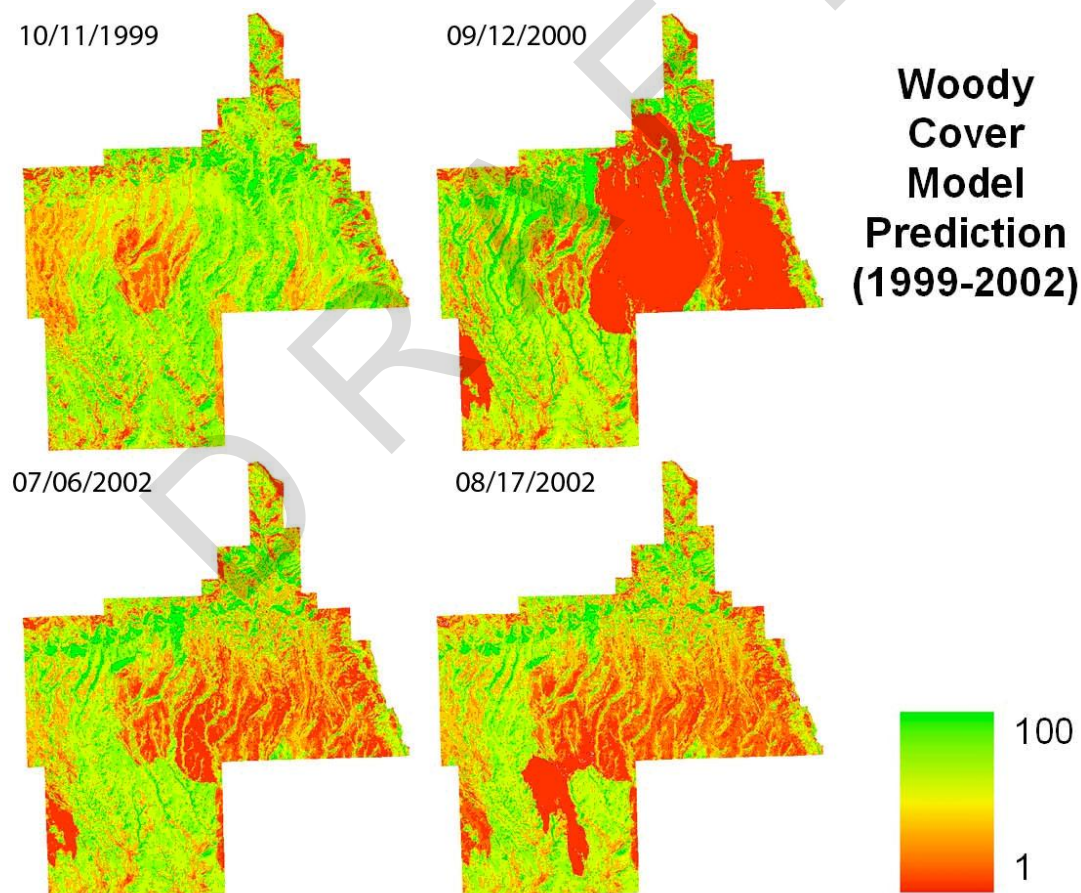


Figure 24. Woody vegetation cover modeled with ANGLE at MEVE from 1999 to 2002.

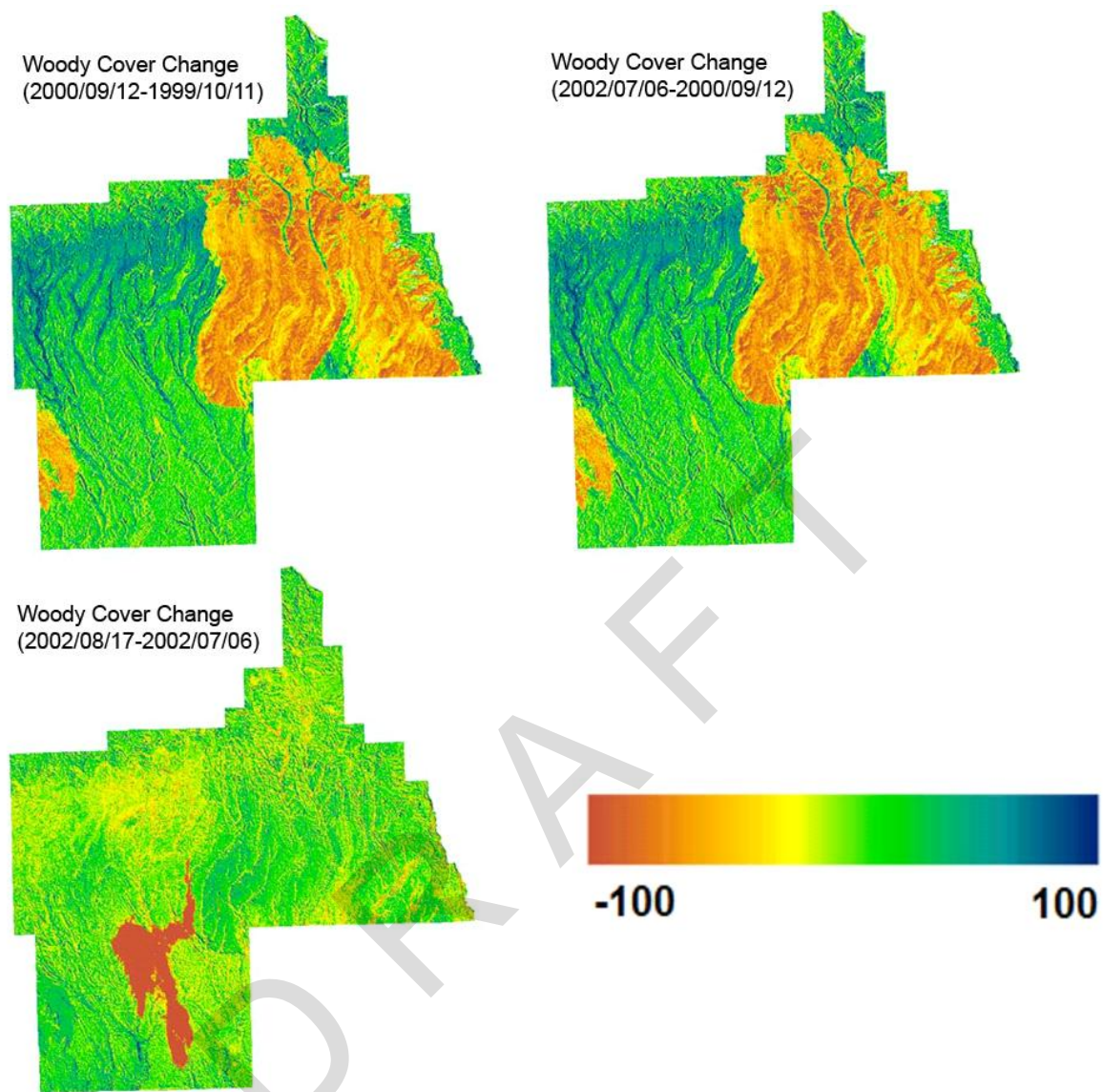


Figure 25. Woody cover change for MEVE.

4.2.2. Canyonlands National Park

CANY is very sparsely vegetated. The error associated with the continuous model of woody tree cover is relatively large when compared with mean vegetation cover. Due to the uncertainty in the output, the continuous model of woody cover was not used for change detection.

Because no park-wide vegetation cover map was available from NPSVM at the time of this analysis, CANY field plot data were used to evaluate spectral separability, but with a slightly different approach from that used for MEVE. Even though more plots were available, no clear spectral separability could be detected using the field plot data and their corresponding label. Therefore, no change detection was applied at CANY.

4.2.3. ZION National Park

The modified NCCN POM method described in section 5.3 was applied to Zion National Park. Due to the rough terrain, the park was divided into SE and NW aspects. All spectral space

partitioning and spectral class characterization was done for each aspect class separately to account for differences introduced by topography.

For change detection, instead of taking the NPSVM vegetation classes directly from the vegetation map, we evaluated different aggregation methods. For each of the polygons defined in the vegetation map, we relabeled it as one of a new set of 19 classes (Table 21), which was based on physiognomic, ecology, and cover information for each polygon. The polygon map was then rasterized with unique identifier assigned to each of these 19 ecological groups. To match the resolution of Landsat image, the resolution of rasterized image was set to 30m.

Table 21. NPSVM aggregated classes used for change detection at ZION.

Class	Name
1	Barren
2	Deciduous Forest
3	Herbaceous Vegetation
4	Open Shrubland
5	Closed Gambel Oak
6	Semi-closed Gambel Oak
7	Other Shrubland
8	Open Coniferous Forest
9	Closed Coniferous Forest
10	Semi-open Coniferous Forest
11	Closed Coniferous Woodland
12	Coniferous Woodland Mixed Shrub
13	Gambel Oak mixed Coniferous Woodland
14	Open Coniferous Woodland
15	Water
16	Floodplain Woodland
17	Land Use
18	Streams
19	Agriculture

Separately, unsupervised k -means classification was used to partition the standardized tasseled cap space into 50 spectral clusters each for SW and NE aspects of ZION. We picked 50 clusters considering the relative small area being studied. However, the approach described here does not have limitations on how many clusters it can handle. Spectral signatures for the spectral clusters defined in standardized spectral space were derived and used for supervised classification for the other image dates (1999 and 2006 Landsat images). This results in a set of spectral separable clusters and the corresponding likelihoods that a given pixel belongs to all the clusters, but none of the spectral classes had any physical meaning yet.

Assigning meaning to the spectrally-separable clusters requires a linkage with the rasterized 19-class ecological grouping image. The image for spectrally separable clusters was transformed to a POM-like image in terms of ZION vegetation ecological group with a two-way table involving this equation:

$$P_i = \sum(P_j * L_{i,j}),$$

where P_i is the likelihood for ecology group i , P_j is the likelihood of spectral cluster j , and $L_{i,j}$ is the likelihood that spectral cluster j belongs to ecology group i . A few exceptions are noteworthy. Topographic shadows on the Landsat image have the potential to weaken the linkage from spectral class to vegetation class. If shadows were included in the calculations, as the sun angle changed among images, so too would the composition in terms of ZION vegetation. Therefore, the shadow spectral clusters were excluded from this POM characterization. By manual examination, spectral clusters that represented shadows were identified for SW and NW aspects.

In addition, among the aggregated classes, agriculture is a dynamic class, and the spectral properties are not consistent; therefore, it was excluded in the POM transition. Floodplain woodland is also a special kind of woodland system. Land use classes include transportation, communications, and utilities, and many of these are linear features and the spectral properties of these different types can vary significantly. Stream classes are subpixel linear features and misregistration error can add significant amount of noise to the spectral signature. Spectral signature for water is very similar to shadow (shadow was excluded from POM analysis). Therefore, water was filtered out also. With all of these types of pixels excluded, the relative likelihood of a given ZION vegetation ecology group for the spectral classes was derived (using the equation above). The result is a two-way table showing the vegetation composition in spectral cluster (Table 22).

Table 22. Aggregated vegetation class summary by spectral cluster.

PHYS CLASS NAME	Barren	Herbaceous		Open Shrubland	Closed Gambel Oak	Semi-closed Gambel Oak	Other Shrubland	Open Coniferous Forest	Closed Coniferous Forest	Semi-open Coniferous Forest	Closed Coniferous Woodland	Oak mixed Coniferous Woodland		Open Coniferous Woodland	Water	Floodplain Woodland	Land Use	Streams	Agriculture
		Deciduous Forest	Vegetation									Woodland Shrub	Woodland						
Phys_class_1	2383	9	18	643	3	8	371	1	0	2	17	262	40	713	0	2	21	21	129
Phys_class_2	2075	1	2	248	5	2	22	0	0	4	5	97	5	399	0	1	73	4	14
Phys_class_3	2096	13	73	754	10	19	925	0	1	7	41	673	86	1145	0	4	30	38	337
Phys_class_4	1739	5	28	192	0	3	168	0	0	4	5	62	18	211	0	6	10	11	189
Phys_class_5	1916	16	186	948	8	27	1150	3	1	13	44	1313	137	1383	0	6	40	41	576
Phys_class_6	775	91	88	372	41	90	849	7	5	18	95	780	254	1233	0	28	95	47	517
Phys_class_7	2599	3	103	514	8	4	382	3	0	8	26	182	20	781	0	3	169	12	204
Phys_class_8	1969	4	358	1132	12	7	1108	0	2	7	55	483	47	1562	2	20	201	49	888
Phys_class_9	2422	6	93	1010	25	7	2032	0	6	13	157	359	36	1067	3	17	316	62	331
Phys_class_10	1190	36	425	1011	31	54	1869	0	2	13	173	2522	435	1999	0	6	60	55	696
Phys_class_11	1710	3	1457	1951	7	20	2639	2	1	25	48	1589	86	2127	2	27	146	54	1603
Phys_class_12	1077	147	230	640	112	242	1874	7	15	51	449	2232	822	2630	2	74	140	105	658
Phys_class_13	1220	42	427	1274	54	91	2392	5	9	31	412	4145	618	3586	0	64	154	80	1178
Phys_class_14	3021	8	458	1676	17	14	2679	1	10	22	340	1512	42	3109	4	47	439	110	777
Phys_class_15	891	406	345	444	309	547	1949	20	44	75	621	1393	942	1574	5	214	258	171	628
Phys_class_16	1173	51	237	963	111	122	2238	10	11	36	1022	5185	874	3862	3	107	154	123	360
Phys_class_17	2773	15	229	1398	26	32	1960	5	15	34	1237	5260	146	4620	9	95	373	151	179
Phys_class_18	974	134	293	595	321	257	2337	8	51	106	1569	3398	1270	3191	4	239	162	188	155
Phys_class_19	1174	44	162	739	70	105	1761	2	21	43	2739	6965	513	3910	2	144	120	166	36
Phys_class_20	3179	9	75	1070	25	44	907	7	7	35	653	3268	82	2911	2	33	126	62	4
Phys_class_21	3687	16	21	883	37	94	561	7	15	92	1003	2283	117	2177	12	42	14	79	3
Phys_class_22	5179	19	21	690	78	82	708	24	31	167	556	797	244	1337	37	75	7	69	9
Phys_class_23	1419	33	60	790	88	102	1146	14	22	66	4308	7011	395	4266	3	113	69	168	9
Phys_class_24	758	189	307	375	404	387	2367	16	75	123	2588	3562	1139	2933	7	259	95	195	45
Phys_class_25	1114	32	43	471	154	134	964	12	36	86	6239	5159	729	2971	2	99	25	78	5
shadow	0	0	0	0	0	0	0	0	0	0	0	0	0	0	0	0	0	0	0
Phys_class_27	1704	32	19	473	108	114	768	15	39	107	4668	2760	658	2150	3	52	8	58	2
Phys_class_28	711	179	127	284	477	449	1896	22	118	163	3685	3706	1281	2468	5	276	55	161	24
Phys_class_29	719	101	46	189	514	295	1401	32	221	222	5150	3061	1497	1882	3	187	26	109	7
Phys_class_30	580	428	633	245	537	677	1946	28	69	110	784	1166	842	1160	11	268	173	122	171
Phys_class_31	351	818	674	148	551	605	1265	19	68	95	192	217	288	265	7	235	170	94	420
Phys_class_32	385	406	136	157	963	618	1610	24	166	218	3199	1779	1591	1386	3	275	67	114	7
Phys_class_33	410	843	643	756	1045	1036	3330	31	105	164	1430	1181	1117	1114	7	357	115	144	50

*Note: not all the spectral clusters are shown

This process created images of likelihood in terms of selected aggregated vegetation classes. Changes were identified as likelihood change in the map classes (Figure 27). To identify the change between the two dates, the most likely class for each date was derived first from the

transformed likelihood class map (Figure 26). Then a direct pixel level comparison of the most likely class image between the two dates was performed. Note that there are situations where the most likely class could be very similar to the second likely class for a given pixel, and that for those situations, it might be useful to examine the second likely class also. As an alternative, a rule can also be defined to name those pixels as mixture of the different composite classes.

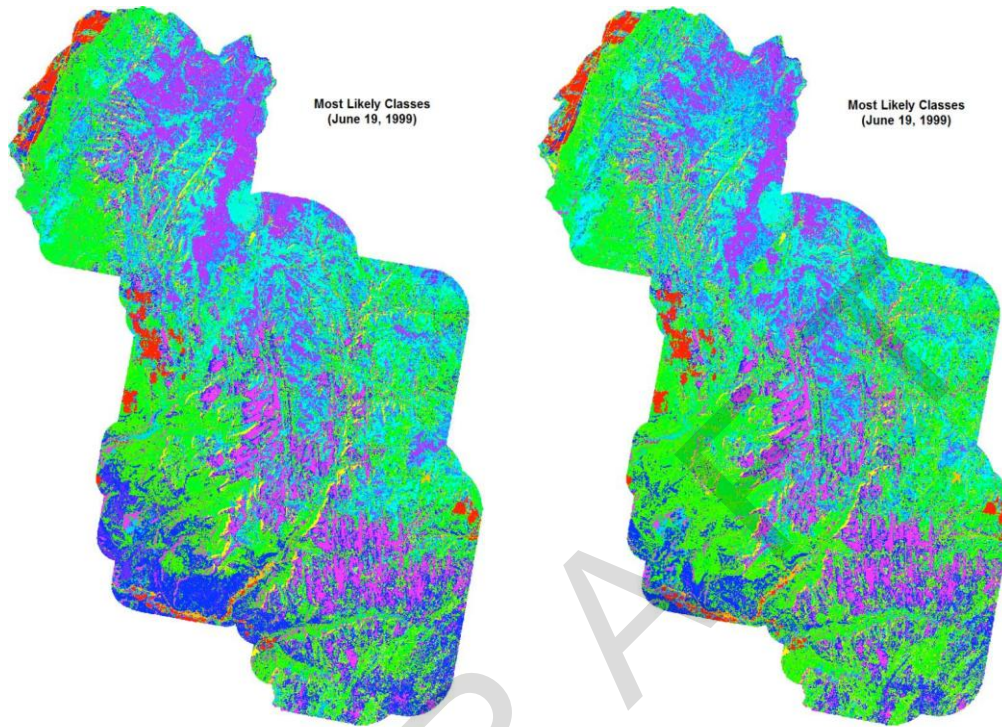


Figure 26. Most likely vegetation classes (based on POM) for ZION for 1999 and 2006.

Changes between the 1999 and 2006 were identified by direct comparison of the most likely images (Figure 26). An additional filter was imposed. Because not all classes in the original park map were spectrally separable as determined by the transformed divergence index, apparent changes among spectrally-inseparable classes could not be defensibly labeled as change. Therefore, if an identified change between two classes with a transformed divergence value of less than 1700, it was treated as no change (Figure 27). The final change map in Figure 26 describes change on the landscape using the spectral data, but describes it in terms of land cover labels that have meaning to the park.



Figure 27. Classes that have changed from 1999 to 2006 at ZION.

Validation is an essential step to assess the quality of map. In the context of developing POM-based change detection map for parks, there was a lack of multi-date reference data corresponding to the image dates analyzed. Available data sources for validation were TM images and sometimes two years of DOQs (digital orthoquads; both color and B/W). In the original NCCN protocols for change detection, we described an approach for direct interpretation of the Landsat imagery as a first phase in potential validation (the S2S validation strategy). Because such an approach is based on the same dataset from which the change maps are produced (the Landsat imagery), a complementary validation approach using DOQs is desirable. Here, we tested the feasibility of conducting a two-date DOQ validation strategy.

Two-date DOQ validation at ZION was conducted as follows. First, DOQs and Landsat imagery must match in date to allow direct comparison. Because DOQs for ZION were available from June 22 and 23, 1999 (from ZION park) and from August 2006 (from the USDA), we had developed all of our change detection maps (i.e., Figure 27) using imagery from the same years. To locate plots for validation, we subtracted the tasseled cap values in 2006 from those in the 1999, classified the resultant difference image into 20 clusters using an unsupervised classification, and then drew 100 stratified random sample plots (of 3 by 3 pixel size). Because DOQ quality is lower than hardcopy stereo-pair airphotos, change classes interpretable from the DOQs are fairly limited. For each sample plot, we determined whether the plot was agriculture or not. If not agriculture, we determined whether the plot had seen no change, an increase or decrease in shrub, or an increase or decrease in tree cover. This formed our reference change dataset.

Matching the POM outputs from the DOQ interpretation required simplification of the POM classes. The POM approach resulted in 161 change classes (as defined in Table 21). To make the comparison feasible, the 161 POM derived change classes were collapsed to the same terms as were used in DOQ interpretation based on understanding the relative proportions of shrub and tree cover in the original NPS map classes. For example, closed coniferous wood to semi-closed gambel oak was recoded as a decrease in tree cover.

We then compared the DOQ-interpreted change with the collapsed POM change labels. The results are shown in Table 23. Care must be taken in interpreting this table. More than two-thirds of the plots show no change or are in the agricultural land use. With so few actual change plots, a plot-by-plot error matrix is essentially meaningless statistically. Therefore, this table presents only the total count in each category (each row) derived from the DOQ interpretation and from the POM approach. As such, it indicates that the POM and the DOQ approaches agree well in overall landscape proportions of the different classes, but it should not be construed as a true error assessment of the POM method. To build a defensible error matrix, plot count would need to be increased by approximately an order of magnitude or more, which was impractical.

Generally speaking, however, the DOQ interpretation approach appeared to be technically feasible, and the comparison with the POM results was straightforward.

Table 23. Validation interpretation for Zion and POM based changes

Type	DOQ Interpretation	POM Most Likely
No change	63	67
Agriculture	11	0
Decrease Shrub	8	8
Increase Shrub	5	9
Decrease Tree	5	14
Increase Tree	3	2
No Image	4	0
Shadowed	1	0
Total	100	

4.2.4. Wupatki National Monument

The method described in section 4.2.3 is a generic method which can use any existing map. For WUPA, the NPS vegetation map was used to characterize the spectral classes. In the WUPA vegetation map, the polygons were labeled using several different classifications, including VEG_NAME, ECO, PHYS, ASSN_NAME etc. In the subsequent analysis, VEG_NAME was used as training data (Figure 28). There are 35 different VEG_NAME classes defined in the WUPA vegetation map (Table 24), including 26 vegetation based, 2 geomorphologic based, and 7 Anderson Level II land-use units. The vegetation map is polygon based, which was rasterized using the MAP_CODE in table 23 for each class.

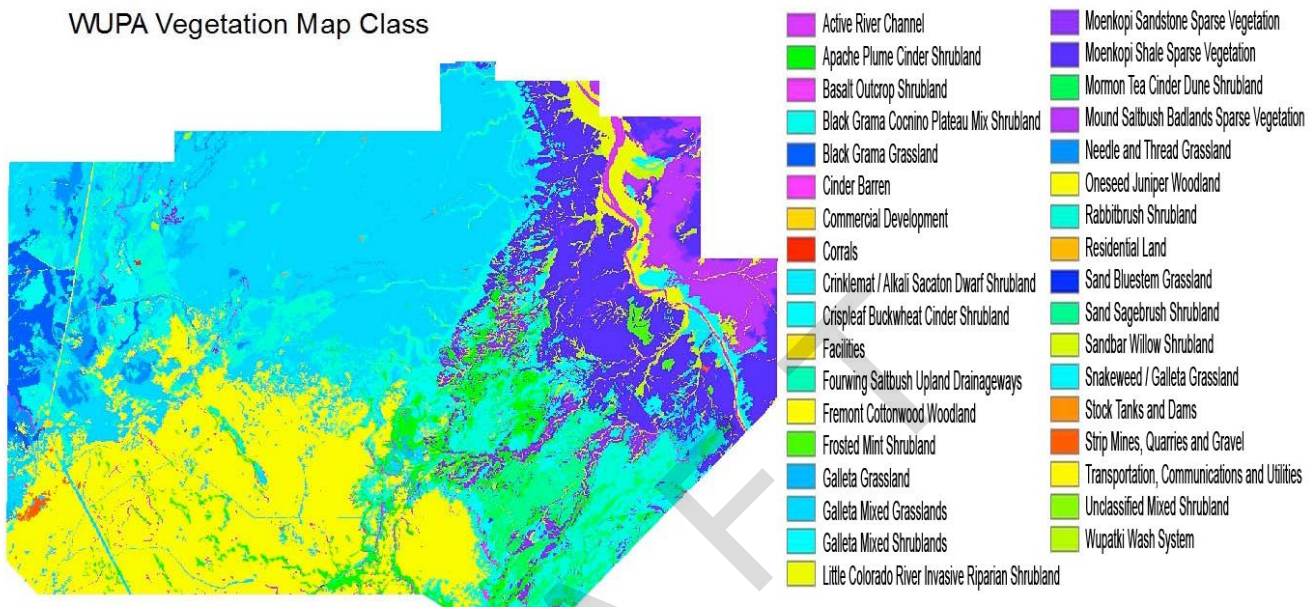


Figure 28. WUPA vegetation map from NPSVM project.

Table 24. WUPA vegetation name and map code defined in WUPA NPSVM project.

MAP_CODE	VEG_NAME
* 1	Cinder Barren
2	Basalt Outcrop Shrubland
* 3	Active River Channel
4	Mound Saltbush Badlands Sparse Vegetation
5	Moenkopi Sandstone Sparse Vegetation
6	Moenkopi Shale Sparse Vegetation
7	Sand Bluestem Grassland
8	Black Grama Grassland
9	Needle –and-Thread Grassland
10	Galleta Grassland
11	Galleta Mixed Grasslands
12	Crinkleemat / Alkali Sacaton Dwarf Shrubland
13	Snakeweed / Galleta Grassland
14	Galleta Mixed Shrublands
15	Crispleaf Buckwheat Cinder Shrubland
16	Black Grama Coconino Plateau Mixed Shrubland
17	Rabbitbrush Shrubland
18	Fourwing Saltbush Upland Drainageways
19	Sand Sagebrush Shrubland
20	Mormon Tea Cinder Dune Shrubland
21	Apache Plume Cinder Shrubland
22	Frosted Mint Shrubland
23	Unclassified Mixed Shrubland
24	Wupatki Wash System
25	Sandbar Willow Shrubland
26	Little Colorado River Invasive Riparian Shrubland
27	Oneseed Juniper Woodland
28	Fremont Cottonwood Woodland
** 29	Transportation, Communications, and Utilities
** 30	Facilities
** 31	Commercial Development
** 32	Residential Land
** 33	Stock Tanks and Dams
** 34	Strip Mines, Quarries and Gravel Pits
** 35	Corrals

* geomorphologic based class ** Anderson Level II land-use class

The vegetation map was based on Color IR photos from 1996 acquired by Merrick & Co. of Aurora, Colorado at 1:12000 scale. To best match that map date, a Landsat image from 1996 was used as the baseline image to build spectral properties for the WUPA vegetation classes.

The same modified NCCN POM approach was applied to the WUPA imagery. Unsupervised classification was applied to standardized tasseled cap space to create 50 spectral classes, which were then applied to the imagery (see Figure 29). This was applied to both dates of imagery,

resulting in two 50-layer probability images. To assign meaningful labels in terms of vegetation component, the composition of each NPS vegetation map VEG_NAME for each unsupervised class was summarized in a summary table (Table 25). The values in Table 25 are the number of pixels. The columns are the classes defined in WUPA vegetation map, and each row represents an unsupervised classification class (the spectral class). The distribution of spectral classes within each NPS vegetation class was derived by calculating the proportion of pixels within each NPS vegetation map class, which were used later to translate the probability of membership in terms of spectral classes into NPS vegetation class, in this case, VEG_NAME.

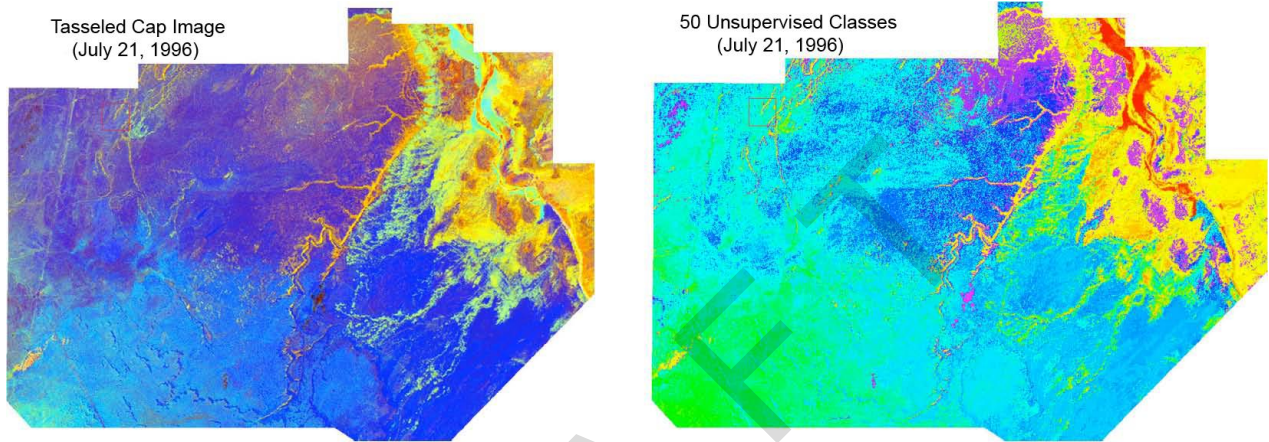


Figure 29. Unsupervised classification of standardized tasseled cap (right) and the tasseled cap image (left).

POM as Baseline Mapping

Even though there was no explicit effort to create baseline maps in the POM approach, this most likely class image derived from unsupervised classification (i.e., Figure 30) can be used as an extension of NPS vegetation baseline map to other image dates and even outside the park boundary. An accuracy matrix for the most likely class for 1996 and the NPS vegetation map was derived (Table 26).

Table 26. Error matrix of POM most likely class

	1	2	3	4	5	6	7	8	9	10	11	12	13	14	15	16	17	18	19	20	21	22	23	24	25	26	27	28			
	NPS CLASS NAME																														
1 Cider Barren	0	0	0	0	0	0	0	0	0	0	0	0	0	0	0	0	0	0	0	0	0	0	0	0	0	0	0	0	0		
2 Beach Outcrop Woodland	14	0	0	0	0	0	0	0	0	0	0	0	0	0	0	0	0	0	0	0	0	0	0	0	0	0	0	0	0		
3 Active River Channel	0	0	0	0	0	0	0	0	0	0	0	0	0	0	0	0	0	0	0	0	0	0	0	0	0	0	0	0	0		
4 Mixed Softleaf Redwood Sparse V.	1	5	575	8138	278	14605	0	4	74	0	534	25	36	1090	0	1483	5	0	1	0	24	61	0	1393	21	931	43	0	28	32	
5 Montane Sandstone Sparse Vegetation	63	163	52	55	7068	7238	0	408	295	68	4818	29	140	556	0	1344	1338	0	407	32	3332	0	8	2395	2	206	7638	0	19	44	
6 Montane Shale Sparse Vegetation	0	0	0	0	0	0	0	0	0	0	0	0	0	0	0	0	0	0	0	0	0	0	0	0	0	0	0	0	0	0	
7 Sandstone Woodland	0	0	0	0	0	0	0	0	0	0	0	0	0	0	0	0	0	0	0	0	0	0	0	0	0	0	0	0	0	0	
8 Black Grama Grassland	28	267	12	22	2047	3855	0	1110	1979	1289	36795	222	5626	1097	1	7621	5836	0	310	22	1508	1	36	1653	1	15	1747	1	11	79	
9 Heather and Thread Grassland	35	200	4	0	474	3537	0	863	3327	1517	28972	245	381	1337	7	8726	8235	0	351	21	988	0	27	533	0	0	2483	0	0	0	
10 Galena Grassland	16	288	7	9	62	647	0	877	1237	1330	32677	179	388	686	3	1275	4926	0	44	5	650	3	3	152	0	10	294	0	2	94	
11 Galena Mixed Grasslands	6	8	7	114	49	2034	0	215	199	277	20030	143	130	345	0	1648	587	0	8	1	120	29	0	382	0	138	86	0	82	95	
12 Goldenrod / Red Seedling Sage	29	30	0	0	0	0	0	0	0	0	0	0	0	0	0	0	0	0	0	0	0	0	0	0	0	0	0	0	0	0	
13 Goldenrod / Galena Grassland	6	32	30	11	128	444	0	132	85	70	2896	13	106	127	0	363	94	0	20	2	241	0	0	177	0	1	131	0	4	82	
14 Galena Mixed Woodlands	0	0	0	0	0	0	0	0	0	0	0	0	0	0	0	0	0	0	0	0	0	0	0	0	0	0	0	0	0	0	0
15 Cragged Redwood Cider Shrub	805	148	0	0	380	41	0	0	14	862	1	11	512	1066	133	7119	0	0	0	0	0	0	0	0	0	0	0	0	0	0	0
16 Black Grama Coniferous Pines Mix	0	0	0	0	0	0	0	0	0	0	0	0	0	0	0	0	0	0	0	0	0	0	0	0	0	0	0	0	0	0	0
17 Redwood Woodland	91	144	0	0	321	386	0	21	218	331	1781	67	170	1236	65	1153	1000	0	3171	913	1768	0	17	310	0	0	2324	0	36	70	
18 Younging Softleaf Woodland	0	0	0	0	0	0	0	0	0	0	0	0	0	0	0	0	0	0	0	0	0	0	0	0	0	0	0	0	0	0	0
19 Sand Sagebrush Woodland	231	263	0	0	204	437	0	11	526	287	2637	43	547	2250	139	1883	1396	0	2367	137	5124	0	4	409	0	0	5448	0	8	44	
20 Monsoon Tea Cider Shrub Woodland	83	206	0	0	509	86	0	0	332	80	343	0	233	180	111	338	5229	0	2387	1102	5441	0	230	0	0	4485	1	8	51	1	
21 Apache Pines Cider Woodland	88	131	4	0	206	19	0	1	146	47	234	0	81	135	53	189	209	0	430	101	1120	0	91	0	0	4468	0	0	0	0	0
22 Fremont Pine Woodland	5	386	79	6454	466	20335	0	30	380	16	20846	136	111	2096	0	3348	344	0	5	0	148	0	0	214	0	0	404	0	2	82	
23 Undershrub Woodland	0	0	0	0	0	0	0	0	0	0	0	0	0	0	0	0	0	0	0	0	0	0	0	0	0	0	0	0	0	0	0
24 Riparian Wetland System	0	14	12	44	194	2657	0	112	253	9	1182	39	129	160	0	398	91	0	18	2	163	0	0	0	0	0	0	0	0	0	0
25 Southern Willow Woodland	0	0	0	0	0	0	0	0	0	0	0	0	0	0	0	0	0	0	0	0	0	0	0	0	0	0	0	0	0	0	0
26 Little Colorado River Riparian R.	0	4	809	333	220	532	0	0	1	2	45	43	89	0	19	2	0	0	0	0	0	0	0	0	0	0	0	0	0	0	0
27 Openwood Juniper Woodland	883	138	0	0	1262	349	0	17	93	30	3887	8	132	206	44	1021	1397	0	816	130	3393	0	1	287	0	0	1423	0	8	89	
28 Fremont Cottonwood Woodland	0	0	0	0	0	0	0	0	0	0	0	0	0	0	0	0	0	0	0	0	0	0	0	0	0	0	0	0	0	0	0
Accuracy	0	0	53	38	63	19	0	77	33	38	16	36	4	0	70	0	13	0	24	20	5	91	0	0	0	63	77	8	36	1	
Fuzzy Accuracy	72	57	86	80	54	73	0	89	87	95	95	93	86	87	81	41	87	0	87	32	27	96	32	68	99	70	77	8	36	1	

The overall accuracy was 26%. Several reasons can be attributed for the low accuracy: (1) the classes are defined by spectral properties and not all of the 28 NPS vegetation map class can be reliably separated by Landsat spectral information. (2) The NPS vegetation map was polygon based and was developed from air photos. The local heterogeneity and low vegetation cover in WUPA makes the spectral properties within the same polygon vary significantly. (3) The class used for comparison is the most likely class; by doing so, a fuzzy classification was turned into a hard classification.

Various spectral distance metrics have been developed to evaluate spectral separability among different classes, including Jeffries-Matusita distance, divergence, transformed divergence (TD), etc. Here, transformed divergence was used to evaluate the spectral separability. Many NPS vegetation classes are not spectrally separable from each other, i.e. their TD < 1.7. Taking this into consideration, the confusion matrix was re-evaluated with spectrally unseparable classes combined, resulting in a new accuracy of 59%.

A direct comparison of the two most likely classes was used to generate a change image. Due to the similarities between NPS vegetation classes, and how most likely classes are labeled, when change was detected by comparing the most likely classes and the pair of classes was not spectrally separable, then it was considered as no change. Using 1996 as the base map, we applied these rules to the 1996 vs. 2001 change interval and developed a five-year change detection map (Figure 31).

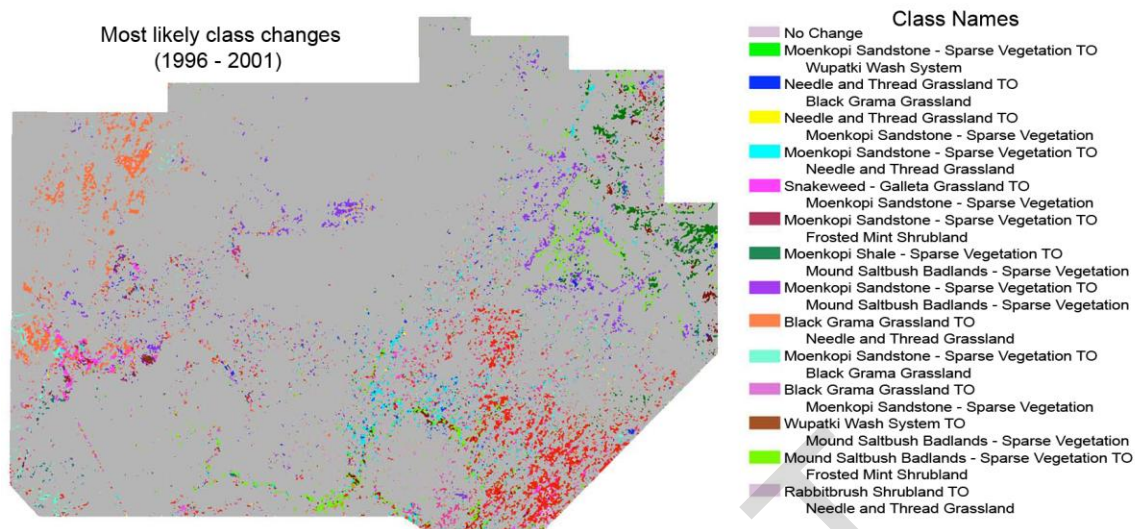


Figure 31. Most likely classes that have changed (using POM) from 1996 to 2001 at WUPA.

Without a reliable change data source for change that occurred, it is hard to validate the change detected between 1996 and 2001.

The big potential problem with this approach is the same as any change detection method based on a two-date comparison: vegetation phenological change. While efforts were made to select images as close as possible to each other in Julian Days, the phenological cycles still have great potential effects on the change detected, especially in this sparsely vegetated environment. Any class transitions that could also be explained by simple changes in the relative greenness in the two years are suspect in such a two-date change detection approach. This is essentially unavoidable if only two dates of imagery are used. Models of phenology using ancillary climate data or MODIS data may be used to ameliorate this potential effect, but these would then introduce new uncertainties into the final product. More promising, however, is the use of sequential years of Landsat TM imagery, where year to year variation becomes noise around longer-term trends. We have developed a trajectory-based approach to pick up such trends, and expect that it could be particularly effective in these systems where phenological state is variable from one year to the next.

5. Conclusions

Overall summary

In general, these pilot studies show that the use of Landsat imagery for baseline mapping and change detection within the parks of the CP requires great care. Results from MEVE and CANY suggest that continuous-variable modeling of woody cover is possible, particularly if more reference data are available. Results at CANY and ZION suggest that mapping based on the NPSVM maps is also possible, but that special aggregation of spectrally-similar vegetation classes must occur before mapping can be robust. Finally, the modified NCCN POM approach shows promise in capturing and labeling the changes that occur over time, but that spectral noise caused by variation in vegetation phenology and sun angle could lead to false positives or negatives, a problem common to all two-change detection approaches.

Specific key points are:

Baseline mapping:

- Field plots collected in support of the NPSVM program were often not appropriate for our mapping purposes. Plots were often: (1) not representative of local conditions ; (2) in topographic shadow (Figure 13, right); and (3) misregistered geographically. Manual filtering of problematic plots can provide a reasonable set of potentially usable plots.
- Woody vegetation was consistently the only vegetation variable that could reliably be modeled with continuous variables. Reference data for such model building must resolve cover into a sufficient number of categories for continuous variables. The derived tasseled cap angle consistently worked well for predicting cover. Predictions of woody cover within +/-10% absolute cover were possible at both MEVE and CANY. However, because woody cover at CANY tops out at 40%, this absolute error is proportionally large and perhaps larger than is tolerable for some applications. Additionally, the resources needed for photointerpretation of woody cover in parks where field data are not well resolved may be unrealistic.
- For baseline landcover mapping, the field plots did not sample all landcover classes equally. Combined with the general issues of field data, this meant that rules for classified map generation often did not allow for sufficient spectral separation between classes. Significantly more plots would be needed, at potentially great expense, to compensate for this effect. Therefore, we conclude that field plot data alone are not a pragmatic means of building landcover maps in these systems.
- Landcover maps based on Landsat data are more appropriately constructed using existing NPSVM maps based on airphotos and field data. The NPSVM vegetation classification can be grouped according to vegetation name, ecological type, or physiognomic types. In all three cases, the original class labels contain too much spectral overlap among classes, in part because of the inherent spectral similarity of some classes and in part because some classes are so rare that statistical summaries are unreliable. For both vegetation name and ecological type groupings, thematic aggregation is needed to obtain sufficient spectral separability to produce reliable maps.
- Land cover change:
- Direct differencing of continuous-variable woody cover at two dates can provide maps of change in woody cover. However, two cautions are needed. First, direct differencing of maps derived from state-variable models compounds the error in both of the state maps. Second, that error is relatively high in systems with low absolute woody cover (such as within CANY).
- The POM approach for change detection does appear to be feasible, and improvements to the method conducted in part for this project means that changes in land cover can be characterized in terms of the cover classes familiar to the parks.
- Change maps can be validated with DOQ interpretation, but because change is relatively rare occurrence on the landscape, a random sample would require many hundreds of plots

to produce error estimates statistically stable enough to fully characterize the error appropriately.

While two-date POM mapping appears to capture the spectral variation appropriately, the spectral variation itself may be caused solely by vegetation phenological change that cannot be separated from actual land cover change. This is essentially unavoidable when using only two dates of imagery, but we expect that a trajectory-based approach that incorporates many sequential years of imagery can significantly reduce this effect.

Literature Cited

- Canty, M.J., Nielsen, A.A., and Schmidt, M. 2004. Automatic radiometric normalization of multitemporal satellite imagery. *Remote Sensing of Environment* 91: 441-451
- Chavez Jr., P.S. 1996. Image-based atmospheric corrections --revisited and improved. *Photogrammetric Engineering & Remote Sensing* 62: 1025-1036
- Kennedy, R.E., and Cohen, W.B. 2003. Automated designation of tie-points for image-to-image coregistration. *International Journal of Remote Sensing* 24: 3467-3490
- Masek, J.G., Huang, C.Q., Wolfe, R., Cohen, W., Hall, F., Kutler, J., and Nelson, P. 2008. North American forest disturbance mapped from a decadal Landsat record. *Remote Sensing of Environment* 112: 2914-2926)